The role of mucus in the cross talk between gut bacteria and the host

Olivia Kober, BSc (Hons)

A thesis submitted in accordance with the requirements for the degree of

Doctor of Philosophy (PhD)

To

The University of East Anglia

Institute of Food Research
Gut Health and Food Safety
Norwich Research Park
Colney
NR4 7UA

September 2013

Abstract

The mammalian gastrointestinal tract is home to a complex microbial community engaged in a dynamic interaction with the immune system. Mucus is the first point of contact of the microbiota with the host, acting as a first line of defence. Furthermore γδ intraepithelial lymphocytes (IELs) respond to the invading bacteria that circumvent the mucus barrier. In this study two approaches were used to investigate the role of mucus in intestinal homeostasis; firstly the impact of γδ IELs on the mucus layer, and secondly the adhesion properties of the gut symbiont *Lactobacillus reuteri* to mucus.

To study the impact of IELs on mucus properties, a γδ T cell-deficient (TCRδ$^{-/-}$) mouse model was used. TCRδ$^{-/-}$ mice showed increased susceptibility to dextran sodium sulphate (DSS)-induced colitis, alterations in mucin expression, glycosylation and goblet cell numbers, but maintained an intact mucus layer *in vivo*. Moreover, TCRδ$^{-/-}$ mice showed reduced levels of interleukin-33 mRNA, a mediator of mucosal healing. An *ex vivo* SI organoid model using input cells from TCRδ$^{-/-}$ mice showed, upon addition of keratinocyte growth factor, increases in crypt length, and both goblet cell numbers and redistribution. These findings provide novel mechanisms by which γδ IELs may modulate mucus properties, explaining the increased susceptibility of TCRδ$^{-/-}$ mice to chemically-induced colitis.

L. reuteri strains protect against DSS-induced colitis in mice. To investigate the importance of *L. reuteri* adhesion to the intestinal mucus layer, the mucus-producing HT29-MTX cell line as well as murine and human intestinal tissues were used in conjunction with chemical treatments. The mucus-binding protein MUB of *L. reuteri* ATCC 53608 was found to promote *L. reuteri* adhesion to mucins in a host and tissue-specific manner and display sialic acid-binding specificities. Together, these data provide insights into *L. reuteri*-mucus interactions; a key factor in influencing host response and exerting health effects.

Preface

The work of this PhD project has resulted in the following publications:

Scientific paper publications:

Kober OI., Ahl D., Carding SC., Holm L., Juge N. *γδ T cell-deficient mice show alterations in mucin expression, glycosylation and goblet cells but maintain an intact mucus layer*. Under revision at Am J Physiol Gastrointest Liver Physiol.

Fuell C., **Kober OI**., Hautefort I., Carding SC., Juge N. *Mice deficient in intestinal γδ intraepithelial lymphocytes show a different mucin O-glycan profile compared to wild-type mice.* Under revision at Glycobiology.

Oral presentations:

Kober O., Holm L., Carding SC. Juge N. *Impact of gamma delta T cells on murine intestinal mucus properties.* Mucins in health and disease, 12th International Workshop on Carcinoma-associated Mucins, Robinson College, Cambridge, UK, 27th-31st July 2013.

Kober O., Holm L., Carding SC. Juge N. *Impact of gamma delta T cells on murine intestinal mucus properties.* Early careers British Society for Immunology Inflammation and Immunology Symposium, University of East Anglia, Norwich, UK, 26th March 2013. (Awarded prize for best oral presentation).

Poster presentations:

Kober O., Holm L., Carding SC. Juge N. *Impact of gamma delta T cells on murine intestinal mucus properties.* British Society for Research on Ageing meeting, University of East Anglia, Norwich, UK, 3rd September 2013.

Kober O., Hautefort I., Holm L., Carding SC., Juge N. *Impact of gamma delta T cells on murine intestinal mucus properties*. Digestive Disease Week 2013, Orange County Convention Centre, Orlando, FL, 18th-21st May 2013.

Kober O., Hautefort I., Holm L., Carding SC., Juge N. *Impact of gamma delta T cells on murine intestinal mucus properties*. Inaugural Annual Symposium, Gut Health and Food Safety ISP, John Innes Conference Centre, Norwich, UK, 5th March 2013.

Kober O., Hautefort I., Holm L., Carding SC., Juge N. *Impact of gamma delta T cells on murine intestinal mucus properties*. Gamma delta T cell conference, Freiburg, Germany, 31st-2nd June 2012.

Kober O., Wakenshaw L., Hautefort I., Carding SC., Holm L., Juge N. *Modulation of the mucus component of intestinal barrier defence in mouse models*. Mucins in Health and Disease, 11th International Workshop on Carcinoma-associated Mucins, Robinson College, Cambridge, UK, 9th-13th July 2011.

Kober O., Wakenshaw L., Hautefort I., Holm L., Carding SC., Juge N. *Modulation of the mucus component of intestinal barrier defence in mouse models*. John Innes Centre, BBSRC conference, John Innes Conference Centre, Norwich, UK, 4th-6th July 2011.

Kober O., Wakenshaw L., Hautefort I., Holm L., Carding SC., Juge N. *Modulation of the mucus component of intestinal barrier defence in mouse models*. IFR Student Science Showcase, Institute of Food Research, Norwich, UK, 1st July 2011.

Kober O., Schreiber O., Jeffers F., Wakenshaw L., Roos S., Holm L., Juge N. *Functional modulation of the rodent mucus layer by gut bacteria*. The molecular biology of inflammatory bowel disease, Biochemical Society Conference, University of Durham, Durham, UK, 20th-22nd March 2011.

Kober O., Jeffers F., Wakenshaw L., Hemmings A., MacKenzie D., Juge N**.** *Functional modulation of the murine mucus layer by gut bacteria*. British Society for Immunology Annual Congress, Arena and Conference Centre, Liverpool, UK, 6th-10th December 2010.

Kober O., Wakenshaw L., Holm L., Carding SC., Juge N. *Functional modulation of the murine mucus layer in response to gut bacteria.* IFR Student Science Showcase, Institute of Food Research, Norwich, UK, 6th May 2010.

Acknowledgements

This PhD was supported by a four-year Biotechnology and Biological Sciences Research Council (BBSRC) Doctoral Training Grant award to the Institute of Food Research.

The first big thank you goes to my supervisors Dr Nathalie Juge and Prof Simon Carding, for supporting me throughout my PhD. Particular thanks go to Nathalie for her inexhaustible time and effort put in during the writing phase of my thesis.

A second thank you goes to everyone who has helped and been involved in my PhD work throughout the four years, particularly Dr Louise Wakenshaw who was a big support during my first two years. This thank you to all extends beyond the work of this PhD, as I have thoroughly enjoyed my life in Norwich during these years.

A huge thank you goes to Alex, who has provided lots of laughter and support during my PhD. You have my eternal gratitude for: being you. Being there. Being amazing.

Finally I would like to thank my examiners Prof Dirk Haller and Dr Claudio Nicoletti for kindly agreeing to read and discuss my work with me.

I would like to dedicate this thesis to my amazing parents. It is through their continuous love and support that I arrived at the stage where I had the option of doing a PhD. Importantly; my parents introduced me to the feel-good movie “The Best Exotic Marigold Hotel”, which taught me a saying that got me through my PhD:

“Everything will be all right in the end…if it’s not all right, then it’s not yet the end.”

Table of contents

List of Figures

List of Tables

Abbreviations

AFM	atomic force microscopy
AhR	aryl hydrocarbon receptor
AMPs	antimicrobial peptides
aRNA	antisense RNA
BabA	blood group antigen-binding adhesin
Benzyl-α-GalNAc	benzyl 2-acetamido-2-deoxy-α-D-galactopyranoside
BSA	bovine serum albumin
CD	Crohn's disease
Cd	cytoplasmic domain
cDNA	complementary deoxyribonucleic acid
Cdx	caudal-related
CF	cystic fibrosis
CFU	colony forming units
CK	cysteine-knot
Clca	calcium-activated chloride channel regulator
CNA	cyanoacetamide
CnBP	collagen binding protein
CT	cytoplasmic tail
DAB	3, 3'-diaminobenzidine
DAI	disease activity index
DAPI	4',6-diamidino-2-phenylindole
DC	distal colon
DCs	dendritic cells
ddH_2O	double distilled water
DMEM	Dulbecco's Modified Eagle's Medium
DNA	deoxyribonucleic acid
DNMTs	DNA methyltransferases
DSS	dextran sodium sulphate
DTT	dithiothreitol
EDTA	ethylenediaminetetraacetic acid

ELISA	enzyme linked immunosorbent assay
ER	endoplasmic reticulum
FAE	follicle-associated epithelium
Fcgbp	fc-gamma binding protein
FCM	flow-cytometry
FCS	foetal calf serum
FITC	fluorescein isothiocyanate
FPLC	fast protein liquid chromatography
Gal	galactose
GalNAc	N-acetylgalactosamine
GALT	gut-associated lymphoid tissue
GI	gastrointestinal
GlcNAc	N-acetylglucosamine
GTs	glycosyltransferases
GuHCl	guanidium chloride
GWAS	genome-wide association study
h	hour(s)
H&E	haematoxylin and eosin Y
HCl	hydrochloric acid
HDACs	histone deacetylases
HI	heat inactivated
HMOs	human milk oligosaccharides
HNF	hepatocyte nuclear factor
HT29-MTX	HT29-methotrexate
IBD	inflammatory bowel disease
IECs	intestinal epithelial cells
IELs	intraepithelial lymphocytes
IF	immunofluorescence
IgA	immunoglobulin A
IL	interleukin
iNOs	inducible nitric oxide synthase
ITF	intestinal trefoil factor
IVT	*in vitro* transcription
kDa	kilo Dalton
KGF	keratinocyte growth factor

LAB	lactic acid bacteria
LDS	lithium dodecyl sulphate
LPS	lipopolysaccharide
LspA	*Lactobacillus* surface protein A
MAA	*maackia amurensis*
MAMPs	microbe-associated molecular patterns
MC	mid colon
MHC	major histocompatibility complex
min	minute(s)
MLN	mesenteric lymph nodes
moDCs	monocyte-derived dendritic cells
MOPS	3-(N-morpholino)propanesulphonic acid
mRNA	messenger ribonucleic acid
MRS	Man, Rogosa and Sharpe
MS	mass spectrometry
MUB	mucus binding protein
MUC	mucin
MW	molecular weight
Neu5Ac	sialic acid
NF-κB	nuclear factor kappa-light-chain-enhancer of activated B cells
NK	natural killer
nNOs	neuronal nitric oxide synthase
NO	nitric oxide
NOS	nitric oxide synthase
NSAIDs	non-steroidal anti-inflammatory drugs
O/N	overnight
PAS/AB	periodic acid Schiff/alcian blue
PBS	phosphate buffered saline
PBS-T	phosphate buffered saline-Tween 20
PCR	polymerase chain reaction
PFA	paraformaldehyde
PG	prostaglandin
PGN	peptidoglycan
pIgR	polymeric immunoglobulin receptor
PNA	peanut agglutinin

PRRs	pattern recognition receptors
PTS	proline, threonine and serine repeats
PVDF	polyvinylidene fluoride
qRT-PCR	quantitative reverse transcription polymerase chain reaction
Rh	rhodamine
RNA	ribonucleic acid
RNase	ribonuclease
RT	room temperature
s	second(s)
SabA	sialic acid-binding adhesin
SasA	*Staphylococcus aureus* surface protein A
SCFAs	short chain fatty acids
SDS-PAGE	sodium dodecyl sulphate polyacrylamide gel electrophoresis
SEA	sea-urchin sperm protein, enterokinase and agrin
Ser	serine
SI	small intestine
SL	sialyllactose
SNA-I	*sambuccus nigra*
SP	sodium periodate
SPF	specific pathogen-free
SPR	surface plasmon resonance
STs	sialyltransferases
T/E	trypsin EDTA
TA	transit amplifying
TFF3	trefoil factor 3
Thr	threonine
TJs	tight junctions
TLRs	toll like receptors
TNB	tris NaCl blocking buffer
TNF	tumour necrosis factor
TR	texas red
UC	ulcerative colitis
UPR	unfolded protein response
VNTR	variable number of tandem repeat
vWF	von Willebrand Factor

WGA	wheat germ agglutinin
wt	wild type
wt/vol	weight per volume
Zg	zymogen granulae

Chapter 1 Introduction

1.1 Structure and function of the vertebrate gastrointestinal (GI) tract

The human gastrointestinal (GI) tract is a system of organs that performs the functions of ingestion, digestion, absorption and defecation. While these functions render the GI tract a highly dynamic environment, factors such as temperature, regional pH, peristalsis and microbial biomass remain continuous. The GI tract can anatomically be divided into the upper GI tract (mouth, pharynx, oesophagus, stomach, and duodenum), and the lower GI tract (small intestine (SI), large intestine (colon) and anus) (Figure 1.1). The ~400 m^2 surface of the adult human GI tract [1] is covered in mucus that is colonised by bacteria soon after birth.

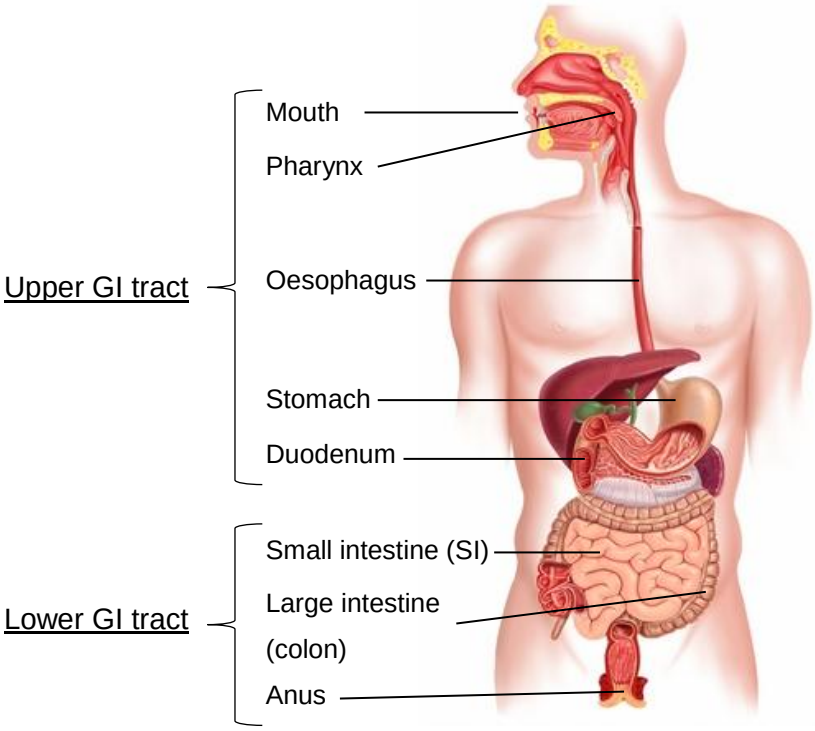

Figure 1.1| Anatomy of the human GI tract. Shown are the upper and lower GI tract with their respective organ constituents [2].

The intestinal epithelium is the most rapidly self-renewing tissue in adult mammals and forms a single-cell layer covering the length of the GI tract (Figure 1.2). It forms the

largest mucosal surface in the human body to create a barrier between the host, the bacteria residing in the GI lumen (microbiota) and luminal contents. While serving to absorb essential nutrients, the epithelium also functions to eliminate harmful pathogens that attempt to invade the underlying tissue. The intestinal epithelium is critically involved in the maintenance of intestinal immune homeostasis by providing a dynamic physical barrier between immune cells and the commensal bacteria, as well as by expressing antimicrobial peptides (AMPs) such as RegIIIγ (Figure 1.2).

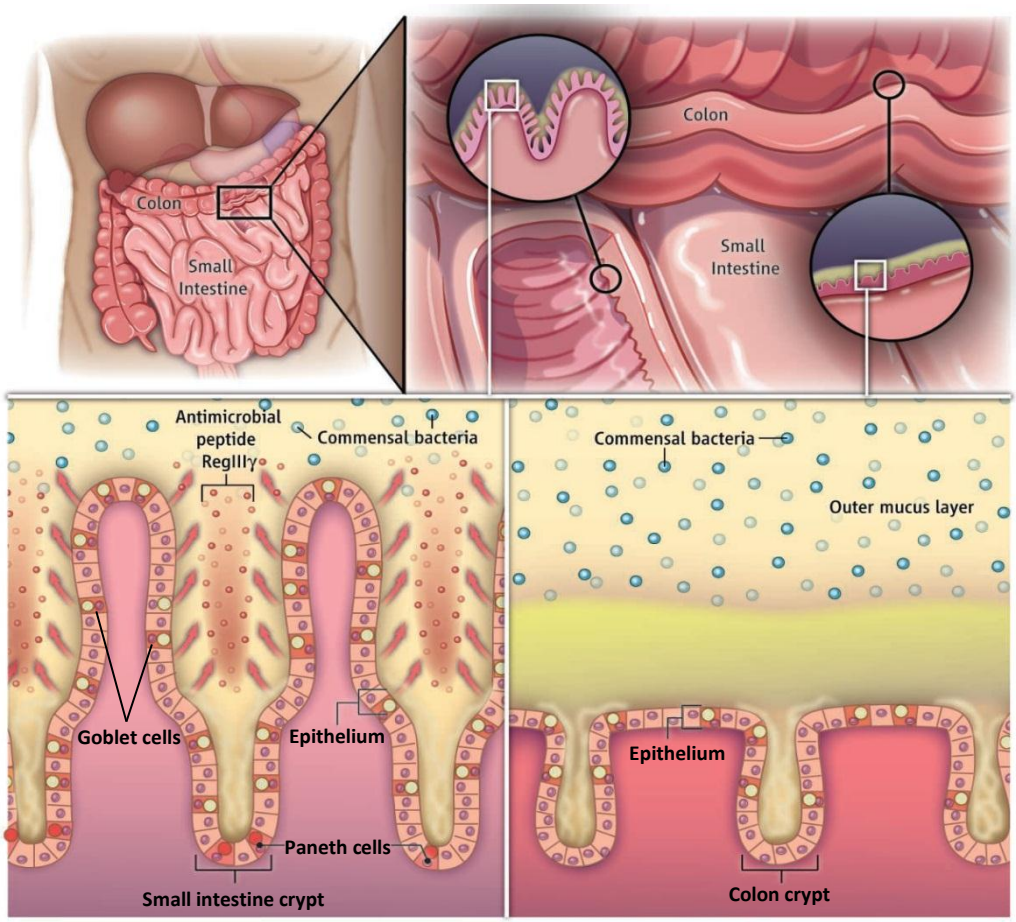

Figure 1.2| Structure of the human lower GI tract. Shown is the SI and colon epithelium with its protective features [3].

The colonic epithelium is a dynamic barrier that is in constant flux [4] and has a well-defined architecture. The colonic mucosa forms invaginations known as crypts of Lieberkühn (Figure 1.3), embedded in connective tissue, whose folding nature provides

a large surface area for maximal absorption. Colonic crypts are composed of four different cell types, namely enterocytes, mucus-secreting goblet cells, stem cells and endocrine cells (Figure 1.3).

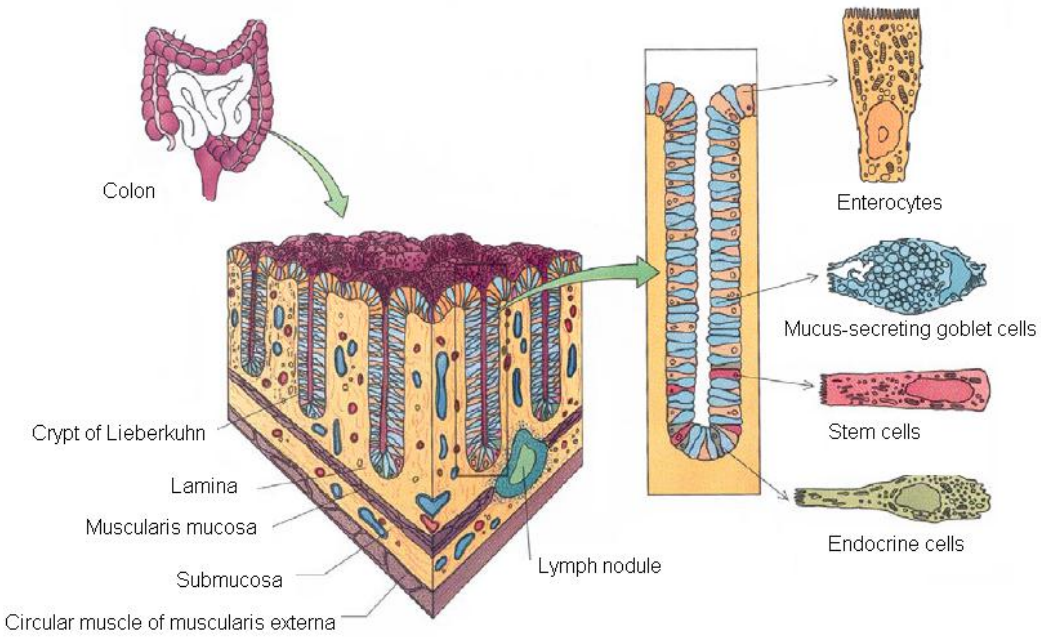

Figure 1.3| Diagrammatic representation of the colon wall and a colonic crypt. Shown are the different wall components in the colon, and one interpretation of the position of the stem cells together with the other differentiated cell types in the colonic crypt [5].

Paneth cells are absent in the colon, but can be found in SI crypts. The epithelium of the murine SI renews every three to five days [6], with the exception of stem cells, which are pluripotent undifferentiated cells with the potential to self-renew, and Paneth cells [7]. Stem cells and their transit-amplifying (TA) daughter cells reside in the intestinal crypts [8]. While enterocytes predominate on the luminal surface, mucus-secreting goblet cells are abundant in the crypt [9]. In the human SI, intestinal epithelial cells migrate from the base of the crypt to the villi where approximately 10^{10} cells are shed per day [10, 11]. The mechanism of cell shedding is central as abundant shedding must be achieved without a loss of intestinal barrier function. 5.3 % of villus sections contain a shedding cell, with an eosin-positive gap, devoid of cellular contents,

often seen within the epithelial monolayer beneath shedding cells [12, 13]. Furthermore, cells always undergo apoptosis during ejection from the monolayer [12].

1.2 The mammalian GI mucus layer

Overlying intestinal epithelial cells (IECs) is the transparent mucus layer that forms a separation between the lumen and the host. The mucus layer serves to lubricate the mucosal surface, to protect underlying IECs from chemical and mechanical stress and bacteria, and as a transport medium between luminal contents and epithelial cells. Furthermore, it provides an habitat for commensal bacteria and signals to the underlying immune system.

The understanding of the biological role of mucus has been limited due to experimental difficulties resulting from the large, oligomerised and highly glycosylated nature of mucins. Conventional tissue fixation methods cross-link proteins and cause the mucus layer to collapse, thus appearing as a thin film in stained tissue sections. Water-free Carnoy fixative is believed to conserve the mucus layer and provide results that are comparable with *in vivo* mucus thickness measurements [14, 15]. However, this approach has been difficult to replicate. To date three approaches are used to study mucus synthesis and secretion. In the human colon, [^{3}H] glucosamine incorporation in cultured specimens has been used [16-18]. A major breakthrough in mucus studies was the development of an *in vivo* mucus thickness measurement system in anaesthetised rodents [19]. The third and most recent approach uses *ex vivo* mouse and human colon, and mouse SI, to measure mucus adhesion, properties, thickness and growth [20].

1.2.1 Structure and organisation of the mammalian GI mucus layer

In the colon, the mucus layer overlying the IECs is composed of two layers; a firm inner layer that cannot be detached, and a loose outer later that can easily be removed by peristalsis and suction [20, 21]. Due to the similarities in the mucin and protein components of these two layers, it is most likely that the loose outer mucus layer is

formed from the firm inner mucus layer. Findings that bacteria produce proteases capable of disrupting the polymeric network of the inner mucus layer [22, 23] may indicate that bacteria play a role in the formation of the loose layer. In the colon, the firmly-attached stratified inner layer has been shown to exclude a majority of the bacteria, while the loose outer layer serves as a habitat for some intestinal commensal microbiota [24-26] (Figure 1.4A & 1.4B). The firm mucus layer is insoluble in the chaotropic salt guanidium choride (GuHCl), a property that may be a reflection of its function as a bacterial barrier [25]. The type of mucus that covers the SI, unlike the colon, is composed of a thinner single layer that is not attached to the epithelium and is permeable to bacteria [26, 27]. Mucus layer differences in the different GI tract locations suggest a functional organisation of the intestinal mucus barrier, where the SI has a loose and penetrable mucus that allows easy penetration of nutrients in contrast to the stomach where the mucus provides physical protection, and to the colon where the mucus separates bacteria from the epithelium [26]. A compact inner mucus layer in the SI would be detrimental to its primary function of nutrient absorption.

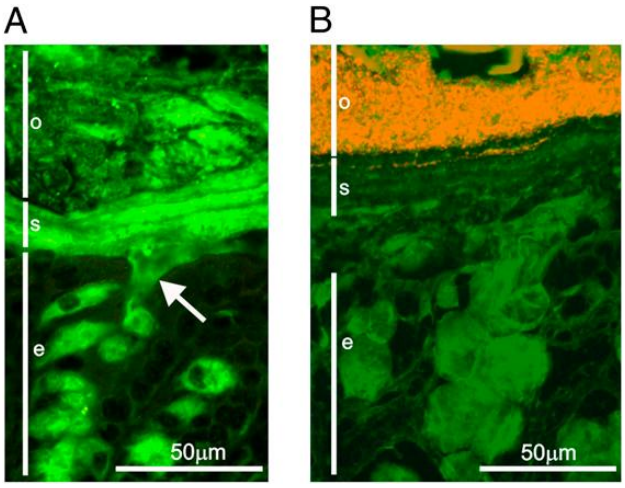

Figure 1.4| Molecular organisation of the intestinal mucus layer. The colonic mucus (green) layer overlying the epithelium (*e*) is composed of a stratified inner layer (*s*) and an outer layer (*o*) (A). *O* provides a habitat for bacteria (red), whereas *s* excludes a majority of bacteria (B), as identified by 16S rRNA FISH staining [21].

The thickness of the mucus layer varies along the GI tract (Figure 1.5), correlating with the microbial burden found in the respective GI regions [28]. In humans, the colonic mucus is thickest in the rectum, reaching up to 284.5 µm, and thinnest in the caecum [29]. *In vivo* mucus thickness measurements revealed that the mean mucus thickness in the colon of rats is 830±110 µm, and that the loose mucus layer performs a rapid regeneration following its removal by suction [19]. An *ex vivo* explant model confirmed a similar mucus thickness in mouse and human tissue, as previously reported *in vivo*, and represents the first study measuring mucus growth as a function of time in live human colon tissue [20]. Mucus regeneration and growth was observed in human (240 µm/h) and mouse (100 µm/h) colon but not in mouse ileum [20].

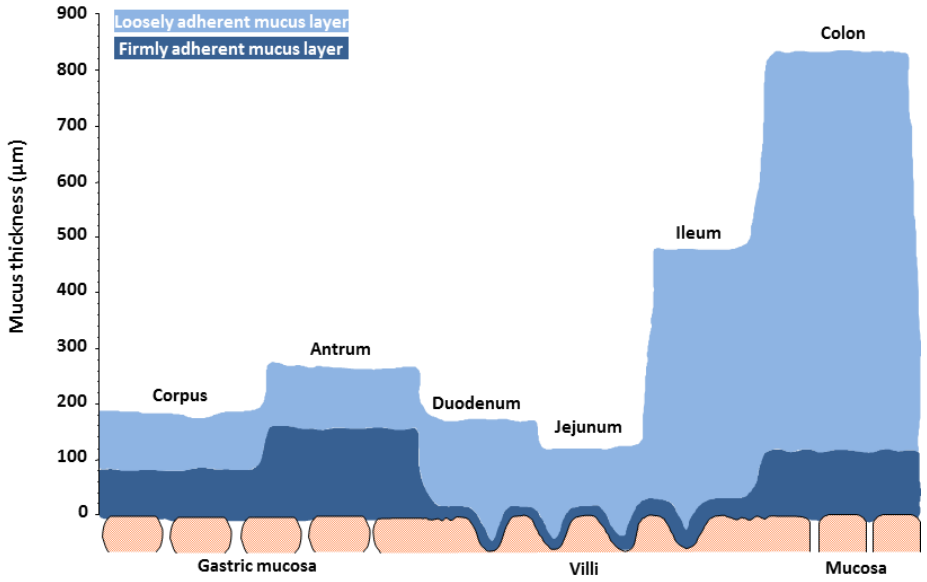

Figure 1.5| Schematic representation of mucus thickness along the GI tract. The *in vivo* thicknesses of the loose and firm mucus layers are shown in the corpus, antrum, mid-duodenum, proximal jejunum, distal ileum and proximal colon of the rat GI tract [19].

The recent discovery of the molecular organisation of the two mucus layers has renewed interest in mucus research, with the potential of elucidating further defence mechanisms of the mucosal immune system. While the IECs with their tight junctions (TJs) were seen as the body's main defence mechanism against opportunistic bacteria

and pathogens, new research may reveal a more important role of mucus than previously anticipated.

1.2.2 Composition of the mammalian GI mucus

Mucus has a high water content and is mainly composed of mucins, but is also made up of a wide variety of non-mucin proteins that are thought to contribute to mucus defense. Non-mucin proteins present in mucus include secretory immunoglobulin A (IgA), lysozyme, defensins and β-galectins. Mucus provides a matrix for AMPs and IgA secreted by IECs, which together restrain and separate commensal bacteria from the epithelial surface [30] (Figure 1.6). AMPs are produced in the SI by Paneth cells and include α-defensins, lysozymes, collectins, histatins and lectins such as RegIIIγ [31, 32]. IgA is the dominant antibody produced in mammals, mostly secreted across mucus-covered membranes, especially in the intestine. The production of IgA is principally initiated in organised lymphoid tissues referred to as Peyer's patches (PPs), where antigen is sampled, processed and presented by dendritic cells (DCs) to activate T cells, which ultimately leads to the development of IgA-producing plasma B cells in the lamina propria [33-35]. This plasma B cell-produced IgA is secreted into the inner and outer mucus layer [25, 36-38]. In mucosal secretions, IgA exists as a complex made of polymeric IgA in association with the secretory component (SC), called sIgA [39]. sIgA is formed from the cleavage from the polymeric immunoglobulin receptor (pIgR), expressed on the basolateral surface of epithelial cells, which ensures the transport of the immunoglobulin across the epithelium [39]. Secretory antibodies influence the commensal microbiota and contribute substantially to the capacity of the mucus to retain and clear potential pathogens [36, 38]. IgA fulfils a neutralising function by clearing potential pathogens at the epithelial interface [40, 41].

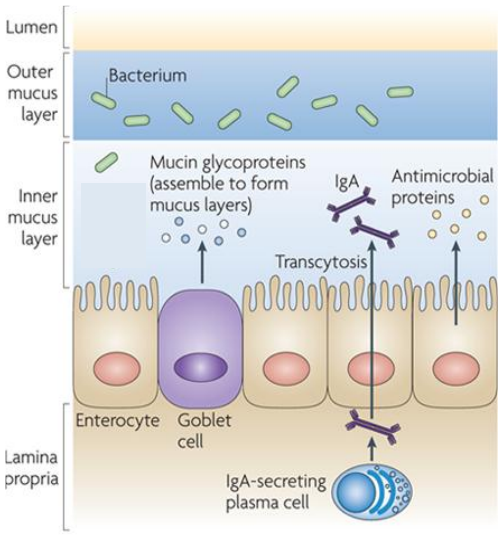

Figure 1.6| Composition of the intestinal mucus layer. The inner mucus layer is composed of mucin glycoproteins, antimicrobial proteins and immunoglobulin A (IgA) to maintain an environment that mainly excludes bacteria (adapted from [42]).

The analysis of the protein composition of the two mucus layers in mouse colon identified more than 1000 proteins, a majority of which had an intracellular origin [43]. Among these, the Fc-gamma binding protein (Fcgbp), zymogen granulae protein (Zg) 16 and calcium-activated chloride channel regulator (Clca) 1 were found strongly associated with Muc2 mucin, suggesting that these may aid in the stabilisation of this mucin [43]. Proteome analysis of the mucin granulae identified two further mucus vesicle-associated proteins (ATPase H^+-transporting lysosomal accessory protein 2 (ATP6AP2) and extended-synaptotagmin 2 (E-Syt2/FAM62B)) as novel potential actors in mucin vesicle secretion [44]. More recently, mucus composition was described not only in the colon, but along the whole length of the GI tract [45], confirming that this association with Muc2 mucin is extensible to the rest of the intestine, from stomach to colon. In light of Muc2 mucin being the major scaffold of intestinal mucus, this association of proteins with Muc2 mucin may suggest their involvement in mucus formation.

1.2.2.1 Mucins

Mucins (MUC for humans and Muc for other species) belong to a family of high-molecular-mass glycoproteins identified as the major structural components of mucus [46, 47]. All mucosal surfaces of the body comprise mucins, with the exact composition of the mucus layer relating to the demands of organ function. To date, twenty-two human mucins have been identified and can be classified into two categories on the basis of their structural characteristics: the secreted mucins, which can be further categorised into gel-forming (MUC2, MUC5AC, MUC5B, MUC6 and MUC19) and non-gel-forming (MUC7, MUC8 and MUC9), and membrane-bound mucins (MUC1, MUC3A, MUC3B, MUC4, MUC10, MUC11, MUC12, MUC13, MUC15, MUC16, MUC17, MUC18, MUC20 and MUC21) [48]. For the majority of these mucins, homologues have been identified in rats and mice (Table 1.1). All mucins are involved in mucosal integrity, but the precise function of various secreted and membrane-bound mucins is not yet entirely known.

Table 1.1| Human MUC genes with homologues in rats and mice.

Gene	Function	GeneAtlas location of highest expression	Selected references
MUC1	Cellular signal transduction, barrier activity	Lungs	[49, 50]
MUC2	Primary extracellular matrix constituent in colon, lubricant activity	Colon	[50, 51]
MUC3A	Epithelial cell protection, adhesion modulation, and signalling	Various	[52]
MUC3B	Possibly cellular signal transduction	Various	[52]
MUC4	Intestinal epithelial cell differentiation, renewal, lubrication	Colon	[53, 54]

MUC5B	Primarily lubricant	Various	[55, 56]
MUC5AC	Major airway mucin, Intestinal epithelial cell differentiation	Trachea, Lungs	[57, 58]
MUC6	Unknown, involved in renal morphogenesis processes	Pancreas, GIT, reproductive system	[58-60]
MUC7	Facilitating clearance of oral bacteria	Salivary gland	[61, 62]
MUC12	May be involved in epithelial cell regulation	Colon	[63]
MUC13	Barrier function in epithelial tissues	Pancreas, small intestine, colon	[64]
MUC15	Barrier function in epithelial tissues	Testis Leydig cell	[65]
MUC16	Unknown, plays a role in ovarian cancer	Lymph nodes, respiratory tract	[66, 67]
MUC17	Extracellular matrix constituent, lubricant activity	Small intestine, stomach	[68, 69]
MUC19	Major gel-forming mucin in the human middle ear	Secretory cells of the ears and eyes	[70]
MUC20	Cellular signal transduction	Intestine, respiratory and urinary tract	[71]

1.2.2.2 Mucin glycosylation

Apomucin is the basic structure of a mucin and it is made up of a core protein backbone with numerous O-linked oligosaccharides and N-glycan chains. Tandemly repeated (TR) motifs rich in proline, threonine (Thr) and serine (Ser) residues (PTS) provide potential sites for extensive O-glycosylation [46, 72]. Marked heterogeneity in the apomucin and oligosaccharide side chains and high carbohydrate content are characteristic for mucins [73]. Mucins are decorated with a dense array of complex O-

linked carbohydrates assembled by the sequential action of glycosyltransferases (GTs). The synthesis of mucin oligosaccharides starts with the transfer of N-acetylgalactosamine (GalNAc) to Ser and Thr residues of the mucin core [74]. The oligosaccharides may be extended with galactose (Gal), N-acetylglucosamine (GlcNAc), GalNAc, fucose or sialic acid (Neu5Ac) [75]. These terminal mucin O-glycans have been proposed to serve as preferential binding sites for intestinal bacteria [48]. In human intestinal mucin, sialic acid increases proportionally from the ileum to the rectum, with a reverse gradient of fucose [76, 77]. The O-glycan structures associated with Muc2 showed that the colon is enriched for sulphated residues [78]. Eight core structures of the mucin O-glycan chain have been identified [79] (Figure 1.7).

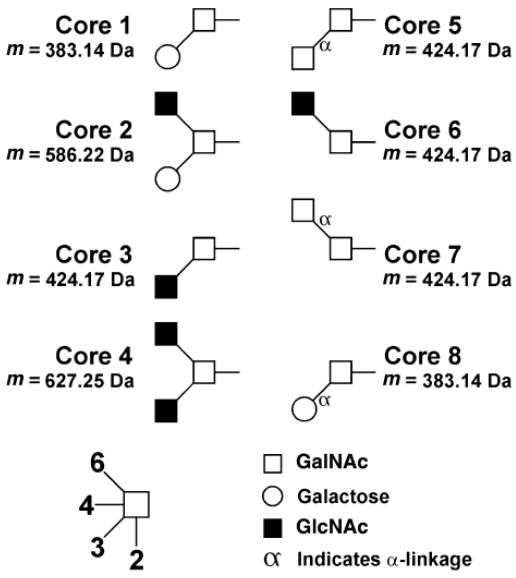

Figure 1.7| The eight different reported core structures of mucin-type O-glycans. The linkage positions are illustrated by the line connecting the monosaccharides, and all linkages not labelled with α are β-anomers. As illustrated, many of the cores have the same mass [79].

The O-glycan structures present in SI and colonic mucins consist predominantly of core 1-4 mucin-type O-glycans containing GalNAc, galactose and N-acetyl-glycosamine [75]. In humans, core-3 and core-4 structures make up the majority of colonic mucin glycans terminated with Neu5Ac [80, 81], whereas murine colonic mucins are instead

characterised by core-1 and core-2 structures with only low amounts of core-3 and core-4 type glycans [82, 83]. In the human SI, the main mucin core structure is core-3, whereas in murine SI mucins core-1 and core-2 glycan structures predominate [77, 84, 85].

1.2.2.3 Mucin biosynthesis and structure

MUC2/Muc2 is the most abundantly expressed secretory mucin in the SI and colon of humans, mice and rats [86], and constitutes the structural component of the mucus layer. Human MUC2 consists of 5,179 amino acids and contains multiple domains arranged in the following order (Figure 1.8): von Willebrand Factor (vWF) D1 domain (D1), D2, D′ and D3, first CysD, small PTS, second CysD, large PTS (tandemly repeated), C-terminal vWF D4, B, C, and a cystine-knot (CK) domain [87].

Figure 1.8| Diagram of the MUC2 protein core. The protein termini contain cysteine-rich regions homologous to von Willebrand Factor (vWF) domains (a); The N-terminal regions of MUC2 proteins contain vWF domain homologues D1, D2, D', and D3 and the C-terminal regions contain vWF domain homologues D4, B, C and CK. These terminal domains are responsible for the extensive polymerisation between mucin monomers, along with the cysteine-rich interruptions between glycosylated tandem repeats (b); The first of the two repetitive domains (c) contains 21 repeats of an irregular motif, whereas the second domain (d) is formed of 50-115 tandem 23 aa motifs (PTTTPITTTTTVTPTPTPTGTQT). Threonine in the repeats are O-glycosylated, forming a densely packed envelope of short branched carbohydrate chains surrounding these regions (adapted from [88]).

During biosynthesis, the primary translational product of full-length MUC2 is quickly dimerised in the endoplasmic reticulum (ER) via disulphide bonds in the CK domain

[89]. The dimers pass through the Golgi apparatus, where the two PTS domains become *O*-glycosylated to form the two mucin domains. In the trans-Golgi network, the glycosylated dimers are then trimerised by disulphide bonding in the vWF D3 [90]. Figure 1.9 shows a schematic representation of the MUC2 mucin with its adopted net-like sheet structure, in comparison with the membrane-tethered MUC1 mucin. During unpacking the MUC2-N ring structure is disrupted, and the mucin domains begin to separate. The net is formed by N-terminal vWF D3 disulphide-linked trimers and C-terminal disulphide-linked dimers of the CK domains.

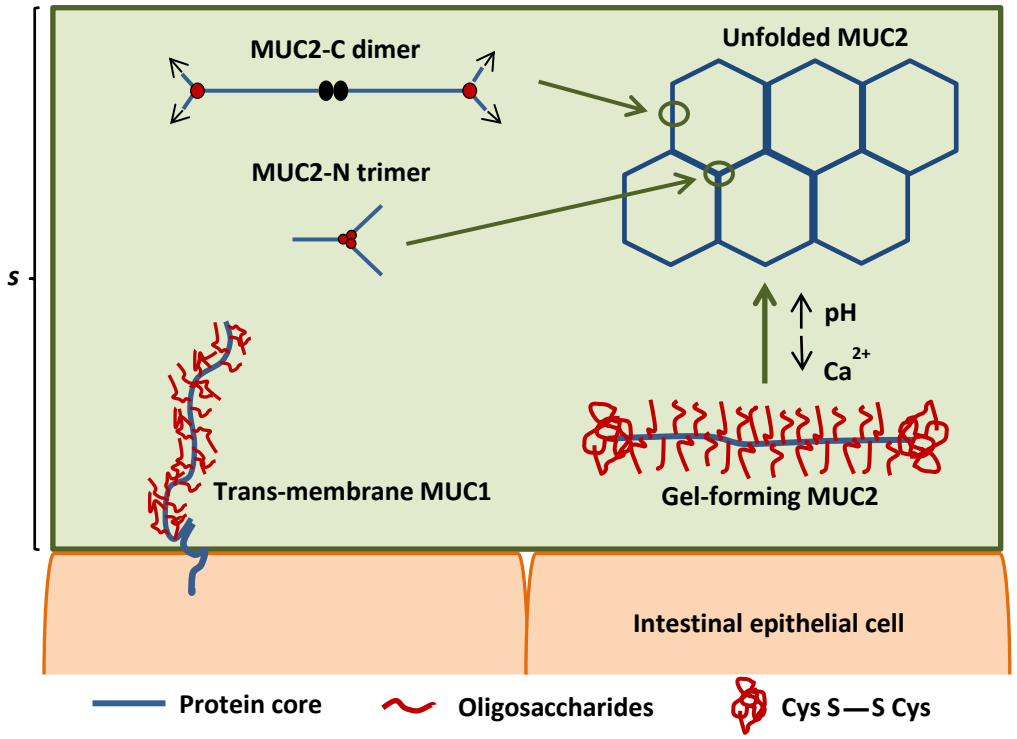

Figure 1.9| Schematic representation of the intestinal membrane-bound and gel-forming mucins. Shown are the mucin protein cores (*blue*) with their associated oligosaccharides (*red*) in the stratified inner mucus layer (*s*). The net-like sheet structure adopted by MUC2 is composed of trimeric disulphide-linked MUC2-N in the sheet corners and dimeric MUC2-C along the sides (adapted from [27]).

MUC1 is the most extensively studied membrane-bound mucin and is the most ubiquitously expressed mucin across all mucosal surfaces (Figure 1.10). Membrane-

bound mucins, such as MUC1 and MUC3, cover the apical surface of mucosal epithelial cells and contain large extracellular variable number of tandem repeat (VNTR) domains predicted to form rigid extended structures [91]. The cytoplasmic domain (Cd) is anchored into the epithelial cell membrane and appears to interact with the cytoskeleton and secondary signalling molecules [92-94]. A series of studies have demonstrated a diverse role of the Cd of MUC1 in intracellular signalling, with potential roles in the physiology of malignant and non-malignant cells; MUC1 Cd phosphorylation via kinases and cell-surface growth factor receptors variously alters the interactions of MUC1 with other proteins such as β-catenin and heat shock protein 90 kD [91, 95-98]. Such interactions are required for the movement of MUC1 Cd to the nucleus or mitochondria, where MUC1 is involved in activating β-catenin-responsive genes and contributing to the resistance to apoptosis and killing by anti-tumour drugs [99-101]. The enormous extracellular mucin domain, ranging from one million up to more than ten million Da in mass [27], interacts with extracellular matrix components and other cells [102-106]. During synthesis most membrane-bound mucins are cleaved in the sea-urchin sperm protein, enterokinase and agrin (SEA) module, and remain non-covalently associated through biosynthesis [107, 108]. The extracellular subunit can be shed from the cell surface via cleavage [109, 110] or physical shear forces [108].

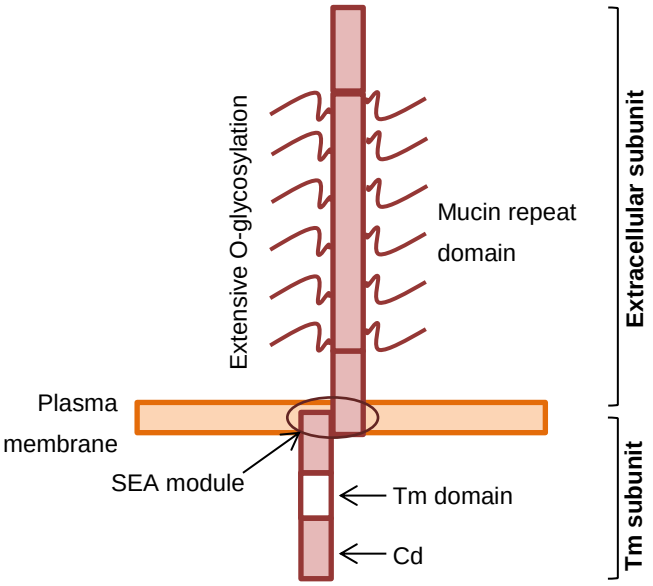

Figure 1.10| Diagram of the MUC1 domain organisation. The trans-membrane (Tm) MUC1 mucin is cleaved in the sea-urchin sperm protein, enterokinase and agrin (SEA) module, in the endoplasmic reticulum (ER), to form an extracellular subunit and a Tm subunit. The extracellular VNTR domain is heavily O-glycosylated, and the complex cytoplasmic domain (Cd) is involved in intracellular signal transduction (adapted from [111]).

1.2.3 Functional importance of mucus in health and disease

Historically, mucus has been associated with protection, lubrication and hydration of the intestinal epithelial layer. Today, the mucus layer is known to play a role in the maintenance of intestinal homeostasis and microbial interactions. The involvement of mucins in epithelial cell renewal and differentiation, cell signalling, and cell adhesion suggests that the aberrant expression or secretion of mucins may impact on IEC function and immune signalling. Indeed, patterns of mucin expression are altered in inflammatory bowel diseases (IBD), cancers and infection [111, 112]. IBD is a collective term for chronic relapsing inflammatory conditions occurring in the GI tract [113, 114]. Crohn's disease (CD) and ulcerative colitis (UC) are two complex forms of IBD. CD and UC show a similar prevalence of 100-150 per 100,000 individuals of European ancestry [115], but show biological differences; CD is a T helper 1-driven disease that can affect

any region of the intestine, whereas UC is a T helper 2-driven disease where inflammation is limited to the colonic mucosa [114, 116, 117]. Like most complex diseases, CD and UC result from a combination of genetic and non-genetic risk factors. An imputation-based association analysis using autosomal genotype-level data from fifteen genome-wide association studies (GWAS) of CD and/or UC identified 163 IBD loci, 71 of which are novel associations [118]. Of these, 110 loci are shared between DC and UC, while 30 loci are classified as CD-specific and the remaining 23 loci as UC-specific. Interestingly, risk alleles at two CD risk loci showed protective effects in UC, which may be a reflection of the biological differences between these two diseases [118]. Of interest here is the association of coding variants in MUC19 with IBD [119]. Alterations in mucin expression, maturation and secretion commonly occur in both CD and UC.

1.2.3.1 Impact of mucus thickness on barrier permeability

Cystic fibrosis (CF) lung disease is caused by mutations in the cystic fibrosis transmembrane conductance regulator (*CFTR*) gene and is the most common genetic form of chronic obstructive pulmonary disease (COPD) [120]. A key element of both chronic and obstructive lung disease, and CF, is the overproduction of mucins in the lungs [121]. The mucus layer of patients with active UC is often thinner and more discontinuous [122]. In the healthy colorectal epithelium MUC2 is abundantly expressed in bulky apical granules of the goblet cells [123]. A complete disappearance of MUC2 has been observed in CD lesions [124]. The causality of this effect has been investigated using mice deficient in Muc2 ($Muc2^{-/-}$), which develop spontaneous chronic intestinal inflammation [125]. $Muc2^{-/-}$ mice show an increase in lymphocyte infiltration, significant growth retardation, failure to gain weight, and develop gross rectal bleeding that is not observed in $Muc2^{+/+}$ or $Muc2^{+/-}$ mice [125]. Increased proliferation and survival of epithelial cells in $Muc2^{-/-}$ mice may be a direct consequence of the exposure of IECs to the luminal contents [126]. The finding that $Muc2^{-/-}$ mice have bacteria in direct contact with the epithelium (Figure 1.11A), and far down the crypt, with inflammation and cancer development [25], supports the proposed protective role of MUC2 in barrier function.

The dextran sodium sulphate (DSS) model of experimental colitis is one of the most widely used animal models of colitis [114]. Exposure of mice to DSS shows that the firm inner mucus layer is no longer free from bacteria, compared to control mice not treated with DSS (Figure 1.11B) [127]. After 24 h of DSS-treatment, the inner mucus layer has largely disappeared, completely losing its organisation after 120 h of DSS-treatment (Figure 1.11B), indicating that alterations in the mucus layer contribute to the colitis phenotype induced by DSS.

These studies indicate the importance of a functional mucus layer in maintaining an homeostatic relationship with the microbiota and protecting the underlying epithelium.

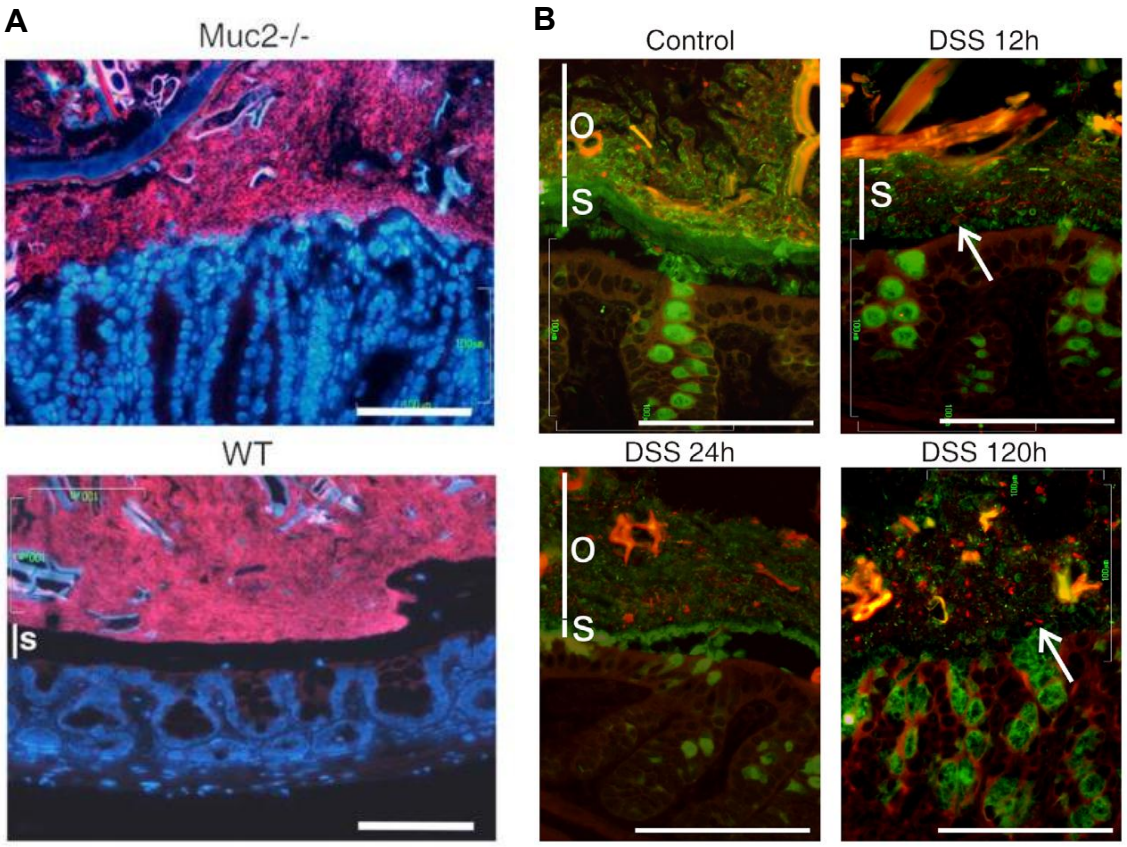

Figure 1.11| Functional importance of mucus. FISH using the EUB338-Alexa Fluor 555 probe (staining bacteria), and DAPI (DNA staining) in the colon show a clear separation of the bacterial DNA and the epithelial surface in WT mice, but not $Muc2^{-/-}$ mice. This separation corresponds to the stratified mucus layer (s) (A). Localisation of bacteria in the colon mucus of mice after DSS treatment for 12, 24, and 120 h, or in untreated control (control). The EUB338-Alexa Fluor 555 probe and anti-Muc2 specific antiserum were used to monitor bacterial penetration and loss of mucus organisation (B). Stratified inner layer (s); outer layer (o); scale bars 50 µm (A), 100 µm (B) (adapted from [25, 127]).

1.2.3.2 Impact of differential mucin expression and glycosylation

In humans, the membrane-bound mucin gene cluster has been implicated in genetic susceptibility to IBD [128]. Ectopic expression of the gastric mucins MUC5AC and MUC6 have been observed in CD, suggesting a role of these mucins in wound healing in addition to their protective function [124]. Upregulation of MUC2 transcription in mucinous carcinoma is caused by altered epigenetic and genetic regulation of MUC2,

such as MUC2 promoter hypomethylation [129]. MUC1 is overexpressed and profoundly hypo-glycosylated in the majority of human adenocarcinomas and their precursor lesions [123], including human IBD [130]. Muc1$^{-/-}$ mice have a thinner inner mucus layer that cannot be removed by suction [131], demonstrating that Muc1 is involved in the regulation of mucus amount and mucus formation, but does not contribute to the attachment of the gastric mucus layer. Muc13 and Muc17 mucins are the main membrane-bound mucins expressed in the intestine under normal physiological conditions [27, 112]. Mice deficient in cell-surface Muc13 develop more severe acute colitis in response to DSS treatment [132]. Muc17 expression is lost in inflammatory, and early and late neoplastic conditions in the colon [133].

Deficiency in the cell-surface Muc1 predisposes mice to intestinal infection with the GI pathogen *Campylobacter jejuni* (*C. jejuni*) [134] and the gastric pathogen *Helicobacter pylori* (*H. pylori*) [135], indicating that Muc1 on the mucosal surface forms a crucial element in the protection against these pathogens. In *H. pylori* infection Muc1 acts by steric hindrance, physically distancing the bacteria from the host cell, and by a release decoy through the detachment of the extracellular domain, preventing prolonged adhesion. Furthermore, Muc1 coating of *H. pylori* via its adhesins Blood group Antigen Binding Adhesin (BabA) and Sialic Acid Binding Adhesin (SabA), limits anchorage to the epithelium by blocking these key adhesins [136]. Infection with the attaching and effacing bacterial pathogens Escherichia coli (E. coli) and Citrobacter rodentium (C. rodentium) causes a dramatic goblet cell depletion in mice, and Muc2 production was shown to be critical for host protection during such infections, by limiting overall pathogen and commensal numbers associated with the colonic mucosal surface [137, 138]

Mucin glycosylation changes have been reported to coincide with inflammation in acute infection and IBD [139]. Alterations in mucin glycosylation cause a defective mucus barrier with increased permeability and susceptibility to DSS-induced colitis [127]. Loss of core-1-derived O-glycans in C1galt1$^{-/-}$ mice causes the rapid induction of severe spontaneous colitis that closely resembles human UC; dramatic thinning and increased permeability of the inner mucus layer [140, 141]. Similarly, mice lacking core-2 β1,6-*N*-acetylglucosaminyl-transferase demonstrate increased intestinal permeability and increased susceptibility to DSS-induced colitis [142]. Mice lacking core-3 β1,3-*N*-acetylglucosaminyl-transferase with defective O-glycans, causing decreased Muc2

synthesis, increased intestinal permeability and susceptibility to DSS-induced colitis [143].

Together these findings indicate that mucins are active participants in the disease pathogenesis that with inappropriate expression or function can perpetuate chronic inflammation and also help drive cancer development. However whether alterations in mucins are a primary contributor to the disease cause or a consequence of inflammation, and whether the effect is direct or indirect, is currently under investigation.

1.2.4 Mechanisms of mucin regulation

The regulation of mucins in normal and pathological states is influenced by an elaborate signalling network initiated by environmental cues, immune cells, and IECs. A large number of biologically active molecules, such as cytokines, growth factors, bacterial products, and other factors, including pH and calcium (Ca^{2+}) concentration, have been shown to regulate mucin synthesis (*in vitro* and *in vivo*) in IECs.

The pH along the secretory pathway shifts gradually, from 7.2 in the ER to 6.0 in the trans-Golgi network and to 5.2 in the secretory granulae, at the same time as the intragranular Ca^{2+} concentration increases. The correct packing and expansion of MUC2 requires an increase in pH and Ca^{2+} removal [144]. The understanding of the packing and release of mucins has important medical implications, such as in cystic fibrosis. Because a correct expansion requires a fast pH increase and Ca^{2+} removal, HCO_3^--containing natural buffers, which fulfil both demands, are likely to be crucial. For example, the cystic fibrosis conductance regulator channel secretes HCO_3^- and is required for intestinal mucus release [145-147]. Lower amounts of HCO_3^- present during mucus secretion would potentially slow down and stop expansion, due to the MUC2 N-terminal rings still being intact. This may cause the viscous mucus phenotype of the disease cystic fibrosis.

When the pH in the gastric lumen is acidic, the mucus layer is important for establishing and maintaining a pH gradient with a neutral pH in the mucus closest to the epithelium. Under normal conditions, the loosely adherent mucus layer of the gastric corpus is not needed for maintaining this neutral pH [148], indicating that the

firmly adherent mucus layer is more important in protecting the gastric mucosa from corrosive acid. The loosely adherent mucus layer has other functions, such as binding luminal noxious agents, binding swallowed nitrite, and continuously releasing nitric oxide (NO) [149]. Prostaglandins (PGs) are important in gastric mucosal protection, and the severe GI side effects of non-steroidal anti-inflammatory drugs (NSAIDs) have to some extent been attributed to the inhibition of the PG-synthesising enzymes and concomitant reduced gastric mucus thickness [150, 151]. In addition, *in vitro* studies have reported that PGE_2 and NO stimulate mucus secretion and that the mucus layer can be altered, such as by a reduction in mature mucin glycosylation, by proteases originating from enteric parasites [23, 152-155]. In rats, application of luminal PGE_2 increased total mucus accumulation rate more than four times compared with control rats, and was shown to be due to increased accumulation of both the firm and the loose mucus layers [131]. NO present in the gastric mucosa can be either nitric oxide synthase (NOS)-derived or generated non-enzymatically in the gastric lumen [156, 157]. Luminal NO stimulation results in an amplified total mucus accumulation rate, compared with untreated rats and mice, and occurs due to increased growth of the firm mucus layer but not an increase in the loose mucus layer [131]. Neuronal nitric oxide synthase (nNOS) is found in the gastric surface mucus cells and has previously been suggested to be involved in mucus secretion [153, 158, 159]. Inducible NOS (iNOS)-derived but not nNOS-derived NO increases mucus accumulation [131]. Furthermore, a new gastroprotective role for iNOS is shown through iNOS-deficient mice, which have a thinner firmly adherent mucus layer and a lower mucus accumulation rate [131].

Cytokines are products of immune cells that are pivotal to important pathophysiological processes, including inflammation. For example, interleukin (IL)-10 contributes to maintaining intestinal homeostasis by suppressing pro-inflammatory cytokine production [160-162]. In case of Muc2 deficiency, anti-inflammatory IL-10 can control epithelial damage to a limited extent [163]. Furthermore, studies using Muc2/IL-10 double knock-out (DKO) mice demonstrate that combined abnormalities in immunoregulatory and epithelial factors greatly accelerate and exacerbate colonic inflammation [163]. Tumour necrosis factor (TNF)-α, interferon (IFN)-γ and IL-6 are significantly upregulated systemically in the Muc2/IL-10 DKO at 5 weeks of age. These pro-inflammatory cytokines play a pivotal role in the pathogenesis of IBD [160-162].

A further feature of IBD is protein misfolding and endoplasmic reticulum (ER) stress. ER stress is emerging as an important contributor to the pathology observed in IBD [164, 165]. Murine models show that defective protein folding or disruption of the unfolded protein response (UPR) causes ER stress and spontaneous intestinal inflammation [166-171]. IL-10 directly modulates conditions within the ER, regulating MUC2 synthesis and secretion under adverse conditions [155]. Furthermore, IL-10 directly regulates MUC2 synthesis and secretion, and when IL-10 is deficient, MUC2 misfolding, ER stress and activation of the UPR occur [155].

The epigenetic mechanisms of human mucin family genes are gradually emerging. Recruitment of diverse transcription factors to mucin genes results in their epigenetic modification by mechanisms including DNA methylation, histone methylation, and histone acetylation/deacetylation [172, 173]. For example, DNA methylation analysis revealed that *MUC1* gene expression is regulated by DNA methylation and histone H3 lysine 9 modification at the *MUC1* promoter [174]. Furthermore, CpG methylation near the *MUC2* transcriptional start site plays a critical role in *MUC2* gene expression [175]. Hypomethylation of *MUC2* plays an important role in the high level of *MUC2* expression in mucinous colorectal cancer [129]. This control of cell differentiation in the GI tract is mediated by several transcription factors, especially those belonging to the hepatocyte nuclear factor (HNF), GATA and Caudal-related (Cdx) families [176-180]. For example, GATA transcription factors are zinc finger proteins belonging to a family of transcription factors involved in development and cell differentiation. During embryonic development GATA-4 mRNA is expressed in the primitive intestine [181, 182] in which Muc2 is also found [183]. Computer analysis of the murine Muc2 promoter sequence [184] revealed the presence of several putative GATA binding sites throughout the promoter region. GATA-4 is expressed in Muc2-expressing goblet cells in the SI, appears as an important general regulator of Muc2 expression and identifies Muc2 as a target gene of GATA-4 in differentiated intestinal mucosa and metaplastic stomach [185]. Further studies are needed to elucidate the relationships among expression levels of mucins, binding of transcriptional regulatory factors, and recruitment of DNA methyltransferases (DNMTs), histone deacetylases (HDACs), methylated DNA binding domain proteins, and polycomb group proteins.

Together, the above shows that mucin regulation results from a dynamic interaction of IECs and the host immune system. Such balanced interactions are necessary for the maintenance of intestinal mucosal homeostasis. Increased knowledge of the mechanisms involved in mucin regulation is vital for the prevention of mucin changes in cancer and inflammatory conditions.

1.3 The human GI immune system

1.3.1 Structure and function of the GI immune system

The GI immune system has the challenge of responding to pathogens while remaining relatively unresponsive to food antigens and the commensal microbiota. The healthy GI mucosa contains the largest repository of immune cells within the human body [186]. After the mucus barrier, the innate immune system serves as the body's second line of defence against invading organisms. This system is non-specific, immediate, and is composed of various cell types; innate leukocytes and phagocytic cells, including natural killer (NK) cells, mast cells, macrophages and DCs along with various granulocytes [187]. The intestinal immune system has co-evolved with the microbiota; a symbiotic relationship that may be threatened by opportunistic invasion of the microbiota. It is well established that colonisation with bacteria is critical for the normal structural and functional development and optimal functioning of the mucosal immune system. For example, germ-free mice exhibit smaller PPs [188] and fewer intraepithelial lymphocytes (IELs) [189], compared to specific pathogen-free or germ-free mice colonised with single or multiple species of bacteria.

The exposed surface of the intestinal mucosa is under constant challenge by ingested foreign antigens in micro-organisms, products of food digestion and drugs. It is therefore not surprising that the intestine contains the largest accumulation of lymphoid tissues in the body, known as the gut-associated lymphoid tissue (GALT), in the form of lymphoid aggregates in PPs and in the lamina propria (solitary lymphoid nodules), and as the scattered lymphocyte populations found in the epithelium and in the lamina propria. One of the key functions of the GALT is to distinguish innocuous antigens from pathogenic micro-organisms and to elicit an appropriate response. Antigens can cross the epithelial surface through breaks in TJs, as for example at villus tips where

epithelial cells are shed, or through the follicle-associated epithelium (FAE) that overlies the organised lymphoid tissues of the intestinal wall [190]. PPs are aggregates of lymphoid tissue found in the SI, although a vast number of much smaller individual follicles also line both the SI and colon. FAE contains M cells whose function it is to transport luminal antigens into the follicle [190]. Antigen-presenting DCs form a bridge between the innate and adaptive immune system by sending processes between gut epithelial cells and sampling commensal and pathogenic gut bacteria, which can subsequently be presented to T and B cells to initiate and adaptive immune response [191, 192]. The gut epithelial barrier therefore represents a highly dynamic structure that limits, but does not exclude, antigens from entering the tissues, while at the same time the immune system continuously samples gut antigens through the FAE and DC processes (Figure 1.12).

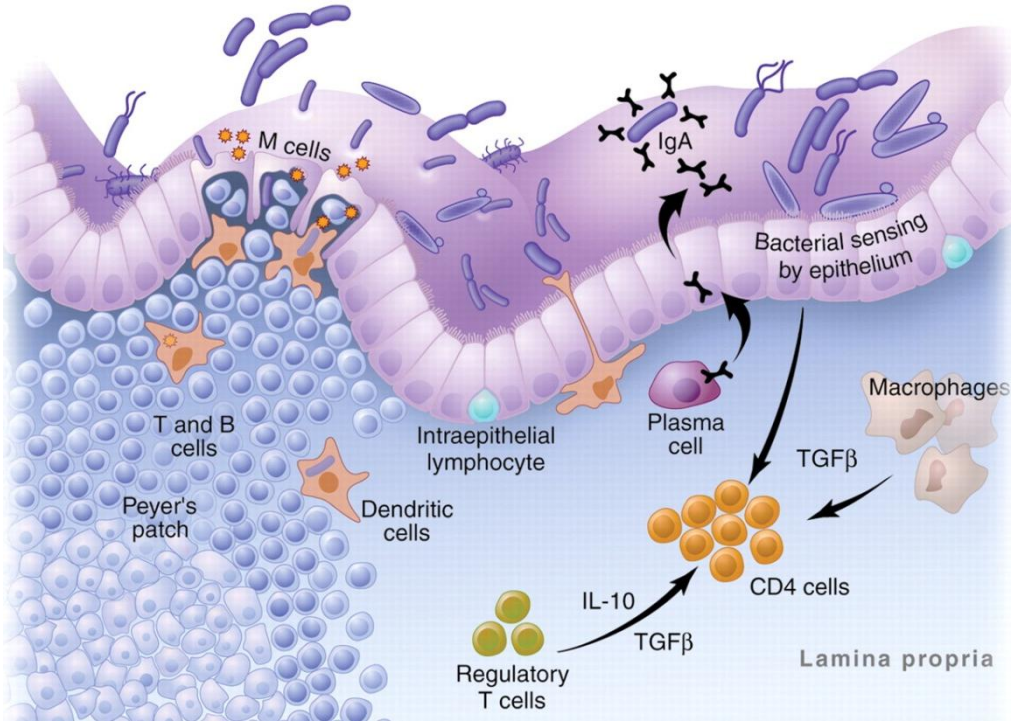

Figure 1.12| Maintenance of an extensive immune system in the intestine. M cells continuously transport luminal bacteria and antigens into the lymphoid tissue. DCs sample bacteria by sending processes through the epithelial barrier. CD8+ and CD4 T cells, macrophages and IgA-producing plasma cells make an enormous contribution to the body's defence. Regulatory T cells and immunosuppressive cytokines serve to inhibit potentially damaging T cell responses [187].

In the intestinal tract of a healthy individual, microbial and food antigens initiate a low level immune response, maintained in a primed but inactive state of suppression [193]. Oral tolerance refers to physiologic induction of tolerance that occurs in the GALT and more broadly at other mucosal surfaces, such as the respiratory tract [194-196]. Oral tolerance and homeostasis are maintained by lymphocytes expressing cell surface markers and anti-inflammatory properties in the GALT. Many inflammatory processes are self-limiting, supporting the existence of endogenous anti-inflammatory mechanisms. This homeostasis is often disturbed in IBD, during which abnormal immune responses to luminal bacteria play a key role in disease pathogenesis [197]. When a disease state is initiated, a potent inflammatory response is orchestrated. The

constitutive presence and trafficking of immune cells into the mucosal compartment has been termed physiologic inflammation [198]. The production of cytokines and other inflammatory mediators can lead to tissue damage and a chronically inflamed mucosa [199].

The exact mechanism of molecular recognition of commensal organisms, food antigens and pathogens by the colonic epithelial surface is still unclear [200]. Pathogen recognition receptors (PRRs) expressed by IECs can induce inflammation upon receptor activation. Toll like receptors (TLRs) consist of ten human PRRs that are homologous to the *Drosophila Toll* protein [201]. In the human SI, the expression of TLR3, TLR4 and TLR5 has been shown on the basolateral surfaces of villus enterocytes [202]. In the human colon, TLR3 and TLR5 are abundantly expressed, whereas TLR2 and TLR4 expression is low [202]. TLRs recognise microbe-associated molecular patterns (MAMPs) in the intestine, which are specific to prokaryotes, and translate them into signals for the expression of antimicrobial peptides, barrier strengthening and proliferation of IECs [203]. TLR co-operation helps to establish a combinatorial repertoire that is able to differentiate between the abundant MAMPs that can be found in nature. In the TLR signalling pathway the adaptor MyD88 was first characterised to play a crucial role, but recent accumulating evidence indicates that TLR signalling pathways consist of a MyD88-dependent pathway that is common to all TLRs, and a MyD88-independent pathway that is atypical to the TLR3- and TLR4 signalling pathways [204]. A signalling cascade leads to the activation of the rapid-acting primary transcription factor nuclear factor (NF)-κB. This transcription activates the expression of genes involved in cell proliferation and inhibition of apoptotic pathways. The essential role for NF-κB in the expression of pro-inflammatory genes, such as TNF-α, IL-1β, IL-6, and IL-8, has led to a vast effort to develop inhibitors of this pathway to aid the treatment of chronic inflammation [205].

Cytokines are a class of small secreted proteins, induced mostly by the activation of NF-κB, and are extensively involved in cellular communication; orchestrating and regulating the processes of immunity and acute and chronic inflammation. Cytokines drive the differentiation of CD4+ T cells into T-helper (T_H) 1 (IL-12), T_H2 (IL-4), and T_H17 (IL-6, TGFβ) cells (Figure 1.13) [206-210]. The effects of both acute and chronic inflammation in IBD are likely to result from the unregulated production of pro-inflammatory cytokines, such as TNF-α, IL-1 and IL-6, or the inadequate synthesis of

anti-inflammatory cytokines, such as IL-4 and IL-10 [211]. The pro-inflammatory cytokines, TNF-α and IL-6, increase mucin secretion in the human colonic LS180 cell line, and increase expression of MUC2, MUC5AC, MUC5B and MUC6 [212]. The T_H2 cytokines IL-4 and IL-9 induce MUC2 and MUC5AC expression, respectively, and mucin production in airway epithelial cells [213-215]. Studies in IL-4 transgenic mice showed that IL-4 induces MUC5AC transcription in non-ciliated cells followed by MUC5AC mucin protein synthesis [216]. The ability of IL-1 to trigger mucin release and to upregulate MUC gene expression was shown in studies of perfused rat colons [217] and the LS180 cell line [212].

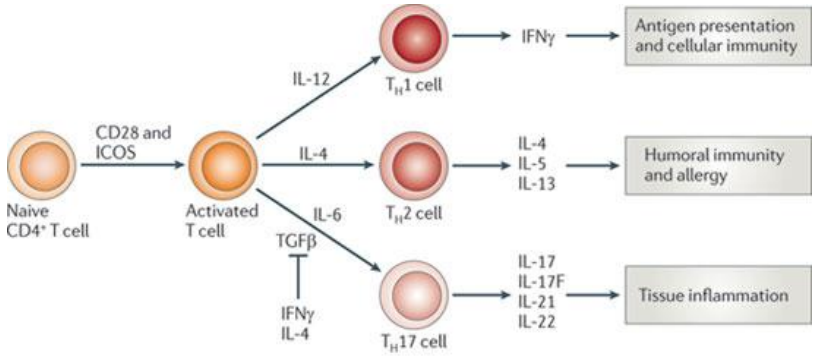

Figure 1.13| General scheme of T-helper cell differentiation. Naive $CD4^+$T cells can differentiate into one of three lineages of effector T helper (T_H) cells; T_H1, T_H2 or T_H17 cells. These cells produce different cytokines and have distinct immunoregulatory functions [210].

A defective or eroded mucus layer can result in a large number of bacteria bypassing the epithelial barrier and binding to TLRs. The subsequent cytokine release activates a strong immune response, decreasing the pH and causing the production of inorganic NOs [218, 219]. This causes structural changes in the epithelium, such as the opening of TJs that serve as intercellular seals, allowing further bacterial invasion and subsequent unfavourable immune activation [220]. Such events occur in inflammatory conditions such as IBD.

1.3.2 Intestinal intraepithelial lymphocytes (IELs)

Through their immediate proximity to antigens in the intestinal lumen and their direct contact with enterocytes, IELs form a potentially important early line of immune defense against invading pathogens [221, 222]. IELs can be split into “type a” that are either TCRαβ^{+}CD8αβ^{+} or TCRαβ^{+}CD4^{+}, or “type b” that consist of the CD8αα^{+} population (TCRαβ and TCRγδ) and the double negative TCRγδ [223]. More than 80 % of human and mouse IELs express CD3 and other markers consistent with their classification as T cells [224, 225]. Higher numbers of IELs are present in the SI (1 IEL for every 10 IECs) compared to the large intestine (1 IEL for every 40 IECs) [226]. IEL numbers are affected by species [227] and external factors, such as the intestinal microbiota [228-230].

The differentiation, activation and functional specialisation of IELs is controlled by interactions with other cell types and soluble factors, and is highly influenced by dietary and microbial products in the intestine. “Natural” IELs (type b) acquire their activated phenotype during development in the thymus in the presence of self-antigens, whereas “induced” IELs (type a) are the progeny of conventional T cells that are activated post-thymically in response to peripheral antigens [231, 232] (Figure 1.14). IELs demonstrate regulatory functions and inhibit excessive inflammatory responses that could be harmful to epithelial barrier integrity [233-237] (Figure 1.14A). However, their heightened activation status and proximity to the intestinal epithelium suggest that IELs may add to immunopathological responses and inflammatory diseases such as IBD [238-241] (Figure 1.14B).

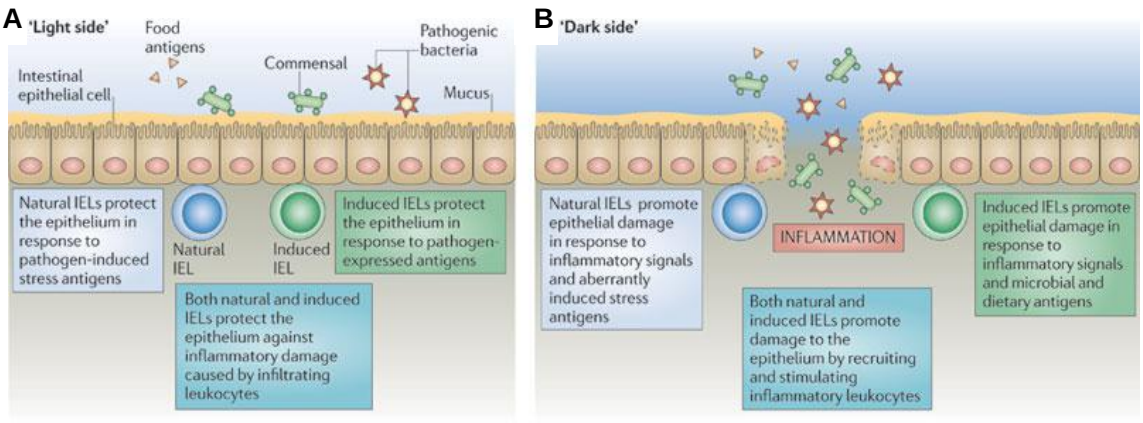

Figure 1.14| The light and the dark side of IELs. Natural and induced IELs have beneficial roles and preserve the epithelium (A), but can also have pathogenic roles by promoting inflammation and through excessive cytotoxicity (B) [232].

1.3.3 Gamma delta (γδ) IELs in the mammalian GI epithelium

TCRγδ^{+}, identified almost thirty years ago [242], constitute up to 60 % of SI IELs [224, 231, 243]. IELs bearing the γδ T cell receptor are strategically intercalated between IECs on the basolateral side of the intestinal TJ barrier (Figure 1.15), for immediate detection of bacteria that penetrate the epithelium. γδ IELs are thought to provide a link between the innate and adaptive immune responses, being able to recognise both native protein antigen and non-protein in a major histocompatibility complex (MHC)-independent manner [244-246]. IEL subsets can be both thymically derived and matured within the intestine, and develop extra-thymically from precursors within the intestine [247-249]. The location and level to which this IEL development occurs depends on age; increasing presence of γδ IELs in athymic nude mice with age revealed that the extra-thymic lymphopoiesis in the gut increases with age [229, 249]. Both thymic and extra-thymic development of γδ IELs is dependent on the IL-7 cytokine, as shown in IL-7$^{-/-}$ mice that lack functional γδ IELs [250-252].

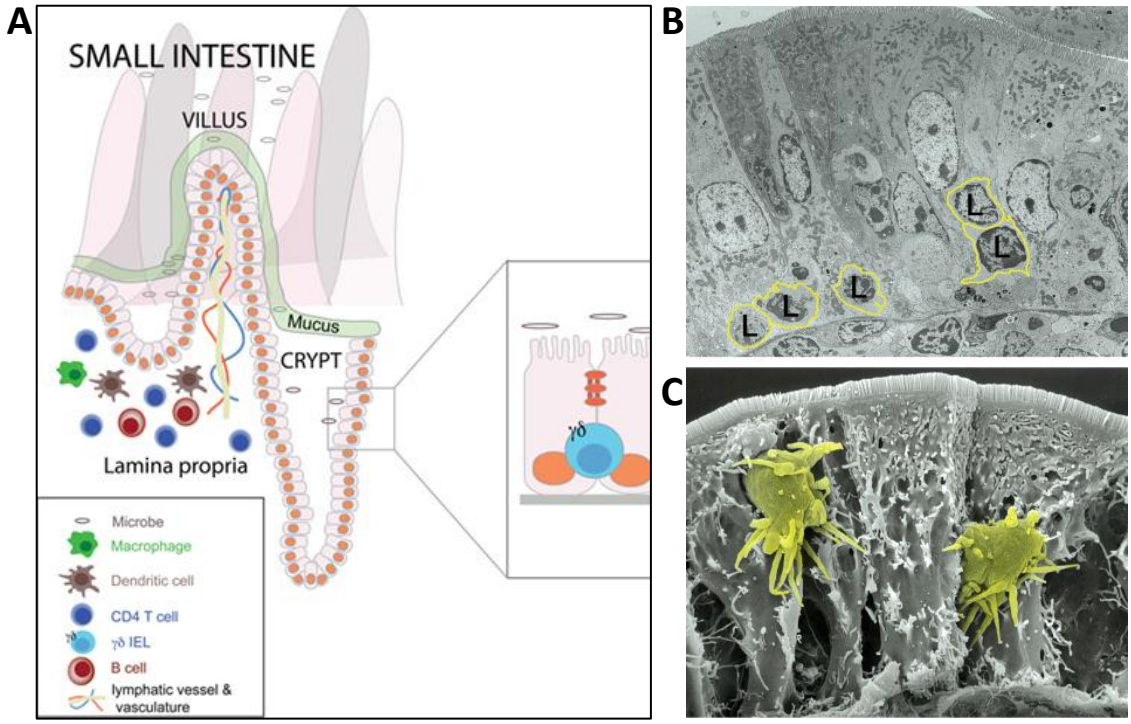

Figure 1.15| Location of γδ IELs in the SI epithelium. γδ IELs are strategically intercalated between epithelial cells (A) [253]. Transmission electron micrographs show that multiple γδ IELs are tightly encased in the epithelium without any visible gaps (B), while scanning electron micrographs show γδ IELs in contact with IECs through spine-like processes and ample space at the basement membrane to move to and fro (C) [254].

Despite published findings on the role of γδ IELs during epithelial repair, inflammation and homeostasis, their functions are not fully understood. The absence of γδ IELs is associated with a reduction in epithelial cell turnover and a down-regulation of the expression of MHC class II molecules, indicating that γδ IELs regulate the generation and differentiation of intestinal epithelial cells to maintain a homeostatic environment [255]. γδ IELs secrete cytokines, chemokines and epithelial growth factors to recruit inflammatory cells, and are active contributors to the promotion of epithelial restitution following injury [255-257]. Intestinal epithelial progenitor proliferation and villus growth is brought about through the localised delivery of keratinocyte growth factor (KGF) by γδ IELs, a unique feature of this T cell population [256, 258]. KGF causes an increase in goblet cell number and trefoil factor (TFF)3 protein expression in the rat intestine [259]. Activated, but not resting γδ IELs express KGF [260]. γδ IELs are activated *in*

vivo to express KGF after DSS treatment, and IEC cell proliferation is decreased in mice deficient in γδ IELs (TCRδ$^{-/-}$) following DSS treatment [256]. This shows that γδ IELs help maintain intestinal integrity by promoting the repair of epithelial lesions, and that γδ IEL-derived KGF forms a component in this protective mechanism. Furthermore, TCRδ$^{-/-}$ mice show a significant decrease in BrdU-labelled epithelial cells in the intestine, suggesting the involvement of γδ IELs in the proliferation of crypt stem cells [255]. Furthermore, γδ IELs have been shown to regulate epithelial regeneration in a DSS-induced colitis model through coordinate expression of genes involved in immunoregulation, inflammatory cell recruitment and antibacterial factors [236] (Figure 1.16). In addition, γδ IELs play a role in infection by maintaining the integrity of intestinal epithelial TJs in response to infection with the protozoan parasite *Toxoplasma gondii* [261].

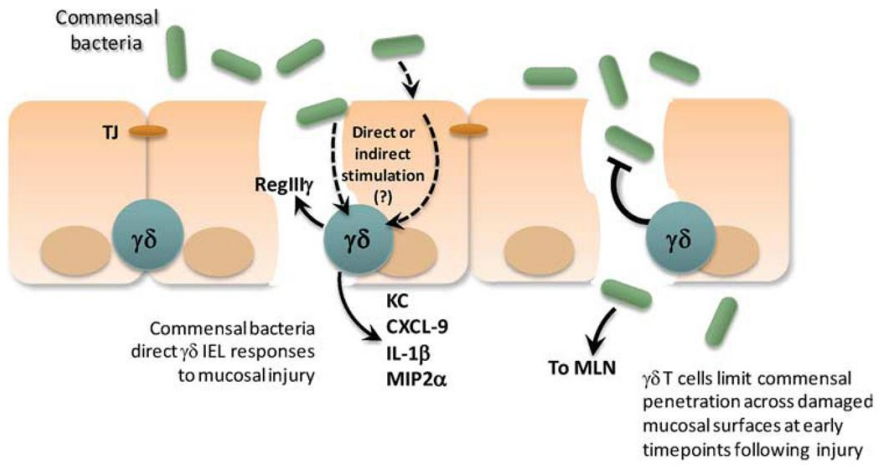

Figure 1.16| The interactions between γδ IELs and the intestinal microbiota during colonic mucosal injury. Commensal bacteria stimulate γδ IELs to express antimicrobial factors (RegIIIγ) and chemotactic cytokines (KC, CXCL-9, IL-1β and MIP2α). Furthermore, γδ IELs limit the penetration of commensal bacteria through mucosal surfaces early on in injury [236].

Further to the above roles during homeostasis and injury, γδ IELs are involved in the regulation of the intestinal microbiota. Commensal bacteria deliver the necessary input, through MyD88-dependent and MyD88-independent pathways, into the γδ IEL response to mucosal injury [236]. Studies in TCRδ$^{-/-}$ mice showed that γδ IELs aid in

the limitation of opportunistic penetration of commensal bacteria across the mucosal surface; a phenomenon seen at early time points of injury by DSS-induced colitis [236]. In the SI, γδ IELs respond to the microbiota not only in the context of injury, but also during homeostasis [262]. The intestinal microbiota induces the expression of antimicrobial factors, including RegIIIγ, in SI γδ IELs [262]. Antibacterial lectin RegIIIγ expression correlates with the physical separation of the microbiota from the host mucosal surface in the SI [263]. This further substantiates the role of IELs and the overlying mucus layer as vital components of the innate immune system. In the intestine, the aryl hydrocarbon receptor (AhR) regulates IEL numbers, and its deficiency compromises IEL maintenance causing alterations in microbial load and composition [264]. Such alterations lead to heightened immune activation and increased susceptibility to epithelial injury, indicating a role of γδ IELs as essential mediators of host-microbial homeostasis at the intestinal mucosal surface.

Together these findings show that γδ IELs play a multifaceted role in the maintenance of mucosal homeostasis following injury, and may be critical mediators of the host response in a dynamic cross-talk between themselves and the intestinal microbiota. Despite the recent advances, we lack details of the molecular processes and responses of γδ IELs, partly due to the experimental challenges; γδ IELs readily undergo spontaneous apoptosis when cultured outside of their intestinal niche [265]. Whether γδ IELs play a role in mucus production or the maintenance of an intact mucus layer, in a homeostatic environment and following mucosal injury, is currently unknown.

1.4 The human GI microbiota

1.4.1 Development and composition of the human GI microbiota

The digestive tract forms an homeostatic environment and is home to ten times as many bacteria as there are human cells [25]. The process of microbial colonisation begins at birth [266], although interactions with microbes prior to birth have been suggested [267]. Natural sources of gut bacteria are represented by the mother's vaginal and faecal microbiota, as well as other environmental microbes [268]. The microbiota is thought to establish itself early on in life, with genetic factors determining

its final composition, and shows substantial diversity in unrelated adults. Microbiota complexity increases with age, reaching a stable climax in adulthood [269].

The intestinal microbiota is largely composed of bacteria (92.9 %), with archaea (0.8 %), eukarya (0.5 %) and viruses (5.8 %) forming small components [270]. Aerobes and facultative anaerobes initiate colonisation of the firstly oxygen-positive environment, but disappear a few weeks after birth to be replaced by a rapidly increasing anaerobic community [271-273]. More than 99 % of the bacteria in the adult intestine are anaerobes, however aerobic bacteria are also present, particularly in the caecum [274]. The infant intestinal microbiota is much less complex than its adult equivalent in terms of total number of bacteria and encountered diversity of microbial taxa [275, 276]. Furthermore, a simplified intestinal microbiota is observed in the elderly population [277].

The microbial burden in the GI tract is tissue specific, displaying an increase along its length, from the oral cavity to the rectum (Figure 1.17A). Being the most metabolically active organ in the body, the colon has the highest bacterial density and species variety, with approximately 10^{13} bacteria per gram of luminal content in the colon, belonging to approximately 500-1000 different species [25]. Microbes preferentially colonise certain areas of the intestine, known as niches. For example, whereas lactobacilli can be found in the stomach, *Escherichia coli* mainly reside in the colon [271]. The human intestinal microbiota consists of several microbial phyla, including *Firmicutes* and *Bacteroides* that together make up the vast majority (>90 %), *Proteobacteria*, *Actinobacteria* and *Verrucomicrobia* (Human microbiome project Nature 2012) (Figure 1.17B). Despite the high inter-individual variation, *Firmicutes* are generally higher in abundance compared to the *Bacteroides* phyla in humans [278-282] and rodents [283, 284]. Figure 1.17C represents the aggregate microbiota composition of the genus *Lactobacillus* as determined from adult faecal samples. The mucosa-associated microbiota differs substantially from the luminal content within the distal GI tract, as well as the faecal microbiota [275, 281, 282, 285, 286]. A major drawback of the use of faecal samples to determine the intestinal microbial composition is the fact that faecal microbiota represents only the distal colon, leaving other parts of the GI tract, particularly the SI, unexplored. The SI is a harsh environment for microbial life because of the short transit time and excretion of digestive enzymes and bile [287], requiring different SI microbes to develop survival strategies of microbes compared

with those residing in the colon. Phylogenetic mapping indicates that *Streptococcus* sp., *Escherichia coli*, *Clostridium* sp. and high G+C organisms are most abundant in the SI, with the composition of these populations fluctuating in time and correlating with the short-chain fatty acid (SCFA) profiles [288]. Comparative functional analysis with faecal metagenomes (complete genetic material in faecal samples) identified functions that are overrepresented in the SI, including simple carbohydrate transport phosphotransferase systems (PTS), central metabolism and biotin production. Moreover, metatranscriptome (mRNA transcripts in a group of species) analysis supported high level in-situ expression of PTS and carbohydrate metabolic genes, especially those belonging to *Streptococcus* sp. [288].

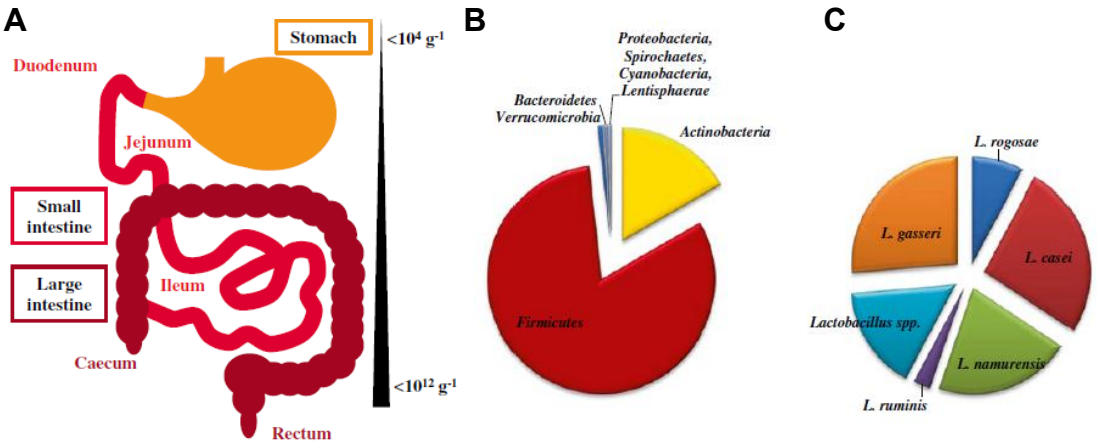

Figure 1.17| Bacterial distribution and abundance in the human GI tract. Schematic representation of the human GI tract showing its different compartments and relative abundance of bacteria (A). Relative abundance of the main microbial phyla detected in the adult fecal samples (B) and aggregate microbiota composition of the genus *Lactobacillus* as determined from adult faecal samples (C) [276, 289].

1.4.2 Role of the human microbiota in the GI tract in health and disease

The symbiotic relationship of the intestinal microbiota with the human host is the consequence of a long history of various co-evolutionary processes, where neither

partner is disadvantaged, and where unique metabolic activities or other benefits are provided to both partners [290].

1.4.2.1 Beneficial role of microbes

Comparative studies with germ-free and conventional animals have recognised that the intestinal microbiota is required for the development of the mucosal immune system and its functioning early on in life, as well as nutrient absorption, epithelial cell renewal and angiogenesis [291-294]. Intestinal microbes are able to influence the expansion and functioning of the murine immune system, as for example the expansion of T cells in the PPs and mesenteric lymph nodes. The intestinal microbiota provides vitamins that are required by the host [295, 296]. A primary role of the microbiota, however, is the digestion of dietary polysaccharides. Non-digested residue that passes from the SI into the colon provides the major source of diet-derived energy for the growth of the colonic microbiota [297]. Several metatranscriptome and metaproteome studies describing the human intestinal microbiota have confirmed the importance of bacterial functions related to carbohydrate metabolism in the colon [298-301]. The colonic microbiota can ferment indigestible dietary fibre to provide energy through the production of SCFAs [302]. The intestinal microbiota in mice can affect the efficiency with which this energy is harvested from the diet and the way that this energy is utilised. Symbiosis appears to exist between the microbiota and the epithelium to maintain epithelial integrity, as is shown by the enhanced increase in gut barrier function in response to recognition of TLR2 and TLR9 ligands [303, 304]. Reductions in mucosal cell turnover, muscle wall thickness, baseline cytokine production, digestive enzyme activity and defective cell-mediated immunity are all associated with the absence of the microbiota [305, 306]. Studies have demonstrated that the commensal microbiota plays a crucial role in the maintenance of intestinal homeostasis during acute DSS-induces colitis. Mice lacking intestinal microbes exhibit increased susceptibility to colonic epithelial damage [307, 308]. The above demonstrates that the intestinal microbiota has important protective, metabolic and trophic functions.

Additionally, the microbiota can prevent the attachment of pathogens to epithelial cells and compete for essential nutrients to prevent the survival of other organisms [309]. When an enteric pathogen by-passes barriers imposed by the commensal microbiota and the epithelial barrier, or when innate immune defects disrupt the natural tolerance

to the resident microbiota, intestinal inflammation occurs [30]. Host defences have the ability to precisely distinguish between commensal microbes and episodic pathogens, through the interpretation of MAMPs via host PRRs [30].

Interestingly, the microbiota also contributes to the thickness and strength of the defensive mucus layer, since it has been shown that several bacterial components such as lipopolysaccharides (LPS) and SCFAs to some extent stimulate mucin production by isolated goblet cells [310-312]. The ability of bacteria to regulate the thickness of the colonic mucus was further demonstrated through mucus thickness measurements in germ-free mice exposed to bacterial peptidoglycan (PGN) and LPS [313] (Figure 1.18).

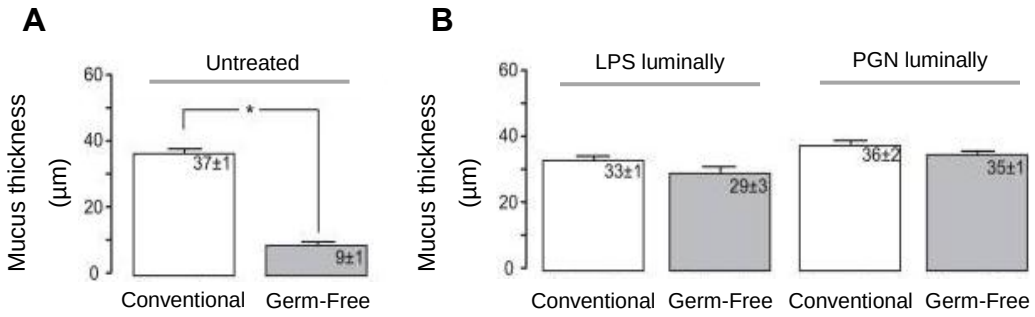

Figure 1.18| Germ-free mice have a thinner mucus layer that can be restored using bacterial products. Thickness (µm) of the adherent mucus in the colon in NMRI mice housed conventionally or under germ-free conditions either with luminal saline (A) or the bacterial products LPS or PGN (B). *p< 0.05 [313].

The mucus-binding capacity of microbes increases the colonisation capacity at the mucosal interface and is important for prolonged intestinal residency of beneficial microbes [88]. The expression of adhesion proteins aids in this process (Table 4.1). Mucus-degrading bacteria have an advantage in the mucosal niche that is rich in endogenous glycoproteins both from excreted mucin proteins and shed IECs. Species of mucin-degrading specialists include: *Akkermansia (A.) municiphila* [314-316], *Bacteroides thetaiotaomicron* [317-319], *Bifidobacterium bifidum* [314, 320-322],

Bacteroides fragilis [323, 324], *Ruminococcus gnavus* [314], and *Ruminococcus torques* [314, 322]. *Akkermansia*-like sequences are universally distributed among animals, ranging from mammals, to non-mammals [270]. This suggests co-evolution of *Akkermansia spp*. with their host and therefore a potential functionality in the GI tract. *A. muciniphila* is a recently discovered mucin-degrading specialist [315]. Members of the genus *Akkermansia* have been suggested as biomarkers for a healthy intestine [325] due to their abundance in the healthy mucosa and their negative correlation with intestinal disorders, including IBD [314]. *B. thetaiotaomicron* is a well-studied mucin-degrading expert that utilises a wide variety of dietary glycans as well as host mucin glycans and human milk oligosaccharides (HMOs) [326]. Members of the microbiota that have adapted to the glycan-rich environment of the intestine are important residents of the human intestine, and could be particularly important for nutrient exchange, communication with the host, development of the immune system and resistance against invading pathogens.

1.4.2.2 Impact of dysbiosis on the host

Numerous factors can harm the beneficial members of the GI tract microbiota, including antibiotic use, psychological and physical stress, radiation, altered GI tract peristalsis, and dietary changes. A disturbance of the normal balance of the intestinal microbiota (dysbiosis) is in part considered responsible for metabolic and inflammatory disorders [327]. In addition, certain diseases have been associated with a particular gut microbe, such as *Helicobacter pylori* in peptic ulcer disease (although 80 % of individuals infected display no symptoms), and *Streptococcus gallolyticus*, in colorectal cancer [328-330]. Obesity and IBD represent the most studied disorders associated with an alteration of the intestinal microbiota composition.

The composition of the diet has been shown to have a significant impact on the content and metabolic activities of the human faecal flora [331]. Metagenomic sequence reads were used for phylogenetic profiling of human faecal samples, and revealed distinct clusters called enterotypes [270]. These enterotypes are identifiable by the variation in the levels of one of three genera: *Bacteroides* (enterotype 1), *Prevotella* (enterotype 2) and *Ruminococcus* (enterotype 3) [270]. Although no clear environmental or genetic explanation was found for the clustering of enterotypes, long-term diet has been

strongly associated with enterotype clustering [332]. A lower proportion of *Bacteroidetes* and a higher proportion of *Actinobacteria* were found in obese individuals, compared to lean individuals [299]. Furthermore, type 2 diabetes, caused by obesity-linked insulin resistance, is associated with a change in microbial composition in the intestine [333]. Although IBD is not associated with a particular gut microbe, chronic microbial infections are associated with its pathology [334-336]. Studies have shown a reduction in general species diversity in the GI tract microbiota in IBD patients, with a decrease in *Firmicutes* and an increase in *Bacteroidetes*, compared to healthy individuals [323, 337-339]. In agreement with these findings, Illumina-based metagenomic sequencing revealed that, on average, IBD patients harboured 25 % fewer bacterial genes when compared to healthy individuals [340]. A dysbiotic mucosal-adherent community enriched in *Proteobacteria* and depleted of *Bacteroidia* members has been associated with chronic inflammation in HIV-infected subjects, demonstrating a link between intestinal microbial populations and immunopathogenesis during progressive HIV infection [341]. Intestinal microbial dysbiosis is not only associated with intestinal diseases, but has also been observed in extra-intestinal diseases such as atopic and allergic diseases, autism, type 2 diabetes and rheumatoid arthritis [342], further highlighting the importance of intestinal microbial homeostasis in human health.

1.4.3 *L. reuteri* in the human GI tract

1.4.3.1 The *Lactobacillus* genus

Lactobacilli belong to the lactic acid bacteria (LAB) due to the nature of the main end product of carbohydrate metabolism; lactic acid. The genus *Lactobacillus* comprises a large (about 145 species) heterogeneous group of low-G+C content gram-positive, non-sporulating, and anaerobic bacteria [343], recognised for its extensive phylogenetic, phenotypic and ecological diversity [344]. The taxonomic classification of the genus *Lactobacillus* is shown in Figure 1.19. Lactobacilli form only a minor proportion (0.01-0.6 %) of the human adult faecal microbiota [345]. The predominant autochthonous *Lactobacillus* species in the GI tract are *L. gasseri*, *L. reuteri*, *L. crispatus*, *L. salivarus* and *L. ruminis* [346].

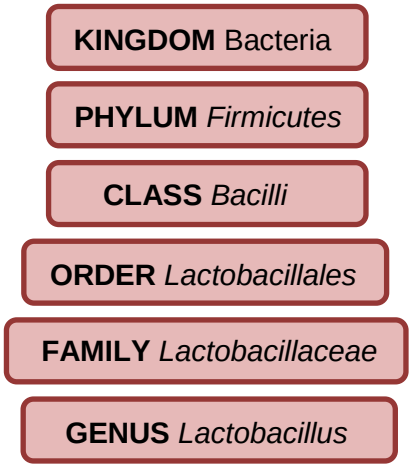

Figure 1.19| Taxonomic classification of the *Lactobacillus* genus.

Symbiotic microorganisms form intimate associations with most members of the animal kingdom [347]. Probiotics are live microorganisms that, when administered in adequate amounts, confer a health benefit on the host (Figure 1.20) [28, 348]. Probiotic bacteria have been used to prevent relapses in UC and may serve as potential prevention and/or treatment methods for diseases of the GI tract [349].

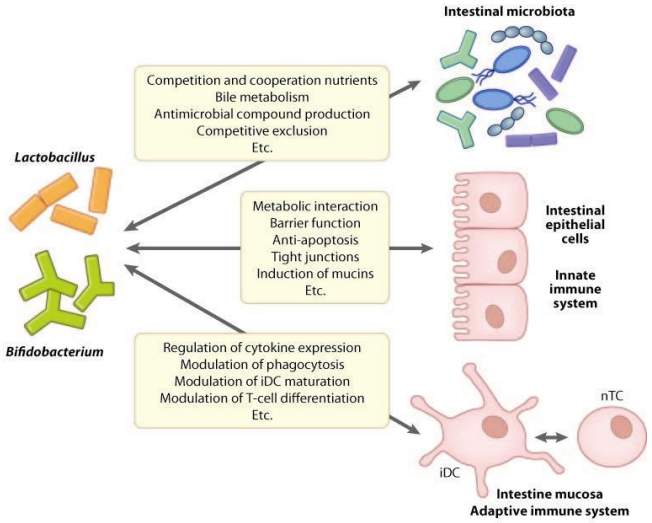

Figure 1.20| Schematic representation of the different modes of interaction that can be anticipated to underlie probiotic effects [28]**.**

Lactobacilli have been shown to exert health benefits under various conditions. The efficacy of some lactobacilli in acute infectious diarrhoea and the prevention of antibiotic-associated diarrhoea has been established [350], with other findings showing that lactobacilli may reduce the recurrence of *Clostridium difficile*-associated diarrhoea [351]. Promising results have been obtained in the prevention of IBD, colorectal cancer and irritable bowel syndrome [352-354]. Different probiotic *Lactobacillus* strains have been associated with different effects related to their specific capacities to express particular surface molecules or to secrete proteins and metabolites that directly interact with host cells. The bacterial envelope of lactobacilli can comprise different cell wall-associated proteins that often consist of repeating domains. It is generally assumed that a good adherence capacity is desirable for probiotic lactobacilli, to promote residence time, pathogen exclusion and host cell interaction [355].

1.4.3.2 Beneficial (probiotic) effects conferred by *L. reuteri*

The beneficial characteristics of *L. reuteri* have been studied intensively during the past three decades because of the common use of different strains as probiotics. *L. reuteri* ATCC 55730 has been shown to have probiotic properties in humans, and is used in the prevention and amelioration of colitis, gastroenteritis and diarrhoea [336, 356-358]. In mice, *L. reuteri* 100-23 has been shown to trigger immune stimulation and regulation via IEC activation and development of regulatory T cells [359, 360]. Furthermore, *L. reuteri* strains (R2LC and JCM 5869 isolated from rat, and ATC PTA 4659 and ATCC 55730 isolated from human) protect against DSS-induced colitis in rats [361]. This protection is associated with reduced P-selectin expression and a decrease in leukocyte- and platelet-endothelial cell interactions. Despite protecting against colitis, treatment with these *L. reuteri* strains did not improve the integrity of the mucus layer or prevent distortion of the mucus microbiota caused by DSS treatment [24]. However, *L. reuteri* decreased bacterial translocation from the intestine to mesenteric lymph nodes during DSS treatment, which may explain how *L. reuteri* ameliorates DSS-induced colitis [24]. It has been shown that the suppression of chemically-induced colitis in mice is associated with an increase in γδ IELs, induced by *L. acidophilus* and *B. longum*, suggesting both a novel importance of γδ IELs in probiotic protection and a new function of these probiotics in the prevention of colitis [362]. The ability of *L. reuteri* to prevent experimental colitis in animal models indicates that the above mentioned immunoregulatory effects of this organism can have a significant benefit for the host [357, 361, 363-365]. Intestinal resistance to the eukaryotic pathogen *Cryptosporidium parvum* was increased by *L. reuteri* in a murine model of acquired immunodeficiency syndrome [366]. Further beneficial attributes of *L. reuteri* are shown in Table 1.2.

Table 1.2| Beneficial attributes of *L. reuteri* studied in human and animal trials and with cell cultures.

Function	Observation	References
Humans		
Prevention of diarrhoea	Reduced duration and severity of diarrhoea caused by rotavirus in children; reduced incidence of diarrhoea in infants.	[367, 368]
Reduction of infant colic	Reduced colicky symptoms in 95% of infants; improved gastric emptying and reduced crying time in premature infants.	[369, 370]
Reduction of IgE-associated eczema and sensitisation	Reduction of IgE-associated eczema in 2 year-olds; reduced levels of TGF-B2.	[371, 372]
Immune stimulations	Short-term survival of *L. reuteri* in the stomach and SI. Stimulation of CD4 lymphocytes.	[373]
Animals		
Immune stimulation	Transient increase in pro-inflammatory cytokines and chemokines in the intestinal tract.	[360]
Immune regulation	Increased levels of regulatory T cells upon colonisation of *Lactobacillus*-free mice with *L. reuteri*	[359]
Cell cultures		
Modulation of immune function in cultured macrophages, DCs and T cells	Reduction in TNF-α production in activated macrophages; reduced production of pro-inflammatory cytokines in DCs, induction of regulatory T cells.	[357, 359, 374-376]

Several clinical trials have shown that *L. reuteri* confers health benefits in humans. In a double-blind, placebo-controlled, randomised trial, *L. reuteri* ATCC 55730 was shown to reduce the severity of diarrhoea of infants in a daycare setting [368]. Immunomodulation has also been shown in humans, where *L. reuteri* ATCC 55730 temporarily colonises the stomach and SI of healthy subjects and increases CD4+ T lymphocytes in the ileum [373]. Recent research has also revealed that *L. reuteri* may play a crucial role in the induction of tolerance in the vertebrate gut; *L. reuteri* inhibited the induction of pro-inflammatory cytokines IL-12, IL-6, and TNF-α, and primed human DCs to drive the development of regulatory T cells [376].

1.4.3.3 Interactions between *L. reuteri* and mucus

A number of colonisation requirements have been identified for *L. reuteri*, including adherence to epithelial cells, mucus-binding ability and fibronectin-binding ability [377-379]. Strain-specific cell surface proteins considered as mucus-binding proteins have been identified in *L. reuteri*, and include the collagen binding protein (CnBP) in *L. reuteri* NCIB11951 [380], Lr W1 in *L. reuteri* JCM 108 [381], and Lar_0958 in MM4-1a [382]. Porcine intestinal mucin and an α-D-galactose-specific lectin were shown to inhibit binding of CnBP to collagen, suggesting a potential lectin-like adhesion to mucus as its binding mechanism [380]. Lr W1 was shown to bind to epithelial cells and mucus [381]. Sequence similarities in CnBP and Lr W1 suggest that mucus binding mechanisms may be similar for these mucus-binding proteins.

The most studied example of mucin-targeting bacterial adhesins is the mucus-binding protein, MUB, produced by *L. reuteri* [377, 383]. MUB is a 358 kDa protein from *L. reuteri* ATCC 53608 (1063) that contains repeated functional domains, termed Mub, responsible for the protein's adhesive properties. The abundance of Mub domains in lactobacilli of the GI tract suggests that the Mub repeat is a functional unit capable of fulfilling an important function in host-microbe interactions. The 14 Mub domains of MUB can be divided into type 1 (six domains) and type 2 (eight highly conserved domains), based on sequence homology. MUB has a YSIRK signal peptide for the translocation across the cytoplasmic membrane, and a C-terminal LPxTG anchor motif (Figure 1.21A). Each Mub repeat consists of the B1 and the B2 domain. The B1 domain of MubR5 (Figure 1.21B) shows structural similarity to the immunoglobulin-binding L protein from *Peptostreptococcus magnus*, and was shown to bind to mammalian immunoglobulins, such as IgA [383]. The mucus-binding ability of MUB to colonic human, guinea pig and rabbit mucus was suggested using the chemically synthesised short MUB_{70} corresponding to the B1 domain of one repeat [384]. The Mub B2 domain is a member of the MucBP domain family (Pfam PF06458), whose sequences are present in all currently available *L. reuteri* strain genomes (JCM1112, 100-23C, DSM 20016, MM2-3, MM4-1, ATCC 55730 and CF48-3A). Several MUB homologues and MucBP domain-containing proteins have been found, but almost exclusively in LAB and predominantly in lactobacilli found naturally in intestinal niches. Binding of MUB to mucus is inhibited by the glycoproteins fetuin and asialofetuin as well as fucose, suggesting that MUB interacts with specific muco-oligosaccharides

[377]. The fact that mucus-binding domains containing multiple Mub domains, were identified in 47 proteins from six *Lactobacillus* genomes, suggests that Mub may play an important role in host-microbe interactions [385] however; the molecular ligands in mucus that are recognised by MUB are unknown, and require investigation in order to better understand the interactions of *L. reuteri* with the host, thereby increasing the knowledge of the potentially beneficial roles of this gut symbiont in the GI tract.

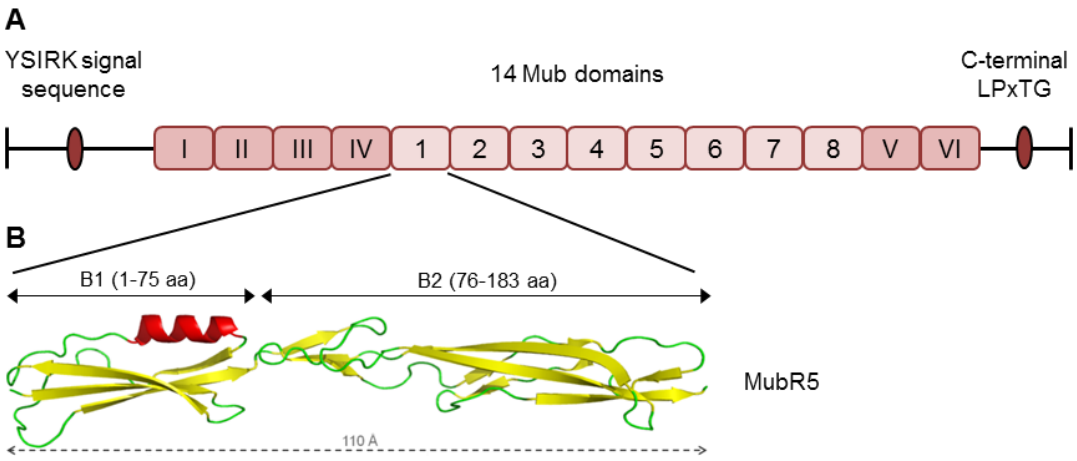

Figure 1.21| Structure of the mucus binding protein MUB of *L. reuteri* ATCC 53608. MUB consists of the YSIRK signal peptide sequence, the 14 Mub repeats and the C-terminal LPxTG anchor motif (A). Crystal structure of the MubR5 repeat (B) [383].

1.5 Aim and objectives

The intestinal mucus layer forms a protective barrier that is in part shaped by the luminal microbiota and by the host immune system, and plays a key role in the maintenance of gut homeostasis. γδ IELs reinforce barrier function by limiting bacterial translocation and regulating IEC generation and differentiation. On the other hand, probiotic bacteria such as *L. reuteri* have been shown to protect against bacterial translocation in mouse models of colitis. With the general aim of increasing our understanding of the role of the much overlooked mucus layer in health and disease, this PhD project explores the relationship and cross-talk between intestinal microbes, the mucus layer, and the intestinal immune system.

Specific objectives:

1. To investigate the impact of γδ IELs on mucus properties, a TCRδ$^{-/-}$ mouse model was used to assess the expression, organisation and glycosylation of intestinal mucus.

2. To explore the specificity of *L. reuteri* adhesion to mucus, an intestinal mucin-producing cell line and mammalian tissue sections were used to assess binding specificity to mucins, mechanisms of adhesion and the impact on the host response.

Chapter 2 Methods

2.1 General Materials

All chemicals were purchased from Sigma-Aldrich, unless otherwise specified. Laboratory reagent supplier names have been indicated in the text; a list of full names and address in in appendix 1. The water used was deionised and ultrapure to a resistance of 18.2 MΩ cm^{-1} (Barnstead Nanopure Diamond).

The composition of phosphate buffered saline (PBS) used throughout the study is 0.01 M phosphate buffer, 0.0027 M potassium chloride and 0.137 M sodium chloride, pH 7.4, at 25 °C. PBS used for molecular biology was purchased as a 10x solution diluted to a 1x concentration, to yield a PBS solution with 0.01 M phosphate buffer and 0.154 M sodium chloride, pH7.4. This was autoclaved before use. All imaging in this study was performed on Carl Zeiss light, fluorescent or confocal microscopes. All incubations in this study were performed at 19-23 °C (room temperature), unless otherwise stated.

2.2 Mice

C57Bl/6J wild type (Harlan Labs) and B6.129P2-$Tcrd^{tm1Mom}$ (TCRδ$^{-/-}$; Jax Laboratories) mice were bred and maintained at a conventional animal unit at the University of East Anglia. All animals were specific pathogen-free (SPF), and had access to a standard mouse diet and water ad libitum. For all studies, 10-20 week-old, age- and sex-matched mice were used. C57BL/6 mice were used as wild type controls. TCRδ$^{-/-}$ mice were used as our immune cell-deficient mouse model that has a neomycin targeted deletion of 4Kb of the Cδ region [386].

2.3 *In vivo* mouse studies

2.3.1 DSS-induced colitis model

2.3.1.1 Induction and assessment of DSS-induced colitis

Colitis was induced by replacing normal drinking water with a 2.5 % solution of dextran sodium sulphate (DSS) (w/v, MW 35-50 kDa; MP Biomedicals) in drinking water provided ad libitum for 7 days. For recovery experiments, mice were given DSS water for 3 days, followed by 3 days of normal drinking water without DSS. All mice used in the DSS studies were 13-20 week old male mice. The severity of colitis was assessed on the basis of stool consistency, faecal blood content (detected using a Haemoccult kit; POCT Ltd, Angus, UK) and weight loss as determined daily throughout the DSS study. These clinical parameters were scored as the disease activity index (DAI) using Cooper and Murthy's scoring system (Table 2.1). Colon length was measured with a millimetre ruler on the final day of the study, as a further measure of severity of colitis.

Table 2.1| Cooper and Murthy's disease activity index (DAI) scoring system.

Score	% Weight loss	Stool consistency	Bleeding
0	None	Well-formed pellet	Haemoccult negative
1	1-5	-	-
2	5-10	Pasty and semi-formed stools	Haemoccult positive
3	10-15	-	-
4	>15	Liquid stools	Gross rectal bleeding

2.3.1.2 Histological analysis of DSS-induced colitis

Segments (0.5 cm) of the ileum, mid-colon and distal colon were fixed in 10 % formalin for a minimum of 24 h. Fixed tissue was placed inside labelled cassettes, incubated in 70 % ethanol for 30 min, processed in a tissue processor (details in appendix 2) and embedded in paraffin wax. Sections (5 µm) were cut using a microtome (Zeiss). Cut paraffin ribbons were placed in a water bath at 37 °C and mounted onto adhesion slides (VWR, Leicestershire, UK). Slides were allowed to dry overnight (O/N) at 37 °C with 5 % CO_2. Sections were deparaffinised twice in xylene (5 min each, Acros Organics, Geel, Belgium), and hydrated in 100 %, 90 % and 70 % ethanol followed by distilled water (5 min each). Nuclei were stained with haematoxylin (BDH, Leicestershire, UK) for 5 min, followed by three washes in tap water. Slides were briefly differentiated in acid-alcohol (96 % ethanol, 1 % HCl) and washed twice in tap water. Eosinophilic structures were stained with Eosin Y for 10 s. Sections were washed in still tap water, and dehydrated in 70 %, 90 %, 100 % ethanol (30 seconds each) and two xylene changes (1 min each). Tissue sections were mounted in DEPEX mounting medium (VWR, Leicestershire, UK) and allowed to dry O/N. Haematoxylin and Eosin Y stained tissue sections were scored blindly by a histologist (James Sington, NNUH) on the basis of epithelial injury, chronic and acute inflammatory infiltrates, number of goblet cells and thickening of the ileum/colon wall (details in appendix 3).

2.3.2 Mucus thickness measurements

Mucus thickness measurements were performed in the Department of Medical Cell Biology at the University of Uppsala, Sweden, where the experimental set-up was kindly made available through a collaboration with Prof Lena Holm. The total mucus thickness (loose and firm) of female C57BL/6 and TCRδ$^{-/-}$ mice was measured in five separate areas using a glass micropipette held by a micromanipulator (Leitz, Wetzlar, Germany) at an angle of 30-35° to the cell surface, as described previously [19]. Briefly, the mice were continuously anaesthetised with inhalation gas (2.2 % isoflurane, 40 % oxygen and 60 % nitrogen) and the body temperature maintained at 37-38 °C. The ileum/distal colon was exteriorised and fitted over a double-bottom mucosal chamber, exposing the mucosa through the hole. The loose mucus layer was then removed by suction and the firm layer covered with carbon particles suspended in a

saline solution, to allow the surface visualisation of the transparent mucus. The firm mucus layer was measured immediately following suction. Readings were repeated after 20, 40 and 60 min. The mucus thickness (*T*) was then calculated using the formula $T = l \times \sin a$, where *l* is the measurement made and *a* is the angle of measurement.

2.4 Biochemistry

2.4.1 Ninhydrin assay

Sialic acid concentration in tissue samples was determined as previously described [387]. Small intestine and colon mucus scrapes were collected from C57BL/6 and TCR$\delta^{-/-}$ mice and immediately frozen on dry ice, before freeze-drying O/N. Mucus samples were diluted in water to 1 mg ml^{-1}. 333 µl of each sample and standard (sialic acid 0-250 µM) was mixed with 333µl glacial acetic acid and 333 µl acidic ninhydrin solution (5 g ninhydrin, 120 ml glacial acetic acid and 80 ml HCl), vortexed and briefly centrifuged to collect the sample at the bottom of the tube. Samples and standards were boiled for 10 min before cooling under a cold stream of water. All samples and standards were briefly centrifuged and transferred to cuvettes. The absorbance at 470 nm was immediately measured using a U-3010 spectrophotometer (Hitachi, Tokyo, Japan). Sample concentration was calculated against the sialic acid standard curve.

2.4.2 Alkaline borohydrate assay

O-glycan concentration in tissue samples was determined as previously described [388]. SI and colon mucus scrapes were collected and diluted as in section 2.4.1. 100 µl of each sample and standard (N-acetylgalactosamine 0-250 µM) was mixed with 120 µl alkaline 2-cyanoacetamide (CNA) reagent (200 µl 0.6 M CNA, 1 ml 0.15 M NaOH) and boiled at 100 °C for 30 min. To this 1 ml of 0.6 M borate buffer (0.3 M sodiumtetraborate, 0.3 M potassium dihydrogenphosphate (Fisher Scientific); pH 8) was added, vortexed and briefly centrifuged. Each standard and sample was added to

an opaque 96-well plate in triplicate and fluorescence measured at λ= 420 nm, with an excitation of λ= 320 nm, using a Microplate reader (BMG Labtech, Offenburg, Germany). Sample concentration was estimated against the N-acetylgalactosamine standard curve.

2.4.3 Faecal IgA ELISA

Faecal pellet samples (50-70 mg) were collected from C57BL/6 or TCRδ$^{-/-}$ mice and homogenised in 100 µl PBS containing 0.01 % sodium azide (NaN_3), per 10 mg of faeces. After centrifugation at 9000 x*g* for 5 min, the supernatants were collected and stored at -80 °C. Samples were diluted (1:200-1:400) and faecal IgA levels were determined using a mouse IgA ELISA quantitation kit (Bethyl Laboratories, Cambridge, UK), following the manufacturer's instructions. Absorbance was determined at a wavelength of 450 nm using a Microplate reader (BMG Labtech).

2.4.4 Intestinal IgA ELISA

C57BL/6 or TCRδ$^{-/-}$ small intestines and colons were extracted and maintained in a Petri dish containing Dubecco's Minimal Essential Media (DMEM; Lonza, Basel, Switzerland). Organs were tied at one end using black silk string (the SI was cut into two halves for easier flushing). Using 1 ml syringes with metal gavage needles, 250-500 µl of ice cold wash solution (8 ml ddH_2O, 1 ml 10x PBS, 1 ml 0.5M EDTA and 20 µl proteinase inhibitor cocktail) was slowly injected into the organ and inverted for 1 min to thoroughly wash intestinal contents. The solution with intestinal contents was transferred into an ice cold 15 ml Falcon tube containing 40 µl of proteinase inhibitor, and mixed briefly by rotation before being placed on dry ice and subsequently frozen at -80 °C until further use. Protein concentrations were estimated using the bicinchoninic acid (BCA) assay, following the manufacturer's instructions. The intestinal IgA ELISA was performed using the Bethyl Laboratories mouse IgA ELISA kit, following manufacturer's instructions.

2.4.5 Total protein extraction from epithelial tissue

Whole small intestines and colons were extracted from C57BL/6 or TCR$\delta^{-/-}$ mice and immediately snap frozen in liquid nitrogen. Frozen samples were crushed to a fine powder using a pestle and mortar, and dissolved in 500 µl NP-40 cell lysis buffer (Invitrogen, Life Technologies Ltd, Paisley, UK), 1 % protease inhibitor cocktail per 200 mg of tissue. Following thorough vortexing, samples were centrifuged at 5000 x*g* for 5 min, and the supernatants collected. Protein concentration was determined using a NanoDrop ND-1000 and samples were frozen at -80 °C until further use.

2.4.6 SDS-PAGE and western blot

Protein extracts (see section 2.4.5) were denatured at 70 °C for 12 min in lithium dodecyl sulphate (LDS) loading buffer and dithiothreitol (DTT) reducing agent, according to manufacturer's instructions (Invitrogen, Life Technologies Ltd, Paisley, UK). A sample concentration of 100 µg protein was loaded onto an Expedeon RunBlue 12 % acrylamide gel electrophoresis was carried out in 3-(N-morpholino)propanesulphonic acid (MOPS) SDS running buffer for 45 min at 180 V constant voltage. Pre-stained 7-175 kDa Molecular Weight protein standard was used as a marker (New England BioLabs). Following three washes in water, gels were stained with Colloidal Blue staining kit (Life Technologies Ltd, Paisley, UK). Gels were de-stained in three washes of water and scanned in a GS-800 calibrated densitometer (Bio-Rad).

The proteins were de-stained by fixing in 10 % (v/v) acetic acid, 50 % (v/v) ethanol for 1 h, then transferring into 10 % (v/v) acetic acid for shaking O/N. The gel was incubated for 1 h in 50 mM Tris-HCl (pH 7.5), 1 % (w/v) SDS; followed by an incubation in Western blotting Transfer Buffer for 5 min before protein transfer. For western blot, proteins were electroblotted onto an ImmobilonTM-P PVDF membrane, following the Novex XCell II blot module protocol for 1 h at 30 V constant voltage in NuPAGE transfer buffer (Life Technologies Ltd, Paisley, UK). After transfer, membranes were blocked in PBS-T (PBS, 0.05 % (w/v) Tween-20), 5 % (w/v) bovine serum albumin (BSA) for 3 h, and incubated with rabbit anti-pIgR (1:500 dilution in PBS-T, 1 % BSA) O/N. Rabbit anti-human β-actin primary antibody (1:1000 dilution in PBS-T, 1 % BSA)

was used as a loading control. Following three washes in PBS-T, the blots were then incubated with goat anti-rabbit IgG-Alkaline Phosphatase conjugate (1:30,000 dilution in PBS-T, 1 % BSA) for 1 h. Following three washes in PBS-T, the blots were incubated with 0.1 M Tris-HCl (pH 9.6) twice for 5 min. For detection, the membranes were incubated with freshly prepared alklaline Phosphatase substrate (0.1 M Tris-HCl, pH 9.6; 100 µg ml^{-1} Nitroblue tetrazolium; 50 µg ml^{-1} 5-bromo-4-chloro-3-indolyl phosphate-toluidine; 4 mM $MgCl_2$) until the desired colour strength develops. Blots were washed in water, blotted dry and scanned in a GS-800 calibrated densitometer (Bio-Rad). Densitometry analysis was perfomed using the AlphaView SA software.

2.4.7 IL-33 ELISA

Protein extracts (see section 2.4.5) were used at a concentration of 2 mg ml^{-1} for colon samples, and 61 mg ml^{-1} for small intestine samples. The IL-33 ELISA was performed using the mouse IL-33 ELISA KIT (Biolegend, London, UK), following the manufacturer's instructions. Absorbance was determined at a wavelength of 450 nm using a Microplate reader (BMG Labtech).

2.4.8 Purification of MUB protein

L. reuteri ATCC 53608 was grown to the early stationary phase by O/N incubation in MRS medium, followed by an O/N incubation in *Lactobacillus* defined medium II (LDMII, see appendix 4). After centrifugation at 7500 rpm for 15 min at 4 °C, the cell pellet was discarded and the medium was filtered through 0.45 µm and 0.2 µm filters before concentrating using VIVAFLOW 200 filtration system (Fisher Scientific, Loughborough, UK) at 4 °C. The filtered protein solution was dialysed two times using PBS (O/N followed by 4 h). The MUB solution was filtered using Ultrafree-Cl 0.45 µm spin columns (UFC0HV25, Millipore) and concentrated with 100K MW cut-off (MWCO) Vivaspin spin concentrators (Sartorius Stedim Biotech, Aubagne Cedex, France). Native MUB was purified by gel filtration using a pre-packed gel filtration Superose 6 HR 16/50 column on an AKTA Fast Protein Liquid Chromatography (FPLC) system

(GE Healthcare, New Jersey, USA). MUB elution fractions were tested by electrophoresis using Tris acetate SDS-PAGE, and the protein concentration determined using a NanoDrop ND-1000 (Thermo Scientific, Waltham, USA).

2.5 Microbiology

2.5.1 *Lactobacillus reuteri* strains and culture conditions

Lactobacillus reuteri (L. reuteri) strains used in this study are shown in Table 2.2. De Man, Rogosa and Sharpe (MRS) culture medium used is composed of 10 mg ml^{-1} peptone, 8 mg ml^{-1} "Lab-Lemco", 4 mg ml^{-1} yeast extract, 20 mg ml^{-1} glucose, 2 mg ml^{-1} dipotassium hydrogen phosphate, 5 mg ml^{-1} sodium acetate $3H_2O$, 2 mg ml^{-1} triammonium citrate, 0.2 mg ml^{-1} magnesium sulphate $7H_2O$, 0.05 mg ml^{-1} Manganese sulphate $4H_2O$ and 1 ml sorbitan mono-oleate. *L. reuteri* cultures were grown from frozen stocks stored at -80 °C in MRS containing 20-50 % (v/v) glycerol. Bacterial cells were grown for 20 h at 37 °C to stationary phase. *L. reuteri* cells were then subcultured in MRS (0.2 % volume) and grown for 16 h at 37 °C to early stationary phase. Cells were centrifuged at 4000 rpm for 5 min at 15 °C, followed by two washes in PBS, and re-suspended in PBS. Using optical density measurements at 600 nm (OD_{600}), a volume of cell suspension representing 1 x 10^9 cells ml^{-1} was collected for further experiments.

Table 2.2| List of *L. reuteri* strains and their sources.

Strain	Isolate	Reference
100-23C	Rat	[389]
DSM 20016	Human	[390]
ATCC 53608	Pig	[378]
1063N	Pig	[391]

2.6 Molecular techniques

2.6.1 Total RNA extraction

2.6.1.1 Total RNA extraction from epithelial tissue

Small intestine and colon epithelial scrapes were collected from C57BL/6 or TCR$\delta^{-/-}$ mice and immediately transferred into 1 ml Tri-reagent and frozen on dry ice. For the extraction of RNA, Tri-reagent samples were thawed, vortexed and incubated for 5 min at RT. 200 µl chloroform was added and vortexed for 15 s followed by a 2 min incubation at RT. Samples were centrifuged at 12 000 x*g* for 15 min at 4 ºC. The upper transparent phase was transferred into a new RNase-free Eppendorf tube. 500 µl isopropanol was added and mixed by inversion, before centrifuging as above. The supernatant was poured off, 1 ml of 70 % ethanol added and mixed by inversion. Samples were centrifuged as above for 10 min. The supernatant was discarded and the pellet left to dry. The pellet was re-suspended in 30 µl RNase-free water, incubated for 5 min and transferred into a new RNase-free Eppendorf tube. DNase I treatment and RNA clean-up was performed using the RNase-free DNase Set and RNeasy Mini kit (Qiagen, West Sussex, UK), following the manufacturer's instructions. The purity, integrity and quantity of RNA was analysed using a NanoDrop ND-1000 and a 2100 Bioanalyser (Agilent Technologies, CA, USA).

2.6.1.2 Total RNA extraction from cell cultures

RNA was extracted from cultured cells using the Rneasy Mini kit (Qiagen, West Sussex, UK), following the manufacturer's instructions. DNase I treatment and RNA clean-up was performed using the RNase-free DNase Set and RNeasy Mini kit (Qiagen, West Sussex, UK), following the manufacturer's instructions. The purity, integrity and quantity of RNA was analysed using a NanoDrop ND-1000 and a 2100 Bioanalyser.

2.6.2 Gene microarray analysis using GeneChips

Target preparation for gene expression analysis was performed by the reverse transcription-*in vitro* transcription (IVT) method using the GeneChip® 3' IVT express kit (Affymetrix, CA, USA), following the manufacturer's instructions. During this process, total RNA (see section 2.6.1.1) was reverse transcribed to synthesize first-strand cDNA. This cDNA was converted to double stranded DNA to serve as a template for transcription. *In vitro* transcription synthesized anti-sense RNA (aRNA) and incorporated a biotin-conjugated nucleotide. The aRNA was then purified to remove unincorporated NTPs, salts, enzymes, and inorganic phosphate. Fragmentation of the biotin-labelled aRNA prepared the sample for hybridisation onto GeneChip 3' expression arrays. This hybridisation was performed following the manufacturer's instructions of the GeneChip® Hybridization, Wash, and Stain Kit (Affymetrix, CA, USA). For this, a hybridisation cocktail was prepared, including the fragmented target, probe array controls, BSA, and herring sperm DNA. This was hybridised to the probe array during a 16 h incubation. Immediately after hybridisation, the probe array underwent an automated washing and staining (streptavidin phycoerythrin conjugate) protocol on the fluidics station. This was followed by scanning of the hybridised probe array by the GeneChip® scanner 3000. The amount of light emitted at 570 nm is proportional to the bound target at each location on the probe array. Custom ClygoV4 oligonucleotide array GeneChips (Glyco_v4a520670F; Scripps Institute, CA, USA) were used for gene expression analysis of ~1260 human probe-ids and ~1246 mouse probe-ids related to glyco-genes (details in appendix 5). GeneChips were analysed by the Scripps institute applying the Limma package in the R software, RMA Express 1.0 and the dChip program to estimate fold changes and standard errors, and to perform quantile normalisation and data normalisation. This allowed the generation of heat maps for data interpretation.

2.6.3 Gene expression analysis using quantitative RT-PCR (qRT-PCR)

Total RNA (see sections 2.6.1.1 and 2.6.1.2) was used to synthesise cDNA using the QuantiTect reverse transcription kit (Qiagen, West Sussex, UK), following the manufacturer's instructions. The qRT-PCR was performed using the QuantiFast SYBRr Green PCR kit (Qiagen, West Sussex, UK), and run in an ABI7500 Taqman

thermocyler (Life Technologies, Paisley, UK). All samples were run in triplicate or, where possible, quadruplicate for each gene tested. The results were analysed using the Taqman SDS system software and Microsoft Excel. Results are representative of the relative quantitation to 18S RNA using the formula $2^{-\Delta Ct}$. Primers for all target genes tested are shown in Table 2.3.

Table 2.3| Primer sequences of target genes used for qRT-PCR expression analysis.

Gene	Primer sequence
Reference gene	
18S	F 5'CACGGGAAACCTCACCCGGC3' R 5'CGGGTGGCTGAACGCCACTT3'
Mucin genes	
Muc1	F 5'TCCTTGCCCTGGCAGTGTGC3' R 5'CCGCCAAAGCTGCCCCAAGT3'
Muc2	F 5'GGCCTCACCACCAAGCGTCC3' R 5'TGGGCTGGCAGGTGGGTTCT3'
Muc3	F 5'GGTCTTCCATGAAACAGACACAGT3' R 5'TGAAGGCCAGCCTCAGCAGGA3'
Muc4	F 5'TTGCACCTGTCCCCCCTGCCT3' R 5'GTTCGCCACCGAGGCGTTGA3'
Muc5AC	F 5'CTGCCCCAAAGGCACCTTCTTAGA3' R 5'TGGGTGCAGGTGCAAATGGCC3'
Muc6	F 5'TGCATGCTCAATGGTATGGT3' R 5'TGTGGGCTCTGGAGAAGAGT3'
Muc12	F 5'GGGACGCTGACCTGCGTGAA3' R 5'TTGGGGCACACGCATTGGGG3'
Muc13	F 5'GCGGTGGAAGCACAGGTCCC3' R 5'TGCTGACCGTGAAGGGGCTG3'
Muc17	F 5'CACACTGGGGCAGAAGGGCG3' R 5'AGGCAGAGGCACTGGGGTCC3'
Muc19	F 5'ACTGGAACCACAGCCAAATC3' R 5'CTACGGCCTGTTTTTCGGTA3'
Glycosyltransferase genes	
C1GalT1	F 5'ACTTAGCTCTGGGAAGGTGCATGG3' R 5'ACAGCATCCAGGACCCTCTATGGGA3'
C1GalT2	F 5'TGGAGCCGTTCTAGATGCGGAAAA3' R 5'GGGGCTTGCAGATGGTGATGCT3'
C2GnT1	F 5'GCTTGATAGGAACTTGGCAGCAC3' R 5'CACCTTCTGGATTTCTTCTGGGTC3'
C2GnT2	F 5'ACCTTCACTCCACATCACTCACGG3' R 5'TTATTCAGCAGAGCCTGGGTCACC3'

C2GnT3	F 5’GCCGCTGTTCTTGCTGTTTTG3’ R 5’GGCCAGATTCTCCTCTCTCAAACG3’
C3GnT	F 5’GGCCAGATTCTCCTCTCTCAAACG3’ R 5’AGTGCTCCGCTGTCCAGTCCA3’
Glyco genes	
IL-33	F 5’TCCTGTCTGTATTGAGAAACCTGA3’ R 5’TTATGGTGAGGCCAGAACGG3’
B3GALT5	F 5’TCACTCACCGGCTGCTCTTT3’ R 5’TGAGCCATCTTTGCCGAGTA3’
CD48	F 5’TGGGAACTGGATTTCAAGGTCAT3’ R 5’TCAGACTCGAAGATTGTCTTTGT3’
CD74	F 5’GGCTAGAGCCATGGATGACC3’ R 5’CACAGGTTTGGCAGATTTCGG3’
LGALS1	F 5’TCAATCATGGCCTGTGGTCT3’ R 5’ATGGGCATTGAAGCGAGGAT3’
COLEC12	F 5’AGGTTTGGTATTCAGGAGGGG3’ R 5’GGTGAGATGTCTCCATGCCA3’
LUM	F 5’ATCCAGAGGCTGGCGTGATT3’ R 5’TCTGTGACCTTACTCTCTTGACAC3’
ANG4	F 5’TGGCCAGCTTTGGAATCACTG3’ R 5’ACAGTATCTGTCGTCCCGGCC3’
Sialyltransferase genes	
ST3Gal-I	F 5’GCCCACTATGCCAGACACTT3’ R 5’TCAGCAGAGTCAAACCCAGC3’
ST3Gal-III	F 5’TGCTGCGGTCATGTAGGAAA3’ R 5’CAGCGGAGTCAAGGGAAAGA3’
ST3Gal-IV	F 5’GGCTCTGGTCCTTGTTGTTG3’ R 5’TCCCTAGAACGGTTGCCAAAA3’
ST3Gal-VI	F 5’CACCCCAAAAGCGCAGATTTATT3’ R 5’CCTGCCTGAAACAGAGTCCAA3’
ST6Gal-I	F 5’TAGACGGGGACGTATCGGA3’ R 5’AAAAACCATCTCAGCATCCGGC3’
ST6Gal-II	F 5’CTAGCCAGCAGGTTTTGTCCA3’ R 5’AAAGAGCATTCGTTGTCGCC3’
ST6GAlNAc-I	F 5’TGTTAGGGACCAGCCATCCA3’ R 5’ATGAACTGGCACCTGGAATC3’
ST6GAlNAc-II	F 5’CGGATGTTGTTGCTCGTTGC3’ R 5’AGTCGGCTCTTTCTGTTTTCC3’

2.7 Tissue histology and antibody-based techniques

2.7.1 Periodic acid Schiff and alcian blue (PAS/AB) staining

Formalin-fixed paraffin-embedded tissue sections were cut, deparaffinised and hydrated as in section 2.3.1.2. Acidic mucins were stained with 1 % alcian blue in 3 % acetic acid (pH 2.5) for 15 min, followed by two washes in still tap water. Sections were treated with 0.5 % periodic acid for 5 min, followed by a further two washes in still tap water. Neutral mucins were stained with Schiff's reagent for 10 min. Tissue sections were washed thoroughly in still tap water. Nuclei were stained with haematoxylin for 1 min, followed by a further two washes in still tap water and brief differentiation in acid-alcohol (96 % ethanol, 1 % HCl). Sections were dehydrated and mounted as in section 2.3.1.2. The number of goblet cells per crypt was calculated from an average of ten crypts per tissue section, for seven mice. Average Crypt lengths (µm) were calculated in a similar manner.

2.7.2 Phloxine-tartrazine staining

Formalin-fixed paraffin-embedded tissue sections were cut, deparaffinised and hydrated as in section 2.3.1.2. Nuclei were stained with haematoxylin for 5 min, followed by three washes in tap water. Slides were briefly differentiated in acid-alcohol and washed two times in tap water. The haematoxylin staining was intensified in Scott's solution (20 mg Calcium chloride, 30 mg magnesium sulphate in 1 L of distilled water) for 1 min, to increase the contrast of the haematoxylin staining. Sections were washed once in tap water. Cytoplasmic components were then stained with Phloxine solution (1 g Phloxine B and 1 g calcium chloride in 100 ml of water) for 20 min. Slides were briefly washed in two changes of tap water. Tissue sections were differentiated with tartrazine in Cellosolve (5 g tartrazine (Fluka Chemika, Buchs, Switzerland) in 200 ml Cellosolve) until only the granules stained intensely red (controlled microscopically). Slides were rinsed briefly in 95 % ethanol, dehydrated, and mounted as in section 2.3.1.2. The number of paneth cells per crypt was calculated from an average of 10 crypts per tissue section, for seven mice.

2.7.3 Fluorescence staining

Formalin-fixed paraffin-embedded tissue sections (5 µm) or frozen tissue sections (6-8 µm) were fixed for 4 min in acetone-methanol (50 % acetone, 50 % methanol), dried and circled with a wax pen. Slides were then washed in wash buffer (PBS, 0.05 % BSA) for 5 min at 60 rpm, followed by a blocking step in block solution (Tris-NaCl-Block (TNB) buffer (PerkinElmer, Cambridgeshire, UK) containing 5 % fresh goat serum (Dako)) for 30 min. Slides were washed as above, dried, and incubated O/N with primary antibody (diluted in TNB buffer) in a humid glass container at 4 °C, or for 2 h with lectins. The primary antibody/lectin was removed and the slides washed three times as described above. Briefly dried slides were incubated for 1 h in the dark with secondary antibody diluted in PBS. Slides were washed in the dark three times as described above. Nuclei were stained with 4',6-diamidino-2-phenylindole (DAPI; Life Technologies Ltd, Paisley, UK) for 10 min in the dark. Slides were washed in the dark three times as described above, before drying and mounting in Hydromount mounting medium (National Diagnostics, Hessle, UK). Stained slides were stored in the dark at 4 °C. The sources and concentrations of antibodies and lectins used are shown in Table 2.4. Fluorescent lectin staining was semi-quantitatively assessed using the ImageJ software system developed by the National Institutes of Health.

Table 2.4| Antibodies and lectins, concentrations and suppliers used for fluorescence staining

Antigen/protein/ sugars/DNA stained	Primary antibody	Secondary antibody/lectin /stain	Conc. [µg/ml]
Chromogranin A	Rabbit polyclonal anti-Chromogranin A (Abcam)	Goat anti-rabbit Alexa 488 (Invitrogen)	2;10
DNA	-	4',6-diamidino-2-phenylindole (DAPI) (Invitrogen)	25
Gal-β(1,3)-GalNAc	-	PNA (Vector Laboratories)	40
IL-33	Rabbit polyclonal anti-IL-33 (Santa Cruz)	Goat anti-rabbit Alexa 488 (Invitrogen)	20;10
Lysozyme	Rabbit anti-Lysozyme concentrate (ZYMED/Invitrogen)	Goat anti-rabbit Alexa 488 (Invitrogen)	1/20;10
MUB	Rabbit anti-MUBR5 (titre 1:200 000)	Goat anti-rabbit Alexa 488 (Invitrogen)	1/100;10
MUC1	Rabbit anti-MUC1 (Santa Cruz)	Goat anti-rabbit Alexa 488 (Invitrogen)	4;10
MUC2	Rabbit anti-MUC2 (Santa Cruz) Mouse anti-MUC2 (Abcam)	Goat anti-rabbit Alexa 488 (Invitrogen) Goat anti-mouse Rhodamine (Abcam)	4;10 10;10
MUC5AC	Rabbit anti-MUC5AC (Santa Cruz)	Goat anti-rabbit Alexa 488 (Invitrogen)	4;10
N-acetyl-D-glucosamine (GlcNAc/NAG)	-	WGA (Vector Laboratories)	40
α-2,3 linked sialic acid	-	MAA (EY Laboratories)	75
α-2,6 linked sialic acid	-	SNA-I (Vector Laboratories)	75
Isotype control	Rabbit IgG (Vector Laboratories)	Goat anti-rabbit Alexa 488 (Invitrogen)	4/10;10
Isotype control	Mouse IgG2b-FITC (Caltag)		10

2.7.4 Periodate treatment

Formalin-fixed paraffin-embedded mouse and human gastric tissue sections were cut, deparaffinised and hydrated as in section 2.3.1.2. Slides were washed in 0.1 M NaAc buffer (0.35 % acetic acid, 0.32 % (w/v) sodium acetate; pH 4.5 or pH 5.5) twice for 5 min, followed by an incubation in periodate buffer (10 mM periodate in 0.1 M NaAc buffer) pH 4.5 (2 h) or pH 5.5 (20 min) in the dark. Slides were washed in 0.1 M NaAc buffer once for 5 min, and twice in PBS. Tissue was reduced by immersion in borate buffer (50 mM $NaBH_4$ in PBS, pH 7.6) for 30 min. Slides were washed twice in PBS for 5 min before blocking in block solution (section 2.7.3) for 1 h. Slides were rinsed with PBS and incubated with lectins or MUB (4 µg ml^{-1} in PBS) O/N at 4 °C. Following three washes in PBS-T for 10 min, slides were incubated with neat antiserum of rabbit anti-MUBR5 diluted in PBS for 3 h. Slides were washes three times in PBS-T for 10 min, and incubated with goat anti-rabbit Alexa Fluor 488 for 1 h in the dark. Following two washes in PBS-T for 10 min, nuclei were stained with DAPI for 10 min in the dark, washed three times and mounted in Hydromount. Sources and concentrations of antibodies and lectins used are shown in Table 2.4.

2.7.5 MUB binding to tissue sections

Mouse and human gastric, small intestine and colon frozen tissue sections were cut, fixed and blocked as described in section 2.7.3. Sections were incubated with 4 µg ml^{-1} MUB diluted in PBS, for 2 h. Two washes (5 min, 60 rpm) were performed before completing the staining protocol as in 2.7.3. The sources and concentrations of antibodies used are shown in Table 2.4.

2.8 Cell culture

2.8.1 *Ex vivo* organoid culture assays

2.8.1.1 Small intestinal crypt isolation

The small intestine was exteriorised from the mice and placed in a Petri dish containing PBS. The SI was cut open longitudinally and washed three times in PBS to remove any faecal matter and luminal contents. The small intestine was cut in 5 mm pieces into a 50 ml Falcon tube containing 15 ml PBS with 2 mM EDTA. This was kept on ice for 30-40 min. Small intestinal crypts were separated from the rest of the tissue through vigorous shaking in the 50 ml Falcon tube. This was repeated 3-4 times in fresh PBS, to obtain a high crypt fraction used for the isolation. This fraction was passed through a 70 µm filter to remove villi. The sample was divided and transferred into two 15 ml tubes (to reduce pellet size), centrifuged at 300 x*g* for 5 min and the supernatant discarded. The pellet was resuspended in 200 µl Matrigel (BD Biosciences, Oxford, UK) and immediately plated out on a pre-warmed 96-well plate in small domes. The plate was incubated at 37 °C for 10 min to allow for the polymerisation of the Matrigel. To each well, 200 µl of complete organoid growth medium (Table 2.6) was added and the plate incubated at 37 °C/5 % CO_2 for culture.

Table 2.5| Composition of complete organoid growth medium describing component functions and concentrations.

Medium/supplement	Function	Conc.
DMEM/F12 (Invitrogen)	Cell culture medium	neat
N2 (Invitrogen)	Recommended for the growth and expression of neuroblastomas and for the survival and expression of post-mitotic neurons in primary cultures from both the peripheral nervous system (PNS) and the central nervous system (CNS).	1x
B27 (Invitrogen)	Supports the growth of neuronal cells without an astrocyte feeder layer and is effective for the growth of neuronal tumour cell lines.	1x
Penicillin/Streptomycin (Lonza)	Effective against Gram-negative and Gram-positive bacteria	1000/1000ml-1
GlutaMax (Invitrogen)	Prevents degradation and ammonia build-up even during long-term cultures	1x
Recombinant murine epidermal growth factor (EGF) (Peprotech)	regulation of cell growth, proliferation, and differentiation	50 ng ml-1
Noggin (Peprotech)	Induces expansion of crypt structures	100 ng ml-1
R-Spondin 1 (R&D Systems)	A Wnt agonist that induces marked crypt hyperplasia *in vivo*	500 ng ml-1
N-acetyl cysteine	Promotes cell growth and survival, and reduces oxidative stress	1mM

2.8.1.2 Small intestinal crypt culture

The complete organoid growth medium was replaced every 3 days, and confluent organoids were passaged every 7 days. To do this, the media was removed from each well and the Matrigel dome broken up using a p1000 pipette. The same pipette tip was used to flush the well twice with 1 ml DMEM/F12. The crypt-media solution was then centrifuged at 300 x*g* for 5 min, and the pellet re-suspended and re-plated as described above.

2.8.1.3 Staining

Organoid cultures used for fluorescence staining were plated out in 24-well plates on glass coverslips, with 1 ml of complete growth medium (see Table 2.5) per well. All fluorescence staining was performed on organoids cultured for four days. The medium was removed from each well and washed with PBS for 5 min (all consecutive washing steps are 5 min). Organoids were fixed with 1 ml 4 % paraformaldehyde (PFA) for 30 min, followed by a further two wash buffer (PBS containing 0.05 % BSA) steps. Organoids were permeabilised with 1 ml 0.2 % Triton X-100 in wash buffer for 60 min. Two washes were performed before blocking with block solution (see section 2.7.3) for 60 min. Organoids were washed in wash buffer twice, followed by an O/N primary antibody (diluted in TNB buffer) incubation at 4 °C. Primary antibody solution was removed and organoids washed three times in wash buffer. Secondary antibody (diluted in PBS) was added to each well for 60 min in the dark. Organoids were washed three times in wash buffer, followed by a 10 min incubation with DAPI (diluted in PBS). Organoids were washed three times in wash buffer. Coverslips were removed from the wells, mounted with Hydromount on glass microscopic slides, and left to dry overnight at 4 °C. The sources and concentrations of antibodies and lectins used are shown in Table 2.4.

2.8.1.4 Small intestinal organoid treatment

Small intestinal organoids were stimulated with 100 ng ml^{-1} recombinant human keratinocyte growth factor (KGF, Peprotech, NJ, USA) in organoid culture medium for 24 h.

2.8.2 HT29-MTX cell culture assays

2.8.2.1 Maintenance of cell stocks

HT29-MTX frozen vials were taken from liquid nitrogen and thawed rapidly at RT. 1 ml of cells was added to 9 ml of pre-warmed complete culture medium (DMEM (Lonza,

Basel, Switzerland) supplemented with 10 % heat inactivated (HI) FCS (Biosera, Sussex, UK) and 1 % L-Glutamine (Lonza, Basel, Switzerland)) and centrifuged at 1000 x*g* for 5 min. The cell pellet was resuspended in 7 ml of complete medium and transferred to a 25 cm^2 culture flask for initial culture. Once confluent, cells were transferred to a 75 cm^2 culture flask and subsequent cell cultures were maintained in 75 cm^2 culture flasks. The volume of complete medium in each flask was 20 ml and was changed every other day. Cells were used between passages 41-60.

2.8.2.2 Cell passaging and seeding

Cells were passaged at a confluency of 80-90 %. The medium was removed from the 75 cm^2 culture flask and replaced with 7 ml of warm Trypsin/EDTA (T/E; Lonza, Basel, Switzerland). Cells were detached from the culture flask surface during a 10-15 min T/E incubation at 37 °C. T/E action was neutralised by the addition of 3 ml of complete medium. Cells were thoroughly suspended in this solution, transferred to a 15 ml Falcon tube and centrifuged at 1000 x*g* for 5 min. A small aliquot was taken and a 10 µl sample counted using a bright line haemocytometer, with four fields counted and averaged to calculate the cell count ml^{-1}. The volume of cell suspension required for the intended cell seeding density was calculated using the formula $z = (1000/n)x$, where z is the µl volume of cell suspension, n is the cell count ml^{-1} , and x is the total number of cells required. Following centrifugation, the supernatant was poured off and the cell pellet thoroughly resuspended in 10 ml of complete medium to form a homogenous single-cell suspension. For cell culture maintenance, a 1:10 or 3:10 ratio was transferred into a new 75 cm^2 culture flask and grown until confluency was reached. For all experiments, cells were seeded at 4×10^4 cells $well^{-1}$ in 24-well plates. For staining experiments, cells were seeded onto glass coverslips, and for all other experiments cells were seeded directly onto the plate. Culture medium in the 24-well plates was changed daily.

2.8.2.3 Staining

Media was removed from the wells, washed with PBS and fixed with 4 % PFA for 10 min. Wells were washed three times with wash buffer. Cell monolayers were incubated with 500 µl primary antibody diluted in TNB buffer O/N at 4 °C. Three washes with wash buffer were performed. Cell monolayers were incubated with secondary antibody diluted in PBS for 1 h in the dark. This was followed by three washes with wash buffer before mounting the slides in Hydromount. Acidic mucins were stained with alcian blue (1 % alcian blue in 3 % acetic acid) for 5 min. Monolayers were washed in PBS three times for 5 min at 80 rpm before mounting in DEPEX mounting medium. Cells were stained with lectins for 2 h, followed by three washes in PBS and mounting of slides in Hydromount. The sources and concentrations of antibodies and lectins used are shown in Table 2.4.

2.8.2.4 *Lactobacillus reuteri* adhesion assays

HT29-MTX cell monolayers (Day 14) were washed twice with PBS. *L. reuteri* cells, prepared as in 2.5.1, were incubated with HT29-MTX cell monolayers at a density of 1 x 10^8 cells ml^{-1} in DMEM (without FCS), for 3 h at 37 °C. Unbound *L. reuteri* cells were removed through three washed with PBS, followed by trypsinisation of bound *L. reuteri* cells and HT29-MTX cells with 250 µl T/E at 37 °C for 10-15 min. T/E was neutralised with 750 µl PBS. Serial dilutions of the suspended *L. reuteri* bacteria in PBS were plated out on modified MRS (MRS supplemented with fructose and maltose) and incubated anaerobically for 24 h at 37 °C. Colony counts were performed and the % adhesion calculated using the formula % adhesion= ratio of colonies/ initial colony count.

Binding of *L. reuteri* strains to the HT29-MTX monolayer was visualised through fluorescence staining. *L. reuteri* cells prepared as in 2.5.1 were resuspended in 1 ml carbonate-bicarbonate buffer. To this, 10 µl of Fluorescein isothiocyanate (FITC) was added to a final concentration of 0.1 mg ml^{-1}. Cells were fluorescently labelled by incubating in the dark for 1 h, before washing three times with PBS to remove any unbound FITC. The FITC-labelled *L. reuteri* cells were resuspended in the desired volume of DMEM, and 1 ml of suspension added to the HT29-MTX monolayers (Day

14), at a cell density of 1 x 10^8 cells ml^{-1}. Plates were incubated in the dark at 37 °C for 3 h, followed by three washes with PBS to remove unbound bacteria. All wells were fixed, stained for MUC5AC using rabbit anti-MUC5AC (Santa Cruz Biotechnology, Heidelberg, Germany), and mounted as in 2.7.3.

L. reuteri adhesion was assessed in competition with sialic acid sugars. *L. reuteri* strains were pre-incubated with sialic acid sugars (N-acetylneuraminic acid or 6'-O-Sialyllactose (Glycom, Lyngby, Denmark); 100 mM) for 15 min. HT29-MTX cell monolayers (Day 14) were washed twice in PBS and incubated with the *L. reuteri* strains at a density of 1 x 10^8 cells ml^{-1} in DMEM (without FCS), for 3 h at 37 °C.

2.8.2.5 Benzyl-α-GalNAc treatment

HT29-MTX monolayers were cultured for 14 days in 24-well plates on glass coverslips. The medium was replaced with DMEM (without FCS) containing 5 mM Benzyl 2-acetamido-2-deoxy-α-D-galactopyranoside (Benzyl-α-GalNAc). Control wells contained DMEM only. HT29-MTX monolayers were cultured for 24 h in the presence of Benzyl-α-GalNAc. The culture medium was removed and wells washed once with PBS. HT29-MTX monolayers were fixed and stained as in section 2.8.2.3. To test the reversibility of the effects of Benzyl-α-GalNAc, HT29-MTX monolayers cultured for 24 h with 5 mM Benzyl-α-GalNAc were washed once and cultured for a further 24 h in culture medium without Benzyl-α-GalNAc. Staining was repeated as above.

2.8.2.6 MUB binding

HT29-MTX monolayers were cultured for 14 days in 24-well plates on glass coverslips. The medium was removed and monolayers washed with PBS before fixation with 4 % PFA for 10 min. HT29-MTX coverslips were washed three times with PBS and blocked in block solution (see section 2.7.3) for 30 min. Following two further washes in PBS, coverslips were incubated with 4 µg ml^{-1} MUB diluted in PBS for 2 h. Cells were washed three times with PBS and incubated with antiserum of rabbit anti-MUBR5

diluted in PBS O/N at 4 °C. Three PBS washes were performed before incubation with goat anti-rabbit Alexa Fluor 488 for 1 h in the dark. Coverslips were washed three times in PBS and mounted in Hydromount. Sources and concentrations of antibodies and lectins used are shown in Table 2.4. MUB adhesion was assessed in competition with sialic acid sugars. MUB (4 µg ml^{-1}) was pre-incubated with sialic acid sugars (N-acetylneuraminic acid or 6'-O-Sialyllactose (Glycom, Lyngby, Denmark); 100 mM) for 1 h. HT29-MTX cell monolayers (Day 14) were washed twice in PBS and incubated with MUB for 2 h.

2.9 Statistical analysis

Data for all experiments carried out in this study was analysed using Microsoft Excel. The Student's T-test was performed for statistical analysis, with degrees of significance represented as *$p<0.05$, **$p<0.01$, ***$p<0.001$ and ***$p<0.0001$.

Chapter 3 Impact of gamma delta (γδ) IELs on murine intestinal mucus properties

3.1 Introduction and objectives

The mammalian gastrointestinal (GI) tract contains a dynamic community of trillions of microorganisms [42]. These microorganisms establish a mutualistic relationship with the host, making essential contributions to mammalian metabolism while occupying a protected, nutrient-rich environment [317]. However the close association of a dense bacterial community with intestinal tissues poses a serious risk to the host. Several immune mechanisms work in concert to limit commensal exposure to the epithelial surface [42]. The composition and functions of the mucus layer (first line of immune defense), and the roles of γδ IELs in the GI tract (second line of immune defense) are discussed in detail in Chapter 1. However, whether γδ IELs contribute to maintaining an intact mucus layer in an homeostatic environment and/or following mucosal injury is currently unknown. In this study the TCRδ$^{-/-}$ mouse model [386] was used to shed light on the role of γδ IELs in modulating mucus expression, organisation and glycosylation.

The objectives of this study are to:

1. Analyse the response of TCRδ$^{-/-}$ mice to DSS-induced colitis.
2. Characterise TCRδ$^{-/-}$ mice in terms of mucus properties, including mucus organisation, mucin expression and glycosylation.
3. Investigate underpinning mechanisms of γδ IEL function using an *ex vivo* SI organoid culture system.

3.2 TCRδ$^{-/-}$ mice are more susceptible to DSS-induced colitis

The use of dextran sodium sulphate (DSS) administered in drinking water is a well-established model system used for the induction of intestinal epithelial cell (IEC) damage [392-394]. Here, DSS-induced acute colitis studies were undertaken in C57BL/6 wild type (wt) and TCRδ$^{-/-}$ mice to compare DSS-susceptibility between the two groups of mice. Acute colitis was induced by replacing normal drinking water with a 2.5 % w/v solution of DSS in drinking water provided ad libitum for 7 days. For recovery experiments, mice were given DSS in drinking water for 3 days, followed by 3 days of drinking water without DSS. The clinical severity of colitis was assessed on the basis of stool consistency, faecal blood content and weight loss as determined daily throughout the DSS study. These clinical parameters were scored as the disease activity index (DAI) as reported by Cooper HS and Murthy SN [393, 395]. Colon length was measured on the final day of the study, as a further measure of severity of colitis. Haematoxylin and Eosin Y (H&E) stained tissue sections were scored blindly by a histologist (James Sington, NNUH) on the basis of epithelial injury, chronic and acute inflammatory infiltrates, number of goblet cells and oedema.

Figure 3.1 demonstrates that TCRδ$^{-/-}$ mice show increased susceptibility to DSS-induced colitis compared to wt mice, in agreement with previous reports [256, 386]. After 7 days of treatment, TCRδ$^{-/-}$ mice rapidly developed severe colitis, and the DAI was significantly higher ($p=0.001$) within 4 days of DSS treatment, compared to DSS-treated wt mice (Figure 3.1A). Furthermore, colon length was significantly shorter in TCRδ$^{-/-}$ mice ($p=0.01$) compared to wt mice, providing a further assessment parameter for the severity of DSS-induced colitis (Figure 3.1B). Blinded histological examination of H&E-stained tissue sections showed that DSS-treated TCRδ$^{-/-}$ mice displayed an increased extent of epithelial injury, showing diffuse injury in more than 50 % of the circumference of the tissue ($p=0.02$) in the distal colon, compared to DSS-treated wt mice (Figure 3.1C). However, the overall histological damage score that combines all parameters assessed (extent of epithelial injury, chronic inflammatory infiltrate, acute inflammatory infiltrate, goblet cell loss and oedema), was similar for the mid-colon and distal colon between the two groups of mice (Figure 3.2), indicating that not all criteria were significantly affected by the lack of γδ IELs at day 7 of this DSS-colitis model.

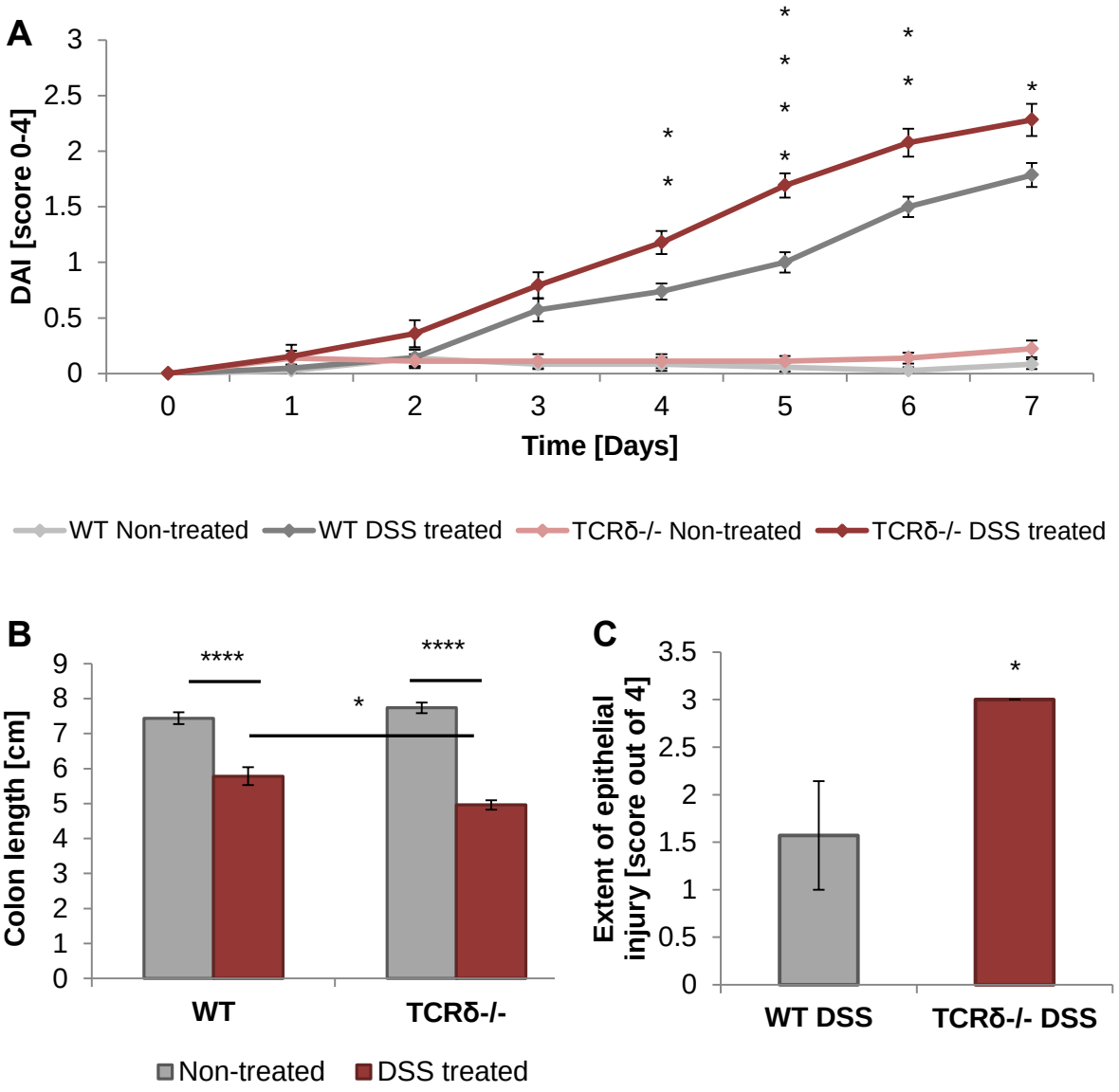

Figure 3.1| TCRδ$^{-/-}$ mice are more susceptible to DSS-induced colitis compared to wt mice. TCRδ$^{-/-}$ and wt mice (n=13 each) were given 2.5 % DSS in drinking water for 7 days. The DAI score for all four groups of mice (wt non-treated, wt DSS-treated, TCRδ$^{-/-}$ non-treated and TCRδ$^{-/-}$ DSS-treated) was calculated daily on the basis of stool consistency, faecal blood content and weight loss (A). Colon length was measured at autopsy using a millimetre ruler on the final day of the DSS study (B). The extent of epithelial injury was scored blindly from H&E stained tissue sections of the distal colon of DSS-treated wt and TCRδ$^{-/-}$ mice (C). DAI, disease activity index; H&E, haematoxylin and Eosin Y; DSS, dextran sodium sulphate; *p<0.05; **p<0.01; ***p<0.001; ***p<0.0001.

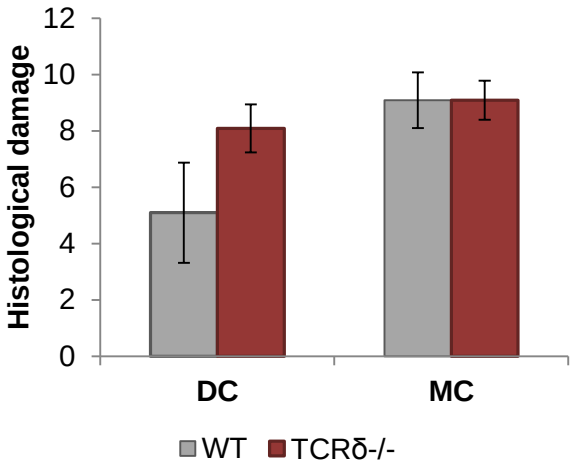

Figure 3.2| Histological damage of distal colon and mid colon tissue of DSS-treated wt and TCRδ$^{-/-}$ mice. The average histological damage score (n=16 each) was calculated from blinded histology scoring of six parameters: epithelial injury, extent of epithelial injury, chronic inflammatory infiltrate, acute inflammatory infiltrate, number of goblet cells, oedema. DC, distal colon; MC, mid-colon.

Figure 3.3 indicates that TCRδ$^{-/-}$ mice showed delayed recovery from DSS treatment, as assessed by the DAI, in agreement with previous reports showing that TCRδ$^{-/-}$ mice are more prone to DSS-induced colitis and show delayed tissue repair after termination of DSS treatment [256]. The DAI was measured daily for 3 days following the termination of DSS treatment. Results showed that at day 5 and day 6 of recovery, DSS-treated TCRδ$^{-/-}$ mice had a significantly higher DAI ($p=0.03$) compared to DSS-treated wt mice, supporting the role of γδ IELs in aiding the recovery process following mucosal injury [255-257].

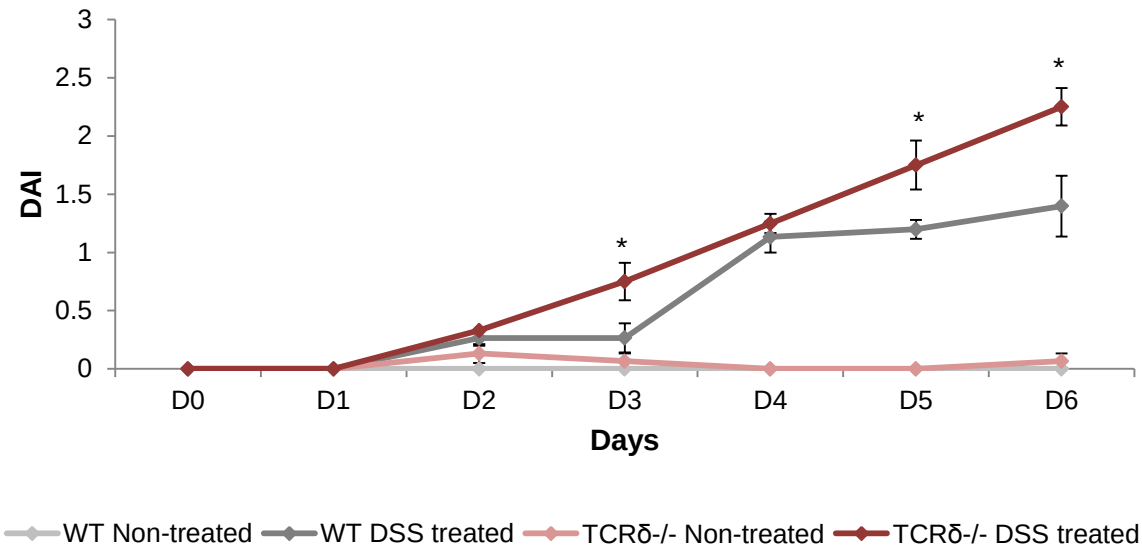

Figure 3.3| TCRδ$^{-/-}$ mice show delayed recovery following DSS-induced colitis. TCRδ$^{-/-}$ and wt mice (n=5) were given 2.5 % DSS in drinking water for 3 days followed by 3 days of normal drinking water without DSS. The DAI score for all four groups of mice (wt non-treated, wt DSS-treated, TCRδ$^{-/-}$ non-treated and TCRδ$^{-/-}$ DSS-treated) was calculated daily on the basis of stool consistency, faecal blood content and weight loss. DAI, disease activity index; DSS, dextran sodium sulphate; *p<0.05.

3.3 Impact of γδ IELs on goblet cells, crypt length and Paneth cells

Goblet cells are specialised mucus-secreting cells that form one of the four differentiated cell types found in the intestinal epithelium [112, 396]. To investigate whether alterations in the mucus of TCRδ$^{-/-}$ mice may contribute to their increased susceptibility to DSS-induced colitis, the morphology of intestinal crypts and the number of goblet cells in wt and TCRδ$^{-/-}$ mice was assessed in healthy and DSS-treated tissue. Paneth cells are lysozyme-secreting cells [31] of the SI epithelium that can exist as an intermediate between Paneth and goblet cells, and have been associated with mucus production [397], thus their relative numbers were also compared in wt and TCRδ$^{-/-}$ mice in this study.

Paraffin-embedded SI and colon tissue sections of healthy and DSS-treated wt and TCRδ$^{-/-}$ mice were stained with periodic acid-Schiff and alcian blue (PAS/AB) to analyse epithelial goblet cells. From this, average goblet cell counts and crypt length measurements were performed in a blinded manner. Paraffin-embedded SI tissue of wt and TCRδ$^{-/-}$ mice was stained with phloxine-tartrazine for the visualisation of crypt Paneth cells. This allowed the calculation of the average Paneth cell number. PAS/AB staining confirmed that mucus was stored within SI and colonic goblet cells in wt and TCRδ$^{-/-}$ mice (Figure 3.4A). Histology revealed a 1.2-fold decrease in the number of goblet cells per crypt in the SI (ileum) of TCRδ$^{-/-}$ mice ($p=0.024$), whereas a 1.3-fold increase was observed in the colon of TCRδ$^{-/-}$ mice ($p=0.0048$), compared to wt mice (Figure 3.4B). These data correlate with a 1.2-fold decrease in crypt length in the SI ($p=0.036$) and a 1.1-fold increase in crypt length in the colon ($p=0.044$) of TCRδ$^{-/-}$ mice compared to wt mice (Figure 3.4C). Phloxine-tartrazine staining confirmed that Paneth cells are filled with eosinophilic granules in wt and TCRδ$^{-/-}$ mice (Figure 3.5A). Results in Figure 3.5B show that Paneth cell numbers were similar in the SI of TCRδ$^{-/-}$ mice, compared to wt mice ($p>0.05$).

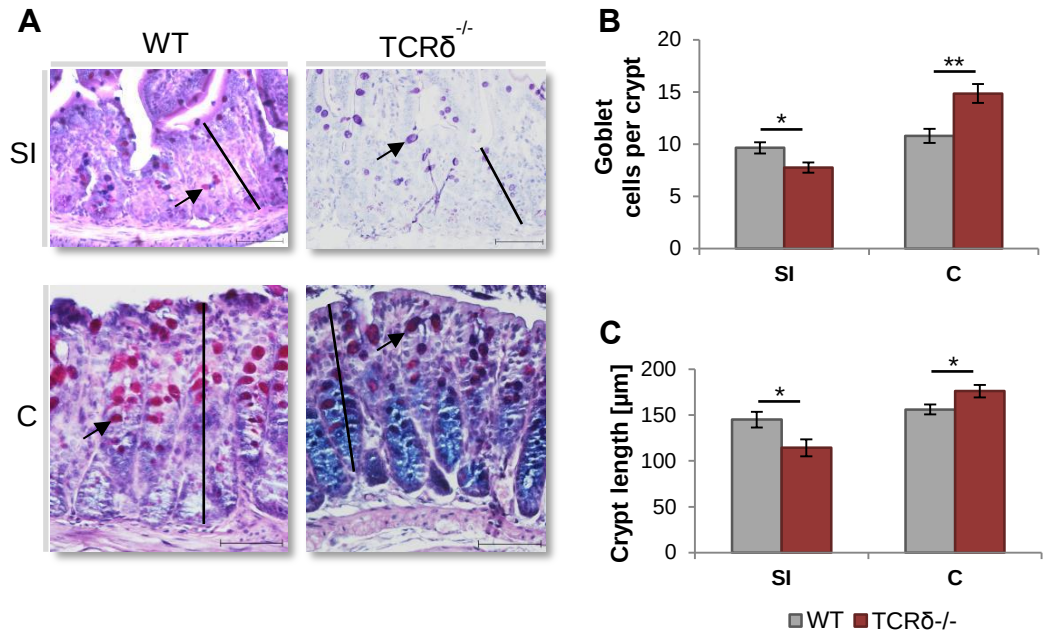

Figure 3.4| Goblet cell counts and crypt length measurements in the SI and colon of wt and TCRδ$^{-/-}$ mice. SI and colon tissues of wt and TCRδ$^{-/-}$ mice (n=7) were stained with PAS/AB (A). Average goblet cell (arrows) number per crypt (B) and crypt length (lines) (C) were calculated from ten crypts per mouse tissue. Magnification, 400x; scale bars, 50 µm; SI, small intestine; C, colon. *p<0.05; **p<0.01.

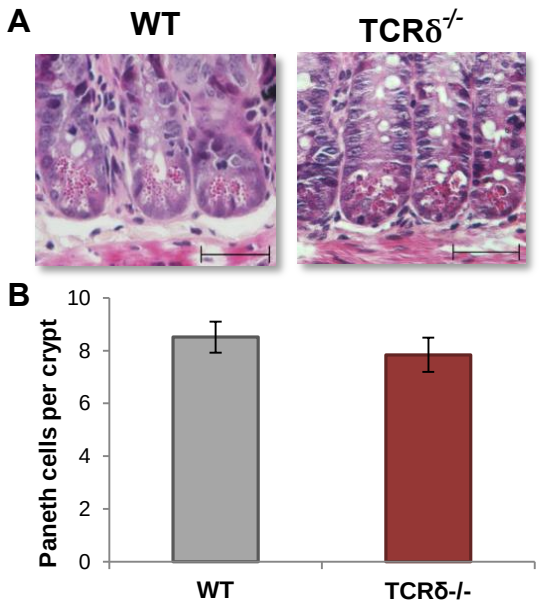

Figure 3.5| Paneth cell counts in the SI of wt and TCRδ$^{-/-}$ mice. SI tissue of wt and TCRδ$^{-/-}$ mice (n=10) was stained with phloxine-tartrazine (A). Average Paneth cell (arrows) number per crypt was calculated from ten crypts per mouse tissue (B). Magnification, x400; scale bars 50 µm.

Following 2.5 % DSS treatment for 7 days, alterations in the goblet cell numbers in the colon were also observed. DSS-treated TCRδ$^{-/-}$ mice showed a significant reduction in the number of goblet cells in the distal colon (p=0.03), compared to DSS-treated wt mice (Figure 3.6A). The model of acute DSS-induced colitis used in this study did not induce inflammation in the SI in both groups of mice (histological scores of 0; data not shown). Histology revealed that DSS treatment of TCRδ$^{-/-}$ mice resulted in extensively damaged colonic epithelium, compared with DSS-treated wt mice, indicating that impaired goblet cell recovery during colitis associates with the more severe inflammation seen in mice lacking γδ IELs. Consistent with goblet cell counts, Muc2 mucin fluorescence staining of distal colon tissue revealed that DSS-treated TCRδ$^{-/-}$ mice showed reduced expression of Muc2 protein compared to DSS-treated wt mice (Figure 3.6B).

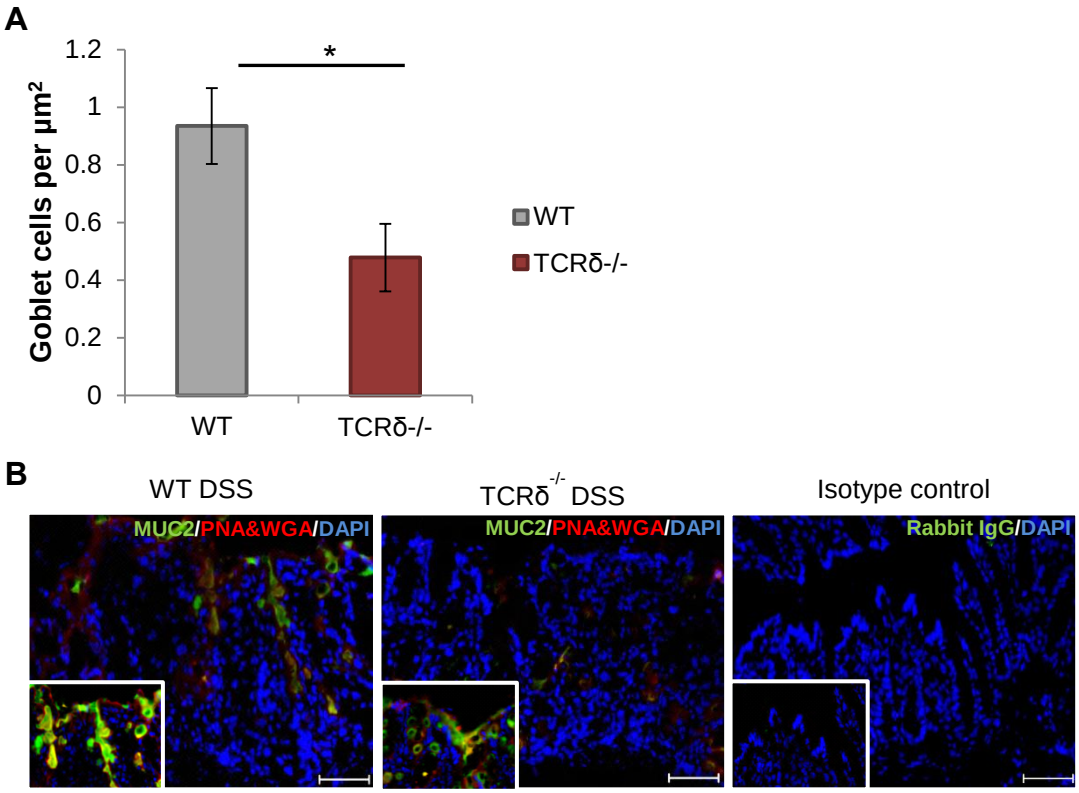

Figure 3.6| Goblet cell counts and Muc2 mucin staining in the colon of wt and TCRδ$^{-/-}$ mice following DSS treatment. Average goblet cell number per µm^2 (n=6) was calculated from tissue area measurements (A). Distal colon sections of DSS-treated wt and TCRδ$^{-/-}$ mice (n=3) were stained with anti-Muc2 (green) and counterstained with PNA and WGA (red) and DAPI (blue). Rabbit IgG represents the isotype control. (B) Magnification, x200; scale bars, 100 µm; Insert magnification, x400; *p<0.05.

3.4 TCRδ$^{-/-}$ mice display an intact mucus layer

TCRδ$^{-/-}$ mice have altered goblet cell numbers in the SI and colon, compared to wt mice (see section 3.3). To determine whether the lack of γδ IELs and the resulting alteration in goblet cell numbers may impact on the architecture and thickness of the mucus layers of TCRδ$^{-/-}$ mice, mucus measurements were performed *in vivo* in the ileum and distal colon of wt and TCRδ$^{-/-}$ mice.

In vivo mucus thickness was measured following previous methods [19]. The intestinal mucus layer was visualised by the addition of charcoal to the exposed ileum or distal colon surface. Mucus thickness was measured using a micropipette attached to a digital micromanipulator. Removal of the loose mucus layer by suction allowed the measurement of the firm and loose mucus layer, as well as the total mucus thickness.

Figure 3.7 reveals that the total mucus layer thickness was 56.2±14.8 µm and 53.3±9.8 µm in the ileum of wt and TCRδ$^{-/-}$ mice, respectively. Total mucus thickness in the distal colon of wt and TCRδ$^{-/-}$ mice was 135.5±21.4 µm and 194.1±59 µm, respectively. The loose mucus layer could be easily aspirated showing that TCRδ$^{-/-}$ mice possessed a distinct outer mucus layer, as shown for wt mice, leaving a thin firmly adherent ileum layer of 23.8±2.1 µm and distal colon layer of 34.2±2.9 µm, compared to 20.6±1.9 µm and 41.7.8±6.0 µm in wt mice, respectively. These results indicate that both firm and loose mucus layer thickness was similar in wt and TCRδ$^{-/-}$ mice ($p>0.05$). Regeneration of the loose mucus layer occurred over a 60 min period following removal of the loose layer, as reported earlier in the ileum and colon of rats, mice, and human explants [19, 20, 313]. The thickness of the firm mucus layer was also measured at the end of the regeneration process, and found to be 27.23±3.3 µm in the ileum and 40.87±2.8 µm in the colon of wt mice and 27.67±2.9 µm in the ileum and 35.53±2.3 µm in the colon of TCRδ$^{-/-}$ mice, thus very similar to the initial measurements, confirming that the procedure did not impact on the integrity of the mucus architecture. These data indicate that the gross molecular organisation of the mucus layer is similar in wt and TCRδ$^{-/-}$ mice.

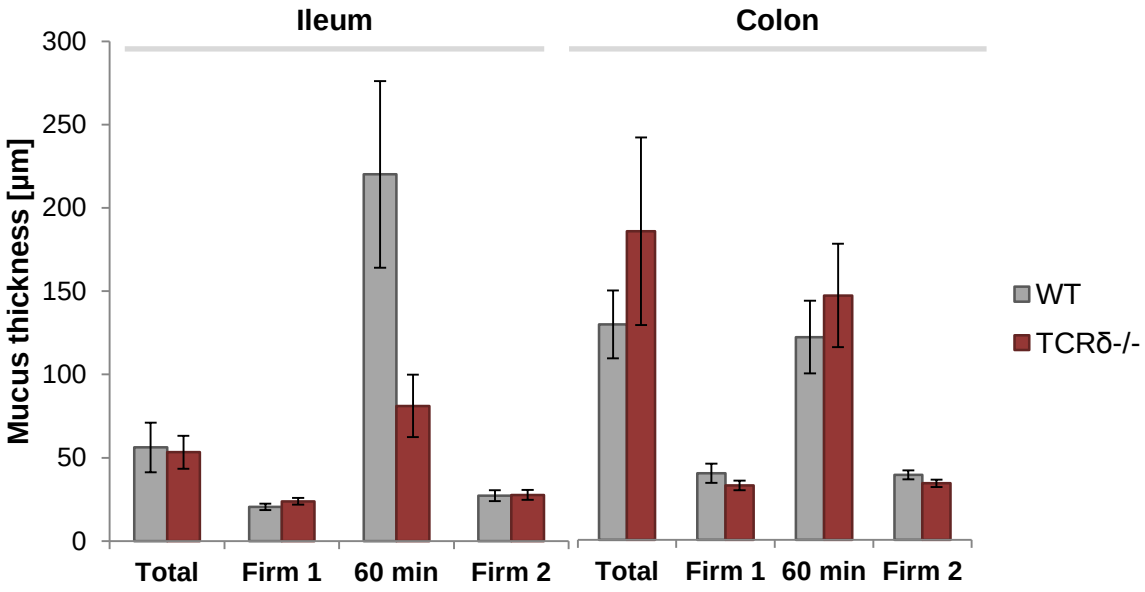

Figure 3.7| *In vivo* mucus measurements in the ileum and distal colon of wt and TCRδ$^{-/-}$ mice. Mucus thickness was measured in wt and TCRδ$^{-/-}$ mice (n=7) *in vivo* using a micromanipulator. Total mucus thickness (Total) indicates the thickness of the firm and loose layer. After removal of the loose layer, firm layer thickness was immediately measured (Firm 1). The mucus layer was allowed to regenerate and then measured (60 min). The firm mucus layer was measured again (Firm 2) to confirm its steady state.

3.5 Impact of γδ IELs on luminal and faecal IgA and intestinal pIgR

To investigate whether the lack of γδ IELs may have an effect on other mucosal secretions, concentrations of immunoglobulin A (IgA) and expression of the polymeric immunoglobulin receptor (pIgR) (see section 1.2.2) were compared in wt and TCRδ$^{-/-}$ mice.

For the quantification of IgA in wt and TCRδ$^{-/-}$ mice by ELISA, two sample types were used: i) faecal pellets and ii) luminal contents collected through intestinal flushes of the SI and colon. Total protein was extracted from SI and colon tissue of the two groups of mice, and pIgR protein expression analysed by western blot.

Figure 3.8A indicates that the faecal IgA concentration was 29.06 µg 100 mg^{-1} in wt mice and 128.85 µg 100 mg^{-1} in TCRδ$^{-/-}$ mice, but statistically similar in both groups of

mice as revealed by the student's T test ($p>0.05$). There was a large variability in faecal IgA concentrations in biological replicates of TCRδ$^{-/-}$ mice, compared to wt mice (Figure 3.8A). Average IgA levels in faecal extracts of wt mice were in agreement with previous findings (27 µg ml^{-1}) [398]. The high variability across biological replicates may suggest that faecal samples are not always reliable for the accurate quantification of IgA. IgA concentrations in wt and TCRδ$^{-/-}$ mice were thus also determined from luminal flush samples of the SI and colon. IgA concentrations were found to be similar ($p>0.05$) for wt and TCRδ$^{-/-}$ mice in both the SI, 0.49 µg mg^{-1} and 3.03 µg mg^{-1} respectively, and colon, 14.77 µg mg^{-1} and 9.4 µg mg^{-1}, respectively (Figure 3.8B). Efficient transport of IgA from the lamina propria into mucosal secretions is mediated by pIgR, and up-regulation of pIgR has been reported in formerly germ-free mice colonised with the commensal *Bacteroides thetaiotamicron* [291]. By western blot, pIgR protein is detected in IECs at a molecular mass of 120 kDa and 100 kDa [399]. In order to separate proteins according to their molecular size, total protein extracts from SI and colon tissue of wt and TCRδ$^{-/-}$ mice were run on an SDS-PAGE gel (Figure 3.9A). Western blot analysis using anti-pIgR antibody against mouse pIgR revealed the presence of two discrete bands at the expected size for mouse pIgR (100 kDa and 120 kDa) for SI wt and TCRδ$^{-/-}$ samples (Figure 3.9B). Densitometric analysis revealed that there was no significant difference in the relative abundance of pIgR in the SI of the two groups of mice (Figure 3.9C). These data are consistent with the IgA concentration in the SI of wt and TCRδ$^{-/-}$ mice (Figure 3.8B). Colon samples displayed a more diffuse pattern with no clear bands that correspond to mouse pIgR, and were therefore not quantified. β-actin was used as a loading control for western blot analysis.

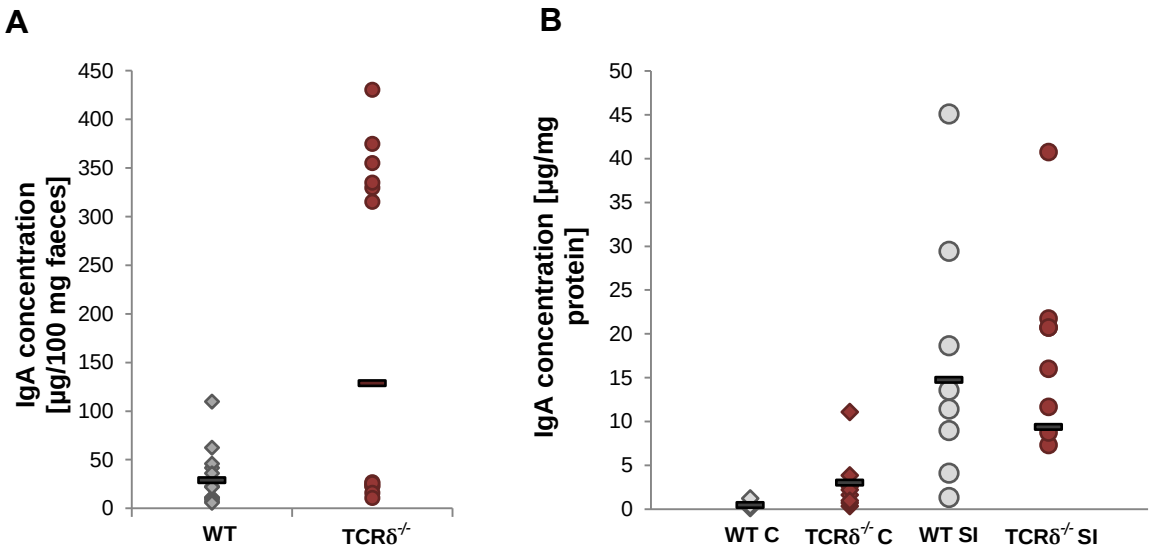

Figure 3.8| Faecal and luminal IgA concentrations in wt and TCRδ$^{-/-}$ mice. IgA concentrations of faecal samples (n=9) (A) and intestinal flush samples (n=8) (B) of wt and TCRδ$^{-/-}$ mice were determined by ELISA. C, colon; SI, small intestine.

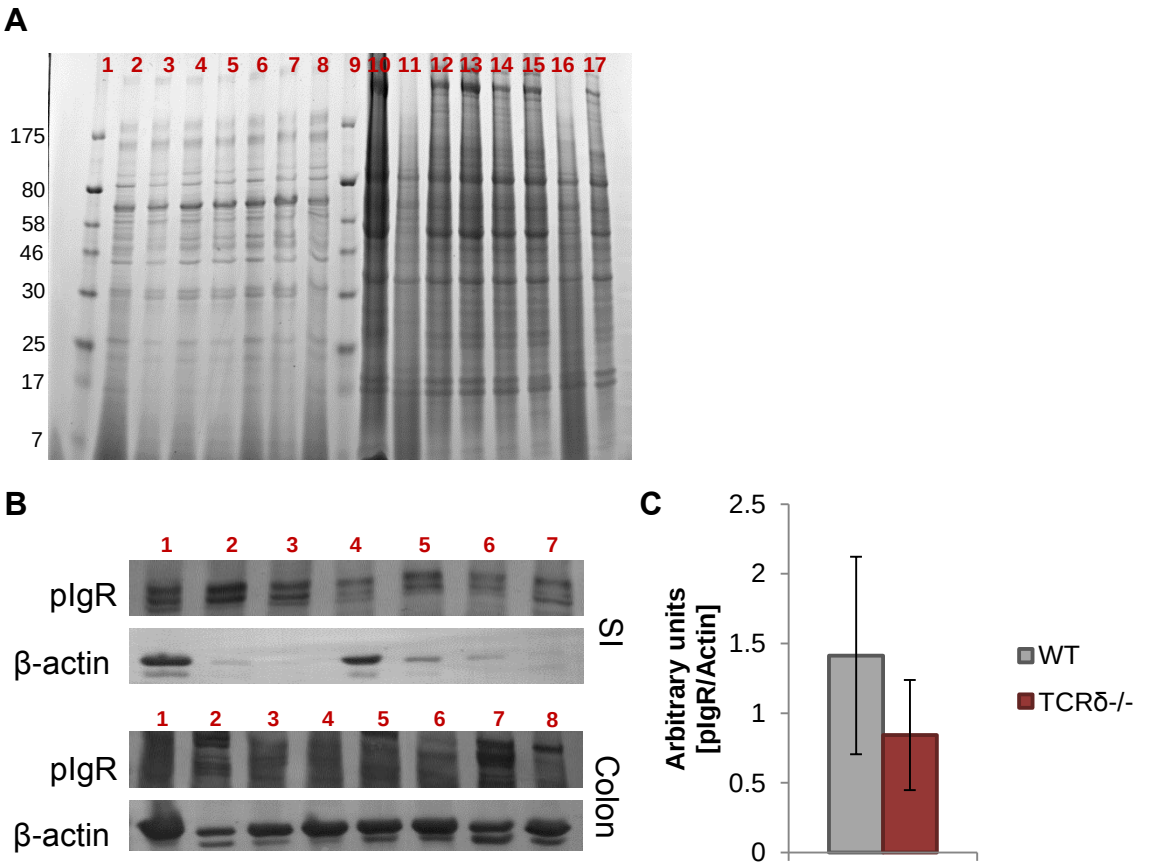

Figure 3.9| pIgR expression in the SI and colon of wt and TCRδ$^{-/-}$ mice. SDS-PAGE of total protein extracts from the SI (n=3/4) and colon (n=4) of wt and TCRδ$^{-/-}$ mice. Lane 1 and 9, Broad range MW marker; Lanes 2-4, wt SI samples; Lanes 5-8, TCRδ$^{-/-}$ SI samples, Lanes 10-13, wt colon; Lanes 14-17 TCRδ$^{-/-}$ colon (A). Western blots of SDS-PAGE of SI (top panel) and colon (bottom panel) protein extracts, probed with anti-pIgR (double band ~100 kDa and ~120 kDa). Top panel: Lanes 1-3, wt SI samples; Lanes 4-7, TCRδ$^{-/-}$ SI samples. Bottom panel: Lanes 1-4 wt colon samples; Lanes 4-8 TCRδ$^{-/-}$ colon samples. β-actin was used as a loading control (B). Relative density was determined for SI wt and TCRδ$^{-/-}$ pIgR bands, represented as the ratio between pIgR and β-actin (C).

3.6 TCRδ$^{-/-}$ mice display altered sialic acid content and glycosyltransferase expression

Aberrant intestinal mucin expression and glycosylation are associated with chronic inflammation and colon cancer in humans [111]. To investigate the potential role of γδ IELs in shaping mucus properties, O-glycan and sialic acid concentrations were determined biochemically from mucus of the SI and colon of wt and TCRδ$^{-/-}$ mice. Furthermore, glycosyltransferase (GT) including sialyltransferase (ST) mRNA expression levels were analysed in the SI and colon of wt and TCRδ$^{-/-}$ mice.

3.6.1 Sialic acid and O-glycan concentrations in wt and TCRδ$^{-/-}$ mice

Sialic acid concentration was determined using the ninhydrin assay, as previously described [387]. TCRδ$^{-/-}$ mice showed a 2-fold decrease ($p=0.04$) in sialic acid concentration in the mucus of the SI, compared to wt mice (Figure 3.10A). Similarly, the sialic acid concentration was 39.5 µM lower in colonic mucus of TCRδ$^{-/-}$ mice ($p=0.03$), compared to wt mice (Figure 3.10A). O-glycan concentration was determined using the alkaline borohydrate assay, as previously described [388]. Figure 3.10B shows that the amount of O-linked oligosaccharide chains was similar in the SI and colon mucus of the two groups of mice.

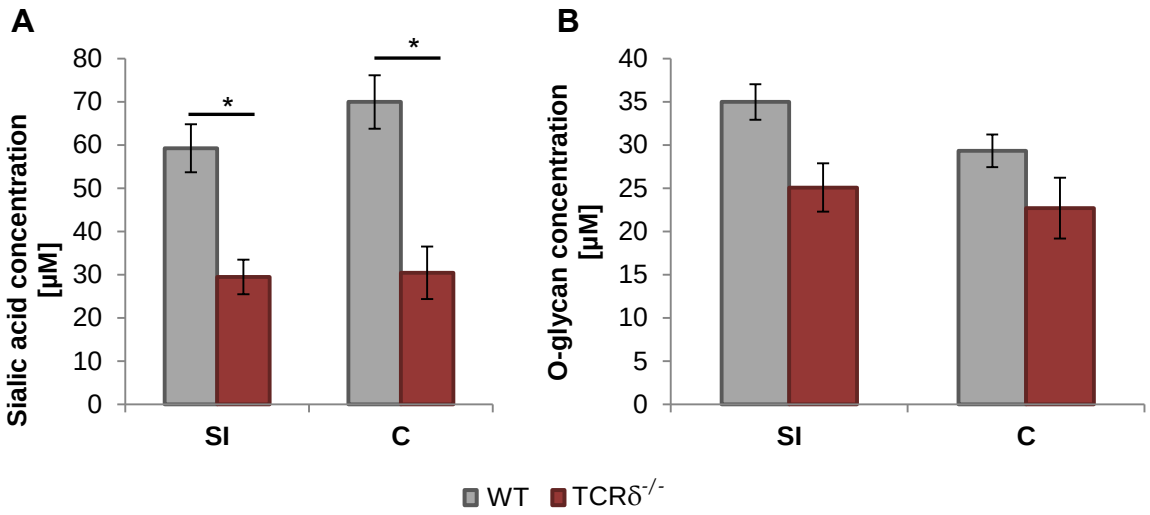

Figure 3.10| Sialic acid and O-glycan concentration analysis in the SI and colon of wt and TCRδ$^{-/-}$ mouse mucus. Sialic acid concentration was determined by ninhydrin colourimetric assay for SI and colon mucus (n=5) (A). O-glycan concentration was determined by alkaline borohydrate colourimetric assay for SI and colon mucus (n=6) (B). SI, small intestine; C, colon; *p<0.05.

To further investigate the marked decrease in sialic acid concentration in the SI and colon of TCRδ$^{-/-}$ mice compared to wt mice, sialic acid lectin (see Table 3.1) binding was compared between the two groups of mice. Wt and TCRδ$^{-/-}$ SI and colon tissue sections were stained with *Sambuccus nigra* (SNA-I) and *Maackia amurensis* (MAA), and the staining was subsequently semi-quantified using the Image J software. Lectin staining images in Figure 3.11A and B showed that both sialic acid-binding lectins bound to intestinal tissue of wt and TCRδ$^{-/-}$ mice, indicating that both α-2,3 sialic acid (MAA) and α-2,6 sialic acid (SNA-I) are present, albeit at a low level. Staining also revealed that α-2,3 sialic acid was more abundant in the SI (Figure 3.11A) compared to the colon (Figure 3.11B). Semi-quantification of the stained images showed that there is no significant difference in SNA-I and MAA lectin staining between the two groups of mice in the SI (Figure 3.11C), but that there was a significantly higher amount of MAA binding (p=0.02) in in the colon of TCRδ$^{-/-}$ mice compared to wt mice (Figure 3.11D). These findings are not in agreement with results in Figure 3.10A, where a significant

decrease in sialic acid content was observed in TCRδ$^{-/-}$ mice compared to wt mice, however the quantification using the ninhydrin assay was deemed more accurate than the method of semi-quantification of lectin stained images using an image software, as reflected by the large error bars within the data set. Future work will include alcian blue staining of tissue sections in order to assess glycosaminoglycan and acidic mucin production in the two groups of mice.

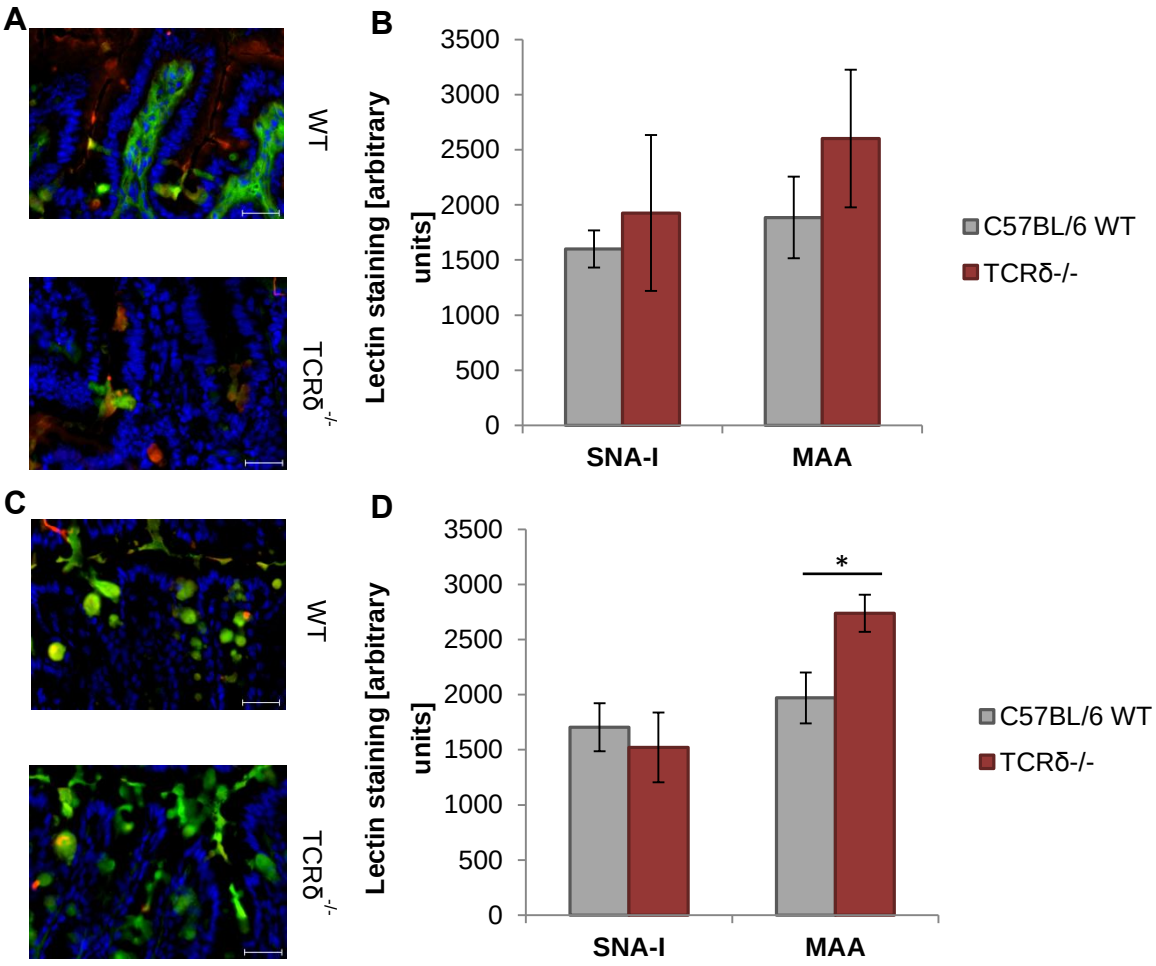

Figure 3.11| Sialic acid lectin staining and semi-quantification in the SI and colon of wt and TCRδ$^{-/-}$ mice. SI (A) and colon (B) tissue sections of wt and TCRδ$^{-/-}$ mice were stained with SNA-I-FITC and MAA-TR (n=5). Sections were counterstained with DAPI. Lectin binding to SI (C) and colon (D) tissue sections was semi-quantified using the Image J software (n=5). Magnification x400; scale bars 50 µm; SNA-I, *Sambuccus nigra* lectin; MAA, *Maackia amurensis* lectin.

3.6.2 Glycosyltransferase and sialyltransferase mRNA levels in wt and TCRδ$^{-/-}$ mice

Here the expression of GT genes involved in the synthesis of the main mucin glycan core structures (*C1GalT1*, *C1GalT2*, *C2GnT1*, *C2GnT2*, *C2GnT3* and *C3GnT*) and STs

involved in chain elongation (*ST3Gal-I*, *ST3Gal-III*, *ST3Gal-IV*, *ST3Gal-VI*, *ST6Gal-I*, *ST6Gal-II*, *ST6GalNAc-I* and *ST6GalNAc-II*) was analysed by qRT-PCR. In mice, C1GalTs, C2GnT1, C2GnT2 and C3GnT1 are expressed in the colon, while C1GalTs, C2GnT1, C2GnT3 and low amounts of C3GnT1 are found in the SI [142, 400, 401]. It was found that core-1 *C1GalT1* and *C1GalT2* displayed the highest GT expression levels, albeit not significantly different between the two groups of mice (data not shown), in agreement with the increased proportion of core-1 structures [82, 83]. Significant differences in gene expression between wt and TCRδ$^{-/-}$ mice were observed for core-2 *C2GnT1* and core-3 *C3GnT* in the SI. Figure 3.11 shows that *C2GnT1* gene expression was 3.7-fold lower (p=0.00013) in TCRδ$^{-/-}$ mice compared to wt mice. A 5-fold decrease was observed in the gene expression level of *C3GnT* (p=0.047) in TCRδ$^{-/-}$ mice compared to wt mice (Figure 3.12). In the colon, GT gene expression was found similar (p>0.05) between the two groups of mice (data not shown). Furthermore, levels of ST gene expression were also similar (p>0.05) in the SI and colon of wt and TCRδ$^{-/-}$ mice (data not shown), suggesting that the observed reduction in sialic acid concentration in TCRδ$^{-/-}$ mice (Figure 3.10A) was not due to changes in ST mRNA expression.

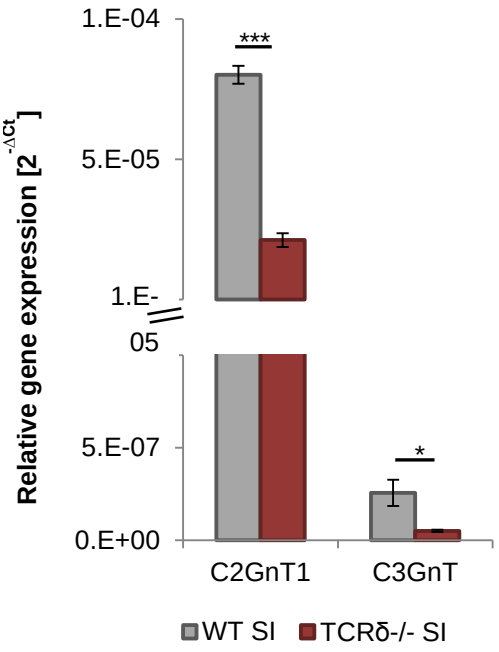

Figure 3.12| Glycosyltransferase gene expression analysis in the SI and colon of wt and TCRδ$^{-/-}$ mice. GT gene expression analysis of the SI and colon of wt and TCRδ$^{-/-}$ mice (n=3) was performed by qRT-PCR, and is represented as relative gene expression ($2^{-\Delta Ct}$). SI, small intestine; *p<0.05; ***p<0.001.

3.7 TCRδ$^{-/-}$ mice display altered cytokine and mucin gene expression

Cytokines are a family of proteins involved in immune signalling. Several cytokines including, for example, IL-1α and IL-18, have been linked to the induction of potent pro-inflammatory responses as well as promoting protection and immune homeostasis [402, 403]. Furthermore, cytokines have been linked to mucus production; for example, IL-13 has been shown to stimulate mucus production in airways [404] and in a human colon cancer cell line [405], IL-1 stimulates mucus production in mouse intestinal explants [406] and airways [407], IL-10 directly regulates Muc2 synthesis [155] and IL-4 increases *MUC2* mRNA in a human colon cancer cell line [405]. To assess the impact of γδ IELs on mucin and cytokine gene expression, microarray and qRT-PCR analyses were performed on SI and colon tissue of wt and TCRδ$^{-/-}$ mice.

3.7.1 Gene microarray and cytokine analysis in wt and TCRδ$^{-/-}$ mice

For a large scale gene expression analysis of glyco-genes, mRNAs were extracted from SI and colon epithelial scrapes of wt and TCRδ$^{-/-}$ mice and subjected to analysis on a custom Affymetrix-based DNA microarray (Glyco_v4a520670F; Scripps Institute, CA, USA), containing murine cytokine genes, made available by the Consortium for Functional Glycomics (www.functionalglycomics.org). Triplicate samples of the SI and colon from separate mice were collected to provide three independent RNA preparations for each mouse strain. Labeled samples were prepared for each RNA and then hybridised to microarrays yielding three sets of data per tissue type and mouse strain.

Microarray analysis revealed that the variability between within group samples was too large to produce conclusive results, but analysis using the non-parametric Rank Product method identified a number of differentially expressed transcripts in the SI and colon of wt and TCRδ$^{-/-}$ mice (Figure 3.13, for details see appendix 6). Of these, a group of genes relevant to this study (IL-33, CD48, CD74, COLEC12, LGALS1, LUM) was selected for further gene expression analysis by qRT-PCR. Figure 3.14A shows that the transcript level of IL-33 in the SI was 3.6-fold lower ($p=0.00031$) in TCRδ$^{-/-}$ mice compared to wt mice. Gene expression of the other five genes selected was similar in the two groups of mice (data not shown). IL-33 (also known as IL-1F11), is the newest identified member of the IL-1 family. To further investigate this marked decrease in IL-33, expression of IL-33 protein was assessed by ELISA and fluorescence staining. ELISA analysis confirmed that IL-33 protein expression was similar in the colon of wt and TCRδ$^{-/-}$ mice ($p>0.05$), whereas levels of IL-33 protein were below detection limit in the SI in both groups of mice (Figure 3.14B). This is in agreement with fluorescence staining of IL-33 in the SI, further confirming its low abundance and indicating that IL-33 protein levels show no marked difference between wt and TCRδ$^{-/-}$ mice (Figure 3.14C). Fluorescence staining showed that IL-33 is localised to the apical surface of the epithelial cells and evenly distributed along villi and crypts of the SI, in both groups of mice (Figure 3.14C).

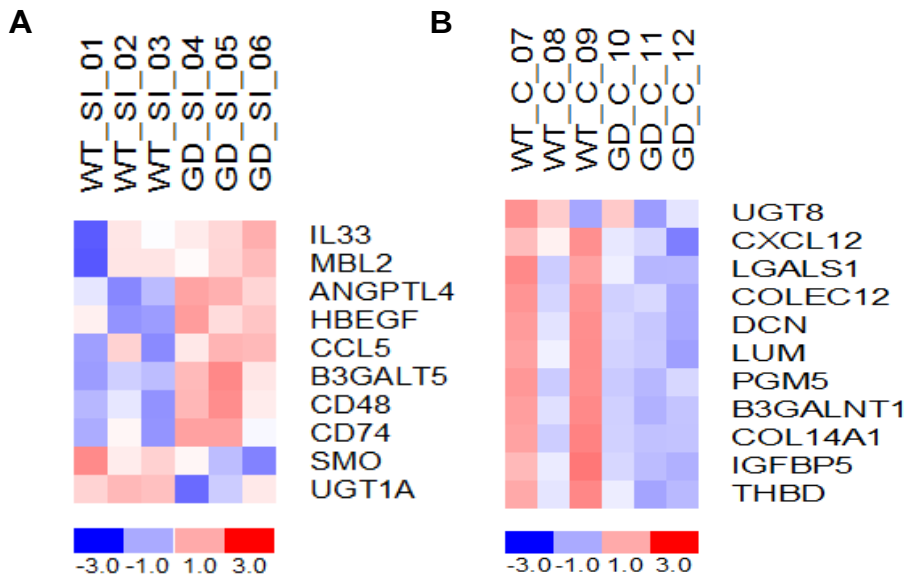

Figure 3.13| Microarray gene expression analysis of the SI and colon from wt and TCRδ$^{-/-}$ mice. Heat maps showing the mean-scaled expression of differentially expressed transcripts in the SI (A) and colon (B) from wt and TCRδ$^{-/-}$ mice (n=3), as identified by the Ranked Product (RP) method. Red indicates increased expression and blue indicates decreased expression.

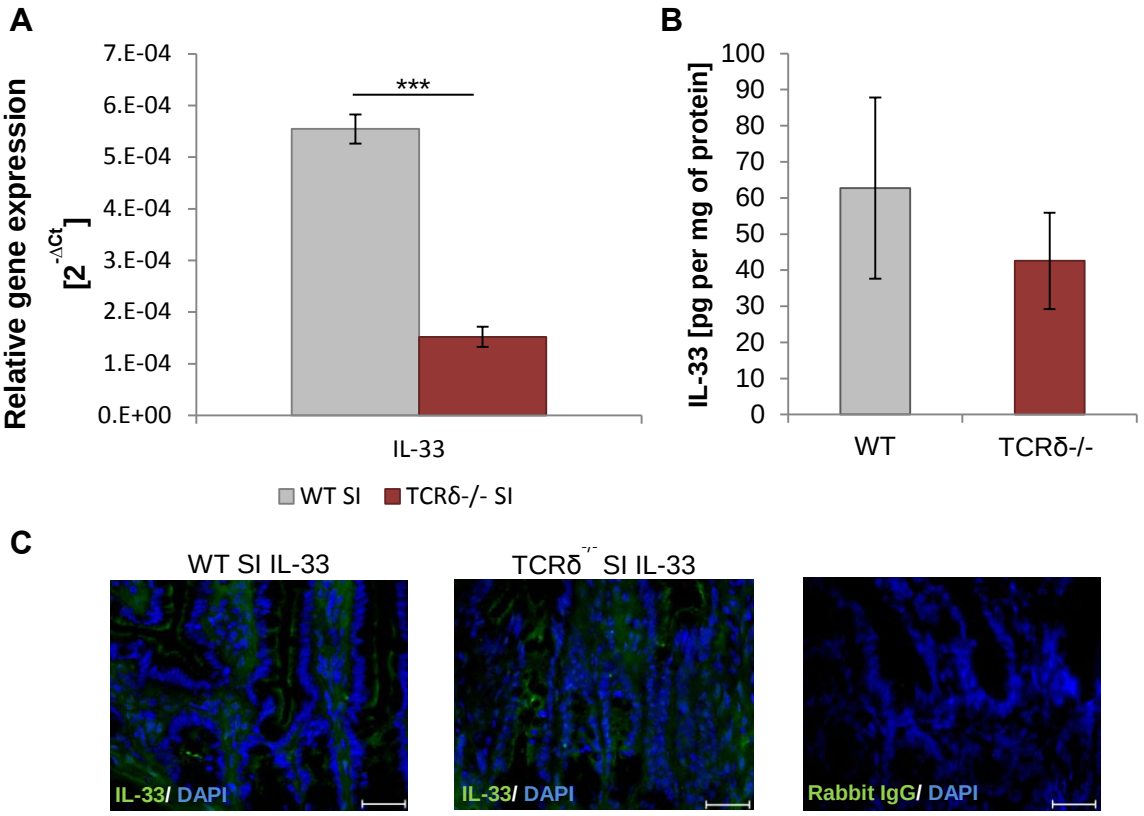

Figure 3.14| IL-33 expression analysis in the SI and colon of wt and TCRδ$^{-/-}$ mice. IL-33 gene expression was analysed in the SI and colon of wt and TCRδ$^{-/-}$ mice (n=3) by qRT-PCR, and is represented as the relative gene expression ($2^{-\Delta Ct}$) (A). IL-33 protein expression in the SI and colon of wt and TCRδ$^{-/-}$ mice (n=4) was analysed by ELISA (B). IL-33 protein expression was further analysed in the SI of wt and TCRδ$^{-/-}$ mice (n=3) by fluorescence staining (C). Sections were counterstained with DAPI (blue). Magnification, x400; scale bars, 50 µm; SI, small intestine; ***p<0.001.

3.7.2 Mucin mRNA levels in wt and TCRδ$^{-/-}$ mice

Next, the mRNA expression of the main intestinal mucins, *Muc1, Muc2, Muc3, Muc4, Muc5AC, Muc6, Muc12, Muc13, Muc17* and *Muc19,* was measured in the SI and colon of wt and TCRδ$^{-/-}$ mice. The secreted Muc2 mucin and the membrane-bound Muc13 and Muc17 mucins are the major mucins expressed in the intestine under normal physiological conditions in humans and mice [27, 112]. In agreement with this, the *Muc2* and *Muc17* mucins were the most highly expressed in the SI and colon of both

groups of mice. There were significant differences in the mRNA expression of the secreted gel-forming *Muc2* and the membrane-bound *Muc3, Muc4, Muc13* and *Muc17* between wt and TCRδ$^{-/-}$ mice. Figure 3.15 shows that a significantly higher level of expression of *Muc2* (p=0.024), *Muc3* (p=0.048) and *Muc17* (p=0.034) mRNA was observed in the SI of TCRδ$^{-/-}$ mice compared to wt mice. In the colon, a significantly higher level of expression of *Muc3* (p=0.0043), *Muc4* (p=0.047) and *Muc13* (p=0.016) mRNA was shown in TCRδ$^{-/-}$ mice compared to wt mice (Figure 3.15). Taken together these findings suggest a role for γδ IELs in the regulation of mucin gene expression.

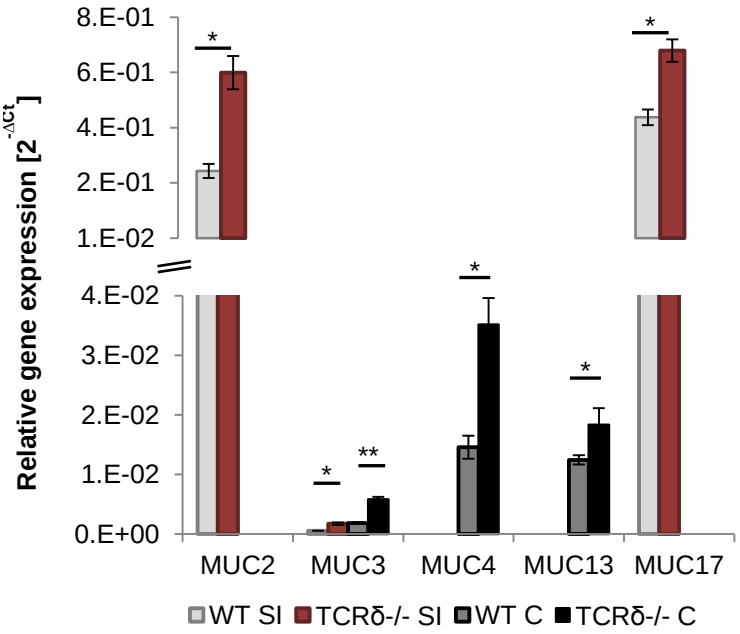

Figure 3.15| Mucin gene expression analysis in the SI and colon of wt and TCRδ$^{-/-}$ mice. Gene expression of *Muc1, Muc2, Muc3, Muc4, Muc5AC, Muc6, Muc12, Muc13, Muc17* and *Muc19* was analysed in the SI and colon of wt and TCRδ$^{-/-}$ mice (n=3) by qRT-PCR, and represented as the relative gene expression ($2^{-\Delta Ct}$). SI, small intestine; C, colon; *p<0.05; **p<0.01.

3.8 TCRδ$^{-/-}$ SI crypt organoid cultures support the role of γδ IELs in the modulation of crypt growth and mucin properties

3.8.1 Characterisation of wt and TCRδ$^{-/-}$ SI organoids

The establishment of a self-renewing long-term intestinal crypt culture system, maintained by a limited number of growth signals in the absence of a non-epithelial cellular niche, simplifies the study of crypt-villus biology [408]. To investigate the possible mechanisms leading to reduced goblet cell numbers and altered mucin expression levels in the SI of TCRδ$^{-/-}$ mice, and to uncouple the potential impact of γδ IELs on intestinal crypts in wt mice, SI crypts were isolated from wt and TCRδ$^{-/-}$ mice and maintained in culture. Organoids were cultured based on published methods [408]. Briefly, crypts were isolated from SI tissue using 2 mM EDTA and re-suspended in a Matrigel matrix. Small domes were plated out in 24-well plates and cultured in a growth factor-rich medium (see Table 2.6). Organoids were passaged every seven days, and maintained in culture for 61 days. Budding crypts and the central lumen of the organoid structures consisted of a single layer of polarised epithelial cells, in agreement with previous reports [408]. Figure 3.16 indicates that the growth pattern of TCRδ$^{-/-}$ SI crypts was similar to that of wt SI crypts; crypts from both groups of mice sealed by day 1 (D1) and continuously budded from the central lumen to form confluent organoids by day 7 (D7).

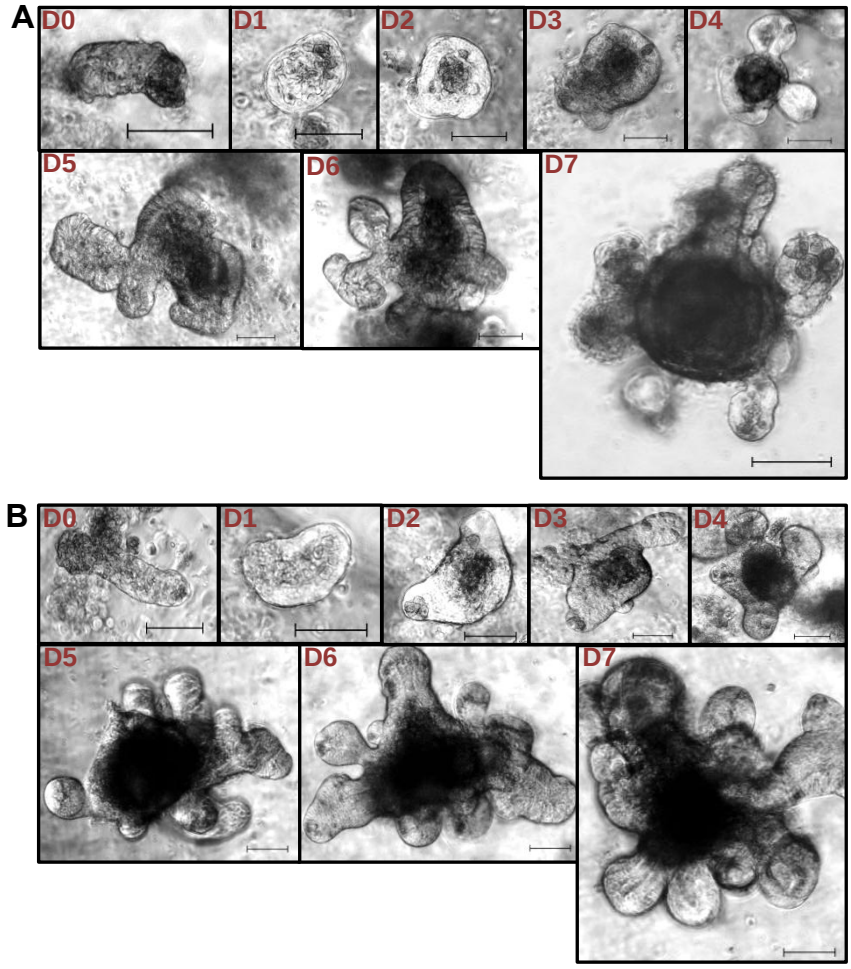

Figure 3.16| TCRδ$^{-/-}$ SI crypts display similar growth patterns compared to wt organoids. Images of SI crypts (n=30-40) that close to form a cyst (D1) to then further develop through the budding of new crypts (arrows) from the cyst body (D2-D7). Day 0 to day 7 images of wt crypts (A) and TCRδ$^{-/-}$ crypts (B) are shown. Magnification x200; scale bars, 50μm; D, day.

For fluorescence staining, SI crypts were cultured for four days to produce organoids composed of numerous newly-formed crypts that could be characterised on the basis of differentiation and integrity markers. Similar phenotypic characteristics were observed between the two groups of mice (Figure 3.17). Enteroendocrine cells (Chromogranin A staining, Figure 3.17A) were scattered throughout the crypt. Goblet cells (MUC2 staining, Figure 3.17B) were observed in the lower third of the crypt, while

Paneth cells (Lysozyme staining, Figure 3.17C) were seen along the whole length of the crypt. Plant lectin (see Table 3.1) staining (peanut agglutinin (PNA) and wheat germ agglutinin (WGA) staining, Figure 3.17D; SNA-I and MAA staining, Figure 3.17E) confirmed expression of extended sugar chains in cultured organoid structures from both groups of mice.

Table 3.1| Specificity of lectins used in this study

Lectin	Abbreviation	Sugar recognition
Maackia amurensis lectin	MAA	α-2,3 neuraminic (sialic) acid
Peanut agglutinin	PNA	Gal-β(1-3)-GalNAc
Sambuccus nigra lectin	SNA-I	α-2,6 neuraminic (sialic) acid
Wheat germ agglutinin	WGA	N-acetylglucosamine (GlcNAc), Neuraminic (sialic) acid

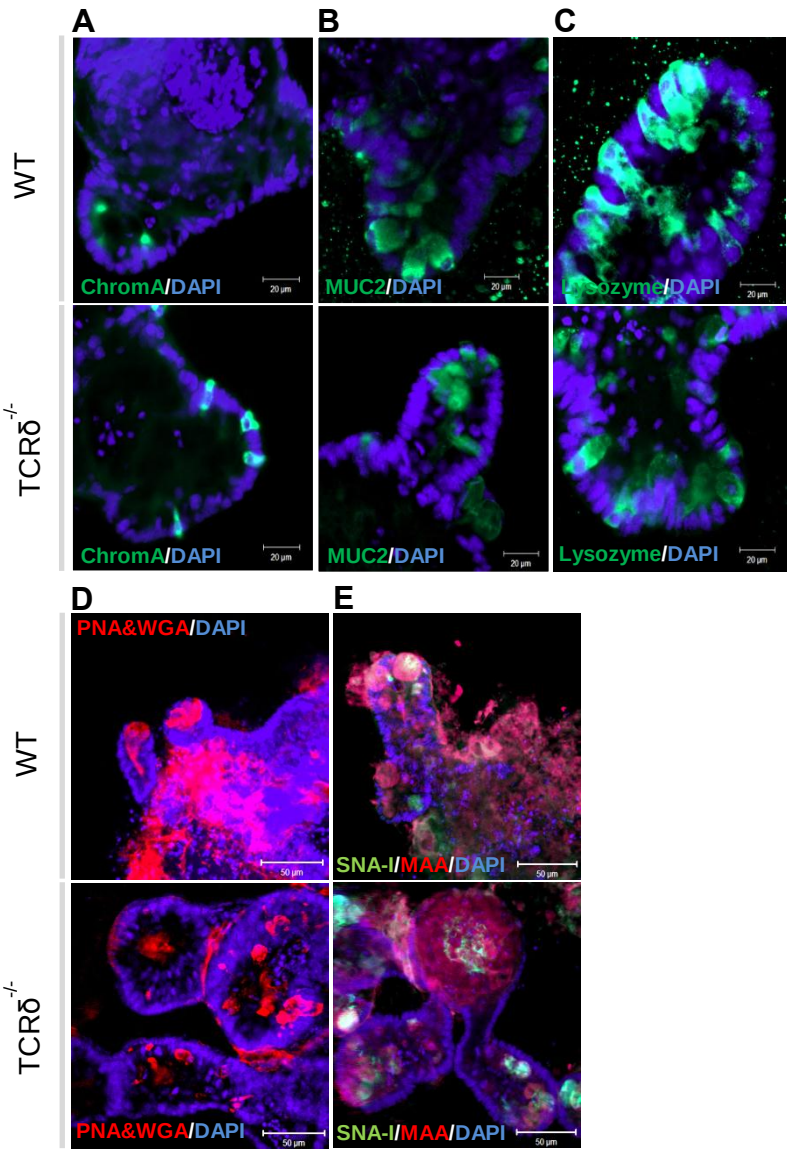

Figure 3.17| TCRδ$^{-/-}$ SI organoid cultures show similar phenotypic characteristics to wt organoids. SI organoids (n=30-40) from both groups of mice were stained with anti-chromogranin A (Chrom A, A), anti-MUC2 (B), anti-Lysozyme (C), PNA and WGA (D) and SNA-I and MAA (E) lectins. Organoids were counterstained with DAPI (blue). Magnification x400.

3.8.2 Role of KGF in goblet cell and crypt properties of SI organoids

The frequency of goblet cells, as determined by anti-MUC2 fluorescence staining of TCRδ$^{-/-}$ crypt organoid cultures was similar to the organoid cultures from wt mice. It was hypothesised that the higher number of goblet cells observed in the SI of wt mice, compared to TCRδ$^{-/-}$ mice (Figure 3.4B), required the presence of γδ IELs that are absent in the wt organoid cultures. KGF plays a critical role in intestinal epithelial growth and maintenance [409, 410], and DSS-activated γδ IELs express KGF in the intestinal mucosa [256]. Here it was investigated whether wt and TCRδ$^{-/-}$ SI organoids would respond to KGF in a similar manner. Four-day organoids were stimulated with 100 ng ml^{-1} KGF in culture medium for 24 h before anti-MUC2 staining was performed. Control organoids were grown in culture medium only. KGF-stimulated organoids showed a marked increase in crypt length and goblet cell number compared to controls (Figure 3.18), similar to responses observed in rat tissue [259, 409], and the phenotype observed in wt tissue (Figure 3.4B), supporting its functional role *in vivo*. Changes in crypt numbers, crypt length and goblet cell numbers per organoid require quantification, which is currently being addressed. Furthermore, Figure 3.18 indicates that goblet cell distributions changed in response to KGF stimulation, with goblet cells being located not just in the lower third of the crypt, but distributed along the entire crypt length. The rapidity (24 h) of the observed response is in accordance with the cell cycle time of the SI crypt proliferating zone being 9-13 h [10]. These findings support a role of KGF-producing cells, which include γδ IELs, in modulating crypt and mucus properties, consistent with the exacerbation of the impact of DSS-treatment in the absence of the γδ IEL-signalling pathway in TCRδ$^{-/-}$ mice.

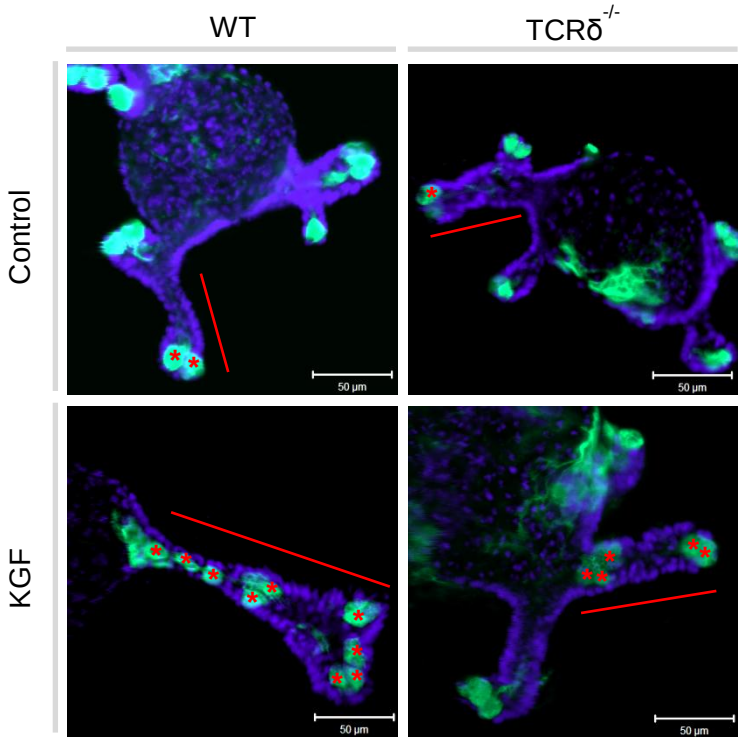

Figure 3.18| Treatment of wt and TCRδ$^{-/-}$ SI organoids with KGF. MUC2-stained organoids grown in normal culture medium (control) (n=60) and culture medium supplemented with KGF (KGF) (n=60) for 24 h. Organoids were counterstained with DAPI (blue). Magnification, x400; KGF, keratinocyte growth factor; bar, crypt length designator; star, goblet cell designator.

3.9 Discussion

In accordance with previous studies [234, 256, 411], TCRδ$^{-/-}$ mice were found to be more susceptible to DSS-induced colitis compared to wt mice. It has been shown that γδ IELs aid in the limitation of opportunistic penetration of commensal bacteria across the mucosal surface; a phenomenon seen at early time points of injury by DSS-induced colitis [236]. γδ IEL activation appears to be dependent on epithelial cell-intrinsic MyD88, a key mediator of microbial-host cross-talk suggesting that epithelial cells supply microbial cues to γδ IELs [412]. Given the role played by the mucus layer in limiting bacterial penetration, it was hypothesised that γδ IELs may reinforce mucus barrier function, thereby decreasing the likelihood of detrimental tissue invasion.

3.9.1 Characterisation of mucus properties in TCRδ$^{-/-}$ mice

Mucus properties in TCRδ$^{-/-}$ mice were investigated on the basis of goblet cell numbers, *in vivo* mucus thickness, mucus composition and mucin and glyco-gene expression. Results from PAS/AB staining of colon tissue suggest that goblet cell depletion in TCRδ$^{-/-}$ mice contributes to the more severe inflammation seen in mice lacking γδ IELs during DSS-induced colitis. Additionally, analysis of *in vivo* intestinal mucus thickness revealed that firm and loose mucus thickness was similar in TCRδ$^{-/-}$ and wt mice, despite goblet cell differences, which may suggest an alteration in the rate of mucus production or secretion. Expression analysis of the intestinal mucin and core GT genes showed major differences occurring in the SI of TCRδ$^{-/-}$ mice, compared to wt mice. This highly altered SI phenotype, compared to the colon, could be associated with the higher abundance of IELs in the SI (1 IEL for every 10 intestinal epithelial cells (IEC)) compared to the large intestine (1 IEL for every 40 IEC) [226].

The addition of O-glycans is a post-translational modification characteristic of secreted and membrane-bound mucins. Mucin glycosylation is characterised by common core structures, which are variously elongated and terminated, comprising the basis for the structural diversity of glycans. Two of the most common mucin-type O-glycans in mouse intestinal mucins are based on the core-1 and core-2 structures [82, 83]. Here *C1GalT1* and *C1GalT2* were most highly expressed in both groups of mice. Expression of both *C2GnT1* and *C3GnT* was down-regulated in the SI of TCRδ$^{-/-}$ mice compared to wt mice. Furthermore mucin sialic acid concentration was decreased in TCRδ$^{-/-}$ mice. However this change did not correlate with changes in gene expression of main ST genes tested. The STs constitute a family of ~20 members [413]. For O-linked mucin glycans, each tissue expresses one or more of the ST3Gal I/II and the ST6GalNAc I–VI enzymes that form the NeuAcα2–3Galβ1–3 (NeuAcα2–6) GalNAcαThr/Ser sequence, the most common O-linked glycan [414]. In light of the similar ST mRNA expression observed between wt and TCRδ$^{-/-}$ mice, the reduced mucin sialic acid concentration in TCRδ$^{-/-}$ mice may be the result of altered bacterial colonisation in these mice. γδ IELs of the SI have been shown to regulate the production of antimicrobial factors, such as RegIIIγ, in response to resident bacterial "pathobionts" that penetrate the intestinal epithelium [236]. Such a response is reduced in TCRδ$^{-/-}$ mice, allowing a different bacterial population to colonise the SI. Indeed gut bacteria, in particular pathogens, have evolved to utilise host sialic acids as a nutrient source and as a major strategy for colonisation and pathogenesis of mammalian mucosal surfaces [415]. Utilisation of

sialic acid by bacteria promotes bacterial survival in mucosal niche environments in several ways, including: (i) nutritional benefits of sialic acid catabolism, (ii) unmasking of cryptic host ligands used for adherence, (iii) participation in biofilm formation and (iv) modulation of immune function [416]. Determining the composition of the mucosa-associated microbiota in TCRδ$^{-/-}$ mice compared to wt littermates will help assess the association between sialic catabolism and pathogenesis.

3.9.2 Impact of γδ IELs on mucosal IgA secretions

Further to mucins, IgA represents an additional immune defence component of the intestinal barrier. In humans, at least 80 % of plasma cells are located in the lamina propria, and together they produce more IgA than any other immunoglobulin isotypes combined [417, 418]. Secreted IgA can neutralise viruses or toxins intraluminally, or during transport via pIgR [419, 420]. IgA also plays a role in preventing commensal bacterial adherence and penetration, or limiting the growth of bacteria and their densities in the lumen of the intestine [38, 421]. IgA levels are close to the detection limit in germ-free animals, with physiological IgA levels being reached within a few weeks following conventionalisation [422-424]. It is worth noting that introduction of commensals is associated with the induction in the intestine of both strain-specific IgA [425] and natural IgA with unknown specificity [424]. Studies have underscored the natural “coating” of commensal bacteria by IgA, a process that may be involved in the sensing of the intestinal microbiota in homeostasis [421, 426, 427]. This is further supported by the fact that pIgR$^{-/-}$ mice display greater susceptibility to DSS-induced colitis compared to wt and IgA$^{-/-}$ mice [428]. In humans, IgA quantification has been assessed by sampling faeces [429, 430] whereas in experimental animals IgA is usually collected by flushing luminal contents [431]. Here, the faecal and luminal IgA concentrations were similar in TCRδ$^{-/-}$ mice compared to wt mice. This is in contrast to studies reporting an 80 % decrease in faecal IgA concentration of TCRδ$^{-/-}$ mice compared to TCRδ$^{+/+}$ control mice [432], however other studies in TCRδ$^{-/-}$ mice showed no differences in faecal and luminal IgA concentrations compared to wt mice [MacPherson, personal correspondence]. Furthermore, pIgR expression was similar in the two groups of mice. Together these findings suggest that the lack of γδ IELs does not affect IgA or pIgR levels in TCRδ$^{-/-}$ mice, and is in agreement with findings that mucus thickness is similar in wt and TCRδ$^{-/-}$ mice.

3.9.3 Impact of γδ IELs on mucin gene expression

Numerous studies have described mucin abnormalities in inflammatory bowel disease (IBD) and cancer, both in animal models and patients [68, 433-436]. Significantly higher gene expression of gel-forming *Muc2* was observed in the SI of TCRδ$^{-/-}$ mice compared to wt mice. MUC2 is the most abundantly expressed secretory mucin in the intestine and is stored in bulky apical granules of the goblet cells which form the characteristic goblet cell thecae [437]. The mucin-containing granules can be secreted from the apical surface both constitutively and in response to a variety of stimuli. In addition, goblet cells can undergo compound exocytis; an accelerated secretory event resulting in the acute release of central mucin granules [438]. As γδ IELs protect against the invasion of intestinal tissues by resident bacteria, specifically during the first few hours after a bacterial encounter [236], increased bacterial translocation in TCRδ$^{-/-}$ mice could trigger increased secretory activity of goblet cells, as recently reported in the case of colonic ischaemia [396]. The maintenance of an apparent intact mucus layer is consistent with previous studies reporting that bacterial penetration in the TCRδ$^{-/-}$ mice did not arise from increased non-specific barrier permeability [236]. Muc2 expression was also down-regulated in MyD88(ΔIEC) mice, consistent with a previously suggested role of the MyD88-dependent signalling pathway in γδ IEL-modulation of mucosal homeostasis [236]. Expression of MUC2 mucin, the structural component of the colonic mucus layer, is lowered in ulcerative colitis (UC) [439]. A primary defect in colonic Muc2 synthesis is observed in IL-10$^{-/-}$ mice, whereas bacterial colonisation and colitis in these mice led to reduced Muc2 sulphation [440]. These quantitative and structural aberrations in Muc2 in IL-10$^{-/-}$ mice likely reduce the ability of the mucosa to cope with non-pathogenic commensal bacteria and may contribute to their susceptibility to develop colitis.

Muc13 and *Muc17* mucins are the main membrane-bound mucins expressed in the intestine under normal physiological conditions [27, 112]. In the colon, significantly higher levels of membrane-bound *Muc3*, *Muc4* and *Muc13* mRNA were measured in TCRδ$^{-/-}$ mice compared to wt mice. MUC13 mucin is the most abundant cell-surface mucin in the normal human GI tract and MUC13 polymorphisms have been linked to IBD [132]. This membrane-bound mucin has recently been shown to have a protective role in the colonic epithelium of mice with disruption or inappropriate expression of *Muc13* predisposing to infectious and inflammatory diseases, and inflammation-induced cancer [132]. Upregulation of *Muc13* gene expression may be an epithelial

protective mechanism induced by the host in the absence of γδ IELs. In addition, results from qRT-PCR showed significantly higher levels of *Muc17* mRNA in the SI of TCRδ$^{-/-}$ mice compared to wt mice. In humans, the region of the membrane-bound mucin gene cluster has been implicated in genetic susceptibility to IBD [128, 441]. *Muc17* expression is lost in inflammatory, and early and late neoplastic conditions in the colon [133], suggesting that *Muc17* may have anti-inflammatory roles, and therefore the observed upregulation of *Muc17* in TCRδ$^{-/-}$ mice compared to wt mice may be a protective mechanism in the SI epithelium.

3.9.4 Impact of KGF on *ex vivo* SI organoids

The differentiation, activation and functional specialisation of IELs are controlled by interactions with other cell types and soluble factors. In particular, activated but not resting γδ IELs can produce KGF [260], a unique feature of this T cell population [256, 258]. It has been reported that intestinal γδ IELs are activated *in vivo* to express KGF after DSS treatment, and that intestinal epithelial cell proliferation is decreased in TCRδ$^{-/-}$ mice following DSS treatment [256]. Here it was shown that KGF treatment can restore goblet cell numbers in *ex vivo* organoid cultures from TCRδ$^{-/-}$ mice, in line with previous reports showing an increase in goblet cell number and trefoil factor 3 (TFF3) protein expression in the rat intestine following KGF treatment [259]. This new line of evidence indicates that γδ IEL-derived KGF could form a component in this protective mechanism. Goblet cell depletion is a characteristic feature of many forms of infectious and non-infectious colitis, particularly UC, although it is not known whether it is a cause or consequence of inflammation [442]. Depletion may occur due to decreases in goblet cell number, decreases in mucin biosynthesis and/or increases in mucin secretion that are not matched by an increase in mucin biosynthesis. Aberrant mucin expression and glycosylation, and altered goblet cell numbers in TCRδ$^{-/-}$ mice may reduce the ability of the mucosa to cope with pathosymbionts, contributing to their increased susceptibility to DSS-induced colitis.

3.9.5 Impact of γδ IELs on IL-33 cytokine expression

Host-derived cytokines have been implicated in the alteration of mucin synthesis and secretions. Expression of the IL-1 family member, IL-33, is increased in the inflamed mucosa of IBD patients *versus* healthy controls, particularly in UC [443-446]. Here, IL-33 gene expression was significantly reduced in the SI of TCRδ$^{-/-}$ mice, perhaps

indicating that IL-33 is a mediator of γδ IELs. However, this was not confirmed by fluorescence staining using anti-IL-33 antibody and would need to be investigated further at the protein level. The increased severity of DSS-induced colitis in TCRδ$^{-/-}$ mice, compared to DSS-treated wt mice, may be due to a potential role of IL-33 in modulating mucin production. Aside from its established function of promoting potent T_H2 immune responses, IL-33 has emerged as an important cytokine in the induction of mucosal healing and restoration of intestinal homeostasis. In support of this concept, a protective role for IL-33 was reported in chemically-induced colitis models [447]. As such, IL-33 follows the trend of several innate-type cytokines, including members of the IL-1 family, that possess dichotomous roles of inducing a potent pro-inflammatory response, while also promoting protection and the return to immune homeostasis. This dual function is best depicted in the intestinal mucosa and is dependent upon the immunological/genetic status of the host and/or the type and phase of the ongoing inflammatory process [402]. IL-33 may have a pro-inflammatory effect on lamina propria immune cells while at the same time promoting wound healing and epithelial repair, when acting on epithelial cells [403]. It is worth noting that IL-33 has been described as a prototypic 'alarmin' that has the ability to signal local, innate immune responses in an effort to mount an effective, physiologic inflammatory reaction to induce mucosal healing and restore intestinal homeostasis [402]. In addition, IL-33 has the ability to potentiate epithelial defenses and enhance mucus production upon parasitic infections [448-451]. *In vitro* it was shown that IL-33 drives protein misfolding and endoplasmic reticulum (ER) stress, and blocks mucin biosynthesis in intestinal and respiratory goblet cells [Hasnain, personal correspondence]. The unfolded protein response (UPR) and ER-associated protein degradation are highly conserved molecular programs that are activated by ER stress, and are critical in the control of protein synthesis and secretion in goblet cells [164]. *In vivo*, T_H1 and T_H17 responses to mucosal pathogens resulted in ER stress and goblet cell failure, whereas T_H2 responses caused high mucus production [Hasnain, personal correspondence]. In inflammatory diseases such as IBD, pathways such as cytokine-induced ER stress exacerbate inflammation by causing mucus depletion to expose the epithelium to the microbiota. The receptor for IL-33 is ST2, a member of the IL-1 family of cytokine receptors [451]. It was demonstrated that IL-33 signal transduction depends on the expression of ST2 [451], but whether ST2 plays a role in T_H2 development remains unclear [452, 453]. The epithelium in macroscopically non-inflamed colon displays abundant ST2, but during chronic inflammation of UC and CD, epithelial-derived ST2

expression is decreased and redistributed to the lamina propria immune cells [445]. Preliminary staining with anti-ST2 shows that ST2 expression is decreased in TCRδ$^{-/-}$ compared to wt mice, however further studies are requried to confirm this. Further mechanistic studies are warranted to determine whether IL-33 is a mediator of activated γδ IELs for maintenance of mucosal homeostasis and whether addition of IL-33 can alleviate acute mucosal injury in these mice.

γδ IELs are involved in the regulation of the mucosal microenvironment in response to intestinal disease, including IBD [444], celiac disease, graft-vs.-host disease [255], and parasite infection [454, 455]. However, the precise role of γδ IELs remains controversial.

In this study, data demonstrating that TCRδ$^{-/-}$ mice show alterations in mucin expression and glycosylation, may compromise the nature of the mucosa-associated microbial community, resulting in increased vulnerability to epithelial damage**.** It remains to be determined how γδ IELs may regulate mucin expression and goblet cell function by investigating several mechanisms, such as the involvement of the IL-33/ST2 axis.

Chapter 4 *L. reuteri* adhesion to mucus *in vitro*

4.1 Introduction and objectives

Gastrointestinal (GI) mucus forms the first point of contact between the intestinal microbiota and the host. Mucin O-glycans (see section 1.2.2.2) have been proposed to serve as preferential binding sites for intestinal bacteria [48], and provide nutritional benefits through catabolism [456, 457], such as sialic acid catabolism [416]. Symbiotic *Lactobacillus* bacteria have been shown to benefit the host through modulating the intestinal immune system and maintaining a balanced intestinal microbiota [458-460]. In order to fully understand the mutualistic relationship of intestinal commensals, it is vital to elucidate the mechanisms that facilitate host-microbe interactions. The *Lactobacillus* species *reuteri* was used in this study as a model gut symbiont since it is found to inhabit the GI tract of many vertebrate species including, humans, pigs, horses, rodents, birds, and fish, providing an excellent model to investigate host adaptation [461]. A number of colonisation requirements have been identified for *Lactobacillus reuteri* (*L. reuteri*), including adherence to epithelial cells, mucus-binding ability and fibronectin-binding ability [377-379]. However, compared with the current understanding of the adhesive mechanisms of numerous human pathogenic bacteria, knowledge on the surface molecules mediating *Lactobacillus* adhesion to the intestinal mucosa and their corresponding receptors is ill-defined.

A simple model to assess the adhesion of bacterial strains to intestinal mucus is based on the immobilisation of commercially available mucin on a micro-well plate surface [462, 463]. These assays revealed the importance of strain-specific cell surface proteins in the adhesion to mucins (Table 4.1). The most studied example of mucin-targeting bacterial adhesins is the canonical mucus-binding protein, MUB, produced by *L. reuteri* [377, 383, 391] (see section 1.4.3.3). Despite recent advances, the nature of the molecular ligands remains to be identified and whether MUB recognises mucin O-glycans as previously postulated, is still a matter of debate [377, 464].

Table 4.1| Mucus adhesion-promoting proteins in Lactobacillus spp.

Protein	Information	Strain	References
MUB	Demonstrates binding to mucus *in vitro*	*L. reuteri ATCC 53608*	[465]
MucBP Domain containing proteins	Implicated in mucus adhesion	13 known *Lactobacillus spp.*	[391]
Pili	Pilin subunit SpaC binds to mucus in vitro	*L. johnsonii, L. rhamnosus GG*	[466-468]
32-Mmubp	Demonstrates binding to mucus *in vitro*	*L. fermentum BCS87*	[469]
S1pA	Knockouts show diminished adhesion to mucus *in vitro*	*L. acidophilus NCFM*	[470]
MapA	Demonstrates binding to mucus *in vitro*	*L. reuteri 104R*	[471, 472]
EF-Tu	Expression upregulated in the presence of mucus	*L. johnsonii NCC533 La1*	[473-477]

Here a well-established mucus-producing colorectal carcinoma cell line (HT29-MTX) as well as murine and human intestinal tissues, were used in conjunction with chemical treatments to investigate the adhesion specificities and impact of selected strains of the model gut symbiont *L. reuteri* to mucus.

The objectives of this study are to:

1. Investigate the binding ability of selected *L. reuteri* strains to the mucin-producing HT29-MTX cell line.
2. Explore the effect of selected *L. reuteri* strains on HT29-MTX mucin gene expression.
3. Determine binding specificities of *L. reuteri* strains and their adhesion protein(s) to mucin types, using HT29-MTX cells and murine/human tissue.
4. Identify the binding specificities of MUB protein to mucin glycans using chemically treated cells and tissues.

4.2 Characterisation of the HT29-MTX cell line

HT-29 human colorectal adenocarcinoma cells selected by adaptation to 10^{-5} M methotrexate (HT29-MTX) have been identified as a homogenous cell population of a differentiated phenotype, producing high amounts of mucin [478]. The mucin secretion of the cells is a growth-related phenomenon that begins once the HT29-MTX cells have reached confluency [479]. In order to determine the mucus-producing phenotype of this cell line, mucin gene and protein expression were characterised in HT29-MTX cell monolayers in a time course experiment from confluency (day 7) up to day 28 of initial seeding. The cells were seeded into 24-well plates on glass coverslips at a density of 4 x 10^4 cells $well^{-1}$, and incubated without passaging for a period of 28 days. Secreted mucin expression was assessed at days 7, 14, 21 and 28 by anti-MUC2/5AC fluorescence staining and qRT-PCR gene expression analysis of *MUC2/5AC*. Acidic mucopolysaccharide production was assessed by alcian blue staining.

Figure 4.1A shows representative (n=9) images of MUC2 and MUC5AC protein expression at selected time points. At confluency (day 7), mucin protein expression was at its lowest level. MUC2 and MUC5AC staining increased from approximately 5 % at day 7 to approximately 30 % at day 14. MUC2 and MUC5AC protein expression levels at day 14 and day 21 were similar and thus day 14 was selected as the optimal time point for all subsequent experiments. The progressive increase in mucus-expressing cells with increased culture time is in agreement with previous observations [479], although in the present study the mucus layer covering the HT29-MTX cell

monolayer was not seen to reach 100 % confluency. However, compared to day 7, *MUC2* gene expression levels remained similar ($p>0.05$) throughout the time course despite a trend for increasing levels of expression (Figure 4.1B), and *MUC5AC* gene expression levels were seen to significantly decrease at day 14 ($p=0.03$), day 21 ($p=7.46x10^{-28}$), and were below detection limit at day 28 (Figure 4.1C). The observed increase in mucin protein secretion at selected time points does therefore not correlate with mucin mRNA expression patterns. qRT-PCR analyses of mucin transcripts in HT29-MTX cells have shown that the genes become expressed at different time points before confluency, and that their levels reach a maximal level with the induction of cell differentiation [480]. It has previously been reported that the expression of mucin mRNAs occurs earlier than the production of mucus in differentiated cells, suggesting that the mucin biosynthesis involves a growth-related time lag between the activation of the mucin genes and the onset of glycosylation [479]. Furthermore, it has been shown that secretion of MUC5AC mucin increased without upregulation of *MUC5AC* gene expression in HT29-MTX cells [481].

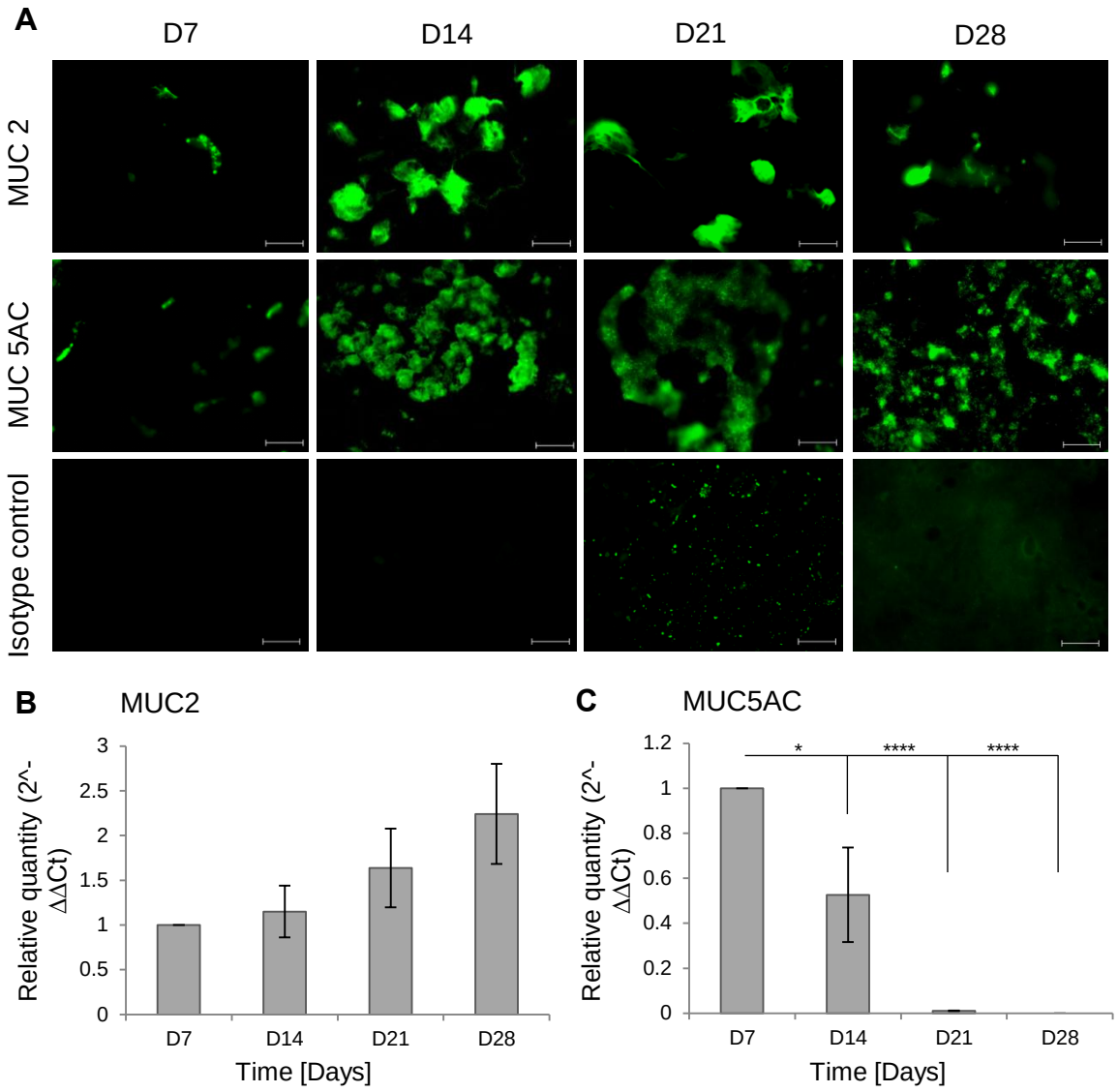

Figure 4.1| Mucin characterisation of the HT29-MTX cell line. HT29-MTX cell monolayers (n=9) were stained with anti-MUC2 and anti-MUC5AC rabbit polyclonal antibodies and anti-rabbit Alexa Fluor 488 secondary antibody at day 7 (confluency), 14, 21 and 28 (A). Rabbit IgG served as the isotype control. qRT-PCR gene expression analysis of MUC2 (B) and MUC5AC (C) was performed at day 7, 14, 21 and 28. Relative quantity relative to day 7 is represented (B, C). Magnification x400; scale bars 50 µm; D, day; *p<0,05; ****p<0.0001.

Alcian blue is a polyvalent basic dye containing four isothiouronium residues and can bind negatively charged macromolecules (e.g. mucopolysaccharides) through electrostatic forces. Alcian blue is widely used for staining glycosaminoglycans and acidic mucins, but mucins with low acidic glycan contents are not detected. Alcian blue staining was previously used to assess mucin production in the HT29-MTX-E12 cell line [482]. Figure 4.2 shows representative images of alcian blue staining of HT29-MTX monolayers at selected time points. At confluency (day 7), a small proportion of cells stained blue, and a steady increase in alcian blue staining was seen at days 14, 21 and 28. After 14 days of growth, approximately 60 % of the HT29-MTX cell culture stained with alcian blue compared to approximately 30 % at day 7. The level of alcian blue staining is most intense at day 28, covering approximately 80 % of the total area. This indicates that, although mucin protein expression remained similar after day 14 of culture (Figure 4.1), a progressive increase in mucin glycosylation was observed with increased culture time of HT29-MTX cells.

Taken together, the characterisation data show that the HT29-MTX cell line confirmed mucin protein expression and that day 14 proves as an optimal time point for mucus secretion, and was therefore selected in the rest of the study for mucus adhesion assays with selected *L. reuteri* strains.

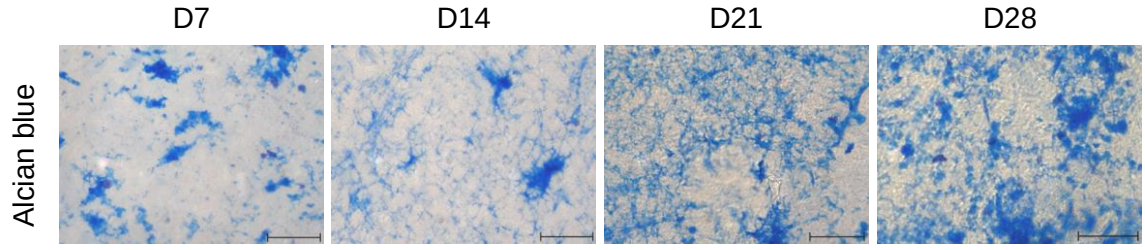

Figure 4.2| Acidic mucopolysaccharide characterisation of the HT29-MTX cell line. HT29-MTX cell monolayers were stained with alcian blue at day 7 (confluency), 14, 21 and 28. Magnification x400; scale bars 50 µm; D, day.

4.3 Adhesion of selected *L. reuteri* strains to the HT29-MTX cell monolayer

The characterised HT29-MTX monolayer was used to investigate the binding of *L. reuteri* strains to mucus. To compare the adhesion of *L. reuteri* strains isolated from different vertebrate hosts, three *L. reuteri* strains were chosen: 100-23C (rat), ATCC 53608 (pig) and DSM 20016 (human). Moreover, the MUB-mutant *L. reuteri* 1063N (pig) strain was included in adhesion assays to compare binding abilities with the MUB-positive *L. reuteri* ATCC 53608 wild-type. The extracellular 353 kDa MUB from *L. reuteri* ATCC 53608 contains two types of related amino acid repeats (Mub1 and Mub2); six copies (RI-RVI) of the type 1 repeat (Mub1) and eight copies (R1-R8) of the type 2 repeat (Mub2) [377]. The 1063N strain harbours a frameshift mutation in the MubR2 repeat, resulting in the expression of a C-terminally truncated MUB that is unable to anchor to the cell wall [391]. For adhesion assays, HT29-MTX cells were seeded into 24-well plates at a density of 4×10^4 cells $well^{-1}$, and incubated without passaging for a period of 14 days. Cell monolayers were then incubated with *L. reuteri* at 1×10^8 cells ml^{-1} in DMEM (without FCS) for 3 h at 37 °C. Non-adherent bacteria were removed by repetitive washes. Percentage adhesion was assessed by a colony count assay. Furthermore, adhesion was visualised by fluorescence microscopy.

Quantitative determination of the cell-associated *L. reuteri* bacteria revealed that 3 h post incubation, all four selected *L. reuteri* strains adhered to the apical surface of the HT29-MTX cell monolayer, with varying degrees of adhesion (10.5-48.22 %, Figure 4.3A). The MUB-positive *L. reuteri* strain ATCC 53608 showed a 2.5-4.5 fold increase in binding to the cell line compared to 100-23C, 1063N and DSM 20016 ($p=0.021$-0.037). Of particular importance is the significantly greater adhesion of the MUB-positive strain ATCC 53608 (48.22 %) compared to the MUB-negative strain 1063N (14.68 %). Adhesion values of strains 100-23C, 1063N and DSM 20016 to the HT29-MTX cell monolayer were similar ($p>0.05$). Fluorescence microscopy images of adhered *L. reuteri* bacteria support the observed binding pattern of the four selected strains (Figure 4.3B), and further confirmed the highly autoaggregating properties of *L. reuteri* ATCC 53608, forming multicellular *L. reuteri* ATCC 53608 aggregates, as previously reported in *L. reuteri* ATCC 53608 cell cultures *in vitro* [391, 483].

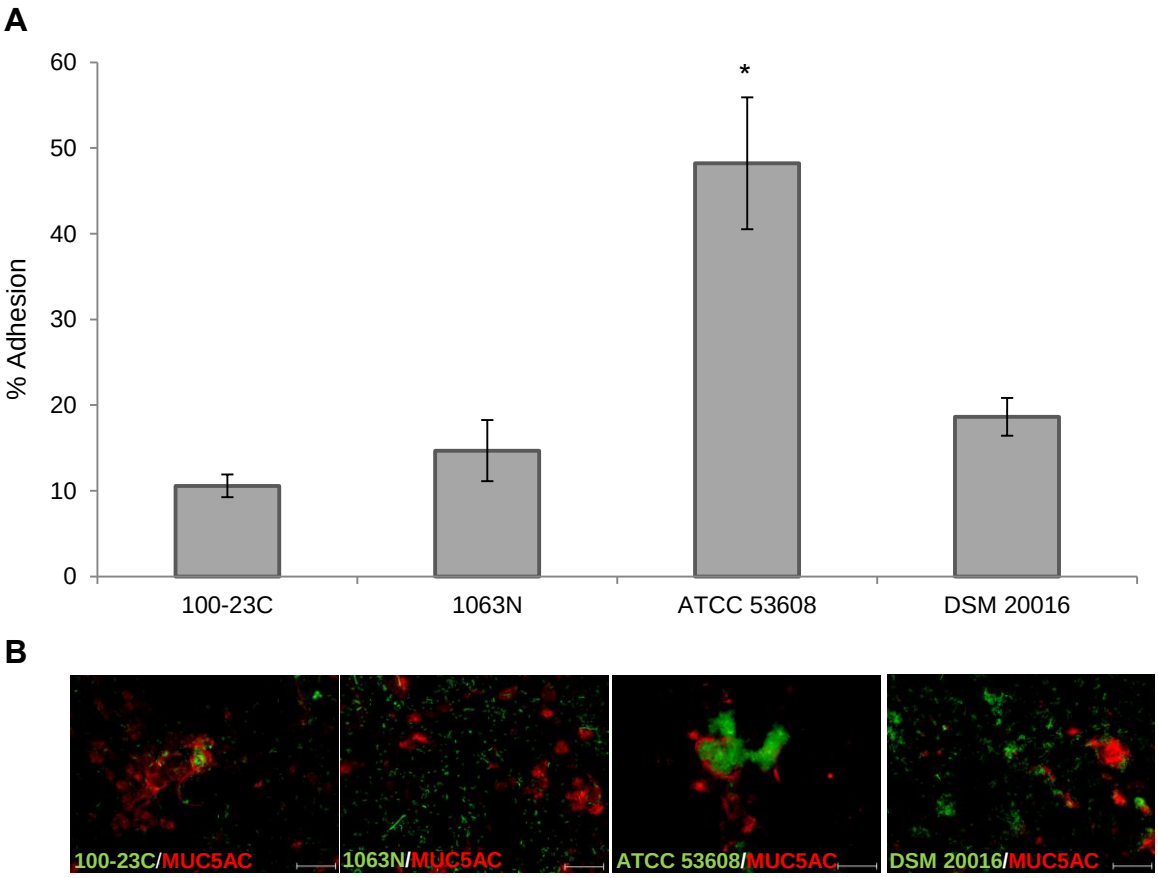

Figure 4.3| *L. reuteri* adhesion to the HT29-MTX cell line. HT29-MTX cell monolayers (n=12) were incubated with *L. reuteri* (100-23C, 1063N, ATCC 53608 or DSM 20016) for 3 h at 37 °C. Percentage adhesion was calculated from colony forming unit counts as the ratio between colonies of adhered bacteria and colonies of initial bacteria added (A). *L. reuteri* adhesion was also assessed by fluorescence imaging of adhered FITC-labelled *L. reuteri* strains on HT29-MTX monolayers stained with anti-MUC5AC rabbit polyclonal primary antibody and anti-rabbit Alexa Fluor 488 secondary antibody (B). Magnification x400; scale bars 50 µm; *p<0.05.

To further investigate the increased mucus-binding ability of strain ATCC 53608 (MUB-positive) compared to strain 1063N (MUB-negative), adhesion of these two strains to HT29-MTX cells was quantified at day 7 (low mucin protein expression) and day 14 (high mucin protein expression), as described above. Figure 4.4 shows that adhesion of the MUB-negative *L. reuteri* 1063N strain is similar at day 7 and day 14 ($p>0.05$),

whereas adhesion increases by 3-fold between these two time points following *L. reuteri* ATCC 53608 incubation (p=0.004). This finding supports the affinity of MUB for mucus, and its role in mediating *L. reuteri* adhesion to the intestinal epithelium *in vitro*.

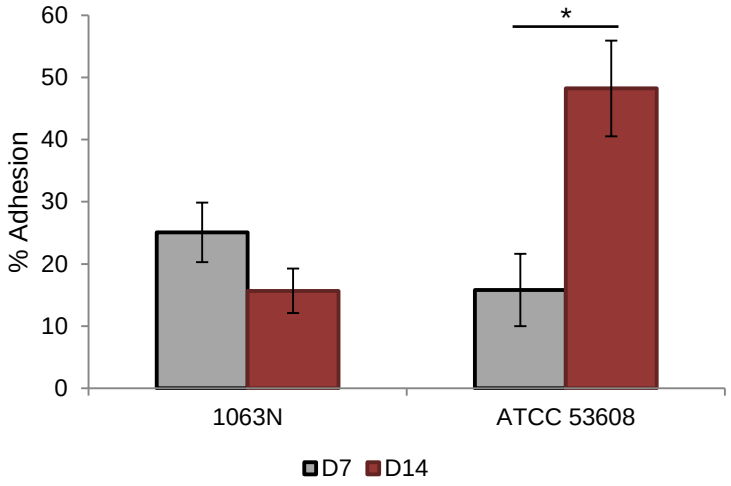

Figure 4.4| *L. reuteri* adhesion to the HT29-MTX cell line at D7 and D14. HT29-MTX cell monolayers (n=12) were incubated with *L. reuteri* (1063N or ATCC 53608) for 3 h at 37 °C. Adhesion of 1063N and ATCC 53608 to HT29-MTX cell monolayers was compared at day 7 (low mucin protein expression) and day 14 (high mucus protein expression). Percentage adhesion was calculated from colony forming unit counts as the ratio between colonies of adhered bacteria and colonies of initial bacteria added. D, day; *p<0.05.

4.4 Effect of selected *L. reuteri* strains on HT29-MTX mucin gene expression

In vitro studies have demonstrated that *Lactobacillus* can inhibit pathogenic epithelial cell adherence through the modulation of intestinal barrier function, such as mucin secretion by host cells [484]. HT29-MTX cells express mainly MUC1, MUC2, MUC3 and MUC5AC [479]. MUC5AC is generally expressed in the respiratory tract, gastric mucosa and reproductive mucosa. The high expression of MUC5AC in HT29-MTX cells is reminiscent of the differentiation of the human foetal colonic epithelium [485]. In

order to investigate the effect of the selected *L. reuteri* strains on mucin gene expression, HT29-MTX cells were seeded into 24-well plates at a density of 4 x 10^4 cells $well^{-1}$, and incubated without passaging for a period of 14 days. Cell monolayers were then incubated with *L. reuteri* (1 x 10^8 cells ml^{-1}) in DMEM (without FCS) for 14 h at 37 °C. Gene expression analysis of *MUC1*, *MUC2*, *MUC3* and *MUC5AC* in response to strains 100-23C, 1063N, ATCC53608 or DSM 20016 was assessed by qRT-PCR. Figure 4.5 shows HT29-MTX mucin gene expression in response to *L. reuteri* strains, expressed as the relative expression level compared to the DMEM-only control. All four *L. reuteri* strains induced membrane-bound *MUC1* gene expression in HT29-MTX cells (p=0.006-0.045), with *L. reuteri* 1063N producing a 2-fold increase (p=0.006). Furthermore, *L. reuteri* 1063N caused a reduction in secreted gel-forming *MUC2* gene expression (p=0.047), and an increase in membrane-bound *MUC3* (p=0.005) and secreted gel-forming *MUC5AC* (p=0.029) gene expression. None of the other *L. reuteri* strains tested (100-23C, ATCC 53608 and DSM 20016) showed an effect on *MUC2*, *MUC3* or *MUCAC* gene expression in HT29-MTX cells. The greatest increase (23-fold) in mucin gene expression was observed for the membrane-bound *MUC3* mucin in response to 1063N. These results are in agreement with previous studies showing upregulation of *MUC3* in HT29 cells in response to different *Lactobacillus* strains, including *L. plantarum* strain 299v, *L. acidophilus* strain DDS-1 and *L. rhamnosus* strain GG [484, 486].

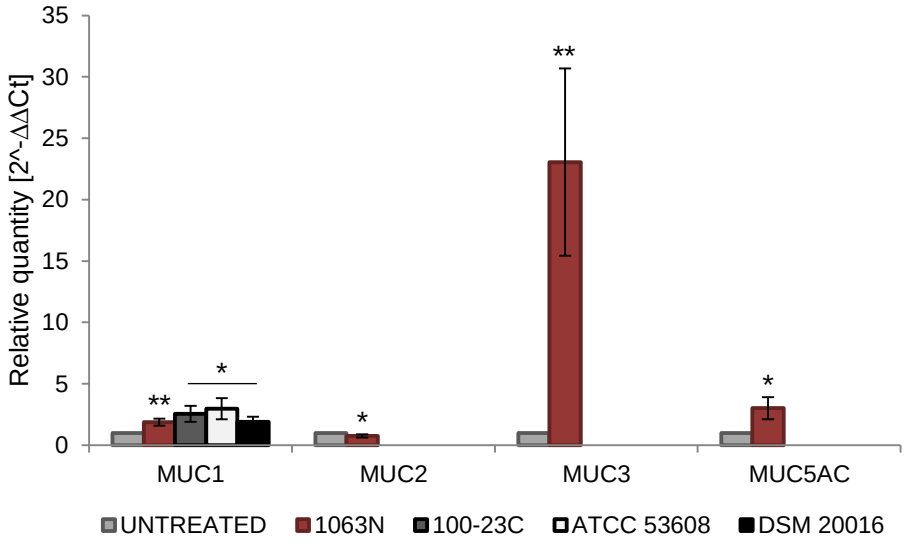

Figure 4.5| HT29-MTX mucin gene expression in response to selected *L. reuteri* strains. HT29-MTX cell monolayers (n=12) were incubated with *L. reuteri* (100-23C, 1063N, ATCC 53608 or DSM 20016) for 14 h at 37 °C. *MUC1*, *MUC2*, *MUC3* and *MUC5AC* mucin gene expression was assessed by qRT-PCR. Gene expression is represented as the relative quantity compared to the untreated control. MUC, mucin; *p<0.05; **p<0.01.

4.5 MUB binding profile and specificity

4.5.1 MUB purification

To further assess the role of MUB in the adhesion of strain ATCC 53608 to the HT29-MTX cell line, compared to 1063N, native MUB was purified from spent media of *L. reuteri* ATCC 53608 cultures. Briefly, low MW proteins were removed from the media and the spent medium concentrated using the Vivaflow system. After extensive dialysis, MUB was purified by size-exclusion chromatography using fast protein liquid chromatography (FPLC) (Figure 4.6A). MUB protein containing fractions were analysed by SDS-PAGE (Figure 4.6B), indicating that MUB protein was successfully purified to apparent homogeneity.

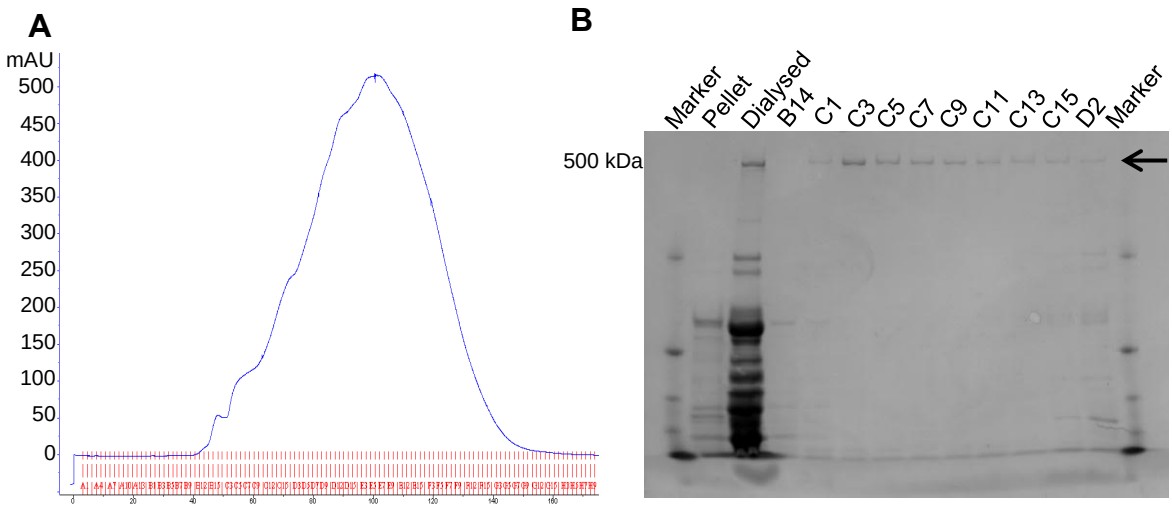

Figure 4.6| Native MUB protein purification from *L. reuteri* ATCC 53608. Elution profile (blue line) of MUB purification sample from FPLC with gel filtration column. Fractions collected are indicated by red lines (A). SDS-PAGE of selected fractions from the gel filtration of MUB purification. Marker, MW marker; B14-D2, selected fractions. MUB indicated by black arrow (B).

MUB ran at an apparent MW of ~ 500 kDa, thus higher than the theoretical MW of 358 kDa, based on amino acid sequence, which may be due to post translational modifications of the native protein, such as glycosylation or phosphorylation. The identity of MUB protein sample, was confirmed by Western blotting using antibodies raised against Mub repeats and by mass spectrometry of the corresponding protein band after trypsin digest (data not shown).

4.5.2 Binding specificity of MUB to HT29-MTX mucin glycans

Adhesion of native purified MUB protein to HT29-MTX cells was first tested under normal culture conditions (as described above). Briefly, MUB was incubated with HT29-MTX cell monolayers for 2 h, and detected using anti-MubR5 antiserum followed by anti-rabbit Alexa Fluor 488 secondary antibody. Fluorescence microscopy showed that

MUB was adhered to mucus droplets overlying the HT29-MTX cell monolayer (Figure 4.7A). The nature of mucus droplets was confirmed by MUC5AC staining (Figure 4.7B).

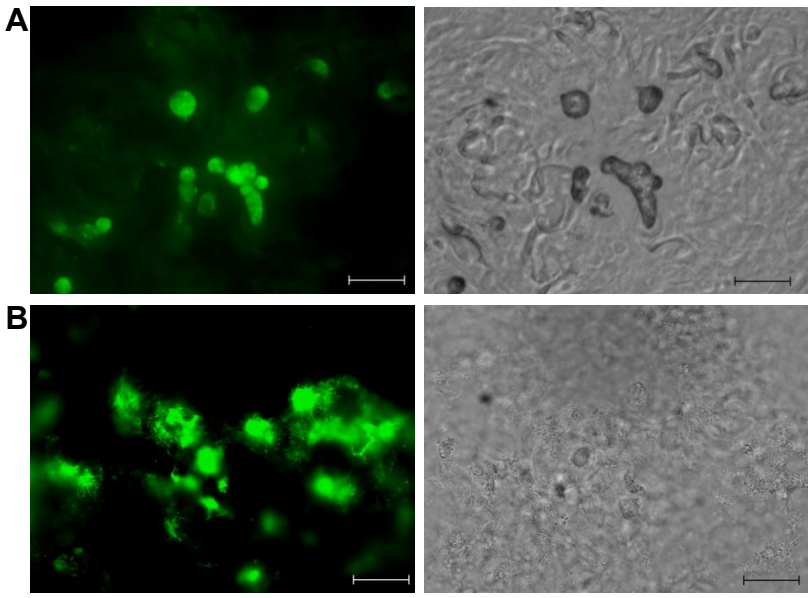

Figure 4.7| MUB protein adheres to mucus droplets on HT29-MTX monolayers. HT29-MTX monolayers (n=12) were incubated with MUB for 2 h at 37 ºC, followed by staining with rabbit anti-MUBR5 and goat anti-rabbit Alexa Fluor 488 secondary antibody (A).HT29-MTX monolayers were stained with polyclonal rabbit anti-MUC5AC followed by goat anti-rabbit Alexa Fluor 488 secondary antibody (B). Bright field images are shown adjacent to fluorescent images to demonstrate the correlation of fluorescence staining with mucus droplet structures. Magnification x400; scale bars, 50 µm.

To determine whether the binding of MUB to mucus was mediated by mucin glycans, HT29-MTX cells were first treated with benzyl 2-acetamido-2-deoxy-α-D-galactopyranoside (benzyl-α-GalNAc), a sugar analogue that acts as an O-glycosylation inhibitor by terminating O-glycan extension [487], prior to MUB binding.

Briefly, HT29-MTX cells were seeded into 24-well plates at a density of 4 x 10^4 cells $well^{-1}$, and incubated without passaging for a period of 14 days. Cell monolayers were incubated with 5 mM benzyl-α-GalNAc for 24 h, before staining with alcian blue, anti-MUC5AC, and plant lectins, SNA-I, peanut agglutinin (PNA) and wheat germ agglutinin (WGA) (Table 3.1). Exposure of HT29-MTX cells to benzyl-α-GalNAc for 24 h led to changes in acidic mucopolysaccharides (Figure 4.8A), mucin secretion (MUC5AC) (Figure 4.8B) and mucin sialylation (SNA-I) (Figure 4.8C), in agreement with previous reports [488, 489]. To test the reversibility of benzyl-α-GalNAc action, monolayers were washed twice following the 24 h benzyl-α-GalNAc incubation, and cultured for a further 24 h with normal culture medium lacking benzyl-α-GalNAc (48 h time point). The 48 h time point demonstrates that the reductions observed in 4.8A, B and C at the 24 h time point are reversible upon removal of the O-glycosylation inhibitor (Figure 4.8A, B and C). Benzyl-α-GalNAc treatment did not cause a reduction in PNA and WGA lectin staining (Figure 4.8D). By contrast, there was a marked reduction in MUB adhesion to treated HT29-MTX cells after 24 h (Figure 4.9A), which was reversible since binding was partially restored after a further 24 h without the inhibitor (Figure 4.9B). Taken together, these results indicate binding specificity of MUB to mucin glycans.

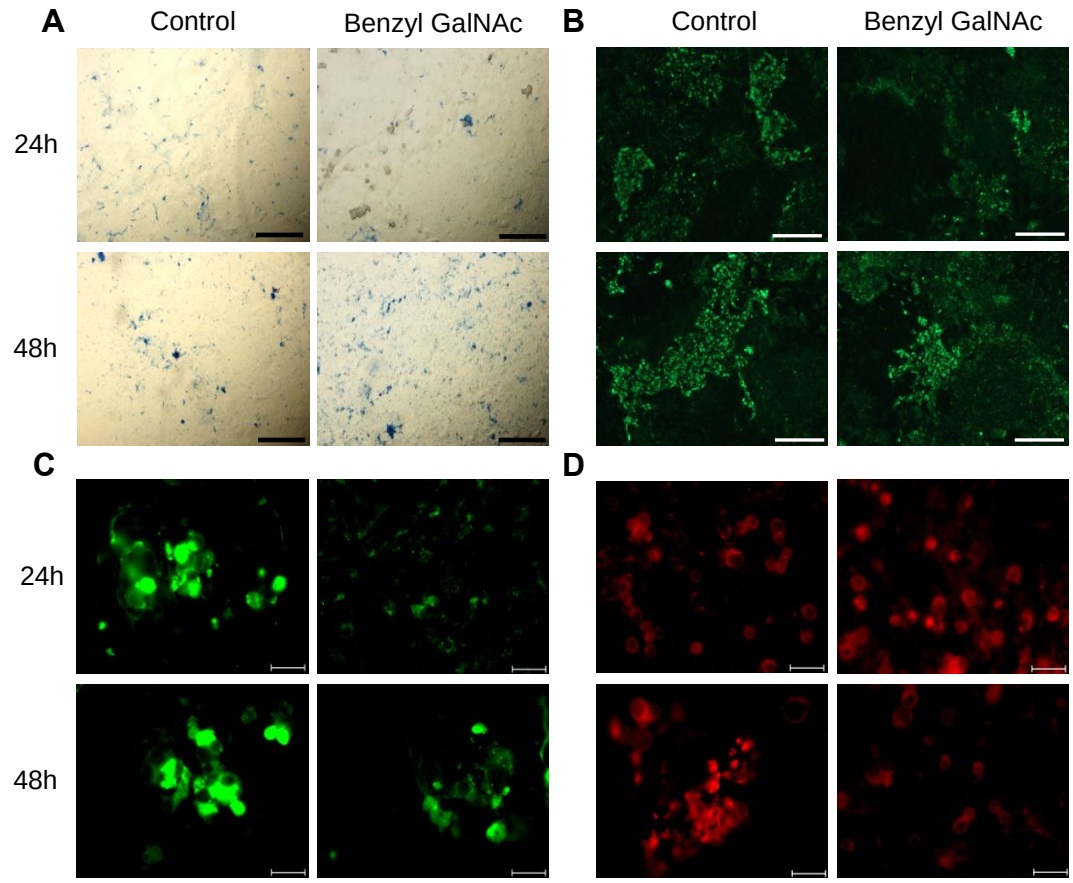

Figure 4.8| The O-glycosylation inhibitor benzyl-α-GalNAc reduces mucin secretion, sialylation and expression of mucopolysaccharides. HT29-MTX monolayers (n=9) were incubated with 5 mM benzyl-α-GalNAc for 24 h and stained with alcian blue (A), anti-MUC5AC (B), SNA-I-FITC (C) or PNA-Rh and WGA-Rh (D). Staining was repeated (A-D) at the 48 h time point (24 h treatment followed by 24 h culture in normal culture medium). Magnification x400, scale bars 50 µm (A,C,D); magnification x100, scale bars 200 µm (B). FITC, Fluorescein isothiocyanate; Rh, Rhodamine.

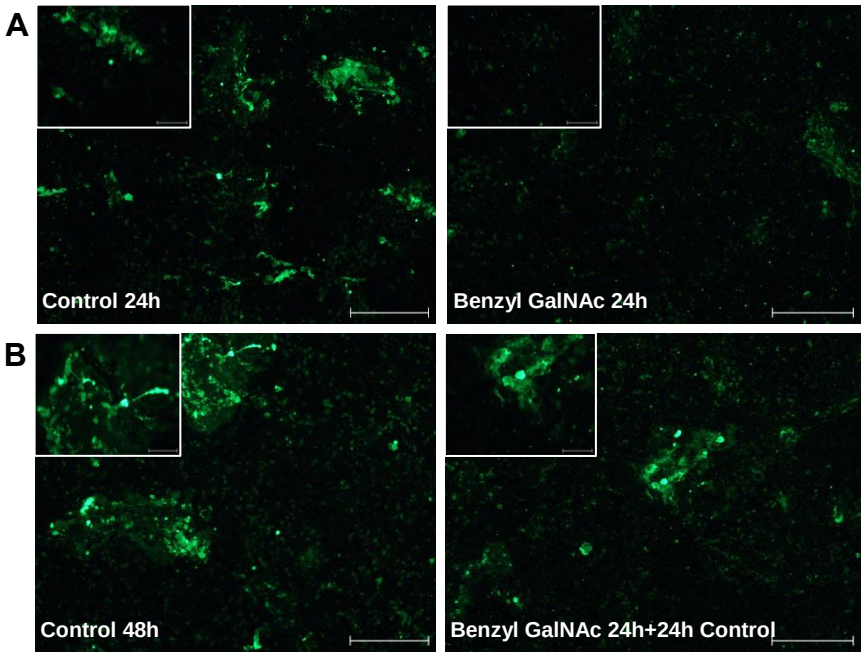

Figure 4.9| Benzyl-α-GalNAc treatment reduces MUB binding to the HT29-MTX cell line. HT29-MTX monolayers (n=9) were incubated with 5mM benzyl-α-GalNAc for 24 h, subsequently incubated with MUB for 2 h and stained with rabbit anti-MUBR5 and goat anti-rabbit Alexa Fluor 488 (A). Staining was repeated at the 48 h time point (24 h treatment followed by 24 h culture in normal culture medium) (B). Magnification x200, scale bars 100 µm; inserts magnification x400; scale bars 50 µm.

4.5.3 Binding specificities of MUB to mucin glycans in host tissues

Given the binding specificity of MUB to specific mucin glycan structures and in light of the differences in mucin O-glycan structures in the SI and colon of humans and mice (section 4.1), it was investigated whether MUB displayed host and/or tissue specificity.

Mouse and human gastric, SI and colon tissue sections were pre-incubated with MUB for 2 h followed by staining for MUB and MUC2. In the mouse, MUB showed gastric binding specificity when compared to the SI and colon (Figure 4.10A top panel). Note that the lack of Muc2 staining in the SI and colon mouse tissue is due to the particular

mouse anti-MUC2 antibody used here, but separate experiments using an alternative rabbit anti-MUC2 antibody confirmed the presence of Muc2 in these sections (Figure 4.10A top panel inserts). Co-staining of MUB and MUC2 was not possible due to the rabbit origin of both antibodies, detected using the same goat anti-rabbit Alexa Fluor 488. In the human tissues, MUB bound to all three tissue types, with particular abundance in the colon (Figure 4.10A bottom panel), in accordance with the high mucin content in this tissue. To investigate whether the murine gastric staining by MUB is representative of higher sialylation in this tissue, mouse gastric, SI and colon tissue sections were stained with SNA-I and MAA sialic acid-specific lectins. Figure 4.10B shows that SNA-I lectin staining is similar in all three tissues, whereas MAA lectin staining is more abundant in gastric tissue compared to the SI and colon. This indicates that α-2,3 linked sialic acid structures are more abundant in gastric tissue compared to the SI and colon, but that their expression is lower than that of α-2,6 linked sialic acid structures in all three tissues. These findings suggest that the increased binding of MUB to gastric tissue may be a consequence of its affinity for α-2,3 linked sialic acid structures.

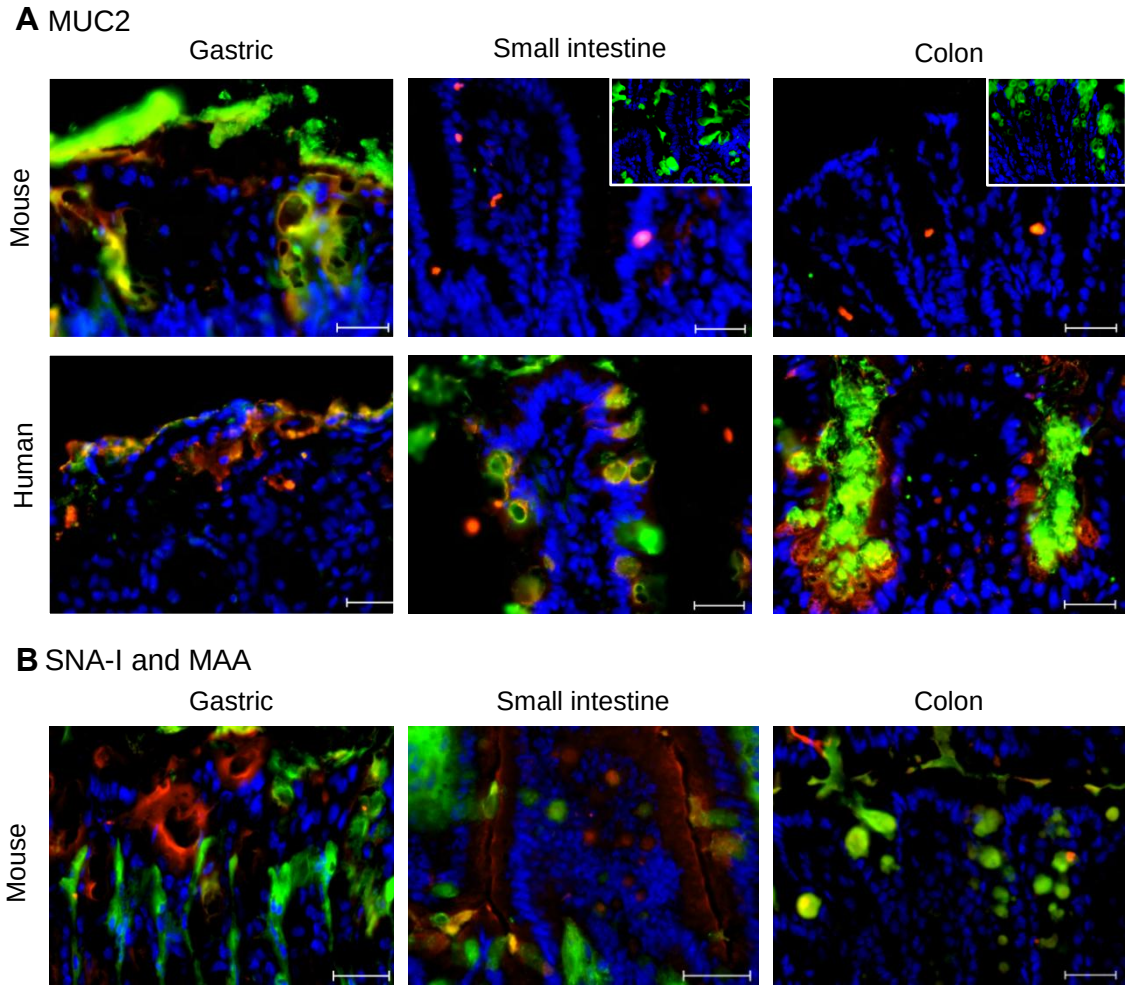

Figure 4.10| Purified MUB protein shows host and tissue specificity. Murine and human gastric, SI and colon tissue (n=3) was incubated with MUB for 2 h at RT and stained with rabbit anti-MUBR5 (green) and mouse anti-MUC2 (red). Mouse SI and colon corner insert images represent tissue stained with rabbit anti-MUC2 (green) only (A). Murine gastric, SI and colon tissue sections were stained with SNA-I-FITC (α-2,6 linked sialic acid specificity; green) and MAA-TR (α-2,3 linked sialic acid specificity; red) lectins (B). Tissue was counterstained with DAPI. Magnification x400, scale bars 50 µm. FITC, Fluorescein isothiocyanate; TR, Texas red.

To further identify the nature of the MUB receptors, murine gastric tissue sections were treated with sodium periodate at pH 5.5 and pH 4.5. Sodium periodate is a mild oxidant that is able to cleave bonds between adjacent carbon atoms that contain hydroxyl

groups (*cis*-glycols), creating two aldehyde groups. Carbohydrate groups in glycoproteins are excellent sites for modification as they allow the conjugation reaction to be directed away from amino acids that may be critical for protein activity. Certain sugar groups are more susceptible to oxidation by sodium periodate, allowing for the cleavage of particular sugars in the polysaccharide chain depending on the treatment conditions applied. Oxidation by sodium periodate at pH 5.5 decreases sialylated structures [490], while treatment with sodium periodate at pH 4.5 abolishes almost all carbohydrate structures [491]. This was shown here by fluorescence staining of mouse gastric tissue with the sialic acid-specific lectin SNA-I (Figure 4.11A), and PNA and WGA lectins (Figure 4.11A). Compared to the PBS control, the level of SNA-I staining was reduced after sodium periodate treatment at pH 5.5. Binding of SNA-I, PNA and WGA was almost completely abolished following treatment at pH 4.5, demonstrating the efficacy of the treatment. Binding of MUB to the epithelial mucus surface was reduced following sodium periodate treatment of gastric tissue (Figure 4.11B), indicating that MUB is adhering to glycan epitopes. Reduced MUB binding at pH 5.5 may be indicative of its sialylated-glycan reactivity. Interestingly, as well as reducing MUB adhesion, treatment of gastric tissue with sodium periodate also seemed to alter the location of MUB binding from the epithelial surface to within the crypts, and potentially goblet cells (Figure 4.11B).

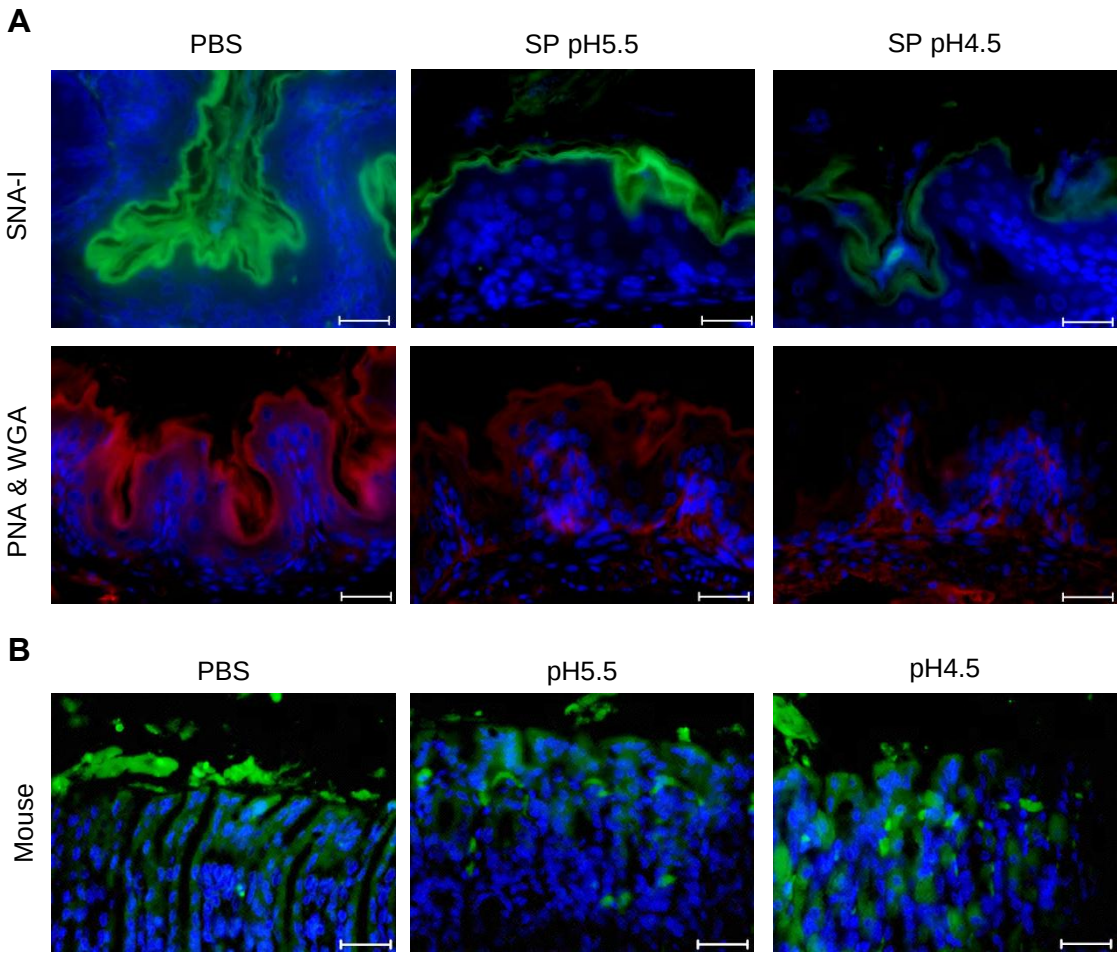

Figure 4.11| Sodium periodate treatment of mouse gastric tissue reduces MUB adhesion. Mouse gastric tissue sections (n=3) were treated with sodium periodate (SP) at pH 5.5 or 4.5. PBS was used as a control. Tissue was stained with the sialic acid-binding lectin SNA-I-FITC, and PNA-Rh and WGA-Rh lectins (A). Tissue was incubated with MUB for 2 h, and subsequently stained with anti-MUBR5 and anti-rabbit Alexa Fluor 488 secondary antibody (B). Sections were counterstained with DAPI. Magnification x400; scale bars 50 µm; PBS, control; pH 5.5, periodate treatment pH 5.5; pH 4.5, periodate treatment pH 4.5; FITC, Fluorescein isothiocyanate; MUB, mucus binding protein; Rh, Rhodamine.

4.6 MUB-mediated *L. reuteri* ATCC 53608 binding profile

In order to further investigate the contribution of MUB mucin glycan specificity to the adhesion of *L. reuteri* strains to mucus, purified MUB was further used in a competition assay. Briefly, HT29-MTX cells were seeded and cultured as above, and pre-incubated with purified MUB protein in DMEM for 2 h at 37 °C, to block potential MUB binding sites. Control wells were incubated with PBS in DMEM. This was followed by incubation with *L. reuteri* 1063N or ATCC 53608 as described above (section 4.3). The percentage adhesion was assessed by a colony count assay.

L. reuteri 1063N adhesion was similar in the PBS control and the MUB pre-incubated cells ($p>0.05$) (Figure 4.12). However, no significant difference in binding was observed for *L. reuteri* ATCC 53608 between the two experimental conditions ($p>0.05$). This may be due to the concentration of MUB used in the assay which may not be sufficient to block available binding sites on the cell line, or due to the fact that binding of purified protein can be more readily displaced by bacteria. An alternative approach would be to pre-incubate bacteria with antibodies directed against Mub repeats (anti-MUBR5 and anti-MUBRI) prior to the adhesion assay [391]. Of note here is that the percentage adhesion of *L. reuteri* ATCC 53608 in Figure 4.12 is approximately 13 % lower compared to Figure 4.4, and is therefore not significantly higher than the *L. reuteri* 1063N strain (as observed in Figure 4.4). This variance in adhesion may be attributed to the amount of mucus expressed by the HT29-MTX monolayer, or the particular *L. reuteri* batch grown for these two experiments that were conducted at different points in time.

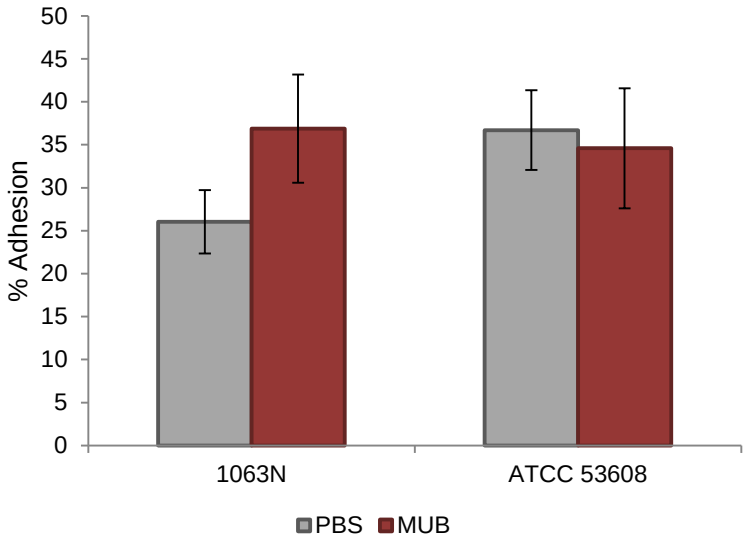

Figure 4.12| *L. reuteri* adhesion following MUB pre-incubation of HT29-MTX cells. HT29-MTX cell monolayers (n=9) were incubated with MUB for 2 h at 37 °C, followed by an incubation with *L. reuteri* (1063N or ATCC 53608) for 3 h at 37 °C. Percentage adhesion was calculated from colony forming unit counts as the ratio between colonies of adhered bacteria and colonies of initial bacteria added. PBS, phosphate buffered saline; MUB, mucus binding protein.

Given the observed specificity of MUB to sialic acid residues (see section 4.5.3), the sialic acid binding specificity of *L. reuteri* 1063N and ATCC 53608 was investigated using the HT29-MTX cell line. HT29-MTX monolayers were first characterised for sialic acid expression using SNA-I and MAA lectins. HT29-MTX monolayers express α-2,6 linked sialic acid, as shown by the SNA-I staining (Figure 4.13A). However, although MAA showed positive staining on mouse and human intestinal tissue sections (Figure 4.10), no MAA lectin binding to HT29-MTX cells was observed (Figure 4.13B), indicating that α-2,3 linked sialic acid structures are absent in the monolayers. Similar binding patterns of SNA-I and MAA to HT29-MTX cells have been reported [492].

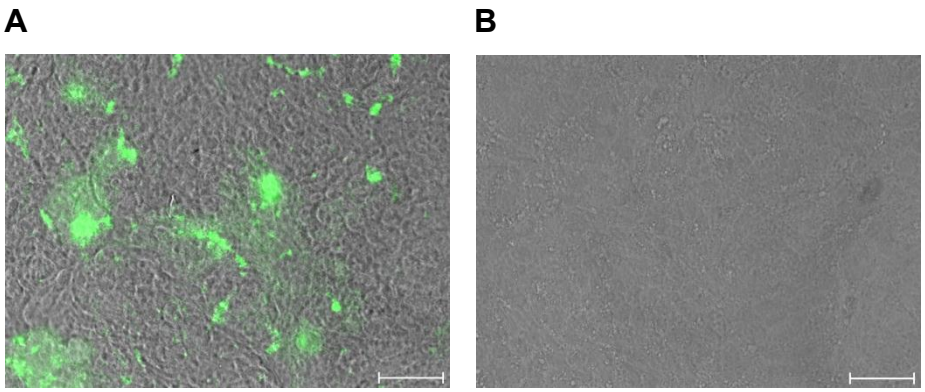

Figure 4.13| Sialic acid lectin characterisation of the HT29-MTX cell monolayer. HT29-MTX monolayers (n=9) were incubated with sialic acid lectins SNA-I-FITC (A) or MAA-TR (B) for 2 h at 37 °C. Lectin staining is shown over bright field channel image. Magnification x400; scale bars 50 µm; FITC, Fluorescein isothiocyanate; TR, Texas red.

HT29-MTX cells were seeded into 24-well plates at a density of 4 x 10^4 cells $well^{-1}$, and incubated without passaging for a period of 14 days. An initial competition assay was performed by attempting to block sialic acid binding sites through the addition of sialic acid lectin SNA-I for 2 h at 37 °C. Cell monolayers were incubated with *L. reuteri* at 1 x 10^8 cells ml^{-1} in DMEM (without FCS) for 3 h at 37 °C. Adhesion was assessed by colony count assays as described above (see section 4.3). A similar level of adhesion ($p>0.05$) was observed for *L. reuteri* 1063N and ATCC 53608 in the presence or absence of sialic acid lectin pre-incubation (Figure 4.14A), as observed above with MUB competition. In a second competition assay, *L. reuteri* 1063N or ATCC 53608 were pre-incubated with the sialic acid sugars Neu5Ac or 6'-O-Sialyllactose (6'-O-SL) for 15 min at RT (Figure 4.14B). Cell monolayers were then incubated with *L. reuteri* at 1 x 10^8 cells ml^{-1} in DMEM (without FCS) for 3 h at 37 °C. Percentage adhesion was assessed by a colony count assay. Adhesion of *L. reuteri* 1063N was similar when cells were pre-incubated with Neu5Ac or 6'-O-SL ($p>0.05$), compared to the PBS control, indicating that *L. reuteri* 1063N has binding specificities for sugars other than Neu5Ac and 6'-O-SL (Figure 4.14B). However, adhesion of *L. reuteri* ATCC 53608 was decreased 3.5-fold ($p=0.01$) and 7-fold ($p=0.006$), compared to the PBS control,

following pre-incubation with Neu5Ac and 6'-O-SL, respectively. This result suggests that MUB has sialic acid sugar specificity, and particularly for 6'-O-SL.

To further investigate this hypothesis, MUB was pre-incubated with sialic acid sugars (Neu5Ac or 6'-O-SL) for 1 h, before incubating with the HT29-MTX monolayers for 2 h at 37 °C (Figure 4.14C). Fluorescence microscopy of MUB adhesion to HT29-MTX cells following pre-incubation with Neu5Ac and 6'-O-SL followed a similar pattern, with binding being reduced following Neu5Ac pre-incubation, and further reduced after incubation with 6'-O-SL, compared to the PBS control (Figure 4.14C). These findings are in accordance with results from sections 4.5.2 and 4.5.3 showing a reduction in MUB binding to intestinal tissue sections following the removal of mucin sialylated glycans or the inhibition of O-glycosylation, thus further suggesting specificity for MUB-mediated *L. reuteri* adhesion to sialylated mucin O-glycans.

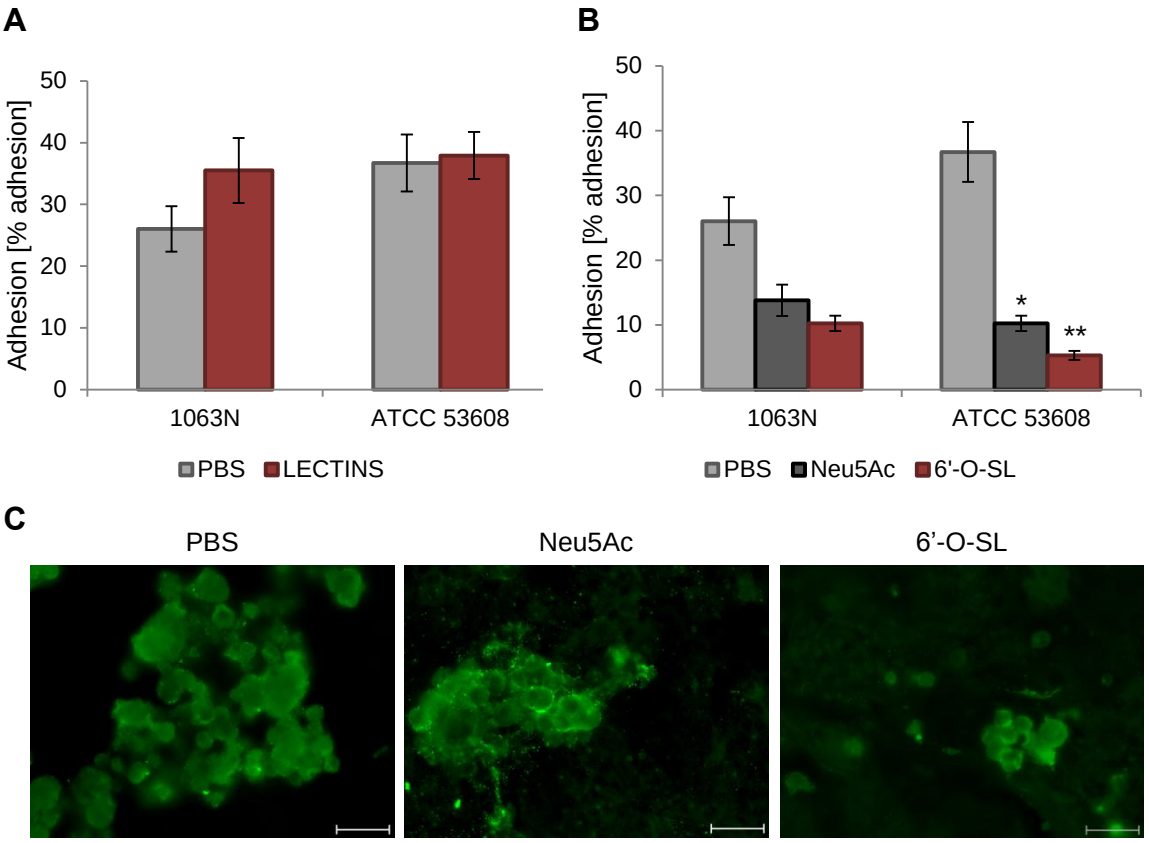

Figure 4.14| *L. reuteri* adhesion in competition with sialic acid lectins and sialic acid sugars. HT29-MTX monolayers (n=9) were incubated with sialic acid lectins (SNA-I and MAA) for 2 h at 37 °C, followed by an incubation with *L. reuteri* (1063N or ATCC 53608) for 3 h at 37 °C (A). *L. reuteri* (1063N or ATCC 53608) strains were pre-incubated with sialic acid sugars (N-acetylneuraminic acid or 6'-O-Sialyllactose) for 15 min, before incubating the HT29-MTX monolayers with the *L. reuteri* strains for 3 h at 37 °C (B). Percentage adhesion was calculated from colony forming unit counts as the ratio between colonies of adhered bacteria and colonies of initial bacteria added. MUB was pre-incubated with sialic acid sugars (N-acetylneuraminic acid or 6'-O-Sialyllactose) for 1 h, before incubating with the HT29-MTX monolayers for 2 h at 37 °C. Monolayers were stained with rabbit anti-MUBR5 and goat anti-rabbit Alexa Fluor 488 (C). Magnification x400; scale bars 50 µm. PBS, phosphate buffered saline; Neu5Ac, N-acetylneuraminic acid; 6'-O-SL, 6'-O-Sialyllactose; *p<0.05; **p<0.01.

4.7 Discussion

4.7.1 *L. reuteri* adhesion and effects on mucin gene expression

Adhesion of bacteria to the intestinal mucosa may prolong their persistence in the GI tract and their beneficial effects to the host, and is thus believed to be a requirement for the compliance of certain probiotic effects, such as immunomodulation and pathogen exclusion [493, 494]. Several reports have been published using human intestinal cell lines as *in vitro* model systems for evaluating the colonisation potential of bacterial strains [495-498]. Mucin production is an important attribute of cell lines for *in vitro* models of the intestinal epithelium, because of the roles played by mucus in the intestine. Bacterial adhesion to the intestinal epithelium influences residence time and the ability of probiotic strains to modulate the immune response(s) and exert health effects in the gut [499].

Results from adhesion experiments described in this study revealed that the binding ability of the selected *L. reuteri* strains to HT29-MTX cells may partly be determined by the nature of the cell-surface protein(s) rather than by their host origin; there was no correlation between species origin and binding i.e. the *L. reuteri* strain isolated from humans did not show significantly higher binding to the human HT29-MTX cell mucus, compared to the rat and pig strains. Similar levels of adhesion of *L. reuteri* were observed for the rat isolate (100-23C), human isolate (DSM 20016) and pig isolate (1063N). However, the 1063N (MUB-negative) mutant showed a significantly reduced binding ability to the human HT29-MTX cells, compared to the MUB-expressing ATCC 53608 wild-type strain, suggesting that MUB has a role in the binding of *L. reuteri* to intestinal mucus. This is in agreement with previous studies showing that mucus binding abilities of *L. reuteri* to mouse mucus *in vitro* correlate with the expression of cell-surface MUB [391]. Additionally, the high adhesion of *L. reuteri* 1063N and ATCC 53608 to HT29-MTX cells observed at day 14 (high mucus protein expression) compared to day 7 (low mucus protein expression), support the role of MUB in facilitating *L. reuteri* adhesion in the presence of mucus, also confirming the mucus-binding specificity of MUB. Differences in aggregation patterns of *Lactobacilli* may also contribute to the observed differences in adhesion abilities [391, 500-502]. A dual role of adhesion and aggregation has previously been reported for the MUB protein in *L.*

reuteri ATCC 53608 [391] and for the transaldolase protein in *Bifidobacterium bifidum* A8 [503].

Some *Lactobacillus* strains appear to possess the capability to upregulate membrane-bound and secreted mucins, although this property is not shared by all probiotic strains. For example, the upregulation of mucin expression was associated with the oral administration of a probiotic preparation (VSL$^{\#}$3) containing four strains of *Lactobacilli (L. casei, L. plantarum, L. acidophilus, and L. delbrueckii subsp. bulgaricus)*, three strains of *Bifidobacteria* and one strain of *Streptococcus salivarius* subsp., which elicited the prevention of flare ups of chronic pouchitis [504]. To determine the impact of *L. reuteri* adhesion properties on the host response, changes in mucin gene expression were investigated in response to the four selected *L. reuteri* isolates. It was hypothesised that *L. reuteri* strains capable of epithelial cell adhesion may affect mucin gene expression *in vitro,* and thereby increase their probiotic potential. qRT-PCR gene expression analyses revealed that the *L. reuteri* isolate 1063N had the highest impact on mucin gene expression in HT29-MTX cells. However, adhesion of *L. reuteri* 1063N to HT29-MTX cells was 33.5 % lower compared to the ATCC 53608 wild-type isolate. This may suggest that adhesion properties are independent of mucin gene expression-modulating properties. Studies investigating the role of mucus in infection with the attaching and effacing bacterial pathogen *Citrobacter rodentium* in mouse models, showed that the gene expression of *Muc2* is significantly reduced at day 10 post-infection, however the biological consequence of this modulation of mucin gene expression currently remains unclear [138]. Here, *L. reuteri* 1063N caused a down-regulation of *MUC2* mRNA. It would be of interest to assess whether changes in *MUC2* mRNA in response to *L. reuteri* 1063N correlate with changes in MUC2 protein. On the one hand, this down-regulation could compromise the host barrier, but on the other hand, a reduction in secreted MUC2 may be important for limiting nutrients and potential attachment sites for pathogenic organisms. In contrast, *L. reuteri* 1063N caused an upregulation of membrane-bound *MUC1* mRNA and *MUC3* mRNA, and secreted *MUC5AC* mRNA. *In vitro*, MUC3 mucin binds numerous enteropathogenic bacteria and viruses [486], stimulates cell migration and prevents apoptosis [505], supporting the importance of this mucin in preventing the attachment of pathogens to intestinal epithelial surfaces and in maintaining the epithelial barrier. In the present work, the highest increase in gene expression was observed for the membrane-bound

MUC3 mucin in response to *L. reuteri* 1063N. An induction of MUC3 was also reported with co-culture of *L. plantarum* 299v or *Lactobacillus rhamnosus* GG with HT29-MTX cells, resulting in the release of a secreted version of the membrane-bound mucin [484]. This secreted version of MUC3 observed by Mack and colleagues could facilitate the clearance of pathogenic organisms through MUC3-microbe interactions also in the loose mucus layer, with subsequent peristalsis, whereas an induction of only the membrane-bound version of MUC3 would require the binding of *Lactobacillus* strains to MUC3 in the firm layer to prevent pathogen binding. Whether *L. reuteri* 1063N used here similarly results in a secreted version of MUC3 requires further investigation. Furthermore, additional work is required to determine the influence of mucin regulation *in vivo*, and its impact on bacteria and the host.

4.7.2 The nature of *L. reuteri* MUB molecular ligands

In bacteria, exported proteins are sorted from the cytoplasm to the bacterial surface or to the surroundings of the microorganism. In probiotic bacteria, these proteins are of special relevance because they may determine important traits such as adhesion to intestinal surfaces and molecular cross-talk with the host. Several bacterial cell-surface proteins have been experimentally shown to be implicated in mucus adhesion, including the MUB of *L. reuteri* 1063 (ATCC 53608) [377], the MUB of *L. acidophilus* NCFM [470], the mannose lectin (Msa) of *L. plantarum* WCFS1 [506] and the *Lactobacillus* surface protein A (LspA) of *L. reuteri* 104R [471, 472]. However, the molecular ligands and implications of these proteins in binding to mucus remain unclear.

MUB binding specificity was investigated in order to understand the underpinning mechanisms that facilitate increased adhesion of *L. reuteri* ATCC 53608 to HT29-MTX cells, compared to *L. reuteri* 1063N. MUB adhesion to gastric tissue was greatly reduced when carbohydrate structures were altered by sodium periodate treatment. Furthermore, binding of MUB was seen to change from an epithelial-surface to an epithelial cell-intrinsic/goblet cell-intrinsic binding phenotype, suggesting that the chemical treatment may disrupt the tissue to make epithelial cell binding sites more accessible to MUB. MUB adhesion to HT29-MTX cells following treatment with the glycosylation inhibitor, benzyl-α-GalNAc, was also markedly reduced. Together, these

findings suggest that MUB binds to mucin glycan structures at the mucosal epithelial surface. This was further reflected by the binding specificity of MUB to murine and human tissue of gastric, SI and colon origin. Whereas MUB was found to adhere to all three tissue types in human, it showed gastric tissue specificity in mice, suggesting that mucin-glycan structures may be dissimilar in gastric tissue compared to the SI and colon. Heavily glycosylated mucins can be modified or terminated with sialic acid groups. Since O-glycomic analyses in mice demonstrated that gastric, SI and colon tissues are all dominated by core-2 O-glycans [82], it was hypothesised that terminal epitopes of glycosylated mucins may be the target of mucus binding proteins. It was shown here that α-2,3 linked sialic acid structures were increased in gastric tissue compared to the SI and colon, but their expression was lower than that of α-2,6 linked sialic acid structures in all three tissues. These findings imply that the increased binding of MUB to gastric tissue may be the result of its affinity for α-2,3 linked sialic acid structures. Further investigations, including the binding of MUB in competition with 3'-O-sialyllactose, would be required to validate these findings.

The specific binding of some bacterial adhesins to sialic acid residues has previously been reported. For example, the sialic acid-binding serine-rich repeat protein (Hsa) of *Streptococcus gordonii* interacts with the carbohydrate portion of the heavily glycosylated gp340 protein found in saliva, tears, the SI and the lungs [507-510], and the *Staphylococcus aureus* surface protein A (SasA) binds to gp340 via the N-acetylneuraminic acid moiety [511]. *Helicobacter pylori* (*H. pylori*) adheres to epithelial cells via bacteria sialic acid-binding lectins [512-514]. *H. pylori* binding to the gastric epithelium has been shown to occur via a glycoprotein containing N-acetylneuraminyl-α (2,3)-lactose [515]. Furthermore, the interaction of *H. pylori* adhesins, such as blood group antigen-binding adhesin (BabA) and sialic acid-binding adhesin (SabA), with several Lewis blood group structures of gastric mucin has been reported [516, 517]. To further investigate the sialic acid binding specificity of *L. reuteri* 1063N and ATCC 53608 in the HT29-MTX cell line, adhesion assays were performed in competition with MUB, sialic acid lectins and sialic acid sugars. These data revealed that *L. reuteri* ATCC 53608 showed binding specificity for Neu5Ac and for 6'-O-sialyllactose. This provides biochemical evidence supporting the probiotic effect of *Lactobacillus* against pathogens, by competing for binding sites, such as *Escherichia coli*, *Vibrio cholerae*,

and *Staphylococcus aureus* that utilise Neu5Ac as a carbon source for growth and colonisation [518-520].

4.7.3 Perspectives and conclusions

Mucus glycoproteins are suggested to act as the molecular receptors of bacterial binding. It has been proposed that bacterial adhesion to mucin glycans is a mechanism by which the host selects bacterial species presenting the complementary adhesins [464]. This study highlights the role of adhesion proteins such as MUB in promoting *Lactobacillus* adhesion to the intestinal epithelium. It was also shown that MUB has sialic acid specificities, particularly towards Neu5Ac and 6'-O-sialyllactose residues; a feature of mucin glycoproteins. The reported specificity of MUB to sialylated structures may explain the regio-specific colonisation of *Lactobacillus* in the vertebrate intestinal tract. Furthermore this study reveals that *L. reuteri* adhesion is necessary but not sufficient for inducing changes in host mucin gene expression.

To date, only indirect evidence has been gathered for adhesion to mucin glycans in *Lactobacillus* species; *L. fermentum* was shown to have affinity to glycoprotein groups on gastric mucus [521], and studies using *L. acidophilus* bacteria suggest binding of lectin-like proteins to the carbohydrate portions of rat colonic mucus [522]. Due to the complexity of the mucin O-glycan structures, having an array of adhesive units with different sugar specificities would be advantageous for a mucus binding protein. Glycan arrays applying mucus and mucins extracted from the intestine, faecal samples, mucus-secreting cell lines or from a commercial source, followed by detailed mucin O-glycan analysis of ligands using mass-spectrometry (MS) would provide alternative methods to assess direct binding and to determine the kinetics of the specific and non-specific interactions involved. Furthermore, more quantitative techniques, such as surface plasmon resonance (SPR) could be used to determine binding of lactobacilli to mucin.

An important aspect of the function of probiotic bacteria is the protection of the host GI micro-environment from invading pathogens. Several reports have demonstrated the ability of probiotic *Lactobacilli* and *Bifidobacteria* to inhibit the cell association and invasion by pathogenic bacteria [484, 500, 523-531]. Further studies to investigate the mechanisms of *L. reuteri* 1063N and ATCC 53608 in the inhibition of adhesion of pathogenic bacteria to HT29-MTX cells, via changes in mucin expression and/or competitive exclusion would be of interest before progressing to the investigation of the role of these strains in animal models and humans.

Chapter 5 Conclusions and perspectives

The focus of this PhD project was to investigate the relationship and cross-talk between intestinal microbes, the mucus layer, and the intestinal immune system, with the general aim of increasing our understanding of the role of the intestinal mucus layer in health and disease. To encompass the above, the first part of this thesis investigated the impact of γδ intraepithelial lymphocyte (IEL) immune cells on the intestinal mucus layer, while the second part shed light on the molecular mechanisms underpinning the adhesion and host response of the gut symbiont *Lactobacillus reuteri* (*L. reuteri)* to intestinal mucus. This discussion summarises the aims and findings of these two parts, the impact in their respective field, and future directions of work, and ends on proposing perspectives of research by building upon the two aspects studied here to bridge the interplay between γδ IELs and *L. reuteri*.

5.1 TCRδ$^{-/-}$ mice show alterations in mucin expression, glycosylation and goblet cells, but maintain an intact mucus layer: conclusions and future work

Intestinal homeostasis is maintained by a hierarchy of immune defences including mucus and immune cells acting in concert to minimise contact between luminal microorganisms and the intestinal epithelial surface. γδ IELs are strategically intercalated at the base of intestinal epithelial cells (IECs); a prime location for an early immune defence. The functions of γδ IELs remain poorly understood, despite reported roles in epithelial restitution and host-microbial homeostasis following injury, and the promotion of barrier maintenance at the intestinal mucosal surface. In light of the functional importance of the mucus layer in maintaining mucosal homeostasis, the relationship between γδ IELs and mucus properties was investigated here, shedding light on the mechanisms underpinning the interplay between these two important host defence mechanisms.

In this study, TCRδ$^{-/-}$ mice were used as a model that lacks γδ IELs, to examine whether and how γδ IELs modulate the properties of the intestinal mucus layer. The TCRδ$^{-/-}$ mice were characterised in terms of mucus properties, and the molecular mechanisms of γδ IEL function were investigated using an *ex vivo* small intestinal (SI) organoid culture system. In accordance with previous findings, data presented here showed an increased susceptibility of TCRδ$^{-/-}$ mice to DSS-induced colitis, which is associated with a reduced number of goblet cells. These alterations in the number of goblet cells correlated with the crypt lengths in the SI and colon of TCRδ$^{-/-}$ mice compared to C57BL/6 wt mice. Such phenotype is reminiscent of characteristic goblet cell depletion (fewer or smaller goblet cell thecae) of many forms of infectious and non-infectious colitis, particularly ulcerative colitis (UC). This phenotype was restored after the addition of keratinocyte growth factor (KGF) to SI organoid cultures from TCRδ$^{-/-}$ mice, showing a marked increase in crypt length, and both goblet cell number and redistribution along the crypts, suggesting a mechanism by which γδ IELs (which produce KGF) modulate crypt and mucus properties. However future work is warranted to determine whether γδ IEL mechanisms of action are direct or indirect i.e. whether γδ IELs secrete factors that directly regulate crypt and mucus properties, or whether it is due to an indirect effect following increased immune-inflammatory stimulation, as suggested by the organoid culture work. The addition of isolated γδ IELs to SI organoid cultures would aid in the elucidation of the mechanisms involved. γδ IELs can be isolated from SI tissue by filtration through a glass wool column and centrifugation through a percoll gradient, to obtain isolated populations of γδ IEL subsets by flow-cytometry (FCM). In particular it would be of interest to determine whether addition of γδ IELs directly impacts on goblet cell numbers and/or mucin gene expression, in the absence of other immune cells in SI organoid cultures.

An alteration in mucus thickness is often associated with disease states in humans such as UC. Despite the reduction of goblet cells observed in TCRδ$^{-/-}$ mice, there was no apparent difference in the thickness or organisation of the inner and outer intestinal mucus layers between TCRδ$^{-/-}$ and wt mice, as measured *in vivo*. However, γδ IEL deficiency led to reduced sialylated mucins in association with increased gene expression of *Muc2* and reduced interleukin-33 (IL-33) mRNA**,** a mediator of mucosal healing and epithelial restoration in the SI. An increased protein expression of Muc2 has been reported for pancreatic adenocarcinomas and gastric carcinomas, and is

usually associated with better patient prognosis. Whether IL-33 is involved in maintaining mucosal homeostasis or alleviating acute mucosal injury in TCRδ$^{-/-}$ mice requires further investigation. Treatment of SI organoids with IL-33 would help to elucidate whether IL-33 is a mediator of γδ IELs to promote mucin biosynthesis. Furthermore, assessing *ST2* gene expression levels by qRT-PCR, and protein levels by ELISA and fluorescence staining, in wt and TCRδ$^{-/-}$ mice, will provide an insight into IL-33 signalling that occurs through this receptor in the absence of γδ IELs. TCRδ$^{-/-}$ mice also showed increased colonic gene expression of membrane-bound mucins, including *Muc13* and *Muc17*. These mucins have been implicated in inflammatory bowel disease (IBD) susceptibility in humans, providing further support for the importance of γδ IELs in the maintenance of mucosal homeostasis. The reported alteration in mucin expression and glycosylation may compromise the nature of the mucosa-associated microbial community, resulting in increased vulnerability to epithelial damage. Determining the composition of the mucosa-associated microbiota in TCRδ$^{-/-}$ mice compared to wt littermates will help assess the association between mucin glycan bacterial metabolism, in particular sialic catabolism, and perhaps pathogenesis.

Collectively, these data provide novel evidence that γδ IELs may play a role in the maintenance of mucosal homeostasis through the regulation of mucin expression, glycosylation and by promoting goblet cell function in the SI. Studies performed here provided some indications of the mechanisms by which γδ IELs modulate mucus properties. A direct role of IL-33/ST2 in this process remains to be demonstrated.

5.2 The mucus-binding protein MUB promotes *L. reuteri* adhesion to the intestinal epithelium and displays sialic acid-binding specificities: conclusions and future work

Mucus is at the interface between the immune system and the microbiota. Unravelling the precise mechanisms of mucus-microbe interactions, and their protective, metabolic and/or immune actions, is essential to our understanding of intestinal homeostasis. Mucins and mucin glycosylation vary along the GI tract, and one of their proposed roles

is to regulate microbial composition. Indeed the diverse mucin glycan structures along the GI tract are believed to provide binding sites for intestinal bacteria, which have adapted to the mucosal environment by expressing the correct complement of adhesins. Given the link between the microbiota and gut inflammatory processes, mucin-binders may represent prime candidates to interact with the host immune system through the production of beneficial metabolites, such as short-chain fatty acids (SCFAs) and polyamines, or by enhancing colonisation resistance and stimulating the immune response. In line with this, microbe adhesion is believed to be a requirement for the realisation of certain probiotic effects, such as immunomodulation and pathogen exclusion. Furthermore, the association with the intestinal mucosa can initiate and extend transient associations, which confer a distinct advantage to these bacteria in the GI tract. In addition certain probiotic strains have been shown to exert a regulatory effect on mucin expression, thereby enhancing their protective effect. However despite the critical role played by the mucus layer in maintaining a homeostatic relationship with the microbiota, knowledge on the nature and structure of bacterial adhesins, as well as their binding specificities to mucin ligands, is limited.

Lactobacilli constitute a normal component of the intestinal microbiota and appear to be a key factor in the processes of competitive exclusion and immunomodulation. Current knowledge suggests that the health-promoting effects of the probiotic *L. reuteri* strain might be partly dependent on its persistence in the intestine and adhesion to mucosal surfaces. The mucus-binding capacity of microbes increases the colonisation capacity at the mucosal interface and has been shown to be important for prolonged intestinal residency of beneficial microbes. In lactobacilli, mucus-binding proteins have been revealed as one class of effector molecules involved in adherence mechanisms of these commensal bacteria to their host. MUB is a mucus-binding protein of *L. reuteri* ATCC 53608 (1063), for which there is limited knowledge on the mucus-binding specificities.

To improve our understanding of the molecular effectors involved in the interaction between GI mucus and *L. reuteri*, the adhesion specificities of *L. reuteri* strains were investigated with the MUB-positive ATCC 53608 and the MUB-negative 1063N, and purified MUB protein, to GI mucins. *L. reuteri* ATCC 53608 showed higher adhesion

ability to the mucin-expressing HT29-MTX cell line compared to the 1063N strain, with adhesion positively correlating with expression of MUC5AC, and indicating *L. reuteri*-mucus interactions. This work also provided evidence for the potential of *L. reuteri* strains to modulate mucin expression; a mechanism by which probiotics may strengthen the mucus barrier to pathogens. Both *L. reuteri* strains induced *MUC1* mRNA, while only *L. reuteri* 1063N caused a reduction in *MUC2* mRNA and an increase in *MUC3* and *MUC5AC* mRNA. The rationale for these changes is not understood and in future work it would be of interest to assess changes in mucins at the protein level, and how they correlate with changes in mucin gene expression. To further investigate how these properties impact on *L. reuteri's* protective role in the host, it would be of interest to compare the potential for *L. reuteri* 1063N and ATCC 53608 strains to limit pathogen adhesion, both *in vitro* and in animal models. Furthermore, investigating the protective effect of these *L. reuteri* strains in a model of inflammation, such as SAMP1/YitFc (SAMP) mice that represent a well-described model of spontaneous Crohn's disease (CD)-like ileitis and gastritis, would be of interest to assess their probiotic potential. HT29-MTX cells used in this study express mainly gastric MUC5AC and the *L. reuteri* strains investigated preferentially colonise the stomach, making the SAMP mouse gastritis model more suitable compared to, for example, the DSS-induced colitis model. Furthermore, work in collaboration with Eva Rajnavolgyi (Debrecen, Hungary) is in progress to measure pro and anti-inflammatory cytokine secretion by monocyte-derived dendritic cells (moDCs) activated in response to different lactobacilli strains, including ATCC 53608 and 1063N.

This study also showed that the contribution of MUB to bacterial adhesion involved specific interactions with mucin glycans. Benzyl-α-GalNAc treatment of HT29-MTX cells caused a reduction in purified MUB protein binding, indicating specificity of MUB to mucin glycans. This was supported by the observed decrease in MUB binding to mouse gastric tissue treated with sodium periodate, suggesting that MUB adheres to sialylated glycan epitopes. Additionally, *L. reuteri* ATCC 53608 and MUB protein adhesion to HT29-MTX cells was reduced in competition with the sialic acid sugars Neu5Ac and 6'-O-SL. Further efforts, such as assays in competition with 3'-O-SL or the use of a range of sialylated mucin substrates, are necessary to fully characterise MUB protein binding specificities to sialic acid structures revealed by this study. Mucin glycan arrays displaying GI tract mucins will be a complementary approach to identify

other potential targets recognised by MUB. Furthermore, the contribution of MUB to mucus interactions could be assessed using methodologies such as atomic force microscopy (AFM) and FCM, allowing a better quantification of the interaction. *H. pylori* is a human pathogen that binds sialic acid structures of gastric mucins via its sialic acid-binding adhesin (SabA), and has been linked to chronic gastritis, gastric and duodenal ulcers, and stomach cancer. Given the similarity in the mucin glycan targets shared between MUB and SabA, it would be of interest to investigate the potential function of *L. reuteri* ATCC 53608 in *H. pylori* exclusion by pre-incubation of HT29-MTX cells with *L. reuteri* ATCC 53608 in a pathogen adhesion assay. Such *in vitro* work can then be followed up by *in vivo* rodent pathogen exclusion studies with *H. pylori* and pre-treatment with *L. reuteri* ATCC 53608.

Deciphering the molecular targets of mucus-binding proteins is important to increase our understanding of host-microbe interactions at the mucosal surface, where bacteria exert their health effect. This knowledge may lead to the identification of new probiotic candidates that display good host attachment and therefore longer residence time in the GI tract; competitive exclusion and immunomodulation mechanisms of such probiotics may aid in the prevention of dysbiosis and the maintenance of a healthy homeostatic environment in the GI tract.

5.3 Investigating the relationship between γδ IELs and *L. reuteri*: future work

The host-microbial symbiosis within the GI tract is fine-tuned at the epithelial interface where the host immune system and the microbiota interact through the mucus layer. Probiotics have been proposed for IBD treatment and clinical studies have reported alleviations of symptoms and prevention of relapses in IBD. The most widely used probiotics are lactobacilli and bifidobacteria but despite the evidence that some probiotics can represent a valid therapeutic approach in IBD treatment, the mechanisms underlying the protection by probiotics in IBD are largely unknown. In addition, not all probiotic strains are able to reduce intestinal inflammation. Since probiotic activity is considered to be genera, species, and strain-specific, investigating the interplay between mucus properties, specific and well-characterised probiotic

strains and immune system is needed to provide mechanistic-based evidences for their protective function. Of interest to this study is the relationship between *L. reuteri* and γδ IELs, and the potential of *L. reuteri* strains to serve as preventive treatment for IBD.

Studies in rats have shown that a *L. reuteri* cocktail, particularly strain R2LC, protects against DSS-induced colitis, highlighting the anti-inflammatory potential of *L. reuteri*. Despite protecting against colitis, treatment with *L. reuteri* did not improve the integrity of the mucus layer or prevent alterations in the mucus microbiota caused by DSS treatment. However, *L. reuteri* did decrease the bacterial translocation from the intestine to the mesenteric lymph nodes (MLN) in rats treated with DSS, which may be an important aspect of the mechanism by which *L. reuteri* ameliorates DSS-induced colitis. Mice lacking γδ IELs are more susceptible to DSS-induced colitis and show increased bacterial translocation compared to wt mice. In light of this, and the above mentioned roles of γδ IELs, we hypothesised that γδ IELs may play an important role in the protective effects induced by *L. reuteri* during DSS-induced colitis. In support of this, studies have shown that pre-treatment with *Lactobacillus acidophilus* and *Bifidobacterium longum* protected against chemically-induced colitis partly via an increase in the γδ IEL population. DSS-induced colitis studies with pre-treatment of *L. reuteri* in wt and TCRδ$^{-/-}$ mice are currently underway in collaboration with Lena Holm (Uppsala, Sweden) in order to address the interplay between *L. reuteri* strains, the mucus layer and γδ IELs in the protection against DSS-induced colitis. The severity of colitis in the two groups of mice will be assessed through body weight, macroscopic and microscopic evaluation of colitis, and compared between *L. reuteri* pre-treated DSS and DSS-only treatment groups. Furthermore, γδ IEL numbers will be assessed in wt DSS and wt *L. reuteri* pre-treated DSS groups to identify whether protection by *L. reuteri* is associated with an increase in γδ IELs. These approaches will increase our understanding of beneficial microbes and their relationship with the host, and provide mechanistic insights and potential novel strategies for the maintenance of a healthy homeostatic intestinal environment to prevent diseases, such as IBD.

Appendix 1

Commercial suppliers of chemicals, reagents and equipment

Abcam
330 Cambridge Science Park
Cambridge, CB4 0FL

Acros Organics (part of Thermo Fisher Scientific)
Bishop Meadow Road
Loughborough, LE11 5RG

Affymetrix
3420 Central Expressway
Santa Clara, CA 95051

Agilent Technologies
5301 Stevens Creek Blvd
Santa Clara, CA 95051

Barnstead (part of Thermo Fisher Scientific)
Bishop Meadow Road
Loughborough, LE11 5RG

BD Biosciences
Between Towns Road
Oxford, OX4 3LY

BDH Laboratory Supplies
Poole,
Dorset, BH15 1TD

Bethyl Laboratories
Munro House, Trafalgar Way, Bar Hill
Cambridge CB23 8SQ

Biolegend
4B Highgate Business Centre, 33 Greenwood Place
London, NW5 1LB

Bio-Rad
Bio-Rad House, Maylands Avenue,
Hemel Hempsted,
Hertfordshire, HP2 7TD

Biosera
2 Birch House, Brambleside
Bellbrook Industrial Estate
East Sussex, TN22 1QQ

BMG Labtech
Allmendgruen 8,
D-77799 Ortenberg
Germany

Caltag
PO Box 6139, Silverstone
Towcester, NN12 8GN

EY Laboratories
107 N. Amphlett Blvd
San Mateo, CA. 94401 USA

Fluka Chemika
Industriestrasse 25,
CH-9470 Buchs
Switzerland

GE Healthcare
101 Carnegie Center
Princeton, NJ 08540
USA

Glycom
Diplomvej 373, 1
DK-2800 Kgs. Lyngby
Denmark

Hitachi
15-1, Konan 2-chome, Minato-ku
Tokyo 108-6020
Japan

Invitrogen
3 Fountain Drive
Inchinnan Business Park
Paisley PA4 9RF, UK

Jackson Laboratories
600 Main Street, Bar Harbor
Maine, 04609 USA

Leitz
Ernst-Leitz-Straße 17-37
Wetzlar, 35578
Germany

Life Technologies Ltd
3 Fountain Drive
Inchinnan Business Park
Paisley PA4 9RF, UK

Lonza
Muechensteinstrasse 38
4002 Basel
Switzerland

Millipore
Merck Millipore Headquarters
290 Concord Road
Billerica, MA 01821

MP Biomedicals
Wellington House, East Road
Cambridge, CB1 1BH

National Diagnostics
Unit 4, Hessle
HU13 9LX

New Englad BioLabs
240 County Road
Ipswich, MA 01938-2723

Peprotech
PeproTech House, 29 Margravine Road
London, W6 8LL

PerkinElmer
204 Science Park, Milton Road
Cambridge, CB4 0GZ

Point Of Care Testing (POCT) Ltd
Unit 18 Arbroath Business Centre, Dens Road,
Arbroath, Angus, DD11 1RS

Qiagen
Qiagen House, Fleming Way
Crawley, West Sussex
RH10 9NQ

R&D Systems
19 Barton Lane, Abingdon Science Park,
Abingdon, OC14 3NB

Santa Cruz Biotechnologies
Bergheimer Str. 89-2
69115 Heidelberg, Germany

Sigma-Aldrich
Fancy Road, Poole
Dorset, BH17 7NH

Thermo Fisher Scientific
Bishop Meadow Road
Loughborough, LE11 5RG

Vector Laboratories
3 Accent Park, Bakewell Road
Peterborough, PE2 6XS

VWR
Hunter Boulevard, Magna Park
Lutterworth, LE17 4XN

Zeiss
PO Box 78, Woodfield Road
Welwyn Garden City, Hertfodshire

Zymed
3 Foundation Drive, Inchinnin Business Park
Paisley, PA4 9RF

Appendix 2

Processing protocol of formalin-fixed tissue

Step	Contents	Duration (min)
1	70 % ethanol	60
2	80 % ethanol	90
3	90 % ethanol	120
4	100 % ethanol	60
5	100 % ethanol	90
6	100 % ethanol	120
7	Xylene	30
8	Xylene	60
9	Xylene	90
10	Wax	60
11	Wax	60
12	Wax	120
13	Wax	120

Appendix 3

Assessment parameters for tissue histology

Parameter scored	Score	Score description
Epithelial injury	0	None
	1	Crypt epithelial injury/flattening ± necrotic debirs in crypt lumen
	2	Erosion in <50% mucosal thickness with basal half crypt preserved
	3	Erosion in >50% mucosal thickness or crypt epithelium completely destroyed
	4	Ulceration involving submucosa (involving muscularis mucosa) or deeper (transmural)
Extent of epithelial injury	0	None
	1	Focal
	2	Multifocal (>2 areas)
	3	Diffuse (> 50% circumference)
Chronic inflammatory cells infiltrate	0	None
	1	Mild
	2	Moderate
	3	Severe
Acute inflammatory cells infiltrate	0	None
	1	Mild (no crypt abscess/cryptitis)

	2	Moderate (occasional crypt abscess/cryptitis)
	3	Severe (frequent crypt abscess/cryptitis)
Number of goblet cells	0	No loss of goblet cells
	1	Loss of goblet cells up to 1/3
	2	Loss of goblet cells up to 2/3
	3	Loss of goblet cells of >2/3
Thickening of the colon/ileum wall (odoema)	0	No thickening of wall
	1	Thickening of submucosa (1/3)
	2	Thickening of submucosa and muscularis propria (2/3)
	3	Thickening of submucosa, muscularis propria and serosa (>2/3)

Appendix 4

Ingredients of LDM II broth

INGREDIENT	AMOUNT PER L
K2HPO4 (anhydrous)	1.5 g
KH2PO4 (anhydrous)	1.5 g
Vitamin-free casamino acids	10 g
Sodium acetate	15 g
Sodium citrate	0.22 g
Tryptophan	50 mg
Asparagine	0.2 g
Cysteine-HCl	0.2 g
Thiamine-HCl	0.2 mg
***para*-Aminobenzoic acid**	0.04 mg
Calcium pantothenic acid	0.4 mg
Niacin	1.0 mg
Pyridoxine-HCl	0.5 mg
Biotin	0.05 mg
Folic acid	0.1 mg
Riboflavin	0.4 mg
Adenine sulphate	10 mg
Uracil	20 mg
Guanine-HCl	10 mg
Cytidine (acid)	50 mg
Thymidine	1.6 µg

Tween-80	1.0 ml
MgSO4.7H2O	0.163 g
MnSO4.H2O	23.4 mg
FeSO4.7H2O	13 mg
Sucrose	20 g

Appendix 5

Glycogene list

Category	Sub-category	Common name
CBP:C-Type Lectin	10-Polycystin	Pkd1 [Polycystin]
CBP:C-Type Lectin	10-Polycystin	Pkd1l2 [Polycystin 1-like protein 2]
CBP:C-Type Lectin	11-Attractin	Atrnl1 [Attractin homolog]
CBP:C-Type Lectin	11-Attractin	Attractin
CBP:C-Type Lectin	12-CTLD + acidic neck	Prg2 [proteoglycan 2 bone marrow]
CBP:C-Type Lectin	12-CTLD + acidic neck	Prg3 [proteoglycan 3; Eosinophil major basic protein homolog]
CBP:C-Type Lectin	13-IDD	DGCR2 DiGeorge syndrome protein C
CBP:C-Type Lectin	14-Endosialin	Cd248 [CD248 antigen endosialin]
CBP:C-Type Lectin	14-Endosialin	CD93 [C1q receptor; Cd93 antigen]
CBP:C-Type Lectin	14-Endosialin	Thbd [Thrombomodulin]
CBP:C-Type Lectin	1-Proteoglycan	Aggrecan
CBP:C-Type Lectin	1-Proteoglycan	Brevican (BCAN)
CBP:C-Type Lectin	1-Proteoglycan	Neurocan
CBP:C-Type Lectin	1-Proteoglycan	Versican (CSPG2, PG-M)

CBP:C-Type Lectin	1-Proteoglycan	Versican (CSPG2, PG-M)
CBP:C-Type Lectin	1-Proteoglycan	Versican (CSPG2, PG-M)
CBP:C-Type Lectin	2-Type 2 Receptor	Asialoglycoprotein receptor R1
CBP:C-Type Lectin	2-Type 2 Receptor	Asialoglycoprotein receptor R2
CBP:C-Type Lectin	2-Type 2 Receptor	CD207 [Langerin]
CBP:C-Type Lectin	2-Type 2 Receptor	CD209a [DC-SIGN]
CBP:C-Type Lectin	2-Type 2 Receptor	CD209b [SIGNR1]
CBP:C-Type Lectin	2-Type 2 Receptor	CD209b [SIGNR1]
CBP:C-Type Lectin	2-Type 2 Receptor	CD209c [SIGNR2]
CBP:C-Type Lectin	2-Type 2 Receptor	CD209d [SIGNR3]
CBP:C-Type Lectin	2-Type 2 Receptor	CD209e [SIGNR4]
CBP:C-Type Lectin	2-Type 2 Receptor	CD209f [SIGNR8]
CBP:C-Type Lectin	2-Type 2 Receptor	CD209g [SIGNR7]
CBP:C-Type Lectin	2-Type 2 Receptor	Clec4a2
CBP:C-Type Lectin	2-Type 2 Receptor	Clec4a3 [dendritic cell inhibitory receptor 3]
CBP:C-Type Lectin	2-Type 2 Receptor	Clec4b1
CBP:C-Type Lectin	2-Type 2 Receptor	Clec4d (Clecsf8), aka MCL
CBP:C-Type Lectin	2-Type 2 Receptor	Clec4e [Mincle; C-type lectin superfamily member 9]
CBP:C-Type Lectin	2-Type 2 Receptor	Clec4f
CBP:C-Type Lectin	2-Type 2 Receptor	Clec4g [LSECtin]
CBP:C-Type Lectin	2-Type 2 Receptor	Fcer2a [Fc receptor IgE low affinity II alpha]
CBP:C-Type Lectin	2-Type 2 Receptor	Fcer2a [Fc receptor IgE low affinity II alpha]
CBP:C-Type Lectin	2-Type 2 Receptor	Lman21 (lectin mannose-binding 2-like; DC-SIGN-X6]
CBP:C-Type Lectin	2-Type 2 Receptor	Mgl1 [macrophage galactose N-acetyl-galactosamine]
CBP:C-Type Lectin	2-Type 2 Receptor	Mgl2 [macrophage galactose N-acetyl-galactosamine]
CBP:C-Type Lectin	2-Type 2 Receptor	Mgl2 [macrophage galactose N-acetyl-galactosamine]
CBP:C-Type Lectin	3-Collectin	Colec10
CBP:C-Type Lectin	3-Collectin	Colec12

CBP:C-Type Lectin	3-Collectin	Colec12
CBP:C-Type Lectin	3-Collectin	Mbl1 [Mannose-binding protein A]
CBP:C-Type Lectin	3-Collectin	Mbl2 [Mannose-binding protein C]
CBP:C-Type Lectin	3-Collectin	Sftpa1 [Surfactant associated protein A- Long Trans]
CBP:C-Type Lectin	3-Collectin	Sftpd [Surfactant associated protein SP-D]
CBP:C-Type Lectin	4-Selectin	Sele [E-Selectin]
CBP:C-Type Lectin	4-Selectin	Sell [L-selectin]
CBP:C-Type Lectin	4-Selectin	Selp [P-selectin]
CBP:C-Type Lectin	5-NK Receptors	CD69
CBP:C-Type Lectin	5-NK Receptors	CD72
CBP:C-Type Lectin	5-NK Receptors	CLEC1a
CBP:C-Type Lectin	5-NK Receptors	CLEC1b
CBP:C-Type Lectin	5-NK Receptors	Clec2d
CBP:C-Type Lectin	5-NK Receptors	Clec2h
CBP:C-Type Lectin	5-NK Receptors	Clec4n [Dectin-2]
CBP:C-Type Lectin	5-NK Receptors	Clec5a [MDL-1]
CBP:C-Type Lectin	5-NK Receptors	Clec7a; dendritic cell-associated C-type lectin 1; Dectin-1
CBP:C-Type Lectin	5-NK Receptors	Klra10; Ly49J
CBP:C-Type Lectin	5-NK Receptors	Klra10; Ly49J
CBP:C-Type Lectin	5-NK Receptors	Klra12; Ly49L1
CBP:C-Type Lectin	5-NK Receptors	Klra13; Ly49M
CBP:C-Type Lectin	5-NK Receptors	Klra15; Ly49O
CBP:C-Type Lectin	5-NK Receptors	Klra15; Ly49O
CBP:C-Type Lectin	5-NK Receptors	Klra17 [LY49Q]
CBP:C-Type Lectin	5-NK Receptors	Klra18 [Ly49R, extensive crosshyb with Klra4,12,33[
CBP:C-Type Lectin	5-NK Receptors	Klra2; Ly49B
CBP:C-Type Lectin	5-NK Receptors	Klra22; Ly49V
CBP:C-Type Lectin	5-NK Receptors	Klra3; Ly49C/Ly49I

CBP:C-Type Lectin	5-NK Receptors	Klra3; Ly49C/Ly49I
CBP:C-Type Lectin	5-NK Receptors	Klra4; Ly49D
CBP:C-Type Lectin	5-NK Receptors	Klra4; Ly49D
CBP:C-Type Lectin	5-NK Receptors	Klra5; LY49E
CBP:C-Type Lectin	5-NK Receptors	Klra5; LY49E
CBP:C-Type Lectin	5-NK Receptors	Klra6; Ly49S
CBP:C-Type Lectin	5-NK Receptors	Klra7; LY49G
CBP:C-Type Lectin	5-NK Receptors	Klra8 [Ly49H/Ly49U]
CBP:C-Type Lectin	5-NK Receptors	Klra9
CBP:C-Type Lectin	5-NK Receptors	Klrb1f [Nkrp1f protein]
CBP:C-Type Lectin	5-NK Receptors	Klrc1 [killer cell lectin-like receptor subfamily C]
CBP:C-Type Lectin	5-NK Receptors	Klrc1 [killer cell lectin-like receptor subfamily C]
CBP:C-Type Lectin	5-NK Receptors	Klrc3 [killer cell lectin-like receptor subfamily C; NKG2 E]
CBP:C-Type Lectin	5-NK Receptors	Klrd1(killer cell lectin-like receptor subfamily D) CD94
CBP:C-Type Lectin	5-NK Receptors	KLRG1 [killer cell lectin-like receptor subfamily G]
CBP:C-Type Lectin	5-NK Receptors	Klrk1 [NKG2 D]
CBP:C-Type Lectin	5-NK Receptors	Klrk1 [NKG2 D]
CBP:C-Type Lectin	5-NK Receptors	Olr1 [oxidized low density lipoprotein (lectin-like)]
CBP:C-Type Lectin	6-MMR	Ly75 [lymphocyte antigen 75; DEC205]
CBP:C-Type Lectin	6-MMR	Ly75 [lymphocyte antigen 75; DEC205]
CBP:C-Type Lectin	6-MMR	Mrc1 [mannose receptor C type 1]
CBP:C-Type Lectin	6-MMR	Mrc2 [mannose receptor C type 2; Endo180 - Long Trans]
CBP:C-Type Lectin	6-MMR	Mrc2 [mannose receptor C type 2; Endo180 - Short trans]
CBP:C-Type Lectin	6-MMR	Pla2r1 [Phospholipase A2 receptor 1]
CBP:C-Type Lectin	6-MMR	Pla2r1 [Phospholipase A2 receptor 1]
CBP:C-Type Lectin	6-MMR	Pla2r1 [Phospholipase A2 receptor 1]
CBP:C-Type Lectin	7-Free CTLDs	Pap [Pancreatitis-associated protein]
CBP:C-Type Lectin	7-Free CTLDs	Reg1 [regenerating islet-derived 1]

CBP:C-Type Lectin	7-Free CTLDs	Reg2 [regenerating islet-derived 2]
CBP:C-Type Lectin	7-Free CTLDs	Reg3d [regenerating islet-derived 3 delta]
CBP:C-Type Lectin	7-Free CTLDs	Reg4 [regenerating islet-derived family member 4]
CBP:C-Type Lectin	8-Simple Type 1 receptors	Chodl [chondrolectin; Layilin homolog]
CBP:C-Type Lectin	8-Simple Type 1 receptors	Chodl [chondrolectin; Layilin homolog]
CBP:C-Type Lectin	8-Simple Type 1 receptors	Layn [Layilin]
CBP:C-Type Lectin	9-Tetranectins	Clec11a [C-type lectin domain family 11 member a]
CBP:C-Type Lectin	9-Tetranectins	Clec3a [C-type lectin domain family 3 member a]
CBP:C-Type Lectin	9-Tetranectins	Clec3b [C-type lectin domain family 3 member b; Tetranectin]
CBP:C-Type Lectin	Novel	Clec14a
CBP:C-Type Lectin	Novel	Frem1 [Fras1 related extracellular matrix protein 1]
CBP:C-Type Lectin	Novel	Mrcl [mannose receptor-like]
CBP:I-Type Lectin	Non-Siglec	CD83
CBP:I-Type Lectin	Non-Siglec	Icam1 [intercellular adhesion molecule possible short variant]
CBP:I-Type Lectin	Non-Siglec	Icam1 [intercellular adhesion molecule]
CBP:I-Type Lectin	Non-Siglec	Icam2 [intercellular adhesion molecule 2]
CBP:I-Type Lectin	Non-Siglec	L1cam [L1 cell adhesion molecule]
CBP:I-Type Lectin	Non-Siglec	L1cam [L1 cell adhesion molecule]
CBP:I-Type Lectin	Non-Siglec	Pecam1 [platelet/endothelial cell adhesion molecule 1]
CBP:I-Type Lectin	Non-Siglec	Pecam1 [platelet/endothelial cell adhesion molecule 1]
CBP:I-Type Lectin	Non-Siglec	Vcam1 [vascular cell adhesion molecule 1]
CBP:I-Type Lectin	Non-Siglec	Vcam1 [vascular cell adhesion molecule 1]
CBP:I-Type Lectin	Siglec	CD22 (Siglec-2)
CBP:I-Type Lectin	Siglec	CD22 (Siglec-2)
CBP:I-Type Lectin	Siglec	CD22 (Siglec-2)
CBP:I-Type Lectin	Siglec	CD33 (Siglec-3)
CBP:I-Type Lectin	Siglec	CD33 (Siglec-3)
CBP:I-Type Lectin	Siglec	MAG [myelin-associated glycoprotein; Siglec-4]

CBP:I-Type Lectin	Siglec	MAG [myelin-associated glycoprotein; Siglec-4]
CBP:I-Type Lectin	Siglec	Siglec1 [Sialoadhesin]
CBP:I-Type Lectin	Siglec	Siglec1 [Sialoadhesin]
CBP:I-Type Lectin	Siglec	Siglec1 [Sialoadhesin]
CBP:I-Type Lectin	Siglec	Siglec15 [sialic acid binding Ig-like lectin 15]
CBP:I-Type Lectin	Siglec	Siglec5 [sialic acid binding Ig-like lectin 5]
CBP:I-Type Lectin	Siglec	Siglec5 [sialic acid binding Ig-like lectin 5]
CBP:I-Type Lectin	Siglec	Siglece [SIGLEC-like 1]
CBP:I-Type Lectin	Siglec	Siglecg [sialic acid binding Ig-like lectin G]
CBP:I-Type Lectin	Siglec	Siglec-H
CBP:I-Type Lectin	Siglec	Siglec-H
CBP:I-Type Lectin	Siglec	Siglec-H
CBP:I-Type Lectin	Siglec	Siglec-H (short form)
Galectin	Galectin	1110067D22Rik [hypothetical protein LOC216551; HSPC159]
Galectin	Galectin	GRIFIN [galectin-related inter-fiber protein; Galectin 11]
Galectin	Galectin	Lgals1 [lectin galactose binding soluble 1; Galectin 1]
Galectin	Galectin	Lgals12 [lectin galactose binding soluble 12; Galectin 12]
Galectin	Galectin	Lgals2 [lectin galactose-binding soluble 2; Galectin 2]
Galectin	Galectin	Lgals3 [Galectin 3]
Galectin	Galectin	Lgals4 [lectin galactose binding soluble 4; Galectin 4 (Lgals4 and Lgals6 overlap heavily)]
Galectin	Galectin	Lgals6 [lectin galactose binding soluble 6; Galectin 6 (Lgals4 and Lgals6 overlap heavily)]
Galectin	Galectin	Lgals7 [lectin galactose binding soluble 7; Galectin 7]
Galectin	Galectin	Lgals8 [lectin galactose binding soluble 8; Galectin 8]
Galectin	Galectin	Lgals9 [lectin galactose binding soluble 9; Galectin 9]
Glycan Degradation	Arylsufatases	Arsa [Arylsulfatase A]
Glycan Degradation	Arylsufatases	Arsb [Arylsulfatase B]

Glycan Degradation	Galactosidase	Gla [alpha-Galactosidase A]
Glycan Degradation	Galactosidase	Glb1 [galactosidase beta 1]
Glycan Degradation	Galactosidase	Glb1 [galactosidase beta 1]
Glycan Degradation	Galactosidase	Glb1 [galactosidase beta 1]
Glycan Degradation	Galactosidase	Glb1 [galactosidase beta 1]
Glycan Degradation	Galactosidase	Glb1 [galactosidase beta 1]
Glycan Degradation	Galactosidase	Glb1 [galactosidase beta 1]
Glycan Degradation	Galactosidase	Glb1l3 [beta-Galactosidase (lactase)]
Glycan Degradation	Glucuronidases	Gusb [glucuronidase beta]
Glycan Degradation	Glucuronidases	Gusb [glucuronidase beta]
Glycan Degradation	Glucuronidases	Gusb [glucuronidase beta]
Glycan Degradation	Glucuronidases	Gusb [glucuronidase beta]
Glycan Degradation	Heparanases	HPSE (Heparanase)
Glycan Degradation	Heparanases	HPSE (Heparanase)
Glycan Degradation	Heparanases	HPSE2 (similar to Heparanase 2;LOC545291)
Glycan Degradation	Hexosaminidases	Hexa [hexosaminidase A]
Glycan Degradation	Hyaluronidases	Hyal1 [hyaluronoglucosaminidase 1]
Glycan Degradation	Hyaluronidases	Hyal1 [hyaluronoglucosaminidase 1]
Glycan Degradation	Hyaluronidases	Hyal2 [hyaluronoglucosaminidase 2]
Glycan Degradation	Hyaluronidases	Hyal2 [hyaluronoglucosaminidase 2]
Glycan Degradation	Hyaluronidases	MGEA5 [meningioma expressed antigen 5 (hyaluronidase)]
Glycan Degradation	Hyaluronidases	MGEA5 [meningioma expressed antigen 5 (hyaluronidase)]
Glycan Degradation	Hyaluronidases	MGEA5 [meningioma expressed antigen 5 (hyaluronidase)]
Glycan Degradation	Iduronidases	Idua [iduronidase alpha-L-]
Glycan Degradation	Lysozomal Enzymes	Aga [aspartylglucosaminidase]
Glycan Degradation	Lysozomal Enzymes	Asah1 [N-acylsphingosine amidohydrolase 1]
Glycan Degradation	Lysozomal Enzymes	Asah1 [N-acylsphingosine amidohydrolase 1]
Glycan Degradation	Lysozomal Enzymes	Ctns [cystinosis nephropathic]

Glycan Degradation	Lysozomal Enzymes	Ctsa [cathepsin A]
Glycan Degradation	Lysozomal Enzymes	Gaa [acid alpha-glucosidase]
Glycan Degradation	Lysozomal Enzymes	Gaa [acid alpha-glucosidase]
Glycan Degradation	Lysozomal Enzymes	Galc [Galactosylceramidase]
Glycan Degradation	Lysozomal Enzymes	Gba [glucosidase beta acid]
Glycan Degradation	Lysozomal Enzymes	Lamp1 [lysosomal membrane glycoprotein 1]
Glycan Degradation	Lysozomal Enzymes	Lamp2 [lysosomal membrane glycoprotein 2]
Glycan Degradation	Lysozomal Enzymes	Lamp2 [lysosomal membrane glycoprotein 2]
Glycan Degradation	Lysozomal Enzymes	Lamp2 [lysosomal membrane glycoprotein 2]
Glycan Degradation	Lysozomal Enzymes	Lamp2 [lysosomal membrane glycoprotein 2]
Glycan Degradation	Lysozomal Enzymes	Lamp2 [lysosomal membrane glycoprotein 2]
Glycan Degradation	Lysozomal Enzymes	Lipa [lysosomal acid lipase A]
Glycan Degradation	Lysozomal Enzymes	Lipa [lysosomal acid lipase A]
Glycan Degradation	Lysozomal Enzymes	Mpi [mannose phosphate isomerase]
Glycan Degradation	Lysozomal Enzymes	Naglu [alpha-N-Acetylglucosaminidase]
Glycan Degradation	Lysozomal Enzymes	Smpd1 [sphingomyelin phosphodiesterase 1 acid]
Glycan Degradation	Lysozomal Enzymes	Smpd1 [sphingomyelin phosphodiesterase 1 acid]
Glycan Degradation	Mannosidases	Man2a1 [mannosidase 2 alpha 1]
Glycan Degradation	Mannosidases	Man2a2 [mannosidase 2 alpha 2]
Glycan Degradation	Mannosidases	Man2a2 [mannosidase 2 alpha 2]
Glycan Degradation	Mannosidases	Man2a2 [mannosidase 2 alpha 2]
Glycan Degradation	Mannosidases	Man2B1 [mannosidase 2 alpha B1]
Glycan Degradation	Mannosidases	Manba [mannosidase beta A lysosomal]
Glycan Degradation	Mannosidases	Manba [mannosidase beta A lysosomal]
Glycan Degradation	Mannosidases	Manba [mannosidase beta A lysosomal]
Glycan Degradation	Miscellaneous	Gm2a [GM2 ganglioside activator protein]
Glycan Degradation	Miscellaneous	Naga [N-acetyl galactosaminidase alpha]
Glycan Degradation	Miscellaneous	Naga [N-acetyl galactosaminidase alpha]

Glycan Degradation	Miscellaneous	Npl [N-acetylneuraminate pyruvate lyase]
Glycan Degradation	Sialidases	Neu1 [neuraminidase 1]
Glycan Degradation	Sialidases	Neu2 [neuraminidase 2]
Glycan Degradation	Sialidases	Neu3 [neuraminidase 3]
Glycan Degradation	Sulfatase	Galns [galactosamine (N-acetyl)-6-sulfate sulfatase]
Glycan Degradation	Sulfatases	Ids [iduronate 2-sulfatase]
Glycan Degradation	Sulfatases (hep sulfate glucosamine-6 endosulfatase)	Sulf1 [sulfatase 1]
Glycan Degradation	Sulfatases (hep sulfate glucosamine-6 endosulfatase)	Sulf1 [sulfatase 1]
Glycan degradation	Sulfatases (hep sulfate glucosamine-6 endosulfatase)	Sulf2 [sulfatase 2]
Glycan Degradation	Sulfohydrolases	Sgsh [N-sulfoglucosamine sulfohydrolase (sulfamidase)]
Glycan-transferase	CS GalNAc/GlcA Transferase	Chsy1 [Carbohydrate (chondroitin) synthase 1]
Glycan-transferase	CS GalNAc/GlcA Transferase	D1Bwg1363e [DNA segment, Chr 1, Brigham & Women's Genetics 1363 expressed; aka chondroitin polymerizing factor isoform a]
Glycan-transferase	Fucosyl-T	Fut1 [fucosyltransferase 1]
Glycan-transferase	Fucosyl-T	Fut1 [fucosyltransferase 1]
Glycan-transferase	Fucosyl-T	Fut10 [fucosyltransferase 10]
Glycan-transferase	Fucosyl-T	Fut10 [fucosyltransferase 10]
Glycan-transferase	Fucosyl-T	Fut11 [alpha (1 3) fucosyltransferase]
Glycan-transferase	Fucosyl-T	Fut2 [fucosyltransferase 2]
Glycan-transferase	Fucosyl-T	Fut2 [fucosyltransferase 2]
Glycan-transferase	Fucosyl-T	Fut4 [fucosyltransferase 4]
Glycan-transferase	Fucosyl-T	Fut4 [fucosyltransferase 4]
Glycan-transferase	Fucosyl-T	Fut4 [fucosyltransferase 4]
Glycan-transferase	Fucosyl-T	Fut7 [fucosyltransferase 7]
Glycan-transferase	Fucosyl-T	Fut8 [fucosyltransferase 8]

Glycan-transferase	Fucosyl-T	Fut8 [fucosyltransferase 8]
Glycan-transferase	Fucosyl-T	Fut9 [fucosyltransferase 9]
Glycan-transferase	Fucosyl-T	Pofut1 [protein O-fucosyltransferase 1]
Glycan-transferase	Fucosyl-T	Pofut1 [protein O-fucosyltransferase 1]
Glycan-transferase	Fucosyl-T	Pofut2 [protein O-fucosyltransferase 2]
Glycan-transferase	Fucosyl-T	Sec1 [secretory blood group 1]
Glycan-transferase	GalNAc-T	B4galnt1 [beta-1 4-N-acetylgalactosaminyltransferase]
Glycan-transferase	GalNAc-T	B4galnt1 [beta-1 4-N-acetylgalactosaminyltransferase]
Glycan-transferase	GalNAc-T	B4galnt1 [beta-1 4-N-acetylgalactosaminyltransferase]
Glycan-transferase	GalNAc-T	B4galnt2 [beta-1 4-N-acetyl-galactosaminyl transferase 2]
Glycan-transferase	GalNAc-T	B4galnt3 [beta-1 4-N-acetyl-galactosaminyl transferase 3]
Glycan-transferase	GalNAc-T	B4galnt4 [beta-1 4-N-acetyl-galactosaminyl transferase 4]
Glycan-transferase	GalNAc-T	B4galnt4 [beta-1 4-N-acetyl-galactosaminyl transferase 4]
Glycan-transferase	GalNAc-T	Galnact1 (4732435N03Rik) [CSGalNAcT1/ChGalNAcT1]
Glycan-transferase	GalNAc-T	Galnact2 [Chondroitin sulfate GalNAcT-2]
Glycan-transferase	GalNAc-T	Galnt1 [UDP-N-acetyl-alpha-D-galactosamine:polypeptide N-acetylgalactosaminyltransferase 1]
Glycan-transferase	GalNAc-T	Galnt10 [UDP-N-acetyl-alpha-D-galactosamine:polypeptide N-acetylgalactosaminyltransferase 10]
Glycan-transferase	GalNAc-T	Galnt10 [UDP-N-acetyl-alpha-D-galactosamine:polypeptide N-acetylgalactosaminyltransferase 10]
Glycan-transferase	GalNAc-T	Galnt11 [UDP-N-acetyl-alpha-D-galactosamine:polypeptide N-acetylgalactosaminyltransferase 11]
Glycan-transferase	GalNAc-T	Galnt12 [UDP-N-acetyl-alpha-D-galactosamine:polypeptide N-acetylgalactosaminyltransferase 12]
Glycan-transferase	GalNAc-T	Galnt13 [UDP-N-acetyl-alpha-D-galactosamine:polypeptide N-acetylgalactosaminyltransferase 13]
Glycan-transferase	GalNAc-T	Galnt14 [mpp-GalNAc-T14; UDP-N-acetyl-alpha-D-galactosamine:polypeptide N-

		acetylgalactosaminyltransferase 14]
Glycan-transferase	GalNAc-T	Galnt14 [UDP-N-acetyl-alpha-D-galactosamine:polypeptide N-acetylgalactosaminyltransferase 14]
Glycan-transferase	GalNAc-T	Galnt15 [UDP-N-acetyl-alpha-D-galactosamine: polypeptide N-acetylgalactosaminyltransferase15]
Glycan-transferase	GalNAc-T	Galnt16[UDP-N-acetyl-alpha-D-galactosamine:polypeptide N-acetylgalactosaminyltransferase-16]
Glycan-transferase	GalNAc-T	Galnt17[UDP-N-acetyl-alpha-D-galactosamine:polypeptide N-acetylgalactosaminyltransferase-17
Glycan-transferase	GalNAc-T	Galnt18 [UDP-N-acetyl-alpha-D-galactosamine:polypeptide N-acetylgalactosaminyltransferase-18]
Glycan-transferase	GalNAc-T	Galnt19[UDP-N-acetyl-alpha-D-galactosamine:polypeptide N-acetylgalactosaminyltransferase-19]
Glycan-transferase	GalNAc-T	Galnt2 [UDP-N-acetyl-alpha-D-galactosamine:polypeptide N-acetylgalactosaminyltransferase 2]
Glycan-transferase	GalNAc-T	Galnt20[UDP-N-acetyl-alpha-D-galactosamine:polypeptide N-acetylgalactosaminyltransferase-20]
Glycan-transferase	GalNAc-T	Galnt3 [UDP-N-acetyl-alpha-D-galactosamine:polypeptide N-acetylgalactosaminyltransferase 3]
Glycan-transferase	GalNAc-T	Galnt4 [UDP-N-acetyl-alpha-D-galactosamine:polypeptide N-acetylgalactosaminyltransferase 4]
Glycan-transferase	GalNAc-T	Galnt5 [UDP-N-acetyl-alpha-D-galactosamine:polypeptide N-acetylgalactosaminyltransferase 5]
Glycan-transferase	GalNAc-T	Galnt6 [UDP-N-acetyl-alpha-D-galactosamine:polypeptide N-acetylgalactosaminyltransferase 6]
Glycan-transferase	GalNAc-T	Galnt7 [UDP-N-acetyl-alpha-D-galactosamine: polypeptide N-acetylgalactosaminyltransferase 7]
Glycan-transferase	GalNAc-T	Galnt7 [UDP-N-acetyl-alpha-D-galactosamine: polypeptide N-

		acetylgalactosaminyltransferase 7]
Glycan-transferase	GalNAc-T	Galnt9 [UDP-N-acetyl-alpha-D-galactosamine:polypeptide N-acetylgalactosaminyltransferase 9]
Glycan-transferase	GalNAc-T	Gbgt1 [globoside alpha-1,3-N-acetylgalactosaminyltransferase 1; a3GalNAcT(FS)]
Glycan-transferase	Gal-T	4833446K15Rik [hypothetical protein LOC78923]
Glycan-transferase	Gal-T	4833446K15Rik [hypothetical protein LOC78923]
Glycan-transferase	Gal-T	4833446K15Rik [hypothetical protein LOC78923]
Glycan-transferase	Gal-T	A4GalT [alpha 1 4-galactosyltransferase]
Glycan-transferase	Gal-T	Abo [cis AB transferase]
Glycan-transferase	Gal-T	AK015826 [Similar to GalNAc transferase 10 isoform a]
Glycan-transferase	Gal-T	B3galnt1 [UDP-GalNAc:betaGlcNAc beta 1,3-galactosaminyltransferase, polypeptide 1]
Glycan-transferase	Gal-T	B3galnt2 [UDP-GalNAc:betaGlcNAc beta 1,3-galactosaminyltransferase, polypeptide 2]
Glycan-transferase	Gal-T	B3galnt2 [UDP-GalNAc:betaGlcNAc beta 1,3-galactosaminyltransferase, polypeptide 2]
Glycan-transferase	Gal-T	B3galnt2 [UDP-GalNAc:betaGlcNAc beta 1,3-galactosaminyltransferase, polypeptide 2]
Glycan-transferase	Gal-T	b3galt1 [UDP-Gal:betaGlcNAc beta 1,3-galactosyltransferase, polypeptide 1]
Glycan-transferase	Gal-T	b3galt1 [UDP-Gal:betaGlcNAc beta 1,3-galactosyltransferase, polypeptide 1]
Glycan-transferase	Gal-T	b3galt1 [UDP-Gal:betaGlcNAc beta 1,3-galactosyltransferase, polypeptide 1]
Glycan-transferase	Gal-T	b3galt2 [UDP-Gal:betaGlcNAc beta 1,3-galactosyltransferase, polypeptide 2]
Glycan-transferase	Gal-T	B3galt4 [UDP-Gal:betaGalNAc beta 1,3-galactosyltransferase, polypeptide 4]
Glycan-transferase	Gal-T	b3galt5 [UDP-Gal:betaGlcNAc beta 1,3-galactosyltransferase, polypeptide 5]
Glycan-transferase	Gal-T	b3galt6 [UDP-Gal:betaGal beta 1,3-galactosyltransferase, polypeptide 6]
Glycan-transferase	Gal-T	B3gnt8 [UDP-GlcNAc:betaGal beta-1,3-N-acetylglucosaminyltransferase 8]
Glycan-transferase	Gal-T	b4galt1 [UDP-Gal:betaGlcNAc beta 1,4- galactosyltransferase, polypeptide 1]
Glycan-transferase	Gal-T	b4galt2 [UDP-Gal:betaGlcNAc beta 1,4- galactosyltransferase, polypeptide 2]

Glycan-transferase	Gal-T	b4galt3 [UDP-Gal:betaGlcNAc beta 1,4-galactosyltransferase, polypeptide 3]
Glycan-transferase	Gal-T	b4galt4 [UDP-Gal:betaGlcNAc beta 1,4-galactosyltransferase, polypeptide 4]
Glycan-transferase	Gal-T	b4galt5 [UDP-Gal:betaGlcNAc beta 1,4-galactosyltransferase, polypeptide 5]
Glycan-transferase	Gal-T	b4galt6 [UDP-Gal:betaGlcNAc beta 1,4-galactosyltransferase, polypeptide 6]
Glycan-transferase	Gal-T	b4GalT7 [Xylosylprotein beta1,4-galactosyltransferase, polypeptide 7 (galactosyltransferase I)]
Glycan-transferase	Gal-T	b4GalT7 [Xylosylprotein beta1,4-galactosyltransferase, polypeptide 7 (galactosyltransferase I)]
Glycan-transferase	Gal-T	C1galt1 [core 1 synthase]
Glycan-transferase	Gal-T	C1galt1c1 [C1GALT1-specific chaperone 1]
Glycan-transferase	Gal-T	Ggta1 [glycoprotein galactosyltransferase alpha 1 3]
Glycan-transferase	Gal-T	Ugt8a [UDP galactosyltransferase 8A]
Glycan-transferase	Gal-T	Ugt8a [UDP galactosyltransferase 8A]
Glycan-transferase	GlcNAc-T	Gyltl1b [glycosyltransferase-like 1B]
Glycan-transferase	GlcNAc-T	Gyltl1b [glycosyltransferase-like 1B]
Glycan-transferase	GlcNAc-T	Mgat5b [mannoside acetylglucosaminyltransferase 5]
Glycan-transferase	GlcNAc-T	4933434I20Rik [hypothetical protein LOC67555; GlcNAcT VI
Glycan-transferase	GlcNAc-T	A4gnT [alpha-1 4-N-acetylglucosaminyltransferase]
Glycan-transferase	GlcNAc-T	B3gnt 5 [UDP-GlcNAc:betaGal beta-1,3-N-acetylglucosaminyltransferase 5]
Glycan-transferase	GlcNAc-T	B3gnt1 [UDP-GlcNAc:betaGal beta-1,3-N-acetylglucosaminyltransferase 1]
Glycan-transferase	GlcNAc-T	B3gnt2 [UDP-GlcNAc:betaGal beta-1,3-N-acetylglucosaminyltransferase 2]
Glycan-transferase	GlcNAc-T	B3gnt3 [UDP-GlcNAc:betaGal beta-1,3-N-acetylglucosaminyltransferase 3]
Glycan-transferase	GlcNAc-T	B3gnt4 [UDP-GlcNAc:betaGal beta-1,3-N-acetylglucosaminyltransferase 4]
Glycan-transferase	GlcNAc-T	B3gnt6 [UDP-GlcNAc:betaGal beta-1,3-N-acetylglucosaminyltransferase 6 (core 3 synthase)]
Glycan-transferase	GlcNAc-T	B3gnt7 [UDP-GlcNAc:betaGal beta-1,3-N-acetylglucosaminyltransferase 7]
Glycan-transferase	GlcNAc-T	C76566 [hypothetical protein LOC97440; beta-1,3-galactosyltransferase-related protein gene]

Glycan-transferase	GlcNAc-T	Dpagt1 [Dolichyl-phosphate (UDP-N-acetylglucosamine) acetylglucosaminephosphotransferase 1 (GlcNAc-1-P transferase)]
Glycan-transferase	GlcNAc-T	Dpagt1 [Dolichyl-phosphate (UDP-N-acetylglucosamine) acetylglucosaminephosphotransferase 1 (GlcNAc-1-P transferase)]
Glycan-transferase	GlcNAc-T	Extl1 [Exostoses (multiple)-like 1]
Glycan-transferase	GlcNAc-T	Extl2 [Exotoses (multiple)-like 2]
Glycan-transferase	GlcNAc-T	Extl3 [exostoses (multiple)-like 3]
Glycan-transferase	GlcNAc-T	Extl3 [exostoses (multiple)-like 3]
Glycan-transferase	GlcNAc-T	Gcnt1 [Glucosaminyl (N-acetyl) transferase 1, core 2]
Glycan-transferase	GlcNAc-T	Gcnt1 [Glucosaminyl (N-acetyl) transferase 1, core 2]
Glycan-transferase	GlcNAc-T	Gcnt2 [Glucosaminyl (N-acetyl) transferase 2, I-branching enzyme]
Glycan-transferase	GlcNAc-T	Gcnt2 [glucosaminyl (N-acetyl) transferase 2]
Glycan-transferase	GlcNAc-T	Gcnt3 [Glucosaminyl (N-acetyl) transferase 3, mucin type]
Glycan-transferase	GlcNAc-T	Gcnt3 [Glucosaminyl (N-acetyl) transferase 3, mucin type]
Glycan-transferase	GlcNAc-T	Large [like-glycosyltransferase]
Glycan-transferase	GlcNAc-T	Lfng [lunatic fringe gene homolog]
Glycan-transferase	GlcNAc-T	Mfng [O-fucosylpeptide 3-beta-N-acetylglucosaminyltransferase; manic fringe homolog]
Glycan-transferase	GlcNAc-T	Mgat1 [mannoside acetylglucosaminyltransferase 1]
Glycan-transferase	GlcNAc-T	Mgat2 [mannoside acetylglucosaminyltransferase 2]
Glycan-transferase	GlcNAc-T	Mgat3 [mannoside acetylglucosaminyltransferase 3]
Glycan-transferase	GlcNAc-T	Mgat4a [mannoside acetylglucosaminyltransferase 4a]
Glycan-transferase	GlcNAc-T	Mgat4b [mannoside acetylglucosaminyltransferase 4]
Glycan-transferase	GlcNAc-T	Mgat4c [mannoside acetylglucosaminyltransferase 4c]
Glycan-transferase	GlcNAc-T	Mgat5 [mannoside acetylglucosaminyltransferase 5]
Glycan-transferase	GlcNAc-T	Mgat5 [mannoside acetylglucosaminyltransferase 5]
Glycan-transferase	GlcNAc-T	Mgat5 [mannoside acetylglucosaminyltransferase 5]
Glycan-transferase	GlcNAc-T	OGT1 [O-linked N-acetylglucosamine (GlcNAc) transferase (UDP-N-

		acetylglucosamine:polypeptide-N-acetylglucosaminyl transferase)]
Glycan-transferase	GlcNAc-T	OGT1 [O-linked N-acetylglucosamine (GlcNAc) transferase (UDP-N-acetylglucosamine:polypeptide-N-acetylglucosaminyl transferase)]
Glycan-transferase	GlcNAc-T	Pigp [Phosphatidylinositol glycan anchor biosynthesis, class P; Down syndrome critical region protein c]
Glycan-transferase	GlcNAc-T	Pigp [Phosphatidylinositol glycan anchor biosynthesis, class P; Down syndrome critical region protein c]
Glycan-transferase	GlcNAc-T	Pomgnt1 [Protein O-linked mannose beta1,2-N-acetylglucosaminyltransferase]
Glycan-transferase	GlcNAc-T	Rfng [O-fucosylpeptide 3-beta-N-acetylglucosaminyltransferase; Radical fringe]
Glycan-transferase	Glc-T	ALG05 [Asparagine-linked glycosylation 5 homolog (yeast, dolichyl-phosphate beta-glucosyltransferase)]
Glycan-transferase	Glc-T	ALG05 [Asparagine-linked glycosylation 5 homolog (yeast, dolichyl-phosphate beta-glucosyltransferase)]
Glycan-transferase	Glc-T	ALG05 [Asparagine-linked glycosylation 5 homolog (yeast, dolichyl-phosphate beta-glucosyltransferase)]
Glycan-transferase	Glc-T	ALG06 [Asparagine-linked glycosylation 6 homolog (yeast, alpha-1,3,-glucosyltransferase)]
Glycan-transferase	Glc-T	ALG08 [Asparagine-linked glycosylation 8 homolog (yeast, alpha-1,3-glucosyltransferase]
Glycan-transferase	Glc-T	ALG10b [Asparagine-linked glycosylation 10 homolog B (yeast, alpha-1,2-glucosyltransferase)]
Glycan-transferase	Glc-T	B3gat2 [Beta-1,3-glucuronyltransferase 2 (glucuronosyltransferase S)]
Glycan-transferase	Glc-T	B3gat2 [Beta-1,3-glucuronyltransferase 2 (glucuronosyltransferase S)]
Glycan-transferase	Glc-T	Ugcg [UDP-glucose ceramide glucosyltransferase]
Glycan-transferase	Glc-T	Ugcg [UDP-glucose ceramide glucosyltransferase]
Glycan-transferase	Glc-T	Ugcgl1 [UDP-glucose ceramide glucosyltransferase-like 1]
Glycan-transferase	Glc-T	Ugcgl1 [UDP-glucose ceramide glucosyltransferase-like 1]
Glycan-transferase	Glc-T	Ugcgl2 [UDP-glucose ceramide glucosyltransferase-like 2]

Glycan-transferase	Glc-T	Ugcgl2 [UDP-glucose ceramide glucosyltransferase-like 2]
Glycan-transferase	Glc-T	Ugcgl2 [UDP-glucose ceramide glucosyltransferase-like 2]
Glycan-transferase	GlcUA-T	B3gat3 [Beta-1,3-glucuronyltransferase 3 (glucuronosyltransferase I)]
Glycan-transferase	GlcUA-T	B3gat3 [Beta-1,3-glucuronyltransferase 3 (glucuronosyltransferase I)]
Glycan-transferase	GlcUA-T	B3gat3 [Beta-1,3-glucuronyltransferase 3 (glucuronosyltransferase I)]
Glycan-transferase	GlcUA-T	Ugt1a(1-10) [UDP glycosyltransferase 1 family polypeptide]
Glycan-transferase	GlcUA-T	Ugt1a(1-10) [UDP glycosyltransferase 1 family polypeptide]
Glycan-transferase	GlcUA-T	Ugt1a(1-10) [UDP glycosyltransferase 1 family polypeptide]
Glycan-transferase	GlcUA-T	Ugt2a1 [UDP glucuronosyltransferase 2 family, polypeptide A1]
Glycan-transferase	GlcUA-T	Ugt2a1 [UDP glucuronosyltransferase 2 family, polypeptide A1]
Glycan-transferase	GlcUA-T	Ugt2a1 [UDP glucuronosyltransferase 2 family, polypeptide A1]
Glycan-transferase	GlcUA-T	Ugt2b5 [UDP glucuronosyltransferase 2 family, polypeptide B5]
Glycan-transferase	GlcUA-T	Ugt2b5 [UDP glucuronosyltransferase 2 family, polypeptide B5]
Glycan-transferase	HS GlcNAc/GlcA Transferase	Ext1 [exostosin 1]
Glycan-transferase	HS GlcNAc/GlcA Transferase	Ext2 [exostosin 2]
Glycan-transferase	HS GlcNAc/GlcA Transferase	Ext2 [exostosin 2]
Glycan-transferase	HS GlcNAc/GlcA Transferase	Ext2 [exostosin 2]
Glycan-transferase	HS GlcNAc/GlcA Transferase	Ext2 [exostosin 2]
Glycan-transferase	HS GlcNAc/GlcA Transferase	Ext2 [exostosin 2]
Glycan-transferase	HS GlcNAc/GlcA Transferase	Has1 [hyaluronan synthase1]
Glycan-transferase	HS GlcNAc/GlcA Transferase	Has1 [hyaluronan synthase1]
Glycan-transferase	HS GlcNAc/GlcA Transferase	Has2 [hyaluronan synthase 2]
Glycan-transferase	HS GlcNAc/GlcA Transferase	Has3 [hyaluronan synthase 3]
Glycan-transferase	HS GlcNAc/GlcA Transferase	Has3 [hyaluronan synthase 3]
Glycan-transferase	Man-T	Alg1 [Asparagine-linked glycosylation 1 homolog (yeast, beta-1,4-mannosyltransferase)]
Glycan-transferase	Man-T	Alg12 [Asparagine-linked glycosylation 12 homolog (yeast, alpha-1,6-mannosyltransferase)]

Glycan-transferase	Man-T	ALG13 [Asparagine-linked glycosylation 13 homolog (S. cerevisiae); glycosyltransferase 28 domain containing 1]
Glycan-transferase	Man-T	ALG13 [Asparagine-linked glycosylation 13 homolog (S. cerevisiae); glycosyltransferase 28 domain containing 1]
Glycan-transferase	Man-T	Alg2 [Asparagine-linked glycosylation 2 homolog (yeast, alpha-1,3-mannosyltransferase)]
Glycan-transferase	Man-T	Alg9 [Asparagine-linked glycosylation 9 homolog (yeast, alpha 1,2 mannosyltransferase); aka Dibd1, disrupted in bipolar disorder 1 homolog]
Glycan-transferase	Man-T	Chga [chromogranin A]
Glycan-transferase	Man-T	Dpm1 [Dolichol-phosphate (beta-D) mannosyltransferase 1]
Glycan-transferase	Man-T	Dpm2 [Dolichol-phosphate (beta-D) mannosyltransferase 2]
Glycan-transferase	Man-T	Piga [Phosphatidylinositol glycan anchor biosynthesis, class A]
Glycan-transferase	Man-T	Piga [Phosphatidylinositol glycan anchor biosynthesis, class A]
Glycan-transferase	Man-T	Pigb [Phosphatidylinositol glycan anchor biosynthesis, class B]
Glycan-transferase	Man-T	Pigb [Phosphatidylinositol glycan anchor biosynthesis, class B]
Glycan-transferase	Man-T	Pigm [Phosphatidylinositol glycan anchor biosynthesis, class M]
Glycan-transferase	Man-T	Pigq [Phosphatidylinositol glycan anchor biosynthesis, class Q]
Glycan-transferase	Man-T	Pigq [Phosphatidylinositol glycan anchor biosynthesis, class Q]
Glycan-transferase	Man-T	Pigq [Phosphatidylinositol glycan anchor biosynthesis, class Q]
Glycan-transferase	Man-T	Pigq [Phosphatidylinositol glycan anchor biosynthesis, class Q]
Glycan-transferase	Man-T	Pigq [Phosphatidylinositol glycan anchor biosynthesis, class Q]
Glycan-transferase	Man-T	Pomt1 [protein-O-mannosyltransferase 1]
Glycan-transferase	Man-T	Pomt2 [Protein-O-mannosyltransferase 2]
Glycan-transferase	Man-T	Pomt2 [Protein-O-mannosyltransferase 2]
Glycan-transferase	Miscellaneous	Glce [D-glucuronyl C5-epimerase]
Glycan-transferase	N-glycans-transferase	Dad1 [defender against cell death protein 1]
Glycan-transferase	N-glycans-transferase	Dad1 [defender against cell death protein 1]
Glycan-transferase	N-glycans-transferase	Ddost [Dolichyl-di-phosphooligosaccharide-protein glycotransferase]

Glycan-transferase	N-glycans-transferase	Rpn1 [Ribophorin I]
Glycan-transferase	N-glycans-transferase	Rpn2 [Ribophorin II]
Glycan-transferase	Sia-T	St3gal6 [ST3 beta-galactoside alpha-2,3-sialyltransferase 6]
Glycan-transferase	Sia-T	St3gal1 [ST3 beta-galactoside alpha-2,3-sialyltransferase 1]
Glycan-transferase	Sia-T	St3gal2 [ST3 beta-galactoside alpha-2,3-sialyltransferase 2]
Glycan-transferase	Sia-T	St3gal2 [ST3 beta-galactoside alpha-2,3-sialyltransferase 2]
Glycan-transferase	Sia-T	St3gal2 [ST3 beta-galactoside alpha-2,3-sialyltransferase 2]
Glycan-transferase	Sia-T	St3gal3 [ST3 beta-galactoside alpha-2,3-sialyltransferase 3; sialyltransferase 6]
Glycan-transferase	Sia-T	St3gal4 [ST3 beta-galactoside alpha-2,3-sialyltransferase 4]
Glycan-transferase	Sia-T	St3gal5 [ST3 beta-galactoside alpha-2,3-sialyltransferase 5]
Glycan-transferase	Sia-T	St6gal1 [Beta galactoside alpha 2,6 sialyltransferase 1]
Glycan-transferase	Sia-T	St6gal2 [Beta galactoside alpha 2,6 sialyltransferase 2]
Glycan-transferase	Sia-T	St6gal2 [Beta galactoside alpha 2,6 sialyltransferase 2]
Glycan-transferase	Sia-T	St6galnac1 [ST6 (alpha-N-acetyl-neuraminyl-2,3-beta-galactosyl-1,3)-N-acetylgalactosaminide alpha-2,6-sialyltransferase 1]
Glycan-transferase	Sia-T	St6galnac2 [ST6 (alpha-N-acetyl-neuraminyl-2,3-beta-galactosyl-1,3)-N-acetylgalactosaminide alpha-2,6-sialyltransferase 2]
Glycan-transferase	Sia-T	St6galnac3 [ST6 (alpha-N-acetyl-neuraminyl-2,3-beta-galactosyl-1,3)-N-acetylgalactosaminide alpha-2,6-sialyltransferase 3]
Glycan-transferase	Sia-T	St6galnac4 [ST6 (alpha-N-acetyl-neuraminyl-2,3-beta-galactosyl-1,3)-N-acetylgalactosaminide alpha-2,6-sialyltransferase 4]
Glycan-transferase	Sia-T	St6galnac4 [ST6 (alpha-N-acetyl-neuraminyl-2,3-beta-galactosyl-1,3)-N-acetylgalactosaminide alpha-2,6-sialyltransferase 4]
Glycan-transferase	Sia-T	St6galnac5 [ST6 (alpha-N-acetyl-neuraminyl-2,3-beta-galactosyl-1,3)-N-acetylgalactosaminide alpha-2,6-sialyltransferase 5]
Glycan-transferase	Sia-T	St6galnac6 [ST6 (alpha-N-acetyl-neuraminyl-2,3-beta-galactosyl-1,3)-N-acetylgalactosaminide alpha-2,6-sialyltransferase 6]
Glycan-transferase	Sia-T	St6galnac6 [ST6 (alpha-N-acetyl-neuraminyl-2,3-beta-galactosyl-1,3)-N-

		acetylgalactosaminide alpha-2,6-sialyltransferase 6]
Glycan-transferase	Sia-T	St8sia1 [ST8 alpha-N-acetyl-neuraminide alpha-2,8-sialyltransferase 1]
Glycan-transferase	Sia-T	St8sia2 [ST8 alpha-N-acetyl-neuraminide alpha-2,8-sialyltransferase 2]
Glycan-transferase	Sia-T	St8sia3 [ST8 alpha-N-acetyl-neuraminide alpha-2,8-sialyltransferase 3]
Glycan-transferase	Sia-T	St8sia4 [ST8 alpha-N-acetyl-neuraminide alpha-2,8-sialyltransferase 4]
Glycan-transferase	Sia-T	St8sia4 [ST8 alpha-N-acetyl-neuraminide alpha-2,8-sialyltransferase 4]
Glycan-transferase	Sia-T	St8sia4 [ST8 alpha-N-acetyl-neuraminide alpha-2,8-sialyltransferase 4]
Glycan-transferase	Sia-T	St8sia5 [ST8 alpha-N-acetyl-neuraminide alpha-2,8-sialyltransferase 5]
Glycan-transferase	Sia-T	St8sia6 [ST8 alpha-N-acetyl-neuraminide alpha-2,8-sialyltransferase 6]
Glycan-transferase	Sulfo-T	4631426J05Rik [GalNAc4ST-6ST; N-acetylgalactosamine 4-sulfate]
Glycan-transferase	Sulfo-T	Chst1 [Carbohydrate (keratan sulfate Gal-6) sulfotransferase 1]
Glycan-transferase	Sulfo-T	Chst10 [Carbohydrate sulfotransferase 10]
Glycan-transferase	Sulfo-T	Chst10 [Carbohydrate sulfotransferase 10]
Glycan-transferase	Sulfo-T	Chst11 [Carbohydrate sulfotransferase 11]
Glycan-transferase	Sulfo-T	Chst12 [Carbohydrate sulfotransferase 12]
Glycan-transferase	Sulfo-T	Chst13 [Carbohydrate (chondroitin 4) sulfotransferase 13]
Glycan-transferase	Sulfo-T	Chst14 [Carbohydrate (N-acetylgalactosamine 4-0) sulfotransferase 14; aka dermatan-4-sulfotransferase-1]
Glycan-transferase	Sulfo-T	Chst2 [carbohydrate sulfotransferase 2]
Glycan-transferase	Sulfo-T	Chst3 [Carbohydrate (chondroitin 6/keratan) sulfotransferase 3]
Glycan-transferase	Sulfo-T	Chst4 [Carbohydrate (chondroitin 6/keratan) sulfotransferase 4]
Glycan-transferase	Sulfo-T	Chst5 [Carbohydrate (N-acetylglucosamine 6-O) sulfotransferase 5]
Glycan-transferase	Sulfo-T	Chst7 [Carbohydrate (N-acetylglucosamino) sulfotransferase 7]
Glycan-transferase	Sulfo-T	Chst8 [Carbohydrate (N-acetylgalactosamine 4-0) sulfotransferase 8]
Glycan-transferase	Sulfo-T	Chst8 [Carbohydrate (N-acetylgalactosamine 4-0) sulfotransferase 8]
Glycan-transferase	Sulfo-T	Chst9 [Carbohydrate (N-acetylgalactosamine 4-0) sulfotransferase 9]
Glycan-transferase	Sulfo-T	Gal3st1 [Galactose-3-O-sulfotransferase 1]
Glycan-transferase	Sulfo-T	Gal3st2 [Galactose-3-O-sulfotransferase 2]

Glycan-transferase	Sulfo-T	Gal3st3 [galactose-3-O-sulfotransferase 3]
Glycan-transferase	Sulfo-T	Gal3st4 [Galactose-3-O-sulfotransferase 4]
Glycan-transferase	Sulfo-T	Hs2st1 [heparan sulfate 2-O-sulfotransferase 1]
Glycan-transferase	Sulfo-T	Hs3st1 [Heparan sulfate (glucosamine) 3-O-sulfotransferase 1]
Glycan-transferase	Sulfo-T	Hs3st2 [Heparan sulfate (glucosamine) 3-O-sulfotransferase 2]
Glycan-transferase	Sulfo-T	Hs3st2 [Heparan sulfate (glucosamine) 3-O-sulfotransferase 2]
Glycan-transferase	Sulfo-T	Hs3st3a1 [Heparan sulfate (glucosamine) 3-O-sulfotransferase 3A1]
Glycan-transferase	Sulfo-T	Hs3st3b1 [Heparan sulfate (glucosamine) 3-O-sulfotransferase 3B1]
Glycan-transferase	Sulfo-T	Hs3st5 [Heparan sulfate (glucosamine) 3-O-sulfotransferase 5]
Glycan-transferase	Sulfo-T	Hs3st6 [Heparan sulfate (glucosamine) 3-O-sulfotransferase 6]
Glycan-transferase	Sulfo-T	Hs6st1 [Heparan sulfate 6-O-sulfotransferase 1]
Glycan-transferase	Sulfo-T	Hs6st2 [Heparan sulfate 6-O-sulfotransferase 2]
Glycan-transferase	Sulfo-T	Hs6st3 [Heparan sulfate 6-O-sulfotransferase 3]
Glycan-transferase	Sulfo-T	Ndst1 [N-deacetylase/N-sulfotransferase (heparan glucosaminyl) 1]
Glycan-transferase	Sulfo-T	Ndst1 [N-deacetylase/N-sulfotransferase (heparan glucosaminyl) 1]
Glycan-transferase	Sulfo-T	Ndst1 [N-deacetylase/N-sulfotransferase (heparan glucosaminyl) 1]
Glycan-transferase	Sulfo-T	Ndst2 [N-deacetylase/N-sulfotransferase (heparan glucosaminyl) 2]
Glycan-transferase	Sulfo-T	Ndst3 [N-deacetylase/N-sulfotransferase (heparan glucosaminyl) 3]
Glycan-transferase	Sulfo-T	Ndst4 [N-deacetylase/N-sulfotransferase (heparin glucosaminyl) 4]
Glycan-transferase	Sulfo-T	Tpst2 [protein-tyrosine sulfotransferase 2]
Glycan-transferase	Sulfo-T	Ust [uronyl-2-sulfotransferase]
Glycan-transferase	Sulfo-T	Ust [uronyl-2-sulfotransferase]
Glycan-transferase	Sulfo-T	Dsel [dermatan sulfate epimerase-like; NCAG1 similar to sulfotransferase]
Glycan-transferase	Xyl-T	Xylt1 [xylosyltransferase I]
Glycan-transferase	Xyl-T	Xylt1 [xylosyltransferase I]
Glycan-transferase	Xyl-T	Xylt2 [xylosyltransferase II]
Glycoprotein	Serum Glycoprotein	Ahsg [alpha-2-HS-glycoprotein; Fetuin]
Glycoproteins	Mucins	Capn1 [calpain 1]

Glycoproteins	Mucins	Capn1 [calpain 1]
Glycoproteins	Mucins	Capn1 [calpain 1]
Glycoproteins	Mucins	Cd164 [CD164 antigen]
Glycoproteins	Mucins	Cd164l2 [CD164 sialomucin-like 2]
Glycoproteins	Mucins	Dmbt1 [deleted in malignant brain tumors 1]
Glycoproteins	Mucins	Emr1 [EGF-like module containing, mucin-like, hormone receptor-like sequence 1]
Glycoproteins	Mucins	Emr1 [EGF-like module containing, mucin-like, hormone receptor-like sequence 1]
Glycoproteins	Mucins	Emr4 [EGF-like module containing, mucin-like, hormone receptor-like sequence 4]
Glycoproteins	Mucins	Fcrla [Fc receptor homolog expressed in B cells]
Glycoproteins	Mucins	Fcrlb [Fc receptor-like B]
Glycoproteins	Mucins	Havcr1 [hepatitis A virus cellular receptor 1]
Glycoproteins	Mucins	Havcr2 [hepatitis A virus cellular receptor 2]
Glycoproteins	Mucins	Itgae, integrin, alpha E, epithelial-associated
Glycoproteins	Mucins	Itgae, integrin, alpha E, epithelial-associated
Glycoproteins	Mucins	Mcam [melanoma cell adhesion molecule]
Glycoproteins	Mucins	Mcoln1 [mucolipin 1]
Glycoproteins	Mucins	Mcoln2 [mucolipin 2]
Glycoproteins	Mucins	Mcoln3 [mucolipin 3]
Glycoproteins	Mucins	Muc1 [mucin 1 transmembrane]
Glycoproteins	Mucins	Muc10 [mucin 10]
Glycoproteins	Mucins	Muc13 [mucin 13, epithelial transmembrane]
Glycoproteins	Mucins	Muc15 [mucin 15]
Glycoproteins	Mucins	Muc19 [mucin 19]
Glycoproteins	Mucins	Muc2 [mucin 2]
Glycoproteins	Mucins	Muc20 [mucin 20]
Glycoproteins	Mucins	Muc3 [mucin 3]
Glycoproteins	Mucins	Muc4 [mucin 4]
Glycoproteins	Mucins	Muc4 [mucin 4]

Glycoproteins	Mucins	Muc4 [mucin 4]
Glycoproteins	Mucins	Muc5ac [mucin 5 subtypes A and C]
Glycoproteins	Mucins	Muc5b [mucin 5 subtype B tracheobronchial]
Glycoproteins	Mucins	Muc6 [mucin 6, gastric]
Glycoproteins	Mucins	Mupcdh [mucin-like protocadherin]
Glycoproteins	Mucins	Ovgp1 [oviductal glycoprotein 1]
Glycoproteins	Mucins	Timd2 [T-cell immunoglobulin and mucin domain containing 2]
Glycoproteins	Mucins	Timd4, T-cell immunoglobulin and mucin domain containing 4
Glycoproteins	Mucins	Umod [uromodulin]
intracellular protein transport	Golgi tethering factor	Cog1 [component of oligomeric golgi complex 1]
intracellular protein transport	Golgi tethering factor	Cog2 [component of oligomeric golgi complex 2]
intracellular protein transport	Golgi tethering factor	Cog2 [component of oligomeric golgi complex 2]
intracellular protein transport	Golgi tethering factor	Cog3 [component of oligomeric golgi complex 3]
intracellular protein transport	Golgi tethering factor	Cog4 [component of oligomeric golgi complex 4]
intracellular protein transport	Golgi tethering factor	Cog5 [component of oligomeric golgi complex 5]
intracellular protein transport	Golgi tethering factor	Cog6 [component of oligomeric golgi complex 6]
intracellular protein transport	Golgi tethering factor	Cog6 [component of oligomeric golgi complex 6]
intracellular protein transport	Golgi tethering factor	Cog7 [component of oligomeric golgi complex 7]
intracellular protein transport	Golgi tethering factor	Cog8 [component of oligomeric golgi complex 8]
intracellular protein transport	Golgi tethering factor	Cog8 [component of oligomeric golgi complex 8]
Miscellaneous	Miscellaneous	V1rc19 [vomeronasal 1 receptor C19]
Notch pathway	Notch Ligands	Dll1 [delta-like 1]
Notch pathway	Notch Ligands	Dll3 [delta-like 3]
Notch pathway	Notch Ligands	Dll4 [delta-like 4]
Notch pathway	Notch Ligands	Jag1 [jagged1]
Notch pathway	Notch Ligands	Jag2 [Jagged2]
Notch pathway	Notch Receptors	Notch1 [Notch gene homolog 1]
Notch pathway	Notch Receptors	Notch2 [Notch gene homolog 2]

Notch pathway	Notch Receptors	Notch2 [Notch gene homolog 2]
Notch pathway	Notch Receptors	Notch3 [Notch gene homolog 3]
Notch pathway	Notch Receptors	Notch4 [Notch gene homolog 4]
Notch pathway	Notch Receptors	Notch4 [Notch gene homolog 4]
Notch pathway	Notch Target Genes	Hes1 [hairy and enhancer of split 1]
Notch pathway	Notch Target Genes	Hes2 [hairy and enhancer of split 2]
Notch pathway	Notch Target Genes	Hes3 [hairy and enhancer of split 3]
Notch pathway	Notch Target Genes	Hes5 [hairy and enhancer of split 5]
Notch pathway	Notch Target Genes	Hes6 [hairy and enhancer of split 6]
Notch pathway	Notch Target Genes	Hes6 [hairy and enhancer of split 6]
Notch pathway	Notch Target Genes	Hes7 [hairy and enhancer of split 7]
Notch pathway	Notch Target Genes	Ncstn [Nicastrin]
Notch pathway	Notch Target Genes	Psen1 [presenilin 1]
Notch pathway	Notch Target Genes	Psen1 [presenilin 1]
Notch pathway	Notch Target Genes	Psen2 [presenilin 2]
Notch pathway	Notch Target Genes	Psen2 [presenilin 2]
Notch pathway	Notch Target Genes	Rbpj [Recombination signal binding protein for immunoglobulin kappa J region]
Nuc. Sugar	Nuc. Sugars Transporters	Slc35a1 [Solute carrier family 35 (CMP-sialic acid transporter), member 1]
Nuc. Sugar	Nuc. Sugars Transporters	Slc35a2 [Solute carrier family 35 (UDP-galactose transporter), member A2]
Nuc. Sugar	Nuc. Sugars Transporters	Slc35a2 [Solute carrier family 35 (UDP-galactose transporter), member A2]
Nuc. Sugar	Nuc. Sugars Transporters	Slc35a3 [Solute carrier family 35 (UDP-N-acetylglucosamine (UDP-GlcNAc) transporter), member 3]
Nuc. Sugar	Nuc. Sugars Transporters	Slc35a4 [solute carrier family 35 member A4]
Nuc. Sugar	Nuc. Sugars Transporters	Slc35a5 [solute carrier family 35 member A5]
Nuc. Sugar	Nuc. Sugars Transporters	Slc35b1 [solute carrier family 35 member B1]
Nuc. Sugar	Nuc. Sugars Transporters	Slc35b2 [solute carrier family 35 member B2]
Nuc. Sugar	Nuc. Sugars Transporters	Slc35b2 [solute carrier family 35 member B2]
Nuc. Sugar	Nuc. Sugars Transporters	Slc35b3 [solute carrier family 35 member B3]

Nuc. Sugar	Nuc. Sugars Transporters	Slc35b3 [solute carrier family 35 member B3]
Nuc. Sugar	Nuc. Sugars Transporters	Slc35b4 [solute carrier family 35 member B4]
Nuc. Sugar	Nuc. Sugars Transporters	Slc35c1 [GDP-fucose transporter 1]
Nuc. Sugar	Nuc. Sugars Transporters	Slc35c2 [solute carrier family 35 member C2]
Nuc. Sugar	Nuc. Sugars Transporters	Slc35d1 [(one of several shorter splice variants) Solute carrier family 35 (UDP-glucuronic acid/UDP-N-acetylgalactosamine dual transporter), member D1]
Nuc. Sugar	Nuc. Sugars Transporters	Slc35d1 [(one of several shorter splice variants) Solute carrier family 35 (UDP-glucuronic acid/UDP-N-acetylgalactosamine dual transporter), member D1]
Nuc. Sugar	Nuc. Sugars Transporters	Slc35d1 [(one of several shorter splice variants) Solute carrier family 35 (UDP-glucuronic acid/UDP-N-acetylgalactosamine dual transporter), member D1]
Nuc. Sugar	Nuc. Sugars Transporters	Slc35d1 [Solute carrier family 35 (UDP-glucuronic acid/UDP-N-acetylgalactosamine dual transporter), member D1]
Nuc. Sugar	Nuc. Sugars Transporters	Slc35d2 [solute carrier family 35 member D2]
Nuc. Sugar	Nuc. Sugars Transporters	Slc35d3 [solute carrier family 35 member D3]
Nuc. Sugar	Nuc. Sugars Transporters	Slc35e1 [solute carrier family 35 member E1]
Nuc. Sugar	Nuc. Sugars Transporters	Slc35e3 [solute carrier family 35 member E3]
Nuc. Sugar	Nuc. Sugars Transporters	Slc35e4 [solute carrier family 35 member E4]
Nuc. Sugar	Nuc. Sugars Transporters	Slc35f1 [solute carrier family 35 member F1]
Nuc. Sugar	Nuc. Sugars Transporters	Slc35f2 [solute carrier family 35 member F2]
Nuc. Sugar	Nuc. Sugars Transporters	Slc35f3 [solute carrier family 35 member F3]
Nuc. Sugar	Nuc. Sugars Transporters	Slc35f4 [solute carrier family 35 member F4]
Nuc. Sugar	Nuc. Sugars Transporters	Slc35f4 [solute carrier family 35 member F4]
Nuc. Sugar	Nuc. Sugars Transporters	Slc35f4 [solute carrier family 35 member F4]
Nuc. Sugar	Nuc. Sugars Transporters	Slc35f5 [solute carrier family 35 member F5]
Nuc. Sugar	Nucleotide Synthesis	Cmah [Cytidine monophospho-N-acetylneuraminic acid hydroxylase]
Nuc. Sugar	Nucleotide Synthesis	Cmah [Cytidine monophospho-N-acetylneuraminic acid hydroxylase]
Nuc. Sugar	Nucleotide Synthesis	Cmah [Cytidine monophospho-N-acetylneuraminic acid hydroxylase]
Nuc. Sugar	Nucleotide Synthesis	Cmah [Cytidine monophospho-N-acetylneuraminic acid hydroxylase]

Nuc. Sugar	Nucleotide Synthesis	Cmas [Cytidine monophospho-N-acetylneuraminic acid synthetase]
Nuc. Sugar	Nucleotide Synthesis	Fpgt [Fucose-1-phosphate guanylyltransferase]
Nuc. Sugar	Nucleotide Synthesis	Gale [Galactose-4-epimerase, UDP]
Nuc. Sugar	Nucleotide Synthesis	Galk1 [galactokinase 1]
Nuc. Sugar	Nucleotide Synthesis	Galk2 [galactokinase 2]
Nuc. Sugar	Nucleotide Synthesis	Galk2 [galactokinase 2]
Nuc. Sugar	Nucleotide Synthesis	Galt [galactose-1-phosphate uridylyltransferase]
Nuc. Sugar	Nucleotide Synthesis	Galt [galactose-1-phosphate uridylyltransferase]
Nuc. Sugar	Nucleotide Synthesis	Gfpt1 [glutamine-fructose-6-phosphate transaminase 1]
Nuc. Sugar	Nucleotide Synthesis	Gfpt1 [glutamine-fructose-6-phosphate transaminase 1]
Nuc. Sugar	Nucleotide Synthesis	Gfpt2 [glutamine-fructose-6-phosphate transaminase 2
Nuc. Sugar	Nucleotide Synthesis	Gmds [GDP-mannose 4, 6-dehydratase]
Nuc. Sugar	Nucleotide Synthesis	Gmds [GDP-mannose 4, 6-dehydratase]
Nuc. Sugar	Nucleotide Synthesis	Gmppa [GDP-mannose pyrophosphorylase A]
Nuc. Sugar	Nucleotide Synthesis	Gmppa [GDP-mannose pyrophosphorylase A]
Nuc. Sugar	Nucleotide Synthesis	Gmppb [GDP-mannose pyrophosphorylase B]
Nuc. Sugar	Nucleotide Synthesis	Gne [glucosamine; epimerase]
Nuc. Sugar	Nucleotide Synthesis	Gnpda1 [glucosamine-6-phosphate deaminase/isomerase 1 (oscillin)]
Nuc. Sugar	Nucleotide Synthesis	Gnpda2 [glucosamine-6-phosphate deaminase 2]
Nuc. Sugar	Nucleotide Synthesis	Gnpnat1 [glucosamine-phosphate N-acetyltransferase 1]
Nuc. Sugar	Nucleotide Synthesis	Gpi1 [glucose phosphate isomerase]
Nuc. Sugar	Nucleotide Synthesis	Hk1 [hexokinase 1]
Nuc. Sugar	Nucleotide Synthesis	Hk1 [hexokinase 1]
Nuc. Sugar	Nucleotide Synthesis	Khk [ketohexokinase (fructokinase)]
Nuc. Sugar	Nucleotide Synthesis	Nagk [N-acetylglucosamine kinase; GlcNAc/ManNAc kinase]
Nuc. Sugar	Nucleotide Synthesis	Nans [Neu5Ac 9-phosphate synthase; N-acetylneuraminic acid synthase (sialic acid synthase)]
Nuc. Sugar	Nucleotide Synthesis	Nans [Neu5Ac 9-phosphate synthase; N-acetylneuraminic acid synthase (sialic acid

		synthase)]
Nuc. Sugar	Nucleotide Synthesis	Papss1 [PAPS synthetase-1; 3'-phosphoadenosine 5'-phosphosulfate synthase 1]
Nuc. Sugar	Nucleotide Synthesis	Papss2 [PAPS synthetase-2; 3'-phosphoadenosine 5'-phosphosulfate synthase 2]
Nuc. Sugar	Nucleotide Synthesis	Pgm1 [phosphoglucomutase 1]
Nuc. Sugar	Nucleotide Synthesis	Pgm2 [phosphoglucomutase 2]
Nuc. Sugar	Nucleotide Synthesis	Pgm2l1 [phosphoglucomutase 2-like 1]
Nuc. Sugar	Nucleotide Synthesis	Pgm3 [phosphoglucomutase 3]
Nuc. Sugar	Nucleotide Synthesis	Pgm3 [phosphoglucomutase 3]
Nuc. Sugar	Nucleotide Synthesis	Pgm3 [phosphoglucomutase 3]
Nuc. Sugar	Nucleotide Synthesis	Pgm5 [phosphoglucomutase 5]
Nuc. Sugar	Nucleotide Synthesis	Pgm5 [phosphoglucomutase 5]
Nuc. Sugar	Nucleotide Synthesis	Pmm1 [phosphomannomutase 1]
Nuc. Sugar	Nucleotide Synthesis	Pmm1 [phosphomannomutase 1]
Nuc. Sugar	Nucleotide Synthesis	Pmm2 [phosphomannomutase 2]
Nuc. Sugar	Nucleotide Synthesis	Renbp [renin binding protein; GlcNAc 2-epimerase]
Nuc. Sugar	Nucleotide Synthesis	TSTA3 [GDP fucose synthetase; tissue specific transplantation antigen P35B]
Nuc. Sugar	Nucleotide Synthesis	Uap1 [UDP-N-acetylglucosamine pyrophosphorylase 1]
Nuc. Sugar	Nucleotide Synthesis	Uap1 [UDP-N-acetylglucosamine pyrophosphorylase 1]
Nuc. Sugar	Nucleotide Synthesis	Uap1l1 [UDP-N-acteylglucosamine pyrophosphorylase 1-like]
Nuc. Sugar	Nucleotide Synthesis	Ugdh [UDP-Glucose Dehydrogenase]
Nuc. Sugar	Nucleotide Synthesis	Ugp2 [UDP-glucose pyrophosphorylase 2; uridine diphosphoglucose pyrophosphorylase 2]
Nuc. Sugar	Nucleotide Synthesis	Uxs1 [UDP-Glucuronic acid Decarboxylase 1]
xAdhesion Molecule	Adhesion Molecule	Bsg [basigin; neurothein (CD147)]
xAdhesion Molecule	Adhesion Molecule	Cd2 [CD2 antigen; LFA-2]
xAdhesion Molecule	Adhesion Molecule	Cd48 [CD48 antigen; BCM1]
xAdhesion Molecule	Selectin & Selectin Ligands	Cd34 [CD34 antigen]
xAdhesion Molecule	Selectin & Selectin Ligands	Glycam1 [glycosylation dependent cell adhesion molec]

xAdhesion Molecule	Selectin & Selectin Ligands	Madcam1 [Mucosal vascular addressin cell adhesion molecule 1]
xAdhesion Molecule	Selectin & Selectin Ligands	Madcam1 [Mucosal vascular addressin cell adhesion molecule 1]
xAdhesion Molecule	Selectin & Selectin Ligands	Selplg [selectin platelet (p-selectin) ligand]
xAdhesion Molecule	Selectin & Selectin Ligands	Selplg [selectin platelet (p-selectin) ligand]
xAdhesion Molecule	Selectin & Selectin Ligands	Selplg [selectin platelet (p-selectin) ligand]
xAdhesion Molecule	Selectin Ligand	Emcn [Endomucin, Muc14]
xAdhesion Molecule	Selectin Ligand	Emcn [Endomucin]
xAdhesion Molecule	Selectin Ligand	Podxl2 [podocalyxin-like 2; Endoglycan]
xAdhesion Molecule	Selectin Ligand	Podxl2 [podocalyxin-like 2; Endoglycan]
xChemokine	C-CL&R	Ccl1 [chemokine (C-C motif) ligand 1]
xChemokine	C-CL&R	Ccl11 [small chemokine (C-C motif) ligand 11; Eotaxin-1]
xChemokine	C-CL&R	Ccl17 [chemokine (C-C motif) ligand 17]
xChemokine	C-CL&R	Ccl21a/c [chemokine (C-C motif) ligand 21a/c (serine)]
xChemokine	C-CL&R	Ccl21b [chemokine (C-C motif) ligand 21b (serine)]
xChemokine	C-CL&R	Ccl22 [chemokine (C-C motif) ligand 22]
xChemokine	C-CL&R	Ccl24 [chemokine (C-C motif) ligand 24]
xChemokine	C-CL&R	Ccl24 [chemokine (C-C motif) ligand 24]
xChemokine	C-CL&R	Ccl25 [chemokine (C-C motif) ligand 25]
xChemokine	C-CL&R	Ccl27 [chemokine (C-C motif) ligand 27]
xChemokine	C-CL&R	Ccl27 [chemokine (C-C motif) ligand 27]
xChemokine	C-CL&R	Ccl27 [chemokine (C-C motif) ligand 27]
xChemokine	C-CL&R	Ccr10 [chemokine (C-C motif) receptor 10]
xChemokine	C-CL&R	Ccrl1 [chemokine (C-C motif) receptor-like 1]
xChemokine	CXCL&R	Cx3cl1 [chemokine (C-X3-C motif) ligand 1]
xChemokine	CXCL&R	Cx3cr1 [chemokine (C-X3-C) receptor 1]
xChemokine	CXCL&R	Cxcl1 [chemokine (C-X-C motif) ligand 1; (GRO beta)]
xChemokine	CXCL&R	Cxcl10 [chemokine (C-X-C motif) ligand 10; (IP-10)]
xChemokine	CXCL&R	Cxcl11 [chemokine (C-X-C motif) ligand 11; (I-TAC)]

xChemokine	CXCL&R	Cxcl12 [Chemokine (C-X-C motif) ligand 12; stromal cell derived factor 1 isoform alpha]
xChemokine	CXCL&R	Cxcl12 [Chemokine (C-X-C motif) ligand 12; stromal cell derived factor 1 isoform alpha]
xChemokine	CXCL&R	Cxcl13 [chemokine (C-X-C motif) ligand 13]
xChemokine	CXCL&R	Cxcl15 [chemokine (C-X-C motif) ligand 15; lungkine]
xChemokine	CXCL&R	Cxcl2 [chemokine (C-X-C motif) ligand 2]
xChemokine	CXCL&R	Cxcl4 [chemokine (C-X-C motif) ligand 4; (PF4)]
xChemokine	CXCL&R	Cxcl5 [chemokine (C-X-C motif) ligand 5; (ENA-78)]
xChemokine	CXCL&R	Cxcl9 [chemokine (C-X-C motif) ligand 9; Mig]
xChemokine	CXCL&R	Cxcr3 [chemokine (C-X-C motif) receptor 3]
xChemokine	CXCL&R	Cxcr4 [chemokine (C-X-C motif) receptor 4]
xChemokine	CXCL&R	Cxcr5 (Blr1) [Burkitt lymphoma receptor 1]
xChemokine	CXCL&R	Cxcr6 [chemokine (C-X-C motif) receptor 6]
xChemokine	CXCL&R	Ppbp [pro-platelet basic protein]
xChemokine	MCP	Ccl12 [chemokine (C-C motif) ligand 12]
xChemokine	MCP	Ccl7 [chemokine (C-C motif) ligand 7]
xChemokine	MCP	Ccl8 [chemokine (C-C motif) ligand 8]
xChemokine	MCP	Ccr2 [chemokine (C-C motif) receptor 2]
xChemokine	MCP	Ccr2 [chemokine (C-C motif) receptor 2]
xChemokine	MIP	Ccl20 [chemokine (C-C motif) ligand 20]
xChemokine	MIP	Ccl20/LARC [chemokine (C-C motif) ligand 20]
xChemokine	MIP	Ccl3 [chemokine (C-C motif) ligand 3; (LD78_MIP1a)]
xChemokine	MIP	Ccl4 [chemokine (C-C motif) ligand 4; (MIP1b)]
xChemokine	MIP	Ccl9 [chemokine (C-C motif) ligand 9; (MIP1 g)]
xChemokine	MIP	Ccr1 [chemokine (C-C motif) receptor 1]
xChemokine	MIP	Ccr1l1 [chemokine (C-C motif) receptor 1-like 1]
xChemokine	MIP	Ccr3 [CC chemokine receptor 3]

xChemokine	MIP	Ccr4 [chemokine (C-C motif) receptor 4]
xChemokine	MIP	Ccr5 [chemokine (C-C motif) receptor 5]
xChemokine	MIP	Ccr6 [chemokine (C-C motif) receptor 6]
xChemokine	MIP	Ccr7 [chemokine (C-C motif) receptor 7]
xChemokine	MIP	Ccr8 [chemokine (C-C motif) receptor 8]
xChemokine	MIP	Ccr9 [chemokine (C-C motif) receptor 9]
xChemokine	MIP	Ccr9 [chemokine (C-C motif) receptor 9]
xChemokine	MIP	Cxcl14 [Chemokine (C-X-C motif) ligand 14; MIP-2g; kidney-expressed chemokine CXC]
xChemokine	Miscellaneous	Cntfr [ciliary neurotrophic factor receptor]
xChemokine	Miscellaneous	Cntfr [ciliary neurotrophic factor receptor]
xChemokine	Miscellaneous	Erbb3 [v-erb-b2 erythroblastic leukemia viral oncogene]
xChemokine	Miscellaneous	Erbb4 [v-erb-a erythroblastic leukemia viral oncogene]
xChemokine	Miscellaneous	Kit [c-kit]
xChemokine	Miscellaneous	Ptprt [protein tyrosine phosphatase receptor type T]
xChemokine	Miscellaneous	Xcl1 [chemokine (C motif) ligand 1; Lymphotactin]
xChemokine	Miscellaneous	Xcr1 [chemokine (C motif) receptor 1; Lymphotactin Receptor}
xChemokine	RANTES	Ccl5 [chemokine (C-C motif) ligand 5; Tcell-specific protein (RANTES)]
xChemokine	RANTES	Ccl5 [chemokine (C-C motif) ligand 5; Tcell-specific protein (RANTES)]
xCytokine	GDNF&R	Gdnf [glial cell line derived neurotrophic factor]
xCytokine	GDNF&R	Gfra1 [glial cell line derived neurotrophic factor family receptor alphafamily receptor alpha 1]
xCytokine	GDNF&R	Gfra2 [GFRalpha2; glial cell line derived neurotrophic factor family receptor alpha 3
xCytokine	GDNF&R	Gfra2 [glial cell line derived neurotrophic factor family receptor alpha 2]
xCytokine	GDNF&R	Gfra2 [glial cell line derived neurotrophic factor family receptor alpha 2]
xCytokine	GDNF&R	Gfra3 [Glial cell line derived neurotrophic factor family receptor alpha 3]
xCytokine	GDNF&R	Gfra4 [Glial cell line derived neurotrophic factor family receptor alpha 4]
xCytokine	GDNF&R	Gfra4 [Glial cell line derived neurotrophic factor family receptor alpha 4]

xCytokine	GDNF&R	Gfra4 [Glial cell line derived neurotrophic factor family receptor alpha 4]
xCytokine	GDNF&R	Gfra4 [Glial cell line derived neurotrophic factor family receptor alpha 4]
xCytokine	Interferon	Ifnab [interferon alpha family gene B]
xCytokine	Interferon	Ifnab [interferon alpha family gene B]
xCytokine	Interferon	Ifnar1 [interferon (alpha and beta) receptor 1]
xCytokine	Interferon	Ifnar1 [interferon (alpha and beta) receptor 1]
xCytokine	Interferon	Ifnar2 [interferon (alpha and beta) receptor 2]
xCytokine	Interferon	Ifnar2 [interferon (alpha and beta) receptor 2]
xCytokine	Interferon	Ifnb1 [interferon beta 1 fibroblast]
xCytokine	Interferon	Ifng [interferon gamma]
xCytokine	Interferon	Ifngr1 [interferon gamma receptor 1]
xCytokine	Interferon	Ifngr2 [interferon gamma receptor 2]
xGrowth Factors & Receptors	Angiopoietin	Angpt1 [angiopoietin 1]
xGrowth Factors & Receptors	Angiopoietin	Angpt2 [angiopoietin 2]
xGrowth Factors & Receptors	Angiopoietin	Angpt4 [angiopoietin 4]
xGrowth Factors & Receptors	Angiopoietin	Angptl1 [angiopoietin-like 1]
xGrowth Factors & Receptors	Angiopoietin	Angptl1 [angiopoietin-like 1]
xGrowth Factors & Receptors	Angiopoietin	Angptl2 [angiopoietin-like 2]
xGrowth Factors & Receptors	Angiopoietin	Angptl2 [angiopoietin-like 2]
xGrowth Factors & Receptors	Angiopoietin	Angptl2 [angiopoietin-like 2]
xGrowth Factors & Receptors	Angiopoietin	Angptl3 [angiopoietin-like 3]
xGrowth Factors & Receptors	Angiopoietin	Angptl4 [angiopoietin-like 4]
xGrowth Factors & Receptors	Angiopoietin	Angptl6 [angiopoietin-like 6]
xGrowth Factors & Receptors	Angiopoietin	Angptl7 [angiopoietin-like 7]
xGrowth Factors & Receptors	BMP	Bmp1 [bone morphogenetic protein 1]
xGrowth Factors & Receptors	BMP	Bmp10 [bone morphogenetic protein 10 preproprotein]
xGrowth Factors & Receptors	BMP	Bmp15 [bone morphogenetic protein 15]
xGrowth Factors & Receptors	BMP	Bmp2 [bone morphogenetic protein 2]

xGrowth Factors & Receptors	BMP	Bmp3 [bone morphogenetic protein 3]
xGrowth Factors & Receptors	BMP	Bmp3 [bone morphogenetic protein 3]
xGrowth Factors & Receptors	BMP	Bmp4 [bone morphogenetic protein 4]
xGrowth Factors & Receptors	BMP	Bmp5 [bone morphogenetic protein 5]
xGrowth Factors & Receptors	BMP	Bmp6 [bone morphogenetic protein 6]
xGrowth Factors & Receptors	BMP	Bmp7 [bone morphogenetic protein 7]
xGrowth Factors & Receptors	BMP	Bmp7 [bone morphogenetic protein 7]
xGrowth Factors & Receptors	BMP	Bmp8a [bone morphogenetic protein 8a]
xGrowth Factors & Receptors	BMP	Bmp8b [bone morphogenetic protein 8b]
xGrowth Factors & Receptors	BMP	Bmpr1a [bone morphogenetic protein receptor type 1A]
xGrowth Factors & Receptors	BMP	Bmpr1a [bone morphogenetic protein receptor type 1A]
xGrowth Factors & Receptors	BMP	Bmpr1b [bone morphogenetic protein receptor type 1B]
xGrowth Factors & Receptors	BMP	Bmpr2 [bone morphogenic protein receptor type II]
xGrowth Factors & Receptors	EGF	Areg [Amphiregulin]
xGrowth Factors & Receptors	EGF	Btc [betacellulin epidermal growth factor family]
xGrowth Factors & Receptors	EGF	Egfr [epidermal growth factor receptor isoform 1]
xGrowth Factors & Receptors	EGF	Egfr [epidermal growth factor receptor isoform 2]
xGrowth Factors & Receptors	EGF	Egfr [epidermal growth factor receptor]
xGrowth Factors & Receptors	EGF	Fbln5 [fibulin 5]
xGrowth Factors & Receptors	EGF	Fbln5 [fibulin 5]
xGrowth Factors & Receptors	EGF	Hbegf [heparin-binding EGF-like growth factor]
xGrowth Factors & Receptors	EGF	Hbegf [heparin-binding EGF-like growth factor]
xGrowth Factors & Receptors	EGF	Odz4 [odd Oz/ten-m homolog 4]
xGrowth Factors & Receptors	EGF	Odz4 [odd Oz/ten-m homolog 4]
xGrowth Factors & Receptors	EGF	Odz4 related transcript AK053790
xGrowth Factors & Receptors	EGF	Odz4 related transcript ten-m4
xGrowth Factors & Receptors	EGF	Odz4 related transcript ten-m4
xGrowth Factors & Receptors	FGF&R	Fgf1 [fibroblast growth factor 1]

xGrowth Factors & Receptors	FGF&R	Fgf10 [fibroblast growth factor 10]
xGrowth Factors & Receptors	FGF&R	Fgf11 [fibroblast growth factor 11]
xGrowth Factors & Receptors	FGF&R	Fgf12 [fibroblast growth factor 12]
xGrowth Factors & Receptors	FGF&R	Fgf12 [fibroblast growth factor 12]
xGrowth Factors & Receptors	FGF&R	Fgf13 [fibroblast growth factor 13]
xGrowth Factors & Receptors	FGF&R	Fgf14 [fibroblast growth factor 14]
xGrowth Factors & Receptors	FGF&R	Fgf14 [fibroblast growth factor 14]
xGrowth Factors & Receptors	FGF&R	Fgf15 [fibroblast growth factor 15]
xGrowth Factors & Receptors	FGF&R	Fgf16 [fibroblast growth factor 16]
xGrowth Factors & Receptors	FGF&R	Fgf17 [fibroblast growth factor 17]
xGrowth Factors & Receptors	FGF&R	Fgf18 [fibroblast growth factor 18]
xGrowth Factors & Receptors	FGF&R	Fgf2 [fibroblast growth factor 2]
xGrowth Factors & Receptors	FGF&R	Fgf20 [fibroblast growth factor 20]
xGrowth Factors & Receptors	FGF&R	Fgf21 [fibroblast growth factor 21]
xGrowth Factors & Receptors	FGF&R	Fgf22 [fibroblast growth factor 22]
xGrowth Factors & Receptors	FGF&R	Fgf22 [fibroblast growth factor 22]
xGrowth Factors & Receptors	FGF&R	Fgf23 [fibroblast growth factor 23]
xGrowth Factors & Receptors	FGF&R	Fgf3 [fibroblast growth factor 3]
xGrowth Factors & Receptors	FGF&R	Fgf4 [fibroblast growth factor 4]
xGrowth Factors & Receptors	FGF&R	Fgf5 [fibroblast growth factor 5]
xGrowth Factors & Receptors	FGF&R	Fgf6 [fibroblast growth factor 6]
xGrowth Factors & Receptors	FGF&R	Fgf7 [fibroblast growth factor 7]
xGrowth Factors & Receptors	FGF&R	Fgf7 [fibroblast growth factor 7]
xGrowth Factors & Receptors	FGF&R	Fgf8 [fibroblast growth factor 8]
xGrowth Factors & Receptors	FGF&R	Fgf9 [fibroblast growth factor 9]
xGrowth Factors & Receptors	FGF&R	Fgf9 [fibroblast growth factor 9]
xGrowth Factors & Receptors	FGF&R	Fgfr1 [fibroblast growth factor receptor 1]
xGrowth Factors & Receptors	FGF&R	Fgfr1 [fibroblast growth factor receptor 1]

xGrowth Factors & Receptors	FGF&R	Fgfr2 [fibroblast growth factor receptor 2]
xGrowth Factors & Receptors	FGF&R	Fgfr2 [fibroblast growth factor receptor 2]
xGrowth Factors & Receptors	FGF&R	Fgfr2 [fibroblast growth factor receptor 2]
xGrowth Factors & Receptors	FGF&R	Fgfr3 [fibroblast growth factor receptor 3]
xGrowth Factors & Receptors	FGF&R	Fgfr4 [fibroblast growth factor receptor 4]
xGrowth Factors & Receptors	FGF&R	Fibp [FGF intracellular binding protein]
xGrowth Factors & Receptors	FGF&R	Fibp [FGF intracellular binding protein]
xGrowth Factors & Receptors	FGF&R	Fibp [FGF intracellular binding protein]
xGrowth Factors & Receptors	FGF&R	Fibp [FGF intracellular binding protein]
xGrowth Factors & Receptors	GDF	Gdf1 [growth differentiation factor 1]
xGrowth Factors & Receptors	GDF	Gdf10 [growth differentiation factor 10]
xGrowth Factors & Receptors	GDF	Gdf11 [growth differentiation factor 11]
xGrowth Factors & Receptors	GDF	Gdf15 [growth differentiation factor 15]
xGrowth Factors & Receptors	GDF	Gdf2 [growth differentiation factor 2]
xGrowth Factors & Receptors	GDF	Gdf3 [growth differentiation factor 3]
xGrowth Factors & Receptors	GDF	Gdf3 [growth differentiation factor 3]
xGrowth Factors & Receptors	GDF	Gdf5 [growth differentiation factor 5]
xGrowth Factors & Receptors	GDF	Gdf6 [growth differentiation factor 6]
xGrowth Factors & Receptors	GDF	Gdf7 [growth differentiation factor 7]
xGrowth Factors & Receptors	GDF	Gdf9 [growth differentiation factor 9]
xGrowth Factors & Receptors	GMCSF	Bdnf [brain derived neurotrophic factor]
xGrowth Factors & Receptors	GMCSF	Csf1 [colony stimulating factor 1]
xGrowth Factors & Receptors	GMCSF	Csf1 [colony stimulating factor 1]
xGrowth Factors & Receptors	GMCSF	Csf1 [colony stimulating factor 1]
xGrowth Factors & Receptors	GMCSF	Csf1 [colony stimulating factor 1]
xGrowth Factors & Receptors	GMCSF	Csf1 [colony stimulating factor 1]
xGrowth Factors & Receptors	GMCSF	Csf1r [colony stimulating factor 1 receptor]
xGrowth Factors & Receptors	GMCSF	Csf1r [colony stimulating factor 1 receptor]

xGrowth Factors & Receptors	GMCSF	Csf1r [colony stimulating factor 1 receptor]
xGrowth Factors & Receptors	GMCSF	Csf2 [colony stimulating factor 2]
xGrowth Factors & Receptors	GMCSF	Csf2ra [colony stimulating factor 2 receptor alpha]
xGrowth Factors & Receptors	GMCSF	Csf2rb [colony stimulating factor 2 receptor beta]
xGrowth Factors & Receptors	GMCSF	Csf2rb2 [colony stimulating factor 2 receptor beta 2]
xGrowth Factors & Receptors	GMCSF	Csf3 [colony stimulating factor 3]
xGrowth Factors & Receptors	GMCSF	Csf3r [colony stimulating factor 3 receptor]
xGrowth Factors & Receptors	HGF	Hgf [hepatocyte growth factor]
xGrowth Factors & Receptors	HGF	Hgf [hepatocyte growth factor]
xGrowth Factors & Receptors	HGF	Hgf [hepatocyte growth factor]
xGrowth Factors & Receptors	HGF	Met [met proto-oncogene]
xGrowth Factors & Receptors	HGF	Met [met proto-oncogene]
xGrowth Factors & Receptors	HH/patched/smoothened	Dhh [desert hedgehog]
xGrowth Factors & Receptors	HH/patched/smoothened	Dhh [desert hedgehog]
xGrowth Factors & Receptors	HH/patched/smoothened	Ihh [Indian hedgehog]
xGrowth Factors & Receptors	HH/patched/smoothened	Ihh [Indian hedgehog]
xGrowth Factors & Receptors	HH/patched/smoothened	Ptch1 [patched]
xGrowth Factors & Receptors	HH/patched/smoothened	Ptch1 [patched]
xGrowth Factors & Receptors	HH/patched/smoothened	Ptch2 [patched homolog 2]
xGrowth Factors & Receptors	HH/patched/smoothened	Shh [sonic hedgehog]
xGrowth Factors & Receptors	HH/patched/smoothened	Shh [sonic hedgehog]
xGrowth Factors & Receptors	HH/patched/smoothened	Smo [smoothened]
xGrowth Factors & Receptors	IGF	Igf1 [insulin-like growth factor 1]
xGrowth Factors & Receptors	IGF	Igf1 [insulin-like growth factor 1]
xGrowth Factors & Receptors	IGF	Igf1r [insulin-like growth factor I receptor]
xGrowth Factors & Receptors	IGF	Igf1r [insulin-like growth factor I receptor]
xGrowth Factors & Receptors	IGF	Igf2 [insulin-like growth factor 2]
xGrowth Factors & Receptors	IGF	Igf2 [insulin-like growth factor 2]

xGrowth Factors & Receptors	IGF	Igf2bp1 [insulin-like growth factor 2 mRNA binding protein 1]
xGrowth Factors & Receptors	IGF	Igf2bp2 [insulin-like growth factor 2 mRNA binding protein 2]
xGrowth Factors & Receptors	IGF	Igf2bp3 [insulin-like growth factor 2 mRNA binding]
xGrowth Factors & Receptors	IGF	Igf2bp3 [insulin-like growth factor 2 mRNA binding]
xGrowth Factors & Receptors	IGF	Igf2bp3 [insulin-like growth factor 2 mRNA binding]
xGrowth Factors & Receptors	IGF	Igf2bp3 [insulin-like growth factor 2 mRNA binding]
xGrowth Factors & Receptors	IGF	Igf2r [insulin-like growth factor 2 receptor]
xGrowth Factors & Receptors	IGF	Igfals [insulin-like growth factor binding protein acid labile subunit]
xGrowth Factors & Receptors	IGF	Igfbp1 [insulin-like growth factor binding protein 1]
xGrowth Factors & Receptors	IGF	Igfbp2 [insulin-like growth factor binding protein 2]
xGrowth Factors & Receptors	IGF	Igfbp3 [insulin-like growth factor binding protein 3]
xGrowth Factors & Receptors	IGF	Igfbp4 [insulin-like growth factor binding protein 4]
xGrowth Factors & Receptors	IGF	Igfbp4 [insulin-like growth factor binding protein 4]
xGrowth Factors & Receptors	IGF	Igfbp4 [insulin-like growth factor binding protein 4]
xGrowth Factors & Receptors	IGF	Igfbp5 [insulin-like growth factor binding protein 5]
xGrowth Factors & Receptors	IGF	Igfbp6 [insulin-like growth factor binding protein 6]
xGrowth Factors & Receptors	IGF	Igfbp7 [insulin-like growth factor binding protein 7]
xGrowth Factors & Receptors	IGF	Igfbpl1 [insulin-like growth factor binding protein like 1]
xGrowth Factors & Receptors	IGF	Igfl3 [IGF-like family member 3]
xGrowth Factors & Receptors	Miscellaneous	MDK (neurite GF2)
xGrowth Factors & Receptors	Miscellaneous	NGF rec
xGrowth Factors & Receptors	PDGF	(PDGFC)
xGrowth Factors & Receptors	PDGF	(PDGFD)
xGrowth Factors & Receptors	PDGF	PDGFa polypep var1
xGrowth Factors & Receptors	PDGF	PDGFb polypep var2
xGrowth Factors & Receptors	PDGF	PDGFR alpha
xGrowth Factors & Receptors	PDGF	PDGFR beta
xGrowth Factors & Receptors	TGF beta	ACVR1 [activin A receptor, type 1]

xGrowth Factors & Receptors	TGF beta	Acvr2a [activin receptor IIA]
xGrowth Factors & Receptors	TGF beta	Acvr2b [activin receptor IIB]
xGrowth Factors & Receptors	TGF beta	Acvrl1 [activin A receptor type II-like 1]
xGrowth Factors & Receptors	TGF beta	Chrd [chordin]
xGrowth Factors & Receptors	TGF beta	Chrd [chordin]
xGrowth Factors & Receptors	TGF beta	Fst [follistatin]
xGrowth Factors & Receptors	TGF beta	Fst [follistatin]
xGrowth Factors & Receptors	TGF beta	Inhbc [inhibin beta-C]
xGrowth Factors & Receptors	TGF beta	Inhbe [inhibin beta E]
xGrowth Factors & Receptors	TGF beta	Magi2 [membrane associated guanylate kinase WW and PDZ]
xGrowth Factors & Receptors	TGF beta	Magi2 [membrane associated guanylate kinase WW and PDZ]
xGrowth Factors & Receptors	TGF beta	Nog [noggin]
xGrowth Factors & Receptors	TGF beta	Nog [noggin]
xGrowth Factors & Receptors	TGF beta	Pspn [persephin]
xGrowth Factors & Receptors	TGF beta	Tgfb1 [transforming growth factor beta 1]
xGrowth Factors & Receptors	TGF beta	Tgfb2 [transforming growth factor beta 2]
xGrowth Factors & Receptors	TGF beta	Tgfb3 [transforming growth factor beta 3]
xGrowth Factors & Receptors	TGF beta	Tgfbr1 [transforming growth factor beta receptor I]
xGrowth Factors & Receptors	TGF beta	Tgfbr2 [transforming growth factor beta receptor II]
xGrowth Factors & Receptors	TGF beta	Tgfbr2 [transforming growth factor beta receptor II]
xGrowth Factors & Receptors	TGF beta	Tgfbr3 [transforming growth factor beta receptor III]
xGrowth Factors & Receptors	TGF beta	Tgfbr3 [transforming growth factor beta receptor III]
xGrowth Factors & Receptors	VEGF	Figf [c-fos induced growth factor]
xGrowth Factors & Receptors	VEGF	Flt3 [FMS-like tyrosine kinase 3]
xGrowth Factors & Receptors	VEGF	Flt3l [FMS-like tyrosine kinase 3 ligand; Flt3 ligand]
xGrowth Factors & Receptors	VEGF	Flt3l [FMS-like tyrosine kinase 3 ligand; Flt3 ligand]
xGrowth Factors & Receptors	VEGF	Flt3l [FMS-like tyrosine kinase 3 ligand; Flt3 ligand]
xGrowth Factors & Receptors	VEGF	Flt3l [FMS-like tyrosine kinase 3 ligand; Flt3 ligand]

xGrowth Factors & Receptors	VEGF	Vegfa [vascular endothelial growth factor A]
xGrowth Factors & Receptors	VEGF	Vegfb [vascular endothelial growth factor B]
xGrowth Factors & Receptors	VEGF	Vegfc [vascular endothelial growth factor C]
xGrowth Factors & Receptors	WNT	Fzd1 [frizzled 1]
xGrowth Factors & Receptors	WNT	Fzd10 [frizzled 10]
xGrowth Factors & Receptors	WNT	Fzd10 [frizzled 10]
xGrowth Factors & Receptors	WNT	Fzd2 [frizzled 2]
xGrowth Factors & Receptors	WNT	Fzd3 [frizzled 3]
xGrowth Factors & Receptors	WNT	Fzd4 [frizzled 4]
xGrowth Factors & Receptors	WNT	Fzd5 [frizzled 5]
xGrowth Factors & Receptors	WNT	Fzd6 [frizzled 6]
xGrowth Factors & Receptors	WNT	Fzd7 [frizzled 7]
xGrowth Factors & Receptors	WNT	Fzd8 [frizzled 8]
xGrowth Factors & Receptors	WNT	Fzd9 [frizzled 9]
xGrowth Factors & Receptors	WNT	Wnt1 [wingless-related MMTV integration site 1]
xGrowth Factors & Receptors	WNT	Wnt10a [wingless related MMTV integration site 10a]
xGrowth Factors & Receptors	WNT	Wnt10b [wingless related MMTV integration site 10b]
xGrowth Factors & Receptors	WNT	Wnt11 [wingless-related MMTV integration site 11]
xGrowth Factors & Receptors	WNT	Wnt16 [wingless-related MMTV integration site 16]
xGrowth Factors & Receptors	WNT	Wnt16 [wingless-related MMTV integration site 16]
xGrowth Factors & Receptors	WNT	Wnt2 [wingless-related MMTV integration site 2]
xGrowth Factors & Receptors	WNT	Wnt2b [wingless related MMTV integration site 2b]
xGrowth Factors & Receptors	WNT	Wnt3 [wingless-related MMTV integration site 3]
xGrowth Factors & Receptors	WNT	Wnt3a [wingless-related MMTV integration site 3a]
xGrowth Factors & Receptors	WNT	Wnt4 [wingless-related MMTV integration site 4]
xGrowth Factors & Receptors	WNT	Wnt5a [wingless-related MMTV integration site 5A]
xGrowth Factors & Receptors	WNT	Wnt5b [wingless-related MMTV integration site 5B]
xGrowth Factors & Receptors	WNT	Wnt6 [wingless-related MMTV integration site 6]

xGrowth Factors & Receptors	WNT	Wnt7a [wingless-related MMTV integration site 7A]
xGrowth Factors & Receptors	WNT	Wnt7b [wingless-related MMTV integration site 7B]
xGrowth Factors & Receptors	WNT	Wnt8a [wingless related MMTV integration site 8a]
xGrowth Factors & Receptors	WNT	Wnt8b [wingless related MMTV integration site 8b]
xGrowth Factors & Receptors	WNT	Wnt9a [wingless related MMTV integration site 9a]
xGrowth Factors & Receptors	WNT	Wnt9b [wingless related MMTV integration site 9b]
xInterleukin & Receptors	IL	Il10 [Interleukin-10]
xInterleukin & Receptors	IL	Il11 [interleukin 11]
xInterleukin & Receptors	IL	Il12a [Interleukin-12a]
xInterleukin & Receptors	IL	Il12b [Interleukin-12b]
xInterleukin & Receptors	IL	Il13 [Interleukin-13]
xInterleukin & Receptors	IL	Il15 [Interleukin-15]
xInterleukin & Receptors	IL	Il15 [Interleukin-15]
xInterleukin & Receptors	IL	Il16 [Interleukin-16]
xInterleukin & Receptors	IL	Il16 [Interleukin-16]
xInterleukin & Receptors	IL	Il17a [Interleukin-17a]
xInterleukin & Receptors	IL	Il17b [Interleukin-17b]
xInterleukin & Receptors	IL	Il17c [interleukin 17C]
xInterleukin & Receptors	IL	Il17d [interleukin 17D]
xInterleukin & Receptors	IL	Il17f [interleukin 17F]
xInterleukin & Receptors	IL	Il18 [interleukin 18]
xInterleukin & Receptors	IL	Il19 [interleukin 19]
xInterleukin & Receptors	IL	Il1a [interleukin 1 alpha]
xInterleukin & Receptors	IL	Il1b [Interleukin-1 beta]
xInterleukin & Receptors	IL	Il1f10 [interleukin 1 family member 10]
xInterleukin & Receptors	IL	Il1f5 [Interleukin 1 family member 5]
xInterleukin & Receptors	IL	Il1f6 [Interleukin 1 family member 6]
xInterleukin & Receptors	IL	Il1f8 [interleukin 1 family member 8]

xInterleukin & Receptors	IL	Il1f9 [interleukin 1 family member 9]
xInterleukin & Receptors	IL	Il2 [Interleukin-2]
xInterleukin & Receptors	IL	Il20 [interleukin 20]
xInterleukin & Receptors	IL	Il21 [interleukin 21]
xInterleukin & Receptors	IL	Il21 [interleukin 21]
xInterleukin & Receptors	IL	Il22 [interleukin 22]
xInterleukin & Receptors	IL	Il23a [interleukin 23 alpha subunit p19]
xInterleukin & Receptors	IL	Il25 [Interleukin-25]
xInterleukin & Receptors	IL	Il27 [interleukin 27]
xInterleukin & Receptors	IL	Il28a [interleukin 28A]
xInterleukin & Receptors	IL	Il28b [interleukin 28B]
xInterleukin & Receptors	IL	Il3 [Interleukin-3]
xInterleukin & Receptors	IL	Il33 [interleukin 33]
xInterleukin & Receptors	IL	Il4 [Interleukin-4]
xInterleukin & Receptors	IL	Il5 Interleukin-5]
xInterleukin & Receptors	IL	Il6 [interleukin 6]
xInterleukin & Receptors	IL	Il6st [Interleukin-6 (gp130); interleukin 6 signal transducer]
xInterleukin & Receptors	IL	Il6st [Interleukin-6 (gp130); interleukin 6 signal transducer]
xInterleukin & Receptors	IL	Il7 [Interleukin-7]
xInterleukin & Receptors	IL receptor	Il10ra [interleukin 10 receptor alpha]
xInterleukin & Receptors	IL receptor	Il10rb [interleukin 10 receptor beta]
xInterleukin & Receptors	IL receptor	Il10rb [interleukin 10 receptor beta]
xInterleukin & Receptors	IL receptor	Il11ra2 [interleukin 11 receptor alpha chain 2]
xInterleukin & Receptors	IL receptor	Il11ra2 [interleukin 11 receptor alpha chain 2]
xInterleukin & Receptors	IL receptor	Il12rb1 [interleukin 12 receptor beta 1]
xInterleukin & Receptors	IL receptor	Il12rb2 [interleukin 12 receptor beta 2]
xInterleukin & Receptors	IL receptor	Il13ra1 [interleukin 13 receptor alpha 1]
xInterleukin & Receptors	IL receptor	Il13ra2 [interleukin 13 receptor alpha 2]

xInterleukin & Receptors	IL receptor	Il15ra [interleukin 15 receptor alpha chain]
xInterleukin & Receptors	IL receptor	Il15ra [interleukin 15 receptor alpha chain]
xInterleukin & Receptors	IL receptor	Il15ra [interleukin 15 receptor alpha chain]
xInterleukin & Receptors	IL receptor	Il17ra [interleukin 17 receptor]
xInterleukin & Receptors	IL receptor	Il17rb [interleukin 17 receptor B]
xInterleukin & Receptors	IL receptor	Il17rc [interleukin 17 receptor C]
xInterleukin & Receptors	IL receptor	Il17rc [interleukin 17 receptor C]
xInterleukin & Receptors	IL receptor	Il17rd [interleukin 17 receptor D]
xInterleukin & Receptors	IL receptor	Il17rd [interleukin 17 receptor D]
xInterleukin & Receptors	IL receptor	Il17rd [interleukin 17 receptor D]
xInterleukin & Receptors	IL receptor	Il17re [interleukin 17 receptor E]
xInterleukin & Receptors	IL receptor	Il17re [interleukin 17 receptor E]
xInterleukin & Receptors	IL receptor	Il18r1 [interleukin 18 receptor 1]
xInterleukin & Receptors	IL receptor	Il18r1 [interleukin 18 receptor 1]
xInterleukin & Receptors	IL receptor	Il18r1 [interleukin 18 receptor 1]
xInterleukin & Receptors	IL receptor	Il18rap [interleukin 18 receptor accessory protein]
xInterleukin & Receptors	IL receptor	Il18rap [interleukin 18 receptor accessory protein]
xInterleukin & Receptors	IL receptor	Il18rap [interleukin 18 receptor accessory protein]
xInterleukin & Receptors	IL receptor	Il1r1 [interleukin 1 receptor type I]
xInterleukin & Receptors	IL receptor	Il1r2 [interleukin 1 receptor type II]
xInterleukin & Receptors	IL receptor	Il1rap [interleukin 1 receptor accessory protein]
xInterleukin & Receptors	IL receptor	Il1rap [interleukin 1 receptor accessory protein]
xInterleukin & Receptors	IL receptor	Il1rap [interleukin 1 receptor accessory protein]
xInterleukin & Receptors	IL receptor	Il1rap [interleukin 1 receptor accessory protein]
xInterleukin & Receptors	IL receptor	Il1rapl2 [interleukin 1 receptor accessory protein-like 2]
xInterleukin & Receptors	IL receptor	Il1rapl2 [interleukin 1 receptor accessory protein-like 2]
xInterleukin & Receptors	IL receptor	Il1rapl2 [interleukin 1 receptor accessory protein-like 2]
xInterleukin & Receptors	IL receptor	Il1rl1 [interleukin 1 receptor-like 1]

xInterleukin & Receptors	IL receptor	Il1rl1 [interleukin 1 receptor-like 1]
xInterleukin & Receptors	IL receptor	Il1rl2 [interleukin 1 receptor-like 2]
xInterleukin & Receptors	IL receptor	Il1rn [interleukin 1 receptor antagonist]
xInterleukin & Receptors	IL receptor	Il20ra [interleukin 20 receptor alpha]
xInterleukin & Receptors	IL receptor	Il20rb [interleukin 20 receptor beta]
xInterleukin & Receptors	IL receptor	Il20rb [interleukin 20 receptor beta]
xInterleukin & Receptors	IL receptor	Il21r [interleukin 21 receptor]
xInterleukin & Receptors	IL receptor	Il21r [interleukin 21 receptor]
xInterleukin & Receptors	IL receptor	Il21r [interleukin 21 receptor]
xInterleukin & Receptors	IL receptor	Il21r [interleukin 21 receptor]
xInterleukin & Receptors	IL receptor	Il22ra1 [interleukin 22 receptor alpha 1]
xInterleukin & Receptors	IL receptor	Il22ra2 [interleukin 22 receptor alpha 2]
xInterleukin & Receptors	IL receptor	Il23r [interleukin 23 receptor]
xInterleukin & Receptors	IL receptor	Il27ra [interleukin 27 receptor alpha]
xInterleukin & Receptors	IL receptor	Il28ra [interleukin 28 receptor alpha]
xInterleukin & Receptors	IL receptor	Il2ra [interleukin 2 receptor alpha chain]
xInterleukin & Receptors	IL receptor	Il2rb [interleukin 2 receptor beta chain]
xInterleukin & Receptors	IL receptor	Il2rg [interleukin 2 receptor gamma chain]
xInterleukin & Receptors	IL receptor	Il2rg [interleukin 2 receptor gamma chain]
xInterleukin & Receptors	IL receptor	Il31ra [interleukin 31 receptor A]
xInterleukin & Receptors	IL receptor	Il31ra [interleukin 31 receptor A]
xInterleukin & Receptors	IL receptor	Il31ra [interleukin 31 receptor A]
xInterleukin & Receptors	IL receptor	Il3ra [interleukin 3 receptor alpha chain]
xInterleukin & Receptors	IL receptor	Il4ra [interleukin 4 receptor alpha]
xInterleukin & Receptors	IL receptor	Il4ra [interleukin 4 receptor alpha]
xInterleukin & Receptors	IL receptor	Il5ra [interleukin 5 receptor alpha]
xInterleukin & Receptors	IL receptor	Il6ra [Interleukin-6 R alpha]
xInterleukin & Receptors	IL receptor	Il6ra [Interleukin-6 R alpha]

xInterleukin & Receptors	IL receptor	Il6ra [Interleukin-6 R alpha]
xInterleukin & Receptors	IL receptor	Il7r [interleukin 7 receptor]
xInterleukin & Receptors	IL receptor	Il7r [interleukin 7 receptor]
xInterleukin & Receptors	IL receptor	Il8ra [interleukin 8 receptor alpha]
xInterleukin & Receptors	IL receptor	Il8rb [interleukin 8 receptor beta]
xInterleukin & Receptors	IL receptor	Il8rb [interleukin 8 receptor beta]
xInterleukin & Receptors	IL receptor	Il9r [interleukin 9 receptor]
xMouse Housekeeping	xMouse Housekeeping	1200013P24Rik [RIKEN cDNA 1200013P24 gene]
xMouse Housekeeping	xMouse Housekeeping	2610209M04Rik [putative nucleic acid binding protein RY-1]
xMouse Housekeeping	xMouse Housekeeping	3100004P22Rik [hypothetical protein LOC68035]
xMouse Housekeeping	xMouse Housekeeping	4931406I20Rik [hypothetical protein LOC66743]
xMouse Housekeeping	xMouse Housekeeping	5730453I16Rik [pre-mRNA cleavage factor I 59 kDa subunit]
xMouse Housekeeping	xMouse Housekeeping	9130011J15Rik [hypothetical protein LOC66818]
xMouse Housekeeping	xMouse Housekeeping	Aldoa [aldolase 1 A isoform]
xMouse Housekeeping	xMouse Housekeeping	Aldoa [aldolase 1 A isoform]
xMouse Housekeeping	xMouse Housekeeping	Anapc1 [anaphase promoting complex subunit 1]
xMouse Housekeeping	xMouse Housekeeping	Anapc2 [anaphase promoting complex subunit 2]
xMouse Housekeeping	xMouse Housekeeping	Angel2 [angel homolog 2 (Drosophila)]
xMouse Housekeeping	xMouse Housekeeping	Ankrd17 [ankyrin repeat domain 17]
xMouse Housekeeping	xMouse Housekeeping	Apoa1bp [apolipoprotein A-I binding protein]
xMouse Housekeeping	xMouse Housekeeping	Arfgef1 [ADP-ribosylation factor guanine nucleotide-exchange factor 1(brefeldin A-inhibited)]
xMouse Housekeeping	xMouse Housekeeping	Armc1 [armadillo repeat containing 1]
xMouse Housekeeping	xMouse Housekeeping	Atg5 [autophagy-related 5 (yeast)]
xMouse Housekeeping	xMouse Housekeeping	Atox1 [(antioxidant protein 1) homolog 1 (yeast)]
xMouse Housekeeping	xMouse Housekeeping	Atp6v0d1 [ATPase, H+ transporting, V0 subunit D isoform 1]
xMouse Housekeeping	xMouse Housekeeping	Aup1 [ancient ubiquitous protein]
xMouse Housekeeping	xMouse Housekeeping	Bat5 [HLA-B associated transcript 5]

xMouse Housekeeping	xMouse Housekeeping	BC031181 [hypothetical protein LOC407819]
xMouse Housekeeping	xMouse Housekeeping	Btg2 [B-cell translocation gene 2, anti-proliferative]
xMouse Housekeeping	xMouse Housekeeping	Canx [calnexin]
xMouse Housekeeping	xMouse Housekeeping	Cdc42 [cell division cycle 42 homolog (S. cerevisiae)]
xMouse Housekeeping	xMouse Housekeeping	Cdv3 [carnitine deficiency-associated gene expressed in ventricle 3]
xMouse Housekeeping	xMouse Housekeeping	Cic [capicua homolog (Drosophila)]
xMouse Housekeeping	xMouse Housekeeping	Cks1b [CDC28 protein kinase 1b]
xMouse Housekeeping	xMouse Housekeeping	Cks2 [CDC28 protein kinase regulatory subunit 2]
xMouse Housekeeping	xMouse Housekeeping	Copa [coatomer protein complex subunit alpha]
xMouse Housekeeping	xMouse Housekeeping	Copg [coatomer protein complex, subunit gamma]
xMouse Housekeeping	xMouse Housekeeping	Cox18 [COX18 cytochrome c oxidase assembly homolog]
xMouse Housekeeping	xMouse Housekeeping	Ctbp1 [C-terminal binding protein 1]
xMouse Housekeeping	xMouse Housekeeping	D10Bwg1364e [DNA segment, Chr 10, Brigham & Women's Genetics 1364 expressed]
xMouse Housekeeping	xMouse Housekeeping	Dctn5 [dynactin 5]
xMouse Housekeeping	xMouse Housekeeping	Ddb1 [damage specific DNA binding protein 1]
xMouse Housekeeping	xMouse Housekeeping	Ddx24 [DEAD (Asp-Glu-Ala-Asp) box polypeptide 24]
xMouse Housekeeping	xMouse Housekeeping	Derl1 [Der1-like domain family, member 1]
xMouse Housekeeping	xMouse Housekeeping	Dhrs1 [dehydrogenase/reductase (SDR family) member 1]
xMouse Housekeeping	xMouse Housekeeping	Dlg1 [discs, large homolog 1 (Drosophila)]
xMouse Housekeeping	xMouse Housekeeping	Dscr3 [Down syndrome critical region gene 3]
xMouse Housekeeping	xMouse Housekeeping	Eif5 [eukaryotic translation initiation factor 5]
xMouse Housekeeping	xMouse Housekeeping	Fryl [furry homolog-like isoform 1]
xMouse Housekeeping	xMouse Housekeeping	G3bp2 [Ras-GTPase-activating protein (GAP120)]
xMouse Housekeeping	xMouse Housekeeping	Ganab [alpha glucosidase 2 alpha neutral subunit]
xMouse Housekeeping	xMouse Housekeeping	Gbf1 [golgi-specific brefeldin A-resistance factor 1]
xMouse Housekeeping	xMouse Housekeeping	Gnb1 [guanine nucleotide-binding protein beta-1]
xMouse Housekeeping	xMouse Housekeeping	Golga7 [golgi autoantigen, golgin subfamily a, 7]

xMouse Housekeeping	xMouse Housekeeping	Golm1 [golgi membrane protein 1]
xMouse Housekeeping	xMouse Housekeeping	Gps1 [G protein pathway suppressor 1]
xMouse Housekeeping	xMouse Housekeeping	Gps2 [G protein pathway suppressor 2]
xMouse Housekeeping	xMouse Housekeeping	H2-Ke2 [H2-K region expressed gene 2]
xMouse Housekeeping	xMouse Housekeeping	Hbxip [hepatitis B virus x interacting protein]
xMouse Housekeeping	xMouse Housekeeping	Hdac5 [histone deacetylase 5]
xMouse Housekeeping	xMouse Housekeeping	Hmgn2 [high mobility group nucleosomal binding domain]
xMouse Housekeeping	xMouse Housekeeping	Hnrpul2 [heterogeneous nuclear ribonucleoprotein U-like 2]
xMouse Housekeeping	xMouse Housekeeping	Hp1bp3 [heterochromatin protein 1, binding protein 3]
xMouse Housekeeping	xMouse Housekeeping	Huwe1 [HECT, UBA and WWE domain containing 1]
xMouse Housekeeping	xMouse Housekeeping	ILK [integrin linked kinase]
xMouse Housekeeping	xMouse Housekeeping	Itch [itchy E3 ubiquitin protein ligase]
xMouse Housekeeping	xMouse Housekeeping	Junb [Jun-B oncogene]
xMouse Housekeeping	xMouse Housekeeping	Jund [Jun-D proto-oncogene]
xMouse Housekeeping	xMouse Housekeeping	Lta4h [leukotriene A4 hydrolase]
xMouse Housekeeping	xMouse Housekeeping	Mad2l1bp [MAD2L1 binding protein]
xMouse Housekeeping	xMouse Housekeeping	Mrpl27 [mitochondrial ribosomal protein L27]
xMouse Housekeeping	xMouse Housekeeping	Mrpl43 [mitochondrial ribosomal protein L43]
xMouse Housekeeping	xMouse Housekeeping	Mrpl52 [mitochondrial ribosomal protein L52]
xMouse Housekeeping	xMouse Housekeeping	Mtif2 [mitochondrial translational initiation factor 2]
xMouse Housekeeping	xMouse Housekeeping	Nmt1 [N-myristoyltransferase 1]
xMouse Housekeeping	xMouse Housekeeping	Nubp1 [nucleotide binding protein 1]
xMouse Housekeeping	xMouse Housekeeping	Pabpn1 [poly(A) binding protein, nuclear 1]
xMouse Housekeeping	xMouse Housekeeping	Pcbp1 [poly(rC) binding protein 1]
xMouse Housekeeping	xMouse Housekeeping	Pdpk1 [Phosphoinositide-dependent protein kinase-1 beta (Pdk1beta)]
xMouse Housekeeping	xMouse Housekeeping	Pfdn5 [prefoldin 5]
xMouse Housekeeping	xMouse Housekeeping	Polr2f [polymerase (RNA) II (DNA directed) polypeptide F]
xMouse Housekeeping	xMouse Housekeeping	Ppm1a [protein phosphatase 1A, magnesium dependent, alpha isoform]

xMouse Housekeeping	xMouse Housekeeping	Prdm1 [PR domain containing 1 with ZNF domain]
xMouse Housekeeping	xMouse Housekeeping	Psap [prosaposin]
xMouse Housekeeping	xMouse Housekeeping	Psenen [presenilin enhancer 2 homolog (C. elegans)]
xMouse Housekeeping	xMouse Housekeeping	Psma1 [proteasome (prosome, macropain) subunit, alpha type 1]
xMouse Housekeeping	xMouse Housekeeping	Psmb3 [proteasome beta 3 subunit]
xMouse Housekeeping	xMouse Housekeeping	Psmb5 [proteasome (prosome, macropain) subunit, beta type 5]
xMouse Housekeeping	xMouse Housekeeping	Psmc1 [protease (prosome macropain) 26S subunit]
xMouse Housekeeping	xMouse Housekeeping	Psmc5 [protease (prosome, macropain) 26S subunit, ATPase 5]
xMouse Housekeeping	xMouse Housekeeping	Psph [phosphoserine phosphatase]
xMouse Housekeeping	xMouse Housekeeping	Rab14 [member RAS oncogene family]
xMouse Housekeeping	xMouse Housekeeping	Rab7 [member RAS oncogene family]
xMouse Housekeeping	xMouse Housekeeping	Rfk [riboflavin kinase]
xMouse Housekeeping	xMouse Housekeeping	Riok3 [RIO kinase 3 (yeast)]
xMouse Housekeeping	xMouse Housekeeping	Riok3 [RIO kinase 3 (yeast)]
xMouse Housekeeping	xMouse Housekeeping	Rpl23 [ribosomal protein L23]
xMouse Housekeeping	xMouse Housekeeping	Rpl39l [ribosomal protein L39-like protein]
xMouse Housekeeping	xMouse Housekeeping	Rps27 [ribosomal protein S27]
xMouse Housekeeping	xMouse Housekeeping	Rragc [Ras-related GTP binding C]
xMouse Housekeeping	xMouse Housekeeping	Rrn3 [RNA polymerase I transcription factor homolog (yeast)]
xMouse Housekeeping	xMouse Housekeeping	S100a10 [S100 calcium binding protein A10]
xMouse Housekeeping	xMouse Housekeeping	Sap30l [SAP30-like]
xMouse Housekeeping	xMouse Housekeeping	Sar1a [Sar1agene homolog 1 (S. cerevisiae)]
xMouse Housekeeping	xMouse Housekeeping	Sc4mol [sterol-C4-methyl oxidase-like]
xMouse Housekeeping	xMouse Housekeeping	Snapin [SNAP-associated protein]
xMouse Housekeeping	xMouse Housekeeping	Ssr3 [signal sequence receptor, gamma]
xMouse Housekeeping	xMouse Housekeeping	Tbl3 [transducin (beta)-like 3]
xMouse Housekeeping	xMouse Housekeeping	Tcea1 [transcription elongation factor A (SII) 1]
xMouse Housekeeping	xMouse Housekeeping	Tmem129 [transmembrane protein 129]

xMouse Housekeeping	xMouse Housekeeping	Tmem165 [TPA regulated locus]
xMouse Housekeeping	xMouse Housekeeping	Tmsb10 [thymosin beta 10]
xMouse Housekeeping	xMouse Housekeeping	Trappc4 [trafficking protein particle complex 4]
xMouse Housekeeping	xMouse Housekeeping	Tsnax [translin-associated factor X]
xMouse Housekeeping	xMouse Housekeeping	Txndc12 [endoplasmic reticulum protein ERp19]
xMouse Housekeeping	xMouse Housekeeping	Ube2g1 [ubiquitin-conjugating enzyme E2G 1 (UBC7 homolog, C. elegans)]
xMouse Housekeeping	xMouse Housekeeping	Ube2v1 [ubiquitin-conjugating enzyme E2 variant 1]
xMouse Housekeeping	xMouse Housekeeping	ubiquitin-conjugating enzyme E2R 2 (Ube2r2)
xMouse Housekeeping	xMouse Housekeeping	Vta1 [1110059P08Rik protein]
xMouse Housekeeping	xMouse Housekeeping	Wars [tryptophanyl-tRNA synthetase]
xMouse Housekeeping	xMouse Housekeeping	Xpo7 [exportin 7]
xMouse Housekeeping	xMouse Housekeeping	Ybx1 [nuclease sensitive element binding protein 1]
xMouse Housekeeping	xMouse Housekeeping	Ythdf1 [YTH domain family 1]
xMouse Housekeeping	xMouse Housekeeping	Ywhab [tyrosine 3-monooxygenase/tryptophan]
xMouse Housekeeping	xMouse Housekeeping	Zc3h11a [zinc finger CCCH type containing 11A]
xMouse Housekeeping	xMouse Housekeeping	Zkscan3 [zinc finger with KRAB and SCAN domains 3]
xProteoglycan	BMPG	Agrn [Agrin]
xProteoglycan	BMPG	Agrn [Agrin]
xProteoglycan	BMPG	Agrn [Agrin]
xProteoglycan	BMPG	Bamacan short (CSPG6; Smc3)
xProteoglycan	BMPG	Col18a1 [Collagen 18a1, procollagen type XVIII alpha 1]
xProteoglycan	BMPG	Perlecan (HSPG2)
xProteoglycan	Glypican	Gpc1 [Glypican-1]
xProteoglycan	Glypican	Gpc2 (Glypican-2, cerebroglycan)
xProteoglycan	Glypican	Gpc2 [Glypican-2, cerebroglycan]
xProteoglycan	Glypican	Gpc3 [Glypican-3, OCI-5]
xProteoglycan	Glypican	Gpc3 [Glypican-3, OCI-5]
xProteoglycan	Glypican	Gpc4 [Glypican-4]

xProteoglycan	Glypican	Gpc5 [Glypican-5]
xProteoglycan	Glypican	Gpc5 [Glypican-5]
xProteoglycan	Glypican	Gpc6 [Glypican-6]
xProteoglycan	Glypican	Gpc6 [Glypican-6]
xProteoglycan	Miscellaneous	Spock3 [Testican-3, sparc/osteonectin cwcv and kazal-like domains]
xProteoglycan	Miscellaneous	CD44 (Epican)
xProteoglycan	Miscellaneous	CD44 (Epican)
xProteoglycan	Miscellaneous	Cd74 [CD74 antigen]
xProteoglycan	Miscellaneous	Col14a1 [procollagen type XIV alpha 1]
xProteoglycan	Miscellaneous	Col14a1 [procollagen type XIV alpha 1]
xProteoglycan	Miscellaneous	Col9a2 [procollagen type IX alpha 2]
xProteoglycan	Miscellaneous	Cspg4 [NG2, chondroitin sulfate proteoglycan 4]
xProteoglycan	Miscellaneous	Cspg4 [NG2, chondroitin sulfate proteoglycan 4]
xProteoglycan	Miscellaneous	Dag1 [dystroglycan 1]
xProteoglycan	Miscellaneous	Esm1 [Endocan, endothelial cell-specific molecule 1]
xProteoglycan	Miscellaneous	Esm1 [Endocan, endothelial cell-specific molecule 1]
xProteoglycan	Miscellaneous	Fcmd [Fukuyama type congenital muscular dystrophy]
xProteoglycan	Miscellaneous	Fcmd [Fukuyama type congenital muscular dystrophy]
xProteoglycan	Miscellaneous	Large [like-glycosyltransferase]
xProteoglycan	Miscellaneous	Lepre1 [Leprecan-1]
xProteoglycan	Miscellaneous	Prg4 [Lubricin, proteoglycan 4]
xProteoglycan	Miscellaneous	Prg4 [Lubricin, proteoglycan 4]
xProteoglycan	Miscellaneous	Prg4 [Lubricin, proteoglycan 4]
xProteoglycan	Miscellaneous	Ptprz1 [Phosphacan, protein tyrosine phosphatase receptor type Z]
xProteoglycan	Miscellaneous	Ptprz1 [Phosphacan, protein tyrosine phosphatase receptor type Z]
xProteoglycan	Miscellaneous	Spock1 [Testican-1, sparc/osteonectin cwcv and kazal-like domains]
xProteoglycan	Miscellaneous	Spock1 [Testican-1, sparc/osteonectin cwcv and kazal-like domains]
xProteoglycan	Miscellaneous	Spock1 [Testican-1, sparc/osteonectin cwcv and kazal-like domains]

xProteoglycan	Miscellaneous	Spock2 [Testican-2, sparc/osteonectin cwcv and kazal-like domains]
xProteoglycan	Miscellaneous	Spock2 [Testican-2, sparc/osteonectin cwcv and kazal-like domains]
xProteoglycan	Miscellaneous	Srgn [Serglycin]
xProteoglycan	SLRP	Bgn [Biglycan, PGI]
xProteoglycan	SLRP	Bgn [Biglycan, PGI]
xProteoglycan	SLRP	DCN [Decorin, PGII]
xProteoglycan	SLRP	Fmod [Fibromodulin]
xProteoglycan	SLRP	Lum [Lumican]
xProteoglycan	Syndecan	Sdc1 [Syndecan-1]
xProteoglycan	Syndecan	Sdc2 [Syndecan-2]
xProteoglycan	Syndecan	Sdc3 [Syndecan-3]
xProteoglycan	Syndecan	Sdc3 [Syndecan-3]
xProteoglycan	Syndecan	Sdc4 [Syndecan-4]
xSulfotransferase	Sulfo-T cytosolic	Sult1a1 [phenol sulfotransferase]
xSulfotransferase	Sulfo-T cytosolic	Sult1a1 [phenol sulfotransferase]
xSulfotransferase	Sulfo-T cytosolic	Sult1b1 [thyroid hormone sulfotransferase]
xSulfotransferase	Sulfo-T cytosolic	Sult1c1 [cytosolic sulfotransferase family 1C]
xSulfotransferase	Sulfo-T cytosolic	Sult1c2 [cytosolic sulfotransferase family 1C]
xSulfotransferase	Sulfo-T cytosolic	Sult1d1 [cytosolic sulfotransferase family 1d]
xSulfotransferase	Sulfo-T cytosolic	Sult1e1 [cytosolic sulfotransferase family 1e]
xSulfotransferase	Sulfo-T Protein tyrosine	Tpst1 [tyrosylprotein sulfotransferase 1]
xSulfotransferase	Sulfo-T Protein tyrosine	Tpst2 [tyrosylprotein sulfotransferase 2]

Appendix 6

Details of differentially expressed genes as identified by microarray analysis

Tissue	Gene	Full name	Function
Small intestine	IL-33	Interleukin-33	Promotes a potent Th2 response, mucosal healing and restores intestinal homeostasis following injury
	MBL2	Mannose-binding lectin 2	Activation of the lectin pathway of the complement system
	ANGPTL4	Angiopoietin-related protein 4	Promotes cell migration, increases E-cadherin expression
	HBEGF	Heparin-binding EGF-like growth factor	Associated with a breakdown in gut barrier function
	CCL5	Chemokine (C-C motif) ligand 5	Recruits leukocytes to inflammatory sites, proliferation and activation of natural killer cells
	B3GALT5	beta-1, 3-galactosyltransferase 5	Functions in mucin glycosyltation
	CD48	Cluster of differentiation 48	Regulates HSC and progenitor cell numbers, activates macrophages and T cells to maintain the inflammatory response
	CD74	Cluster of differentiation 74	Pro-inflammatory cytokine that induces NF-κB
	SMO	Smoothened	G protein-coupled receptor, molecular target for teratogen cyclopamine
	UGT1A	UDP glucuronosyltransferase 1 family, polypeptide A cluster	Encodes several UDP-glucuronosyltransferases

Colon	UGT8	UDP glycosyltransferase 8	Synthesis of galactosylceramide,
	CXCL12	Chemokine (C-X-C motif) ligand 12	Pro-inflammatory cytokine chemotactic for polymorphonuclear leukocytes and haematopoietic stem cells
	LGALS1	lectin, galactoside-binding, soluble, 1	Influences viability of enterocytes, integrity of the villus and epithelial barrier function
	COLEC12	Collectin sub-family member 12	Recognition and removal of microorganisms
	DCN	decorin	Component of extracellular matrix involved in matrix assembly, suppresses growth of various tumour cell lines
	LUM	Lumican	Regulates collagen fibril organisation, epithelial cell migration and tissue repair
	PGM5	phosphoglucomutase 5	Interconversion of glucose-1-phosphate and glucose-6-phosphate
	B3GALNT1	beta-1,3-N-acetylgalactosaminyltransferase 1	Encodes membrane-bound glycoproteins with diverse enzymatic functions
	COL14A1	collagen, type XIV, alpha	Adhesive role by integrating collagen bundles
	IGFBP5	insulin-like growth factor binding protein 5	Binds extracellular matrix and regulates mucosal growth response
	THBD	Thrombomodulin	Regulates thrombin generation

References

[1] Mowat AM, Viney JL. The anatomical basis of intestinal immunity. Immunological reviews 1997;156:145-66.

[2] Healthpages. Anatomy and function of the digestive system. 2011.

[3] Johansson MEV, Hansson GC. Keeping Bacteria at a Distance. Science 2011;334:182-3.

[4] Serafini EP, Kirk AP, Chambers TJ. Rate and pattern of epithelial cell proliferation in ulcerative colitis. Gut 1981;22:648-52.

[5] Gartner LP, Hiatt J.L. Colour textbook of histology: W.B. Saunders company; 2001.

[6] Barker N, van Es JH, Kuipers J, Kujala P, van den Born M, Cozijnsen M, et al. Identification of stem cells in small intestine and colon by marker gene Lgr5. Nature 2007;449:1003-7.

[7] Barker N, van de Wetering M, Clevers H. The intestinal stem cell. Genes Dev 2008;22:1856-64.

[8] van der Flier LG, Haegebarth A, Stange DE, van de Wetering M, Clevers H. OLFM4 is a robust marker for stem cells in human intestine and marks a subset of colorectal cancer cells. Gastroenterology 2009;137:15-7.

[9] Barkla DH, Gibson PR. The fate of epithelial cells in the human large intestine. Pathology 1999;31:230-8.

[10] Potten CS. Stem cells in gastrointestinal epithelium: numbers, characteristics and death. Philos Trans R Soc Lond B Biol Sci 1998;353:821-30.

[11] Watson AJ. Apoptosis and colorectal cancer. Gut 2004;53:1701-9.

[12] Bullen TF, Forrest S, Campbell F, Dodson AR, Hershman MJ, Pritchard DM, et al. Characterization of epithelial cell shedding from human small intestine. Lab Invest 2006;86:1052-63.

[13] Watson AJ, Duckworth CA, Guan Y, Montrose MH. Mechanisms of epithelial cell shedding in the Mammalian intestine and maintenance of barrier function. Ann N Y Acad Sci 2009;1165:135-42.

[14] Ota H, Katsuyama T. Alternating laminated array of two types of mucin in the human gastric surface mucous layer. The Histochemical journal 1992;24:86-92.

[15] Johansson ME, Hansson GC. Preservation of mucus in histological sections, immunostaining of mucins in fixed tissue, and localization of bacteria with FISH. Methods Mol Biol 2012;842:229-35.
[16] Finnie IA, Dwarakanath AD, Taylor BA, Rhodes JM. Colonic Mucin Synthesis Is Increased by Sodium-Butyrate. Gut 1995;36:93-9.
[17] Finnie IA, Campbell BJ, Taylor BA, Milton JD, Sadek SK, Yu LG, et al. Stimulation of colonic mucin synthesis by corticosteroids and nicotine. Clin Sci (Lond) 1996;91:359-64.
[18] MacDermott RP, Donaldson RM, Jr., Trier JS. Glycoprotein synthesis and secretion by mucosal biopsies of rabbit colon and human rectum. J Clin Invest 1974;54:545-54.
[19] Atuma C, Strugala V, Allen A, Holm L. The adherent gastrointestinal mucus gel layer: thickness and physical state in vivo. Am J Physiol Gastrointest Liver Physiol 2001;280:G922-9.
[20] Gustafsson JK, Ermund A, Johansson ME, Schutte A, Hansson GC, Sjovall H. An ex vivo method for studying mucus formation, properties, and thickness in human colonic biopsies and mouse small and large intestinal explants. Am J Physiol Gastrointest Liver Physiol 2012;302:G430-8.
[21] Johansson ME, Larsson JM, Hansson GC. The two mucus layers of colon are organized by the MUC2 mucin, whereas the outer layer is a legislator of host-microbial interactions. Proc Natl Acad Sci U S A 2011;108 Suppl 1:4659-65.
[22] van der Post S, Subramani DB, Backstrom M, Johansson ME, Vester-Christensen MB, Mandel U, et al. Site-specific O-glycosylation on the MUC2 mucin protein inhibits cleavage by the Porphyromonas gingivalis secreted cysteine protease (RgpB). J Biol Chem 2013;288:14636-46.
[23] Lidell ME, Moncada DM, Chadee K, Hansson GC. Entamoeba histolytica cysteine proteases cleave the MUC2 mucin in its C-terminal domain and dissolve the protective colonic mucus gel. Proc Natl Acad Sci U S A 2006;103:9298-303.
[24] Dicksved J, Schreiber O, Willing B, Petersson J, Rang S, Phillipson M, et al. Lactobacillus reuteri maintains a functional mucosal barrier during DSS treatment despite mucus layer dysfunction. PLoS One 2012;7:e46399.
[25] Johansson ME, Phillipson M, Petersson J, Velcich A, Holm L, Hansson GC. The inner of the two Muc2 mucin-dependent mucus layers in colon is devoid of bacteria. Proc Natl Acad Sci U S A 2008;105:15064-9.

[26] Ermund A, Schuette A, Johansson ME, Gustafsson JK, Hansson GC. Gastrointestinal mucus layers have different properties depending on location - 1. Studies of mucus in mouse stomach, small intestine, Peyer's patches and colon. Am J Physiol Gastrointest Liver Physiol 2013.

[27] Johansson ME, Ambort D, Pelaseyed T, Schutte A, Gustafsson JK, Ermund A, et al. Composition and functional role of the mucus layers in the intestine. Cell Mol Life Sci 2011;68:3635-41.

[28] Kleerebezem M, Vaughan EE. Probiotic and gut lactobacilli and bifidobacteria: molecular approaches to study diversity and activity. Annu Rev Microbiol 2009;63:269-90.

[29] Matsuo K, Ota H, Akamatsu T, Sugiyama A, Katsuyama T. Histochemistry of the surface mucous gel layer of the human colon. Gut 1997;40:782-9.

[30] Pedron T, Sansonetti P. Commensals, bacterial pathogens and intestinal inflammation: an intriguing menage a trois. Cell Host Microbe 2008;3:344-7.

[31] Porter EM, Bevins CL, Ghosh D, Ganz T. The multifaceted Paneth cell. Cell Mol Life Sci 2002;59:156-70.

[32] Ouellette AJ. Paneth cells and innate mucosal immunity. Current opinion in gastroenterology 2010;26:547-53.

[33] Mestecky J, McGhee JR. Immunoglobulin A (IgA): molecular and cellular interactions involved in IgA biosynthesis and immune response. Advances in immunology 1987;40:153-245.

[34] Nagler-Anderson C. Man the barrier! Strategic defences in the intestinal mucosa. Nature reviews Immunology 2001;1:59-67.

[35] Brandtzaeg P. Induction of secretory immunity and memory at mucosal surfaces. Vaccine 2007;25:5467-84.

[36] Strugnell RA, Wijburg OL. The role of secretory antibodies in infection immunity. Nat Rev Microbiol 2010;8:656-67.

[37] Belzer C, Liu Q, Carroll MC, Bry L. THE ROLE OF SPECIFIC IgG AND COMPLEMENT IN COMBATING A PRIMARY MUCOSAL INFECTION OF THE GUT EPITHELIUM. European journal of microbiology & immunology 2011;1:311-8.

[38] Phalipon A, Cardona A, Kraehenbuhl JP, Edelman L, Sansonetti PJ, Corthesy B. Secretory component: a new role in secretory IgA-mediated immune exclusion in vivo. Immunity 2002;17:107-15.

[39] Rojas R, Apodaca G. Immunoglobulin transport across polarized epithelial cells. Nature reviews Molecular cell biology 2002;3:944-55.

[40] Mantis NJ, Rol N, Corthesy B. Secretory IgA's complex roles in immunity and mucosal homeostasis in the gut. Mucosal immunology 2011;4:603-11.
[41] Ouwehand AC, Derrien M, de Vos W, Tiihonen K, Rautonen N. Prebiotics and other microbial substrates for gut functionality. Current opinion in biotechnology 2005;16:212-7.
[42] Hooper LV, Macpherson AJ. Immune adaptations that maintain homeostasis with the intestinal microbiota. Nature Reviews Immunology 2010;10:159-69.
[43] Johansson ME, Thomsson KA, Hansson GC. Proteomic analyses of the two mucus layers of the colon barrier reveal that their main component, the Muc2 mucin, is strongly bound to the Fcgbp protein. J Proteome Res 2009;8:3549-57.
[44] Rodriguez-Pineiro AM, Post S, Johansson ME, Thomsson KA, Nesvizhskii AI, Hansson GC. Proteomic study of the mucin granulae in an intestinal goblet cell model. J Proteome Res 2012;11:1879-90.
[45] Rodriguez-Pineiro AM, Bergstrom JH, Ermund A, Gustafsson JK, Schuette A, Johansson ME, et al. Gastrointestinal mucus proteome reveals Muc2 and Muc5ac accompanied by a set of core proteins - 2. Studies of mucus in mouse stomach, small intestine, and colon. Am J Physiol Gastrointest Liver Physiol 2013.
[46] Moniaux N, Escande F, Porchet N, Aubert JP, Batra SK. Structural organization and classification of the human mucin genes. Frontiers in bioscience : a journal and virtual library 2001;6:D1192-206.
[47] Porchet N, Buisine MP, Desseyn JL, Moniaux N, Nollet S, Degand P, et al. [MUC genes: a superfamily of genes? Towards a functional classification of human apomucins]. Journal de la Societe de biologie 1999;193:85-99.
[48] Andrianifahanana M, Moniaux N, Batra SK. Regulation of mucin expression: mechanistic aspects and implications for cancer and inflammatory diseases. Biochim Biophys Acta 2006;1765:189-222.
[49] Gendler SJ. MUC1, the renaissance molecule. J Mammary Gland Biol Neoplasia 2001;6:339-53.
[50] Chambers JA, Hollingsworth MA, Trezise AE, Harris A. Developmental expression of mucin genes MUC1 and MUC2. J Cell Sci 1994;107 (Pt 2):413-24.
[51] Allen A, Hutton DA, Pearson JP. The MUC2 gene product: a human intestinal mucin. Int J Biochem Cell Biol 1998;30:797-801.
[52] Pratt WS, Crawley S, Hicks J, Ho J, Nash M, Kim YS, et al. Multiple transcripts of MUC3: evidence for two genes, MUC3A and MUC3B. Biochem Biophys Res Commun 2000;275:916-23.

[53] Carraway KL, Perez A, Idris N, Jepson S, Arango M, Komatsu M, et al. Muc4/sialomucin complex, the intramembrane ErbB2 ligand, in cancer and epithelia: to protect and to survive. Progress in nucleic acid research and molecular biology 2002;71:149-85.
[54] Porchet N, Nguyen VC, Dufosse J, Audie JP, Guyonnet-Duperat V, Gross MS, et al. Molecular cloning and chromosomal localization of a novel human tracheo-bronchial mucin cDNA containing tandemly repeated sequences of 48 base pairs. Biochem Biophys Res Commun 1991;175:414-22.
[55] Desseyn JL, Guyonnet-Duperat V, Porchet N, Aubert JP, Laine A. Human mucin gene MUC5B, the 10.7-kb large central exon encodes various alternate subdomains resulting in a super-repeat. Structural evidence for a 11p15.5 gene family. J Biol Chem 1997;272:3168-78.
[56] Nielsen PA, Bennett EP, Wandall HH, Therkildsen MH, Hannibal J, Clausen H. Identification of a major human high molecular weight salivary mucin (MG1) as tracheobronchial mucin MUC5B. Glycobiology 1997;7:413-9.
[57] Escande F, Aubert JP, Porchet N, Buisine MP. Human mucin gene MUC5AC: organization of its 5'-region and central repetitive region. Biochem J 2001;358:763-72.
[58] Nordman H, Davies JR, Lindell G, de Bolos C, Real F, Carlstedt I. Gastric MUC5AC and MUC6 are large oligomeric mucins that differ in size, glycosylation and tissue distribution. Biochem J 2002;364:191-200.
[59] Toribara NW, Ho SB, Gum E, Gum JR, Jr., Lau P, Kim YS. The carboxyl-terminal sequence of the human secretory mucin, MUC6. Analysis Of the primary amino acid sequence. J Biol Chem 1997;272:16398-403.
[60] Bartman AE, Buisine MP, Aubert JP, Niehans GA, Toribara NW, Kim YS, et al. The MUC6 secretory mucin gene is expressed in a wide variety of epithelial tissues. J Pathol 1998;186:398-405.
[61] Bobek LA, Liu J, Sait SN, Shows TB, Bobek YA, Levine MJ. Structure and chromosomal localization of the human salivary mucin gene, MUC7. Genomics 1996;31:277-82.
[62] Bobek LA, Tsai H, Biesbrock AR, Levine MJ. Molecular cloning, sequence, and specificity of expression of the gene encoding the low molecular weight human salivary mucin (MUC7). J Biol Chem 1993;268:20563-9.
[63] Williams SJ, McGuckin MA, Gotley DC, Eyre HJ, Sutherland GR, Antalis TM. Two novel mucin genes down-regulated in colorectal cancer identified by differential display. Cancer Res 1999;59:4083-9.

[64] Williams SJ, Wreschner DH, Tran M, Eyre HJ, Sutherland GR, McGuckin MA. Muc13, a novel human cell surface mucin expressed by epithelial and hemopoietic cells. J Biol Chem 2001;276:18327-36.
[65] Pallesen LT, Berglund L, Rasmussen LK, Petersen TE, Rasmussen JT. Isolation and characterization of MUC15, a novel cell membrane-associated mucin. Eur J Biochem 2002;269:2755-63.
[66] Yin BW, Dnistrian A, Lloyd KO. Ovarian cancer antigen CA125 is encoded by the MUC16 mucin gene. Int J Cancer 2002;98:737-40.
[67] McLemore MR, Aouizerat B. Introducing the MUC16 gene: implications for prevention and early detection in epithelial ovarian cancer. Biological research for nursing 2005;6:262-7.
[68] Gum JR, Crawley SC, Hicks JW, Szymkowski DE, Kim YS. MUC17, a novel membrane-tethered mucin. Biochem Bioph Res Co 2002;291:466-75.
[69] Moniaux N, Junker WM, Singh AP, Jones AM, Batra SK. Characterization of human mucin MUC17. Complete coding sequence and organization. J Biol Chem 2006;281:23676-85.
[70] Chen Y, Zhao YH, Kalaslavadi TB, Hamati E, Nehrke K, Le AD, et al. Genome-wide search and identification of a novel gel-forming mucin MUC19/Muc19 in glandular tissues. Am J Respir Cell Mol Biol 2004;30:155-65.
[71] Higuchi T, Orita T, Nakanishi S, Katsuya K, Watanabe H, Yamasaki Y, et al. Molecular cloning, genomic structure, and expression analysis of MUC20, a novel mucin protein, up-regulated in injured kidney. J Biol Chem 2004;279:1968-79.
[72] Strous GJ, Dekker J. Mucin-type glycoproteins. Critical reviews in biochemistry and molecular biology 1992;27:57-92.
[73] Gendler SJ, Spicer AP. Epithelial mucin genes. Annu Rev Physiol 1995;57:607-34.
[74] Ju T, Otto VI, Cummings RD. The Tn antigen-structural simplicity and biological complexity. Angew Chem Int Ed Engl 2011;50:1770-91.
[75] Moran AP, Gupta A, Joshi L. Sweet-talk: role of host glycosylation in bacterial pathogenesis of the gastrointestinal tract. Gut 2011;60:1412-25.
[76] Robbe C, Capon C, Maes E, Rousset M, Zweibaum A, Zanetta JP, et al. Evidence of regio-specific glycosylation in human intestinal mucins: presence of an acidic gradient along the intestinal tract. J Biol Chem 2003;278:46337-48.
[77] Robbe C, Capon C, Coddeville B, Michalski JC. Structural diversity and specific distribution of O-glycans in normal human mucins along the intestinal tract. Biochem J 2004;384:307-16.

[78] Karlsson NG, Herrmann A, Karlsson H, Johansson ME, Carlstedt I, Hansson GC. The glycosylation of rat intestinal Muc2 mucin varies between rat strains and the small and large intestine. A study of O-linked oligosaccharides by a mass spectrometric approach. J Biol Chem 1997;272:27025-34.
[79] Jensen PH, Kolarich D, Packer NH. Mucin-type O-glycosylation--putting the pieces together. FEBS J 2010;277:81-94.
[80] Larsson JM, Karlsson H, Sjovall H, Hansson GC. A complex, but uniform O-glycosylation of the human MUC2 mucin from colonic biopsies analyzed by nanoLC/MSn. Glycobiology 2009;19:756-66.
[81] Gill DJ, Clausen H, Bard F. Location, location, location: new insights into O-GalNAc protein glycosylation. Trends in cell biology 2011;21:149-58.
[82] Ismail MN, Stone EL, Panico M, Lee SH, Luu Y, Ramirez K, et al. High-sensitivity O-glycomic analysis of mice deficient in core 2 {beta}1,6-N-acetylglucosaminyltransferases. Glycobiology 2011;21:82-98.
[83] Thomsson KA, Holmen-Larsson JM, Angstrom J, Johansson ME, Xia L, Hansson GC. Detailed O-glycomics of the Muc2 mucin from colon of wild-type, core 1- and core 3-transferase-deficient mice highlights differences compared with human MUC2. Glycobiology 2012;22:1128-39.
[84] Holmen JM, Olson FJ, Karlsson H, Hansson GC. Two glycosylation alterations of mouse intestinal mucins due to infection caused by the parasite Nippostrongylus brasiliensis. Glycoconj J 2002;19:67-75.
[85] Thomsson KA, Hinojosa-Kurtzberg M, Axelsson KA, Domino SE, Lowe JB, Gendler SJ, et al. Intestinal mucins from cystic fibrosis mice show increased fucosylation due to an induced Fucalpha1-2 glycosyltransferase. Biochem J 2002;367:609-16.
[86] Malmberg EK, Noaksson KA, Phillipson M, Johansson ME, Hinojosa-Kurtzberg M, Holm L, et al. Increased levels of mucins in the cystic fibrosis mouse small intestine, and modulator effects of the Muc1 mucin expression. Am J Physiol Gastrointest Liver Physiol 2006;291:G203-10.
[87] Gum JR, Jr., Hicks JW, Toribara NW, Siddiki B, Kim YS. Molecular cloning of human intestinal mucin (MUC2) cDNA. Identification of the amino terminus and overall sequence similarity to prepro-von Willebrand factor. J Biol Chem 1994;269:2440-6.
[88] Van Tassell ML, Miller MJ. Lactobacillus adhesion to mucus. Nutrients 2011;3:613-36.

[89] Lidell ME, Johansson ME, Morgelin M, Asker N, Gum JR, Jr., Kim YS, et al. The recombinant C-terminus of the human MUC2 mucin forms dimers in Chinese-hamster ovary cells and heterodimers with full-length MUC2 in LS 174T cells. Biochem J 2003;372:335-45.
[90] Godl K, Johansson ME, Lidell ME, Morgelin M, Karlsson H, Olson FJ, et al. The N terminus of the MUC2 mucin forms trimers that are held together within a trypsin-resistant core fragment. J Biol Chem 2002;277:47248-56.
[91] Hattrup CL, Gendler SJ. Structure and function of the cell surface (tethered) mucins. Annu Rev Physiol 2008;70:431-57.
[92] Pandey P, Kharbanda S, Kufe D. Association of the DF3/MUC1 breast cancer antigen with Grb2 and the Sos/Ras exchange protein. Cancer Res 1995;55:4000-3.
[93] Li Y, Ren J, Yu W, Li Q, Kuwahara H, Yin L, et al. The epidermal growth factor receptor regulates interaction of the human DF3/MUC1 carcinoma antigen with c-Src and beta-catenin. J Biol Chem 2001;276:35239-42.
[94] Li Q, Ren J, Kufe D. Interaction of human MUC1 and beta-catenin is regulated by Lck and ZAP-70 in activated Jurkat T cells. Biochem Biophys Res Commun 2004;315:471-6.
[95] Kufe DW. Targeting the human MUC1 oncoprotein: a tale of two proteins. Cancer Biol Ther 2008;7:81-4.
[96] Schroeder JA, Thompson MC, Gardner MM, Gendler SJ. Transgenic MUC1 interacts with epidermal growth factor receptor and correlates with mitogen-activated protein kinase activation in the mouse mammary gland. J Biol Chem 2001;276:13057-64.
[97] Ren J, Raina D, Chen W, Li G, Huang L, Kufe D. MUC1 oncoprotein functions in activation of fibroblast growth factor receptor signaling. Mol Cancer Res 2006;4:873-83.
[98] Singh PK, Wen Y, Swanson BJ, Shanmugam K, Kazlauskas A, Cerny RL, et al. Platelet-derived growth factor receptor beta-mediated phosphorylation of MUC1 enhances invasiveness in pancreatic adenocarcinoma cells. Cancer Res 2007;67:5201-10.
[99] Huang L, Ren J, Chen D, Li Y, Kharbanda S, Kufe D. MUC1 cytoplasmic domain coactivates Wnt target gene transcription and confers transformation. Cancer Biol Ther 2003;2:702-6.
[100] Kawano T, Ito M, Raina D, Wu Z, Rosenblatt J, Avigan D, et al. MUC1 oncoprotein regulates Bcr-Abl stability and pathogenesis in chronic myelogenous leukemia cells. Cancer Res 2007;67:11576-84.

[101] Ren J, Agata N, Chen D, Li Y, Yu WH, Huang L, et al. Human MUC1 carcinoma-associated protein confers resistance to genotoxic anticancer agents. Cancer Cell 2004;5:163-75.
[102] Regimbald LH, Pilarski LM, Longenecker BM, Reddish MA, Zimmermann G, Hugh JC. The breast mucin MUC1 as a novel adhesion ligand for endothelial intercellular adhesion molecule 1 in breast cancer. Cancer Research 1996;56:4244-9.
[103] Nath D, Hartnell A, Happerfield L, Miles DW, Burchell J, Taylor-Papadimitriou J, et al. Macrophage-tumour cell interactions: identification of MUC1 on breast cancer cells as a potential counter-receptor for the macrophage-restricted receptor, sialoadhesin. Immunology 1999;98:213-9.
[104] Gubbels JA, Belisle J, Onda M, Rancourt C, Migneault M, Ho M, et al. Mesothelin-MUC16 binding is a high affinity, N-glycan dependent interaction that facilitates peritoneal metastasis of ovarian tumors. Mol Cancer 2006;5:50.
[105] Ciborowski P, Finn OJ. Non-glycosylated tandem repeats of MUC1 facilitate attachment of breast tumor cells to normal human lung tissue and immobilized extracellular matrix proteins (ECM) in vitro: potential role in metastasis. Clin Exp Metastasis 2002;19:339-45.
[106] Komatsu M, Carraway CA, Fregien NL, Carraway KL. Reversible disruption of cell-matrix and cell-cell interactions by overexpression of sialomucin complex. J Biol Chem 1997;272:33245-54.
[107] Wreschner DH, McGuckin MA, Williams SJ, Baruch A, Yoeli M, Ziv R, et al. Generation of ligand-receptor alliances by "SEA" module-mediated cleavage of membrane-associated mucin proteins. Protein Sci 2002;11:698-706.
[108] Macao B, Johansson DG, Hansson GC, Hard T. Autoproteolysis coupled to protein folding in the SEA domain of the membrane-bound MUC1 mucin. Nat Struct Mol Biol 2006;13:71-6.
[109] Thathiah A, Blobel CP, Carson DD. Tumor necrosis factor-alpha converting enzyme/ADAM 17 mediates MUC1 shedding. J Biol Chem 2003;278:3386-94.
[110] Thathiah A, Carson DD. MT1-MMP mediates MUC1 shedding independent of TACE/ADAM17. Biochem J 2004;382:363-73.
[111] Sheng YH, Hasnain SZ, Florin TH, McGuckin MA. Mucins in inflammatory bowel diseases and colorectal cancer. J Gastroenterol Hepatol 2012;27:28-38.
[112] Kim YS, Ho SB. Intestinal goblet cells and mucins in health and disease: recent insights and progress. Curr Gastroenterol Rep 2010;12:319-30.

[113] Okamoto R, Watanabe M. Cellular and molecular mechanisms of the epithelial repair in IBD. Dig Dis Sci 2005;50 Suppl 1:S34-8.
[114] Geier MS, Butler RN, Howarth GS. Inflammatory bowel disease: current insights into pathogenesis and new therapeutic options; probiotics, prebiotics and synbiotics. Int J Food Microbiol 2007;115:1-11.
[115] Loftus EV, Jr. Clinical epidemiology of inflammatory bowel disease: Incidence, prevalence, and environmental influences. Gastroenterology 2004;126:1504-17.
[116] Balding J, Livingstone WJ, Conroy J, Mynett-Johnson L, Weir DG, Mahmud N, et al. Inflammatory bowel disease: the role of inflammatory cytokine gene polymorphisms. Mediators Inflamm 2004;13:181-7.
[117] Brown SJ, Mayer L. The immune response in inflammatory bowel disease. Am J Gastroenterol 2007;102:2058-69.
[118] Jostins L, Ripke S, Weersma RK, Duerr RH, McGovern DP, Hui KY, et al. Host-microbe interactions have shaped the genetic architecture of inflammatory bowel disease. Nature 2012;491:119-24.
[119] Rivas MA, Beaudoin M, Gardet A, Stevens C, Sharma Y, Zhang CK, et al. Deep resequencing of GWAS loci identifies independent rare variants associated with inflammatory bowel disease. Nat Genet 2011;43:1066-73.
[120] Riordan JR, Rommens JM, Kerem B, Alon N, Rozmahel R, Grzelczak Z, et al. Identification of the cystic fibrosis gene: cloning and characterization of complementary DNA. Science 1989;245:1066-73.
[121] Hauber HP, Foley SC, Hamid Q. Mucin overproduction in chronic inflammatory lung disease. Canadian respiratory journal : journal of the Canadian Thoracic Society 2006;13:327-35.
[122] Strugala V, Dettmar PW, Pearson JP. Thickness and continuity of the adherent colonic mucus barrier in active and quiescent ulcerative colitis and Crohn's disease. International journal of clinical practice 2008;62:762-9.
[123] Ho SB, Ewing SL, Montgomery CK, Kim YS. Altered mucin core peptide immunoreactivity in the colon polyp-carcinoma sequence. Oncol Res 1996;8:53-61.
[124] Buisine MP, Desreumaux P, Leteurtre E, Copin MC, Colombel JF, Porchet N, et al. Mucin gene expression in intestinal epithelial cells in Crohn's disease. Gut 2001;49:544-51.
[125] Van der Sluis M, De Koning BA, De Bruijn AC, Velcich A, Meijerink JP, Van Goudoever JB, et al. Muc2-deficient mice spontaneously develop colitis, indicating that MUC2 is critical for colonic protection. Gastroenterology 2006;131:117-29.

[126] Yang K, Popova NV, Yang WC, Lozonschi I, Tadesse S, Kent S, et al. Interaction of Muc2 and Apc on Wnt signaling and in intestinal tumorigenesis: potential role of chronic inflammation. Cancer Res 2008;68:7313-22.
[127] Johansson ME, Gustafsson JK, Sjoberg KE, Petersson J, Holm L, Sjovall H, et al. Bacteria penetrate the inner mucus layer before inflammation in the dextran sulfate colitis model. PLoS One 2010;5:e12238.
[128] Satsangi J, Jewell DP, Bell JI. The genetics of inflammatory bowel disease. Gut 1997;40:572-4.
[129] Okudaira K, Kakar S, Cun L, Choi E, Wu Decamillis R, Miura S, et al. MUC2 gene promoter methylation in mucinous and non-mucinous colorectal cancer tissues. Int J Oncol 2010;36:765-75.
[130] Campbell BJ, Yu LG, Rhodes JM. Altered glycosylation in inflammatory bowel disease: a possible role in cancer development. Glycoconj J 2001;18:851-8.
[131] Phillipson M, Johansson ME, Henriksnas J, Petersson J, Gendler SJ, Sandler S, et al. The gastric mucus layers: constituents and regulation of accumulation. Am J Physiol Gastrointest Liver Physiol 2008;295:G806-12.
[132] Sheng YH, Lourie R, Linden SK, Jeffery PL, Roche D, Tran TV, et al. The MUC13 cell-surface mucin protects against intestinal inflammation by inhibiting epithelial cell apoptosis. Gut 2011;60:1661-70.
[133] Senapati S, Ho SB, Sharma P, Das S, Chakraborty S, Kaur S, et al. Expression of intestinal MUC17 membrane-bound mucin in inflammatory and neoplastic diseases of the colon. J Clin Pathol 2010;63:702-7.
[134] McAuley JL, Linden SK, Png CW, King RM, Pennington HL, Gendler SJ, et al. MUC1 cell surface mucin is a critical element of the mucosal barrier to infection. J Clin Invest 2007;117:2313-24.
[135] McGuckin MA, Every AL, Skene CD, Linden SK, Chionh YT, Swierczak A, et al. Muc1 mucin limits both Helicobacter pylori colonization of the murine gastric mucosa and associated gastritis. Gastroenterology 2007;133:1210-8.
[136] Linden SK, Sheng YH, Every AL, Miles KM, Skoog EC, Florin TH, et al. MUC1 Limits Helicobacter pylori Infection both by Steric Hindrance and by Acting as a Releasable Decoy. PLoS Pathog 2009;5:e1000617.
[137] Bergstrom KS, Guttman JA, Rumi M, Ma C, Bouzari S, Khan MA, et al. Modulation of intestinal goblet cell function during infection by an attaching and effacing bacterial pathogen. Infect Immun 2008;76:796-811.

[138] Bergstrom KS, Kissoon-Singh V, Gibson DL, Ma C, Montero M, Sham HP, et al. Muc2 protects against lethal infectious colitis by disassociating pathogenic and commensal bacteria from the colonic mucosa. PLoS Pathog 2010;6:e1000902.
[139] Corfield AP, Myerscough N, Longman R, Sylvester P, Arul S, Pignatelli M. Mucins and mucosal protection in the gastrointestinal tract: new prospects for mucins in the pathology of gastrointestinal disease. Gut 2000;47:589-94.
[140] Fu J, Wei B, Wen T, Johansson ME, Liu X, Bradford E, et al. Loss of intestinal core 1-derived O-glycans causes spontaneous colitis in mice. J Clin Invest 2011;121:1657-66.
[141] Johansson ME, Gustafsson JK, Holmen-Larsson J, Jabbar KS, Xia L, Xu H, et al. Bacteria penetrate the normally impenetrable inner colon mucus layer in both murine colitis models and patients with ulcerative colitis. Gut 2013.
[142] Stone EL, Ismail MN, Lee SH, Luu Y, Ramirez K, Haslam SM, et al. Glycosyltransferase function in core 2-type protein O glycosylation. Mol Cell Biol 2009;29:3770-82.
[143] An G, Wei B, Xia B, McDaniel JM, Ju T, Cummings RD, et al. Increased susceptibility to colitis and colorectal tumors in mice lacking core 3-derived O-glycans. J Exp Med 2007;204:1417-29.
[144] Ambort D, Johansson ME, Gustafsson JK, Nilsson HE, Ermund A, Johansson BR, et al. Calcium and pH-dependent packing and release of the gel-forming MUC2 mucin. Proc Natl Acad Sci U S A 2012;109:5645-50.
[145] Choi JY, Muallem D, Kiselyov K, Lee MG, Thomas PJ, Muallem S. Aberrant CFTR-dependent HCO3- transport in mutations associated with cystic fibrosis. Nature 2001;410:94-7.
[146] Quinton PM. Cystic fibrosis: impaired bicarbonate secretion and mucoviscidosis. Lancet 2008;372:415-7.
[147] Garcia MA, Yang N, Quinton PM. Normal mouse intestinal mucus release requires cystic fibrosis transmembrane regulator-dependent bicarbonate secretion. J Clin Invest 2009;119:2613-22.
[148] Phillipson M, Atuma C, Henriksnas J, Holm L. The importance of mucus layers and bicarbonate transport in preservation of gastric juxtamucosal pH. Am J Physiol Gastrointest Liver Physiol 2002;282:G211-9.
[149] Petersson J, Phillipson M, Jansson EA, Patzak A, Lundberg JO, Holm L. Dietary nitrate increases gastric mucosal blood flow and mucosal defense. Am J Physiol Gastrointest Liver Physiol 2007;292:G718-24.

[150] Hawkey CJ. Nonsteroidal anti-inflammatory drug gastropathy. Gastroenterology 2000;119:521-35.
[151] Holm L, Phillipson M, Perry MA. NO-flurbiprofen maintains duodenal blood flow, enhances mucus secretion contributing to lower mucosal injury. Am J Physiol Gastrointest Liver Physiol 2002;283:G1090-7.
[152] Allen A, Flemstrom G, Garner A, Kivilaakso E. Gastroduodenal mucosal protection. Physiological reviews 1993;73:823-57.
[153] Brown JF, Hanson PJ, Whittle BJ. Nitric oxide donors increase mucus gel thickness in rat stomach. Eur J Pharmacol 1992;223:103-4.
[154] Hasnain SZ, Thornton DJ, Grencis RK. Changes in the mucosal barrier during acute and chronic Trichuris muris infection. Parasite immunology 2011;33:45-55.
[155] Hasnain SZ, Gallagher AL, Grencis RK, Thornton DJ. A new role for mucins in immunity: insights from gastrointestinal nematode infection. Int J Biochem Cell Biol 2013;45:364-74.
[156] Lundberg JO, Weitzberg E, Gladwin MT. The nitrate-nitrite-nitric oxide pathway in physiology and therapeutics. Nat Rev Drug Discov 2008;7:156-67.
[157] Lundberg JO, Weitzberg E, Cole JA, Benjamin N. Nitrate, bacteria and human health. Nat Rev Microbiol 2004;2:593-602.
[158] Brown JF, Keates AC, Hanson PJ, Whittle BJ. Nitric oxide generators and cGMP stimulate mucus secretion by rat gastric mucosal cells. Am J Physiol 1993;265:G418-22.
[159] Price KJ, Hanson PJ, Whittle BJ. Localization of constitutive isoforms of nitric oxide synthase in the gastric glandular mucosa of the rat. Cell Tissue Res 1996;285:157-63.
[160] Bouma G, Strober W. The immunological and genetic basis of inflammatory bowel disease. Nature reviews Immunology 2003;3:521-33.
[161] Fiocchi C. Inflammatory bowel disease: etiology and pathogenesis. Gastroenterology 1998;115:182-205.
[162] Strober W, Fuss IJ, Blumberg RS. The immunology of mucosal models of inflammation. Annual review of immunology 2002;20:495-549.
[163] van der Sluis M, Bouma J, Vincent A, Velcich A, Carraway KL, Buller HA, et al. Combined defects in epithelial and immunoregulatory factors exacerbate the pathogenesis of inflammation: mucin 2-interleukin 10-deficient mice. Lab Invest 2008;88:634-42.

[164] Hasnain SZ, Lourie R, Das I, Chen AC, McGuckin MA. The interplay between endoplasmic reticulum stress and inflammation. Immunology and cell biology 2012;90:260-70.
[165] McGuckin MA, Eri RD, Das I, Lourie R, Florin TH. ER stress and the unfolded protein response in intestinal inflammation. Am J Physiol Gastrointest Liver Physiol 2010;298:G820-32.
[166] Brandl K, Rutschmann S, Li X, Du X, Xiao N, Schnabl B, et al. Enhanced sensitivity to DSS colitis caused by a hypomorphic Mbtps1 mutation disrupting the ATF6-driven unfolded protein response. Proc Natl Acad Sci U S A 2009;106:3300-5.
[167] Heazlewood CK, Cook MC, Eri R, Price GR, Tauro SB, Taupin D, et al. Aberrant mucin assembly in mice causes endoplasmic reticulum stress and spontaneous inflammation resembling ulcerative colitis. PLoS Med 2008;5:e54.
[168] Kaser A, Lee AH, Franke A, Glickman JN, Zeissig S, Tilg H, et al. XBP1 links ER stress to intestinal inflammation and confers genetic risk for human inflammatory bowel disease. Cell 2008;134:743-56.
[169] Zhao F, Edwards R, Dizon D, Afrasiabi K, Mastroianni JR, Geyfman M, et al. Disruption of Paneth and goblet cell homeostasis and increased endoplasmic reticulum stress in Agr2-/- mice. Dev Biol 2010;338:270-9.
[170] Bertolotti A, Wang X, Novoa I, Jungreis R, Schlessinger K, Cho JH, et al. Increased sensitivity to dextran sodium sulfate colitis in IRE1beta-deficient mice. J Clin Invest 2001;107:585-93.
[171] Wei X, Yang Z, Rey FE, Ridaura VK, Davidson NO, Gordon JI, et al. Fatty acid synthase modulates intestinal barrier function through palmitoylation of mucin 2. Cell Host Microbe 2012;11:140-52.
[172] Vincent A, Perrais M, Desseyn JL, Aubert JP, Pigny P, Van Seuningen I. Epigenetic regulation (DNA methylation, histone modifications) of the 11p15 mucin genes (MUC2, MUC5AC, MUC5B, MUC6) in epithelial cancer cells. Oncogene 2007;26:6566-76.
[173] Yamada N, Kitamoto S, Yokoyama S, Hamada T, Goto M, Tsutsumida H, et al. Epigenetic regulation of mucin genes in human cancers. Clinical epigenetics 2011;2:85-96.
[174] Yamada N, Nishida Y, Tsutsumida H, Hamada T, Goto M, Higashi M, et al. MUC1 expression is regulated by DNA methylation and histone H3 lysine 9 modification in cancer cells. Cancer Res 2008;68:2708-16.

[175] Yamada N, Nishida Y, Yokoyama S, Tsutsumida H, Houjou I, Kitamoto S, et al. Expression of MUC5AC, an early marker of pancreatobiliary cancer, is regulated by DNA methylation in the distal promoter region in cancer cells. Journal of hepato-biliary-pancreatic sciences 2010;17:844-54.
[176] Molkentin JD. The zinc finger-containing transcription factors GATA-4,-5, and-6 - Ubiquitously expressed regulators of tissue-specific gene expression. Journal of Biological Chemistry 2000;275:38949-52.
[177] Montgomery RK, Mulberg AE, Grand RJ. Development of the human gastrointestinal tract: Twenty years of progress. Gastroenterology 1999;116:702-31.
[178] Richmond CA, Breault DT. Regulation of Gene Expression in the Intestinal Epithelium. Prog Mol Biol Transl 2010;96:207-29.
[179] Traber PG, Silberg DG. Intestine-specific gene transcription. Annual Review of Physiology 1996;58:275-97.
[180] Duncan SA, Manova K, Chen WS, Hoodless P, Weinstein DC, Bachvarova RF, et al. Expression of transcription factor HNF-4 in the extraembryonic endoderm, gut, and nephrogenic tissue of the developing mouse embryo: HNF-4 is a marker for primary endoderm in the implanting blastocyst. Proc Natl Acad Sci U S A 1994;91:7598-602.
[181] Morrisey EE, Ip HS, Lu MM, Parmacek MS. GATA-6: a zinc finger transcription factor that is expressed in multiple cell lineages derived from lateral mesoderm. Dev Biol 1996;177:309-22.
[182] Morrisey EE, Ip HS, Tang Z, Lu MM, Parmacek MS. GATA-5: a transcriptional activator expressed in a novel temporally and spatially-restricted pattern during embryonic development. Dev Biol 1997;183:21-36.
[183] Buisine MP, Devisme L, Savidge TC, Gespach C, Gosselin B, Porchet N, et al. Mucin gene expression in human embryonic and fetal intestine. Gut 1998;43:519-24.
[184] Aslam F, Palumbo L, Augenlicht LH, Velcich A. The Sp family of transcription factors in the regulation of the human and mouse MUC2 gene promoters. Cancer Res 2001;61:570-6.
[185] van der Sluis M, Melis MH, Jonckheere N, Ducourouble MP, Buller HA, Renes I, et al. The murine Muc2 mucin gene is transcriptionally regulated by the zinc-finger GATA-4 transcription factor in intestinal cells. Biochem Biophys Res Commun 2004;325:952-60.
[186] Wang D, Dubois RN, Richmond A. The role of chemokines in intestinal inflammation and cancer. Curr Opin Pharmacol 2009;9:688-96.

[187] Macdonald TT, Monteleone G. Immunity, inflammation, and allergy in the gut. Science 2005;307:1920-5.
[188] Moreau MC, Corthier G. Effect of the gastrointestinal microflora on induction and maintenance of oral tolerance to ovalbumin in C3H/HeJ mice. Infect Immun 1988;56:2766-8.
[189] Lefrancois L, Goodman T. In vivo modulation of cytolytic activity and Thy-1 expression in TCR-gamma delta+ intraepithelial lymphocytes. Science 1989;243:1716-8.
[190] Neutra MR, Mantis NJ, Kraehenbuhl JP. Collaboration of epithelial cells with organized mucosal lymphoid tissues. Nat Immunol 2001;2:1004-9.
[191] Rescigno M, Urbano M, Valzasina B, Francolini M, Rotta G, Bonasio R, et al. Dendritic cells express tight junction proteins and penetrate gut epithelial monolayers to sample bacteria. Nat Immunol 2001;2:361-7.
[192] Niess JH, Brand S, Gu X, Landsman L, Jung S, McCormick BA, et al. CX3CR1-mediated dendritic cell access to the intestinal lumen and bacterial clearance. Science 2005;307:254-8.
[193] Miron N, Cristea V. Enterocytes: active cells in tolerance to food and microbial antigens in the gut. Clinical and Experimental Immunology 2012;167:405-12.
[194] Faria AM, Weiner HL. Oral tolerance. Immunological reviews 2005;206:232-59.
[195] Iwata M, Hirakiyama A, Eshima Y, Kagechika H, Kato C, Song SY. Retinoic acid imprints gut-homing specificity on T cells. Immunity 2004;21:527-38.
[196] Mora JR, Iwata M, Eksteen B, Song SY, Junt T, Senman B, et al. Generation of gut-homing IgA-secreting B cells by intestinal dendritic cells. Science 2006;314:1157-60.
[197] McConnell BB, Yang VW. The Role of Inflammation in the Pathogenesis of Colorectal Cancer. Curr Colorectal Cancer Rep 2009;5:69-74.
[198] Zimmerman NP, Vongsa RA, Wendt MK, Dwinell MB. Chemokines and chemokine receptors in mucosal homeostasis at the intestinal epithelial barrier in inflammatory bowel disease. Inflamm Bowel Dis 2008;14:1000-11.
[199] Deban L, Correale C, Vetrano S, Malesci A, Danese S. Multiple pathogenic roles of microvasculature in inflammatory bowel disease: a Jack of all trades. Am J Pathol 2008;172:1457-66.
[200] Furrie E, Macfarlane S, Thomson G, Macfarlane GT. Toll-like receptors-2, -3 and -4 expression patterns on human colon and their regulation by mucosal-associated bacteria. Immunology 2005;115:565-74.

[201] Rock FL, Hardiman G, Timans JC, Kastelein RA, Bazan JF. A family of human receptors structurally related to Drosophila Toll. Proc Natl Acad Sci U S A 1998;95:588-93.
[202] Abreu MT. Toll-like receptor signalling in the intestinal epithelium: how bacterial recognition shapes intestinal function. Nature reviews Immunology 2010;10:131-44.
[203] Abreu MT, Fukata M, Arditi M. TLR signaling in the gut in health and disease. J Immunol 2005;174:4453-60.
[204] Akira S, Takeda K, Kaisho T. Toll-like receptors: critical proteins linking innate and acquired immunity. Nat Immunol 2001;2:675-80.
[205] Karin M, Yamamoto Y, Wang QM. The IKK NF-kappa B system: a treasure trove for drug development. Nat Rev Drug Discov 2004;3:17-26.
[206] O'Garra A, Arai N. The molecular basis of T helper 1 and T helper 2 cell differentiation. Trends in cell biology 2000;10:542-50.
[207] Mayack SR, Berg LJ. Cutting edge: an alternative pathway of CD4+ T cell differentiation is induced following activation in the absence of gamma-chain-dependent cytokine signals. J Immunol 2006;176:2059-63.
[208] Nurieva R, Yang XO, Martinez G, Zhang Y, Panopoulos AD, Ma L, et al. Essential autocrine regulation by IL-21 in the generation of inflammatory T cells. Nature 2007;448:480-3.
[209] Zhou L, Ivanov, II, Spolski R, Min R, Shenderov K, Egawa T, et al. IL-6 programs T(H)-17 cell differentiation by promoting sequential engagement of the IL-21 and IL-23 pathways. Nat Immunol 2007;8:967-74.
[210] Medzhitov R, Shevach EM, Trinchieri G, Mellor AL, Munn DH, Gordon S, et al. Highlights of 10 years of immunology in Nature Reviews Immunology. Nature reviews Immunology 2011;11:693-702.
[211] McKay DM, Baird AW. Cytokine regulation of epithelial permeability and ion transport. Gut 1999;44:283-9.
[212] Enss ML, Cornberg M, Wagner S, Gebert A, Henrichs M, Eisenblatter R, et al. Proinflammatory cytokines trigger MUC gene expression and mucin release in the intestinal cancer cell line LS180. Inflamm Res 2000;49:162-9.
[213] Dabbagh K, Takeyama K, Lee HM, Ueki IF, Lausier JA, Nadel JA. IL-4 induces mucin gene expression and goblet cell metaplasia in vitro and in vivo. J Immunol 1999;162:6233-7.

[214] Cohn L, Homer RJ, MacLeod H, Mohrs M, Brombacher F, Bottomly K. Th2-induced airway mucus production is dependent on IL-4Ralpha, but not on eosinophils. J Immunol 1999;162:6178-83.
[215] Longphre M, Li D, Gallup M, Drori E, Ordonez CL, Redman T, et al. Allergen-induced IL-9 directly stimulates mucin transcription in respiratory epithelial cells. J Clin Invest 1999;104:1375-82.
[216] Temann UA, Prasad B, Gallup MW, Basbaum C, Ho SB, Flavell RA, et al. A novel role for murine IL-4 in vivo: induction of MUC5AC gene expression and mucin hypersecretion. Am J Respir Cell Mol Biol 1997;16:471-8.
[217] Plaisancie P, Barcelo A, Moro F, Claustre J, Chayvialle JA, Cuber JC. Effects of neurotransmitters, gut hormones, and inflammatory mediators on mucus discharge in rat colon. Am J Physiol 1998;275:G1073-84.
[218] Willis RA, Nussler AK, Fries KM, Geller DA, Phipps RP. Induction of nitric oxide synthase in subsets of murine pulmonary fibroblasts: effect on fibroblast interleukin-6 production. Clinical immunology and immunopathology 1994;71:231-9.
[219] Tepperman BL, Brown JF, Whittle BJ. Nitric oxide synthase induction and intestinal epithelial cell viability in rats. Am J Physiol 1993;265:G214-8.
[220] Schulzke JD, Ploeger S, Amasheh M, Fromm A, Zeissig S, Troeger H, et al. Epithelial tight junctions in intestinal inflammation. Ann N Y Acad Sci 2009;1165:294-300.
[221] Lepage AC, Buzoni-Gatel D, Bout DT, Kasper LH. Gut-derived intraepithelial lymphocytes induce long term immunity against Toxoplasma gondii. J Immunol 1998;161:4902-8.
[222] Muller S, Buhler-Jungo M, Mueller C. Intestinal intraepithelial lymphocytes exert potent protective cytotoxic activity during an acute virus infection. J Immunol 2000;164:1986-94.
[223] Hayday A, Theodoridis E, Ramsburg E, Shires J. Intraepithelial lymphocytes: exploring the Third Way in immunology. Nat Immunol 2001;2:997-1003.
[224] Bonneville M, Janeway CA, Jr., Ito K, Haser W, Ishida I, Nakanishi N, et al. Intestinal intraepithelial lymphocytes are a distinct set of gamma delta T cells. Nature 1988;336:479-81.
[225] Ernst PB, Befus AD, Bienenstock J. Leukocytes in the Intestinal Epithelium - an Unusual Immunological Compartment. Immunol Today 1985;6:50-5.

[226] Beagley KW, Fujihashi K, Lagoo AS, Lagoo-Deenadaylan S, Black CA, Murray AM, et al. Differences in intraepithelial lymphocyte T cell subsets isolated from murine small versus large intestine. J Immunol 1995;154:5611-9.
[227] Suzuki H, Jeong KI, Okutani T, Doi K. Regional variations in the distribution of small intestinal intraepithelial lymphocytes in three inbred strains of mice. J Vet Med Sci 2000;62:881-7.
[228] Bandeira A, Mota-Santos T, Itohara S, Degermann S, Heusser C, Tonegawa S, et al. Localization of gamma/delta T cells to the intestinal epithelium is independent of normal microbial colonization. J Exp Med 1990;172:239-44.
[229] Ishimoto Y, Tomiyama-Miyaji C, Watanabe H, Yokoyama H, Ebe K, Tsubata S, et al. Age-dependent variation in the proportion and number of intestinal lymphocyte subsets, especially natural killer T cells, double-positive CD4+ CD8+ cells and B220+ T cells, in mice. Immunology 2004;113:371-7.
[230] Nagura T, Hachimura S, Kaminogawa S, Aritsuka T, Itoh K. Characteristic intestinal microflora of specific pathogen-free mice bred in two different colonies and their influence on postnatal murine immunocyte profiles. Experimental animals / Japanese Association for Laboratory Animal Science 2005;54:143-8.
[231] Guy-Grand D, Cerf-Bensussan N, Malissen B, Malassis-Seris M, Briottet C, Vassalli P. Two gut intraepithelial CD8+ lymphocyte populations with different T cell receptors: a role for the gut epithelium in T cell differentiation. J Exp Med 1991;173:471-81.
[232] Cheroutre H, Lambolez F, Mucida D. The light and dark sides of intestinal intraepithelial lymphocytes. Nature reviews Immunology 2011;11:445-56.
[233] Poussier P, Ning T, Banerjee D, Julius M. A unique subset of self-specific intraintestinal T cells maintains gut integrity. J Exp Med 2002;195:1491-7.
[234] Kuhl AA, Pawlowski NN, Grollich K, Loddenkemper C, Zeitz M, Hoffmann JC. Aggravation of intestinal inflammation by depletion/deficiency of gammadelta T cells in different types of IBD animal models. Journal of leukocyte biology 2007;81:168-75.
[235] Mucida D, Cheroutre H. The many face-lifts of CD4 T helper cells. Advances in immunology 2010;107:139-52.
[236] Ismail AS, Behrendt CL, Hooper LV. Reciprocal interactions between commensal bacteria and gamma delta intraepithelial lymphocytes during mucosal injury. J Immunol 2009;182:3047-54.

[237] Bhagat G, Naiyer AJ, Shah JG, Harper J, Jabri B, Wang TC, et al. Small intestinal CD8+TCRgammadelta+NKG2A+ intraepithelial lymphocytes have attributes of regulatory cells in patients with celiac disease. J Clin Invest 2008;118:281-93.
[238] Kanazawa H, Ishiguro Y, Munakata A, Morita T. Multiple accumulation of Vdelta2+ gammadelta T-cell clonotypes in intestinal mucosa from patients with Crohn's disease. Dig Dis Sci 2001;46:410-6.
[239] Yeung MM, Melgar S, Baranov V, Oberg A, Danielsson A, Hammarstrom S, et al. Characterisation of mucosal lymphoid aggregates in ulcerative colitis: immune cell phenotype and TcR-gammadelta expression. Gut 2000;47:215-27.
[240] Kawaguchi-Miyashita M, Shimada S, Kurosu H, Kato-Nagaoka N, Matsuoka Y, Ohwaki M, et al. An accessory role of TCRgammadelta (+) cells in the exacerbation of inflammatory bowel disease in TCRalpha mutant mice. Eur J Immunol 2001;31:980-8.
[241] Mizoguchi A, Mizoguchi E, de Jong YP, Takedatsu H, Preffer FI, Terhorst C, et al. Role of the CD5 molecule on TCR gammadelta T cell-mediated immune functions: development of germinal centers and chronic intestinal inflammation. Int Immunol 2003;15:97-108.
[242] Saito H, Kranz DM, Takagaki Y, Hayday AC, Eisen HN, Tonegawa S. A third rearranged and expressed gene in a clone of cytotoxic T lymphocytes. Nature 1984;312:36-40.
[243] Goodman T, Lefrancois L. Expression of the gamma-delta T-cell receptor on intestinal CD8+ intraepithelial lymphocytes. Nature 1988;333:855-8.
[244] Born WK, Reardon CL, O'Brien RL. The function of gammadelta T cells in innate immunity. Current opinion in immunology 2006;18:31-8.
[245] Sciammas R, Johnson RM, Sperling AI, Brady W, Linsley PS, Spear PG, et al. Unique antigen recognition by a herpesvirus-specific TCR-gamma delta cell. J Immunol 1994;152:5392-7.
[246] Morita CT, Beckman EM, Bukowski JF, Tanaka Y, Band H, Bloom BR, et al. Direct presentation of nonpeptide prenyl pyrophosphate antigens to human gamma delta T cells. Immunity 1995;3:495-507.
[247] Lefrancois L, Olson S. A novel pathway of thymus-directed T lymphocyte maturation. J Immunol 1994;153:987-95.
[248] Bandeira A, Itohara S, Bonneville M, Burlen-Defranoux O, Mota-Santos T, Coutinho A, et al. Extrathymic origin of intestinal intraepithelial lymphocytes bearing T-cell antigen receptor gamma delta. Proc Natl Acad Sci U S A 1991;88:43-7.

[249] Guy-Grand D, Azogui O, Celli S, Darche S, Nussenzweig MC, Kourilsky P, et al. Extrathymic T cell lymphopoiesis: ontogeny and contribution to gut intraepithelial lymphocytes in athymic and euthymic mice. J Exp Med 2003;197:333-41.
[250] Maki K, Sunaga S, Komagata Y, Kodaira Y, Mabuchi A, Karasuyama H, et al. Interleukin 7 receptor-deficient mice lack gammadelta T cells. Proc Natl Acad Sci U S A 1996;93:7172-7.
[251] Laky K, Lefrancois L, von Freeden-Jeffry U, Murray R, Puddington L. The role of IL-7 in thymic and extrathymic development of TCR gamma delta cells. J Immunol 1998;161:707-13.
[252] Laky K, Lefrancois L, Lingenheld EG, Ishikawa H, Lewis JM, Olson S, et al. Enterocyte expression of interleukin 7 induces development of gammadelta T cells and Peyer's patches. J Exp Med 2000;191:1569-80.
[253] Smith PM, Garrett WS. The gut microbiota and mucosal T cells. Frontiers in microbiology 2011;2:111.
[254] Ishikawa H, Naito T, Iwanaga T, Takahashi-Iwanaga H, Suematsu M, Hibi T, et al. Curriculum vitae of intestinal intraepithelial T cells: their developmental and behavioral characteristics. Immunological reviews 2007;215:154-65.
[255] Komano H, Fujiura Y, Kawaguchi M, Matsumoto S, Hashimoto Y, Obana S, et al. Homeostatic regulation of intestinal epithelia by intraepithelial gamma delta T cells. Proc Natl Acad Sci U S A 1995;92:6147-51.
[256] Chen Y, Chou K, Fuchs E, Havran WL, Boismenu R. Protection of the intestinal mucosa by intraepithelial gamma delta T cells. Proc Natl Acad Sci U S A 2002;99:14338-43.
[257] Jameson J, Ugarte K, Chen N, Yachi P, Fuchs E, Boismenu R, et al. A role for skin gammadelta T cells in wound repair. Science 2002;296:747-9.
[258] Yang H, Antony PA, Wildhaber BE, Teitelbaum DH. Intestinal intraepithelial lymphocyte gamma delta-T cell-derived keratinocyte growth factor modulates epithelial growth in the mouse. J Immunol 2004;172:4151-8.
[259] Fernandez-Estivariz C, Gu LH, Gu L, Jonas CR, Wallace TM, Pascal RR, et al. Trefoil peptide expression and goblet cell number in rat intestine: effects of KGF and fasting-refeeding. Am J Physiol-Reg I 2003;284:R564-R73.
[260] Boismenu R, Havran WL. Modulation of epithelial cell growth by intraepithelial gamma delta T cells. Science 1994;266:1253-5.

[261] Dalton JE, Cruickshank SM, Egan CE, Mears R, Newton DJ, Andrew EM, et al. Intraepithelial gammadelta+ lymphocytes maintain the integrity of intestinal epithelial tight junctions in response to infection. Gastroenterology 2006;131:818-29.
[262] Ismail AS, Severson KM, Vaishnava S, Behrendt CL, Yu X, Benjamin JL, et al. Gammadelta intraepithelial lymphocytes are essential mediators of host-microbial homeostasis at the intestinal mucosal surface. Proc Natl Acad Sci U S A 2011;108:8743-8.
[263] Vaishnava S, Yamamoto M, Severson KM, Ruhn KA, Yu X, Koren O, et al. The antibacterial lectin RegIIIgamma promotes the spatial segregation of microbiota and host in the intestine. Science 2011;334:255-8.
[264] Li Y, Innocentin S, Withers DR, Roberts NA, Gallagher AR, Grigorieva EF, et al. Exogenous stimuli maintain intraepithelial lymphocytes via aryl hydrocarbon receptor activation. Cell 2011;147:629-40.
[265] Yada S, Kishihara K, Kong YY, Nomoto K. Differential requirements of CD45 protein tyrosine phosphatase for cytolytic activities and intrathymic and extrathymic development of intestinal intraepithelial lymphocytes. J Immunol 1998;161:2208-16.
[266] Ley RE, Peterson DA, Gordon JI. Ecological and evolutionary forces shaping microbial diversity in the human intestine. Cell 2006;124:837-48.
[267] Jimenez E, Marin ML, Martin R, Odriozola JM, Olivares M, Xaus J, et al. Is meconium from healthy newborns actually sterile? Research in microbiology 2008;159:187-93.
[268] Vaishampayan PA, Kuehl JV, Froula JL, Morgan JL, Ochman H, Francino MP. Comparative metagenomics and population dynamics of the gut microbiota in mother and infant. Genome biology and evolution 2010;2:53-66.
[269] Hopkins MJ, Sharp R, Macfarlane GT. Age and disease related changes in intestinal bacterial populations assessed by cell culture, 16S rRNA abundance, and community cellular fatty acid profiles. Gut 2001;48:198-205.
[270] Arumugam M, Raes J, Pelletier E, Le Paslier D, Yamada T, Mende DR, et al. Enterotypes of the human gut microbiome. Nature 2011;473:174-80.
[271] Savage DC. Microbial ecology of the gastrointestinal tract. Annu Rev Microbiol 1977;31:107-33.
[272] Yoshioka H, Iseki K, Fujita K. Development and differences of intestinal flora in the neonatal period in breast-fed and bottle-fed infants. Pediatrics 1983;72:317-21.
[273] Dai D, Walker WA. Protective nutrients and bacterial colonization in the immature human gut. Advances in pediatrics 1999;46:353-82.

[274] Vedantam G, Hecht DW. Antibiotics and anaerobes of gut origin. Curr Opin Microbiol 2003;6:457-61.
[275] Eckburg PB, Bik EM, Bernstein CN, Purdom E, Dethlefsen L, Sargent M, et al. Diversity of the human intestinal microbial flora. Science 2005;308:1635-8.
[276] Turroni F, Peano C, Pass DA, Foroni E, Severgnini M, Claesson MJ, et al. Diversity of bifidobacteria within the infant gut microbiota. PLoS One 2012;7:e36957.
[277] Claesson MJ, Cusack S, O'Sullivan O, Greene-Diniz R, de Weerd H, Flannery E, et al. Composition, variability, and temporal stability of the intestinal microbiota of the elderly. Proc Natl Acad Sci U S A 2011;108 Suppl 1:4586-91.
[278] Hong PY, Croix JA, Greenberg E, Gaskins HR, Mackie RI. Pyrosequencing-based analysis of the mucosal microbiota in healthy individuals reveals ubiquitous bacterial groups and micro-heterogeneity. PLoS One 2011;6:e25042.
[279] Shen XJ, Rawls JF, Randall T, Burcal L, Mpande CN, Jenkins N, et al. Molecular characterization of mucosal adherent bacteria and associations with colorectal adenomas. Gut Microbes 2010;1:138-47.
[280] Swidsinski A, Loening-Baucke V, Verstraelen H, Osowska S, Doerffel Y. Biostructure of fecal microbiota in healthy subjects and patients with chronic idiopathic diarrhea. Gastroenterology 2008;135:568-79.
[281] Willing BP, Dicksved J, Halfvarson J, Andersson AF, Lucio M, Zheng Z, et al. A pyrosequencing study in twins shows that gastrointestinal microbial profiles vary with inflammatory bowel disease phenotypes. Gastroenterology 2010;139:1844-54 e1.
[282] Walker AW, Sanderson JD, Churcher C, Parkes GC, Hudspith BN, Rayment N, et al. High-throughput clone library analysis of the mucosa-associated microbiota reveals dysbiosis and differences between inflamed and non-inflamed regions of the intestine in inflammatory bowel disease. BMC microbiology 2011;11:7.
[283] Nava GM, Friedrichsen HJ, Stappenbeck TS. Spatial organization of intestinal microbiota in the mouse ascending colon. ISME J 2011;5:627-38.
[284] Van den Abbeele P, Gerard P, Rabot S, Bruneau A, El Aidy S, Derrien M, et al. Arabinoxylans and inulin differentially modulate the mucosal and luminal gut microbiota and mucin-degradation in humanized rats. Environmental microbiology 2011;13:2667-80.
[285] Zoetendal EG, von Wright A, Vilpponen-Salmela T, Ben-Amor K, Akkermans AD, de Vos WM. Mucosa-associated bacteria in the human gastrointestinal tract are uniformly distributed along the colon and differ from the community recovered from feces. Appl Environ Microbiol 2002;68:3401-7.

[286] Zoetendal EG, Rajilic-Stojanovic M, de Vos WM. High-throughput diversity and functionality analysis of the gastrointestinal tract microbiota. Gut 2008;57:1605-15.
[287] Johnson SA, Jackson S, Abratt VR, Wolfaardt GM, Cordero-Otero R, Nicolson SW. Xylose utilization and short-chain fatty acid production by selected components of the intestinal microflora of a rodent pollinator (Aethomys namaquensis). Journal of comparative physiology B, Biochemical, systemic, and environmental physiology 2006;176:631-41.
[288] Zoetendal EG, Raes J, van den Bogert B, Arumugam M, Booijink CC, Troost FJ, et al. The human small intestinal microbiota is driven by rapid uptake and conversion of simple carbohydrates. ISME J 2012;6:1415-26.
[289] Turroni F, Ventura M, Butto LF, Duranti S, O'Toole PW, Motherway MO, et al. Molecular dialogue between the human gut microbiota and the host: a Lactobacillus and Bifidobacterium perspective. Cell Mol Life Sci 2013.
[290] Marco ML, Pavan S, Kleerebezem M. Towards understanding molecular modes of probiotic action. Current opinion in biotechnology 2006;17:204-10.
[291] Hooper LV, Wong MH, Thelin A, Hansson L, Falk PG, Gordon JI. Molecular analysis of commensal host-microbial relationships in the intestine. Science 2001;291:881-4.
[292] Savage DC. Gastrointestinal microflora in mammalian nutrition. Annu Rev Nutr 1986;6:155-78.
[293] Rawls JF, Samuel BS, Gordon JI. Gnotobiotic zebrafish reveal evolutionarily conserved responses to the gut microbiota. Proc Natl Acad Sci U S A 2004;101:4596-601.
[294] Stappenbeck TS, Hooper LV, Gordon JI. Developmental regulation of intestinal angiogenesis by indigenous microbes via Paneth cells. Proc Natl Acad Sci U S A 2002;99:15451-5.
[295] Bentley R, Meganathan R. Biosynthesis of vitamin K (menaquinone) in bacteria. Microbiol Rev 1982;46:241-80.
[296] Wostmann BS. The germfree animal in nutritional studies. Annu Rev Nutr 1981;1:257-79.
[297] Cummings JH, Macfarlane GT. The control and consequences of bacterial fermentation in the human colon. J Appl Bacteriol 1991;70:443-59.
[298] Gill SR, Pop M, Deboy RT, Eckburg PB, Turnbaugh PJ, Samuel BS, et al. Metagenomic analysis of the human distal gut microbiome. Science 2006;312:1355-9.

[299] Turnbaugh PJ, Hamady M, Yatsunenko T, Cantarel BL, Duncan A, Ley RE, et al. A core gut microbiome in obese and lean twins. Nature 2009;457:480-4.
[300] Booijink CC, Boekhorst J, Zoetendal EG, Smidt H, Kleerebezem M, de Vos WM. Metatranscriptome analysis of the human fecal microbiota reveals subject-specific expression profiles, with genes encoding proteins involved in carbohydrate metabolism being dominantly expressed. Appl Environ Microbiol 2010;76:5533-40.
[301] Klaassens ES, Ben-Amor K, Vriesema A, Vaughan EE, de Vos W. The fecal bifidobacterial transcriptome of adults: a microarray approach. Gut Microbes 2011;2:217-26.
[302] Lomax AR, Calder PC. Prebiotics, immune function, infection and inflammation: a review of the evidence. Br J Nutr 2009;101:633-58.
[303] Madsen K, Cornish A, Soper P, McKaigney C, Jijon H, Yachimec C, et al. Probiotic bacteria enhance murine and human intestinal epithelial barrier function. Gastroenterology 2001;121:580-91.
[304] Cario E, Brown D, McKee M, Lynch-Devaney K, Gerken G, Podolsky DK. Commensal-associated molecular patterns induce selective toll-like receptor-trafficking from apical membrane to cytoplasmic compartments in polarized intestinal epithelium. Am J Pathol 2002;160:165-73.
[305] Klaasen HL, Van der Heijden PJ, Stok W, Poelma FG, Koopman JP, Van den Brink ME, et al. Apathogenic, intestinal, segmented, filamentous bacteria stimulate the mucosal immune system of mice. Infect Immun 1993;61:303-6.
[306] Umesaki Y, Okada Y, Matsumoto S, Imaoka A, Setoyama H. Segmented filamentous bacteria are indigenous intestinal bacteria that activate intraepithelial lymphocytes and induce MHC class II molecules and fucosyl asialo GM1 glycolipids on the small intestinal epithelial cells in the ex-germ-free mouse. Microbiol Immunol 1995;39:555-62.
[307] Pull SL, Doherty JM, Mills JC, Gordon JI, Stappenbeck TS. Activated macrophages are an adaptive element of the colonic epithelial progenitor niche necessary for regenerative responses to injury. Proc Natl Acad Sci U S A 2005;102:99-104.
[308] Rakoff-Nahoum S, Paglino J, Eslami-Varzaneh F, Edberg S, Medzhitov R. Recognition of commensal microflora by toll-like receptors is required for intestinal homeostasis. Cell 2004;118:229-41.

[309] Hooper LV, Xu J, Falk PG, Midtvedt T, Gordon JI. A molecular sensor that allows a gut commensal to control its nutrient foundation in a competitive ecosystem. Proc Natl Acad Sci U S A 1999;96:9833-8.
[310] Barcelo A, Claustre J, Moro F, Chayvialle JA, Cuber JC, Plaisancie P. Mucin secretion is modulated by luminal factors in the isolated vascularly perfused rat colon. Gut 2000;46:218-24.
[311] Smirnova MG, Guo L, Birchall JP, Pearson JP. LPS up-regulates mucin and cytokine mRNA expression and stimulates mucin and cytokine secretion in goblet cells. Cell Immunol 2003;221:42-9.
[312] Willemsen LE, Koetsier MA, van Deventer SJ, van Tol EA. Short chain fatty acids stimulate epithelial mucin 2 expression through differential effects on prostaglandin E(1) and E(2) production by intestinal myofibroblasts. Gut 2003;52:1442-7.
[313] Petersson J, Schreiber O, Hansson GC, Gendler SJ, Velcich A, Lundberg JO, et al. Importance and regulation of the colonic mucus barrier in a mouse model of colitis. Am J Physiol Gastrointest Liver Physiol 2011;300:G327-33.
[314] Png CW, Linden SK, Gilshenan KS, Zoetendal EG, McSweeney CS, Sly LI, et al. Mucolytic bacteria with increased prevalence in IBD mucosa augment in vitro utilization of mucin by other bacteria. Am J Gastroenterol 2010;105:2420-8.
[315] Derrien M, Vaughan EE, Plugge CM, de Vos WM. Akkermansia muciniphila gen. nov., sp. nov., a human intestinal mucin-degrading bacterium. Int J Syst Evol Microbiol 2004;54:1469-76.
[316] Derrien M, Van Baarlen P, Hooiveld G, Norin E, Muller M, de Vos WM. Modulation of Mucosal Immune Response, Tolerance, and Proliferation in Mice Colonized by the Mucin-Degrader Akkermansia muciniphila. Frontiers in microbiology 2011;2:166.
[317] Koropatkin NM, Cameron EA, Martens EC. How glycan metabolism shapes the human gut microbiota. Nature Reviews Microbiology 2012;10:323-35.
[318] Backhed F, Ley RE, Sonnenburg JL, Peterson DA, Gordon JI. Host-bacterial mutualism in the human intestine. Science 2005;307:1915-20.
[319] Xu J, Bjursell MK, Himrod J, Deng S, Carmichael LK, Chiang HC, et al. A genomic view of the human-Bacteroides thetaiotaomicron symbiosis. Science 2003;299:2074-6.
[320] Garrido D, Kim JH, German JB, Raybould HE, Mills DA. Oligosaccharide binding proteins from Bifidobacterium longum subsp. infantis reveal a preference for host glycans. PLoS One 2011;6:e17315.

[321] Crociani F, Alessandrini A, Mucci MM, Biavati B. Degradation of complex carbohydrates by Bifidobacterium spp. Int J Food Microbiol 1994;24:199-210.
[322] Salyers AA, West SE, Vercellotti JR, Wilkins TD. Fermentation of mucins and plant polysaccharides by anaerobic bacteria from the human colon. Appl Environ Microbiol 1977;34:529-33.
[323] Swidsinski A, Weber J, Loening-Baucke V, Hale LP, Lochs H. Spatial organization and composition of the mucosal flora in patients with inflammatory bowel disease. J Clin Microbiol 2005;43:3380-9.
[324] Huang JY, Lee SM, Mazmanian SK. The human commensal Bacteroides fragilis binds intestinal mucin. Anaerobe 2011;17:137-41.
[325] Belzer C, de Vos WM. Microbes inside-from diversity to function: the case of Akkermansia. Isme Journal 2012;6:1449-58.
[326] Sonnenburg JL, Xu J, Leip DD, Chen CH, Westover BP, Weatherford J, et al. Glycan foraging in vivo by an intestine-adapted bacterial symbiont. Science 2005;307:1955-9.
[327] Tamboli CP, Neut C, Desreumaux P, Colombel JF. Dysbiosis as a prerequisite for IBD. Gut 2004;53:1057.
[328] Boleij A, Roelofs R, Schaeps RM, Schulin T, Glaser P, Swinkels DW, et al. Increased exposure to bacterial antigen RpL7/L12 in early stage colorectal cancer patients. Cancer 2010;116:4014-22.
[329] Vanhaecke L, Vercruysse F, Boon N, Verstraete W, Cleenwerck I, De Wachter M, et al. Isolation and characterization of human intestinal bacteria capable of transforming the dietary carcinogen 2-amino-1-methyl-6-phenylimidazo[4,5-b]pyridine. Appl Environ Microbiol 2008;74:1469-77.
[330] Klein RS, Recco RA, Catalano MT, Edberg SC, Casey JI, Steigbigel NH. Association of Streptococcus bovis with carcinoma of the colon. N Engl J Med 1977;297:800-2.
[331] Gibson GR. Dietary modulation of the human gut microflora using prebiotics. Br J Nutr 1998;80:S209-12.
[332] Wu GD, Chen J, Hoffmann C, Bittinger K, Chen YY, Keilbaugh SA, et al. Linking long-term dietary patterns with gut microbial enterotypes. Science 2011;334:105-8.
[333] Larsen N, Vogensen FK, van den Berg FW, Nielsen DS, Andreasen AS, Pedersen BK, et al. Gut microbiota in human adults with type 2 diabetes differs from non-diabetic adults. PLoS One 2010;5:e9085.

[334] Haller D. Nutrigenomics and IBD: the intestinal microbiota at the cross-road between inflammation and metabolism. Journal of clinical gastroenterology 2010;44 Suppl 1:S6-9.
[335] Walzer N, Buchman AL. Development of Crohn's disease in patients with intestinal failure: a role for bacteria? Journal of clinical gastroenterology 2010;44:361-3.
[336] Holma R, Salmenpera P, Lohi J, Vapaatalo H, Korpela R. Effects of Lactobacillus rhamnosus GG and Lactobacillus reuteri R2LC on acetic acid-induced colitis in rats. Scand J Gastroenterol 2001;36:630-5.
[337] Manichanh C, Rigottier-Gois L, Bonnaud E, Gloux K, Pelletier E, Frangeul L, et al. Reduced diversity of faecal microbiota in Crohn's disease revealed by a metagenomic approach. Gut 2006;55:205-11.
[338] Shiga H, Kajiura T, Shinozaki J, Takagi S, Kinouchi Y, Takahashi S, et al. Changes of faecal microbiota in patients with Crohn's disease treated with an elemental diet and total parenteral nutrition. Digestive and liver disease : official journal of the Italian Society of Gastroenterology and the Italian Association for the Study of the Liver 2012;44:736-42.
[339] Hansen J, Gulati A, Sartor RB. The role of mucosal immunity and host genetics in defining intestinal commensal bacteria. Current opinion in gastroenterology 2010;26:564-71.
[340] Qin J, Li R, Raes J, Arumugam M, Burgdorf KS, Manichanh C, et al. A human gut microbial gene catalogue established by metagenomic sequencing. Nature 2010;464:59-65.
[341] Vujkovic-Cvijin I, Dunham RM, Iwai S, Maher MC, Albright RG, Broadhurst MJ, et al. Dysbiosis of the Gut Microbiota Is Associated with HIV Disease Progression and Tryptophan Catabolism. Science translational medicine 2013;5:193ra91.
[342] Gerritsen J, Smidt H, Rijkers GT, de Vos WM. Intestinal microbiota in human health and disease: the impact of probiotics. Genes and Nutrition 2011;6:209-40.
[343] Claesson MJ, van Sinderen D, O'Toole PW. The genus Lactobacillus--a genomic basis for understanding its diversity. FEMS Microbiol Lett 2007;269:22-8.
[344] Makarova KS, Koonin EV. Evolutionary genomics of lactic acid bacteria. J Bacteriol 2007;189:1199-208.
[345] Dal Bello F, Walter J, Hammes WP, Hertel C. Increased complexity of the species composition of lactic acid bacteria in human feces revealed by alternative incubation condition. Microbial ecology 2003;45:455-63.

[346] Walter J, Chagnaud P, Tannock GW, Loach DM, Dal Bello F, Jenkinson HF, et al. A high-molecular-mass surface protein (Lsp) and methionine sulfoxide reductase B (MsrB) contribute to the ecological performance of Lactobacillus reuteri in the murine gut. Appl Environ Microbiol 2005;71:979-86.
[347] Moran NA. Symbiosis. Curr Biol 2006;16:R866-71.
[348] Araya M, Morelli, L., Reid, G., Sanders, M. E. & Stanton, C. Guidelines for the evaluation of probiotics in foods. FAO/WHO report. 2002.
[349] Sartor RB. Therapeutic manipulation of the enteric microflora in inflammatory bowel diseases: antibiotics, probiotics, and prebiotics. Gastroenterology 2004;126:1620-33.
[350] Sazawal S, Hiremath G, Dhingra U, Malik P, Deb S, Black RE. Efficacy of probiotics in prevention of acute diarrhoea: a meta-analysis of masked, randomised, placebo-controlled trials. The Lancet infectious diseases 2006;6:374-82.
[351] Pillai A, Nelson R. Probiotics for treatment of Clostridium difficile-associated colitis in adults. Cochrane database of systematic reviews 2008:CD004611.
[352] Hedin C, Whelani K, Lindsay JO. Evidence for the use of probiotics and prebiotics in inflammatory bowel disease: a review of clinical trials. P Nutr Soc 2007;66:307-15.
[353] Rafter J, Bennett M, Caderni G, Clune Y, Hughes R, Karlsson PC, et al. Dietary synbiotics reduce cancer risk factors in polypectomized and colon cancer patients. Am J Clin Nutr 2007;85:488-96.
[354] Camilleri M. Probiotics and irritable bowel syndrome: rationale, putative mechanisms, and evidence of clinical efficacy. Journal of clinical gastroenterology 2006;40:264-9.
[355] Servin AL. Antagonistic activities of lactobacilli and bifidobacteria against microbial pathogens. FEMS microbiology reviews 2004;28:405-40.
[356] Pena JA, Li SY, Wilson PH, Thibodeau SA, Szary AJ, Versalovic J. Genotypic and phenotypic studies of murine intestinal lactobacilli: species differences in mice with and without colitis. Appl Environ Microbiol 2004;70:558-68.
[357] Pena JA, Rogers AB, Ge Z, Ng V, Li SY, Fox JG, et al. Probiotic Lactobacillus spp. diminish Helicobacter hepaticus-induced inflammatory bowel disease in interleukin-10-deficient mice. Infect Immun 2005;73:912-20.
[358] Klein G, Hallmann C, Casas IA, Abad J, Louwers J, Reuter G. Exclusion of vanA, vanB and vanC type glycopeptide resistance in strains of Lactobacillus reuteri and Lactobacillus rhamnosus used as probiotics by polymerase chain reaction and hybridization methods. J Appl Microbiol 2000;89:815-24.

[359] Livingston M, Loach D, Wilson M, Tannock GW, Baird M. Gut commensal Lactobacillus reuteri 100-23 stimulates an immunoregulatory response. Immunology and cell biology 2010;88:99-102.
[360] Hoffmann M, Rath E, Holzlwimmer G, Quintanilla-Martinez L, Loach D, Tannock G, et al. Lactobacillus reuteri 100-23 transiently activates intestinal epithelial cells of mice that have a complex microbiota during early stages of colonization. J Nutr 2008;138:1684-91.
[361] Schreiber O, Petersson J, Phillipson M, Perry M, Roos S, Holm L. Lactobacillus reuteri prevents colitis by reducing P-selectin-associated leukocyte- and platelet-endothelial cell interactions. Am J Physiol Gastrointest Liver Physiol 2009;296:G534-42.
[362] Roselli M, Finamore A, Nuccitelli S, Carnevali P, Brigidi P, Vitali B, et al. Prevention of TNBS-induced colitis by different Lactobacillus and Bifidobacterium strains is associated with an expansion of gammadeltaT and regulatory T cells of intestinal intraepithelial lymphocytes. Inflamm Bowel Dis 2009;15:1526-36.
[363] Moller PL, Paerregaard A, Gad M, Kristensen NN, Claesson MH. Colitic scid mice fed Lactobacillus spp. show an ameliorated gut histopathology and an altered cytokine profile by local T cells. Inflamm Bowel Dis 2005;11:814-9.
[364] Madsen KL, Doyle JS, Jewell LD, Tavernini MM, Fedorak RN. Lactobacillus species prevents colitis in interleukin 10 gene-deficient mice. Gastroenterology 1999;116:1107-14.
[365] Fabia R, Ar'Rajab A, Johansson ML, Willen R, Andersson R, Molin G, et al. The effect of exogenous administration of Lactobacillus reuteri R2LC and oat fiber on acetic acid-induced colitis in the rat. Scand J Gastroenterol 1993;28:155-62.
[366] Alak JI, Wolf BW, Mdurvwa EG, Pimentel-Smith GE, Adeyemo O. Effect of Lactobacillus reuteri on intestinal resistance to Cryptosporidium parvum infection in a murine model of acquired immunodeficiency syndrome. J Infect Dis 1997;175:218-21.
[367] Shornikova AV, Casas IA, Isolauri E, Mykkanen H, Vesikari T. Lactobacillus reuteri as a therapeutic agent in acute diarrhea in young children. Journal of pediatric gastroenterology and nutrition 1997;24:399-404.
[368] Weizman Z, Asli G, Alsheikh A. Effect of a probiotic infant formula on infections in child care centers: comparison of two probiotic agents. Pediatrics 2005;115:5-9.
[369] Savino F, Pelle E, Palumeri E, Oggero R, Miniero R. Lactobacillus reuteri (American Type Culture Collection Strain 55730) versus simethicone in the treatment of infantile colic: a prospective randomized study. Pediatrics 2007;119:e124-30.

[370] Indrio F, Riezzo G, Raimondi F, Bisceglia M, Cavallo L, Francavilla R. The effects of probiotics on feeding tolerance, bowel habits, and gastrointestinal motility in preterm newborns. J Pediatr 2008;152:801-6.

[371] Bottcher MF, Abrahamsson TR, Fredriksson M, Jakobsson T, Bjorksten B. Low breast milk TGF-beta2 is induced by Lactobacillus reuteri supplementation and associates with reduced risk of sensitization during infancy. Pediatric allergy and immunology : official publication of the European Society of Pediatric Allergy and Immunology 2008;19:497-504.

[372] Abrahamsson TR, Jakobsson T, Bottcher MF, Fredrikson M, Jenmalm MC, Bjorksten B, et al. Probiotics in prevention of IgE-associated eczema: a double-blind, randomized, placebo-controlled trial. J Allergy Clin Immunol 2007;119:1174-80.

[373] Valeur N, Engel P, Carbajal N, Connolly E, Ladefoged K. Colonization and immunomodulation by Lactobacillus reuteri ATCC 55730 in the human gastrointestinal tract. Appl Environ Microbiol 2004;70:1176-81.

[374] Lin JHC, Savage DC. Host Specificity of the Colonization of Murine Gastric Epithelium by Lactobacilli. Fems Microbiology Letters 1984;24:67-71.

[375] Christensen HR, Frokiaer H, Pestka JJ. Lactobacilli differentially modulate expression of cytokines and maturation surface markers in murine dendritic cells. J Immunol 2002;168:171-8.

[376] Smits HH, Engering A, van der Kleij D, de Jong EC, Schipper K, van Capel TM, et al. Selective probiotic bacteria induce IL-10-producing regulatory T cells in vitro by modulating dendritic cell function through dendritic cell-specific intercellular adhesion molecule 3-grabbing nonintegrin. J Allergy Clin Immunol 2005;115:1260-7.

[377] Roos S, Jonsson H. A high-molecular-mass cell-surface protein from Lactobacillus reuteri 1063 adheres to mucus components. Microbiology+ 2002;148:433-42.

[378] Wadstrom T, Andersson K, Sydow M, Axelsson L, Lindgren S, Gullmar B. Surface properties of lactobacilli isolated from the small intestine of pigs. J Appl Bacteriol 1987;62:513-20.

[379] Lindgren SE, Swaisgood HE, Janolino VG, Axelsson LT, Richter CS, Mackenzie JM, et al. Binding of Lactobacillus reuteri to fibronectin immobilized on glass beads. Zentralblatt fur Bakteriologie : international journal of medical microbiology 1992;277:519-28.

[380] Aleljung P, Shen W, Rozalska B, Hellman U, Ljungh A, Wadstrom T. Purification of collagen-binding proteins of Lactobacillus reuteri NCIB 11951. Curr Microbiol 1994;28:231-6.
[381] Wang B, Wei H, Yuan J, Li Q, Li Y, Li N, et al. Identification of a surface protein from Lactobacillus reuteri JCM1081 that adheres to porcine gastric mucin and human enterocyte-like HT-29 cells. Curr Microbiol 2008;57:33-8.
[382] Jeffers F. Investigating the molecular mechanisms of the interactions between Lactobacillus reuteri strains and mucus: University of East Anglia; 2012.
[383] MacKenzie DA, Tailford LE, Hemmings AM, Juge N. Crystal structure of a mucus-binding protein repeat reveals an unexpected functional immunoglobulin binding activity. J Biol Chem 2009;284:32444-53.
[384] Coic YM, Baleux F, Poyraz O, Thibeaux R, Labruyere E, Chretien F, et al. Design of a specific colonic mucus marker using a human commensal bacterium cell surface domain. J Biol Chem 2012;287:15916-22.
[385] Kleerebezem M, Hols P, Bernard E, Rolain T, Zhou M, Siezen RJ, et al. The extracellular biology of the lactobacilli. FEMS microbiology reviews 2010;34:199-230.
[386] Itohara S, Mombaerts P, Lafaille J, Iacomini J, Nelson A, Clarke AR, et al. T cell receptor delta gene mutant mice: independent generation of alpha beta T cells and programmed rearrangements of gamma delta TCR genes. Cell 1993;72:337-48.
[387] Yao K, Ubuka T, Masuoka N, Kinuta M, Ikeda T. Direct determination of bound sialic acids in sialoglycoproteins by acidic ninhydrin reaction. Anal Biochem 1989;179:332-5.
[388] Crowther RS, Wetmore RF. Fluorometric assay of O-linked glycoproteins by reaction with 2-cyanoacetamide. Anal Biochem 1987;163:170-4.
[389] McConnell MAAAM, and G. W. Tannock. Transfer of plasmid pAMß1 between members of the normal microflora inhabiting the murine digestive tract and modification of the plasmid in a Lactobacillus reuteri host. Microb Ecol Hlth Dis 1991;4:343-35.
[390] Kandler O, Stetter KO, Kohl R. Lactobacillus-Reuteri Sp-Nov, a New Species of Heterofermentative Lactobacilli. Zbl Bakt Mik Hyg I C 1980;1:264-9.
[391] Mackenzie DA, Jeffers F, Parker ML, Vibert-Vallet A, Bongaerts RJ, Roos S, et al. Strain-specific diversity of mucus-binding proteins in the adhesion and aggregation properties of Lactobacillus reuteri. Microbiology+ 2010;156:3368-78.
[392] Okayasu I, Hatakeyama S, Yamada M, Ohkusa T, Inagaki Y, Nakaya R. A novel method in the induction of reliable experimental acute and chronic ulcerative colitis in mice. Gastroenterology 1990;98:694-702.

[393] Cooper HS, Murthy SN, Shah RS, Sedergran DJ. Clinicopathologic study of dextran sulfate sodium experimental murine colitis. Lab Invest 1993;69:238-49.
[394] Elson CO, Sartor RB, Tennyson GS, Riddell RH. Experimental models of inflammatory bowel disease. Gastroenterology 1995;109:1344-67.
[395] Murthy SN, Cooper HS, Shim H, Shah RS, Ibrahim SA, Sedergran DJ. Treatment of dextran sulfate sodium-induced murine colitis by intracolonic cyclosporin. Dig Dis Sci 1993;38:1722-34.
[396] Johansson ME, Hansson GC. The goblet cell: a key player in ischaemia-reperfusion injury. Gut 2012.
[397] Troughton WD, Trier JS. Paneth and goblet cell renewal in mouse duodenal crypts. J Cell Biol 1969;41:251-68.
[398] Kamata T, Nogaki F, Fagarasan S, Sakiyama T, Kobayashi I, Miyawaki S, et al. Increased frequency of surface IgA-positive plasma cells in the intestinal lamina propria and decreased IgA excretion in hyper IgA (HIGA) mice, a murine model of IgA nephropathy with hyperserum IgA. J Immunol 2000;165:1387-94.
[399] Shimada S, Kawaguchi-Miyashita M, Kushiro A, Sato T, Nanno M, Sako T, et al. Generation of polymeric immunoglobulin receptor-deficient mouse with marked reduction of secretory IgA. J Immunol 1999;163:5367-73.
[400] Xia L. Core 3-derived O-glycans are essential for intestinal mucus barrier function. Methods Enzymol 2010;479:123-41.
[401] Yeh JC, Ong E, Fukuda M. Molecular cloning and expression of a novel beta-1, 6-N-acetylglucosaminyltransferase that forms core 2, core 4, and I branches. J Biol Chem 1999;274:3215-21.
[402] Lopetuso LR, Scaldaferri F, Pizarro TT. Emerging role of the interleukin (IL)-33/ST2 axis in gut mucosal wound healing and fibrosis. Fibrogenesis & tissue repair 2012;5:18.
[403] Pastorelli L, De Salvo C, Cominelli MA, Vecchi M, Pizarro TT. Novel cytokine signaling pathways in inflammatory bowel disease: insight into the dichotomous functions of IL-33 during chronic intestinal inflammation. Therapeutic advances in gastroenterology 2011;4:311-23.
[404] Cohn L, Whittaker L, Niu N, Homer RJ. Cytokine regulation of mucus production in a model of allergic asthma. Novartis Foundation symposium 2002;248:201-13; discussion 13-20, 77-82.

[405] Iwashita J, Sato Y, Sugaya H, Takahashi N, Sasaki H, Abe T. mRNA of MUC2 is stimulated by IL-4, IL-13 or TNF-alpha through a mitogen-activated protein kinase pathway in human colon cancer cells. Immunology and cell biology 2003;81:275-82.
[406] Han V, Resau J, Prendergast R, Scott A, Levy DA. Interleukin-1 induces mucus secretion from mouse intestinal explants. International archives of allergy and applied immunology 1987;82:364-5.
[407] Tanabe T, Fujimoto K, Yasuo M, Tsushima K, Yoshida K, Ise H, et al. Modulation of mucus production by interleukin-13 receptor alpha2 in the human airway epithelium. Clin Exp Allergy 2008;38:122-34.
[408] Sato T, Vries RG, Snippert HJ, van de Wetering M, Barker N, Stange DE, et al. Single Lgr5 stem cells build crypt-villus structures in vitro without a mesenchymal niche. Nature 2009;459:262-5.
[409] Housley RM, Morris CF, Boyle W, Ring B, Biltz R, Tarpley JE, et al. Keratinocyte growth factor induces proliferation of hepatocytes and epithelial cells throughout the rat gastrointestinal tract. J Clin Invest 1994;94:1764-77.
[410] Iwakiri D, Podolsky DK. Keratinocyte growth factor promotes goblet cell differentiation through regulation of goblet cell silencer inhibitor. Gastroenterology 2001;120:1372-80.
[411] Tsuchiya T, Fukuda S, Hamada H, Nakamura A, Kohama Y, Ishikawa H, et al. Role of gamma delta T cells in the inflammatory response of experimental colitis mice. J Immunol 2003;171:5507-13.
[412] Frantz AL, Rogier EW, Weber CR, Shen L, Cohen DA, Fenton LA, et al. Targeted deletion of MyD88 in intestinal epithelial cells results in compromised antibacterial immunity associated with downregulation of polymeric immunoglobulin receptor, mucin-2, and antibacterial peptides. Mucosal immunology 2012;5:501-12.
[413] Harduin-Lepers A, Mollicone R, Delannoy P, Oriol R. The animal sialyltransferases and sialyltransferase-related genes: a phylogenetic approach. Glycobiology 2005;15:805-17.
[414] Comelli EM, Head SR, Gilmartin T, Whisenant T, Haslam SM, North SJ, et al. A focused microarray approach to functional glycomics: transcriptional regulation of the glycome. Glycobiology 2006;16:117-31.
[415] Severi E, Hood DW, Thomas GH. Sialic acid utilization by bacterial pathogens. Microbiol-Sgm 2007;153:2817-22.
[416] Lewis AL, Lewis WG. Host sialoglycans and bacterial sialidases: a mucosal perspective. Cellular Microbiology 2012;14:1174-82.

[417] Vanderheijden PJ, Stok W, Bianchi ATJ. Contribution of Immunoglobulin-Secreting Cells in the Murine Small-Intestine to the Total Background Immunoglobulin Production. Immunology 1987;62:551-5.
[418] van Egmond M, Damen CA, van Spriel AB, Vidarsson G, van Garderen E, van de Winkel JG. IgA and the IgA Fc receptor. Trends in immunology 2001;22:205-11.
[419] Lycke N, Eriksen L, Holmgren J. Protection against cholera toxin after oral immunization is thymus-dependent and associated with intestinal production of neutralizing IgA antitoxin. Scand J Immunol 1987;25:413-9.
[420] Lycke N, Erlandsson L, Ekman L, Schon K, Leanderson T. Lack of J chain inhibits the transport of gut IgA and abrogates the development of intestinal antitoxic protection. J Immunol 1999;163:913-9.
[421] Fagarasan S, Muramatsu M, Suzuki K, Nagaoka H, Hiai H, Honjo T. Critical roles of activation-induced cytidine deaminase in the homeostasis of gut flora. Science 2002;298:1424-7.
[422] Moreau MC, Ducluzeau R, Guy-Grand D, Muller MC. Increase in the population of duodenal immunoglobulin A plasmocytes in axenic mice associated with different living or dead bacterial strains of intestinal origin. Infect Immun 1978;21:532-9.
[423] Shroff KE, Meslin K, Cebra JJ. Commensal enteric bacteria engender a self-limiting humoral mucosal immune response while permanently colonizing the gut. Infect Immun 1995;63:3904-13.
[424] Talham GL, Jiang HQ, Bos NA, Cebra JJ. Segmented filamentous bacteria are potent stimuli of a physiologically normal state of the murine gut mucosal immune system. Infect Immun 1999;67:1992-2000.
[425] Hapfelmeier S, Lawson MA, Slack E, Kirundi JK, Stoel M, Heikenwalder M, et al. Reversible microbial colonization of germ-free mice reveals the dynamics of IgA immune responses. Science 2010;328:1705-9.
[426] van der Waaij LA, Limburg PC, Mesander G, van der Waaij D. In vivo IgA coating of anaerobic bacteria in human faeces. Gut 1996;38:348-54.
[427] Tsuruta T, Inoue R, Nojima I, Tsukahara T, Hara H, Yajima T. The amount of secreted IgA may not determine the secretory IgA coating ratio of gastrointestinal bacteria. FEMS Immunol Med Microbiol 2009;56:185-9.
[428] Murthy AK, Dubose CN, Banas JA, Coalson JJ, Arulanandam BP. Contribution of polymeric immunoglobulin receptor to regulation of intestinal inflammation in dextran sulfate sodium-induced colitis. J Gastroenterol Hepatol 2006;21:1372-80.

[429] Haneberg B, Aarskog D. Human faecal immunoglobulins in healthy infants and children, and in some with diseases affecting the intestinal tract or the immune system. Clin Exp Immunol 1975;22:210-22.
[430] Jiang ZD, Nelson AC, Mathewson JJ, Ericsson CD, DuPont HL. Intestinal secretory immune response to infection with Aeromonas species and Plesiomonas shigelloides among students from the United States in Mexico. J Infect Dis 1991;164:979-82.
[431] Merchant AA, Groene WS, Cheng EH, Shaw RD. Murine intestinal antibody response to heterologous rotavirus infection. J Clin Microbiol 1991;29:1693-701.
[432] Fujihashi K, Dohi T, Kweon MN, McGhee JR, Koga T, Cooper MD, et al. gamma delta T cells regulate mucosally induced tolerance in a dose-dependent fashion. International Immunology 1999;11:1907-16.
[433] Corazziari ES. Intestinal Mucus Barrier in Normal and Inflamed Colon. Journal of pediatric gastroenterology and nutrition 2009;48:S54-S5.
[434] Ho SB, Niehans GA, Lyftogt C, Yan PS, Cherwitz DL, Gum ET, et al. Heterogeneity of Mucin Gene-Expression in Normal and Neoplastic Tissues. Cancer Research 1993;53:641-51.
[435] Louis NA, Hamilton KE, Canny G, Shekels LL, Ho SB, Colgan SP. Selective induction of mucin-3 by hypoxia in intestinal epithelia. Journal of Cellular Biochemistry 2006;99:1616-27.
[436] Moehle C, Ackermann N, Langmann T, Aslanidis C, Kel A, Kel-Margoulis O, et al. Aberrant intestinal expression and allelic variants of mucin genes associated with inflammatory bowel disease. Journal of molecular medicine 2006;84:1055-66.
[437] Grootjans J, Hundscheid IH, Lenaerts K, Boonen B, Renes IB, Verheyen FK, et al. Ischaemia-induced mucus barrier loss and bacterial penetration are rapidly counteracted by increased goblet cell secretory activity in human and rat colon. Gut 2013;62:250-8.
[438] Deplancke B, Gaskins HR. Microbial modulation of innate defense: goblet cells and the intestinal mucus layer. Am J Clin Nutr 2001;73:1131S-41S.
[439] Tytgat KM, van der Wal JW, Einerhand AW, Buller HA, Dekker J. Quantitative analysis of MUC2 synthesis in ulcerative colitis. Biochem Biophys Res Commun 1996;224:397-405.
[440] Schwerbrock NM, Makkink MK, van der Sluis M, Buller HA, Einerhand AW, Sartor RB, et al. Interleukin 10-deficient mice exhibit defective colonic Muc2 synthesis before

and after induction of colitis by commensal bacteria. Inflamm Bowel Dis 2004;10:811-23.
[441] Satsangi J, Parkes M, Louis E, Hashimoto L, Kato N, Welsh K, et al. Two stage genome-wide search in inflammatory bowel disease provides evidence for susceptibility loci on chromosomes 3, 7 and 12. Nat Genet 1996;14:199-202.
[442] McGuckin MA, Hasnain SZ. There is a 'uc' in mucus, but is there mucus in UC? Gut 2013.
[443] Beltran CJ, Nunez LE, Diaz-Jimenez D, Farfan N, Candia E, Heine C, et al. Characterization of the novel ST2/IL-33 system in patients with inflammatory bowel disease. Inflamm Bowel Dis 2010;16:1097-107.
[444] Kobori A, Yagi Y, Imaeda H, Ban H, Bamba S, Tsujikawa T, et al. Interleukin-33 expression is specifically enhanced in inflamed mucosa of ulcerative colitis. J Gastroenterol 2010;45:999-1007.
[445] Pastorelli L, Garg RR, Hoang SB, Spina L, Mattioli B, Scarpa M, et al. Epithelial-derived IL-33 and its receptor ST2 are dysregulated in ulcerative colitis and in experimental Th1/Th2 driven enteritis. Proc Natl Acad Sci U S A 2010;107:8017-22.
[446] Seidelin JB, Bjerrum JT, Coskun M, Widjaya B, Vainer B, Nielsen OH. IL-33 is upregulated in colonocytes of ulcerative colitis. Immunology letters 2010;128:80-5.
[447] Bamias G, Corridoni D, Pizarro TT, Cominelli F. New insights into the dichotomous role of innate cytokines in gut homeostasis and inflammation. Cytokine 2012;59:451-9.
[448] Moro K, Yamada T, Tanabe M, Takeuchi T, Ikawa T, Kawamoto H, et al. Innate production of T(H)2 cytokines by adipose tissue-associated c-Kit(+)Sca-1(+) lymphoid cells. Nature 2010;463:540-4.
[449] Neill DR, Wong SH, Bellosi A, Flynn RJ, Daly M, Langford TK, et al. Nuocytes represent a new innate effector leukocyte that mediates type-2 immunity. Nature 2010;464:1367-70.
[450] Price AE, Liang HE, Sullivan BM, Reinhardt RL, Eisley CJ, Erle DJ, et al. Systemically dispersed innate IL-13-expressing cells in type 2 immunity. Proc Natl Acad Sci U S A 2010;107:11489-94.
[451] Schmitz J, Owyang A, Oldham E, Song Y, Murphy E, McClanahan TK, et al. IL-33, an interleukin-1-like cytokine that signals via the IL-1 receptor-related protein ST2 and induces T helper type 2-associated cytokines. Immunity 2005;23:479-90.

[452] Hoshino K, Kashiwamura S, Kuribayashi K, Kodama T, Tsujimura T, Nakanishi K, et al. The absence of interleukin 1 receptor-related T1/ST2 does not affect T helper cell type 2 development and its effector function. J Exp Med 1999;190:1541-8.
[453] Townsend MJ, Fallon PG, Matthews DJ, Jolin HE, McKenzie AN. T1/ST2-deficient mice demonstrate the importance of T1/ST2 in developing primary T helper cell type 2 responses. J Exp Med 2000;191:1069-76.
[454] Do JS, Fink PJ, Li L, Spolski R, Robinson J, Leonard WJ, et al. Cutting edge: spontaneous development of IL-17-producing gamma delta T cells in the thymus occurs via a TGF-beta 1-dependent mechanism. J Immunol 2010;184:1675-9.
[455] Edelblum KL, Shen L, Weber CR, Marchiando AM, Clay BS, Wang Y, et al. Dynamic migration of gammadelta intraepithelial lymphocytes requires occludin. Proc Natl Acad Sci U S A 2012;109:7097-102.
[456] Ouwerkerk JP, de Vos WM, Belzer C. Glycobiome: Bacteria and mucus at the epithelial interface. Best practice & research Clinical gastroenterology 2013;27:25-38.
[457] Marcobal A, Southwick AM, Earle KA, Sonnenburg JL. A refined palate: Bacterial consumption of host glycans in the gut. Glycobiology 2013;23:1038-46.
[458] Whelan K, Myers CE. Safety of probiotics in patients receiving nutritional support: a systematic review of case reports, randomized controlled trials, and nonrandomized trials. Am J Clin Nutr 2010;91:687-703.
[459] Zhang M, Wang XQ, Zhou YK, Ma YL, Shen TY, Chen HQ, et al. Effects of oral Lactobacillus plantarum on hepatocyte tight junction structure and function in rats with obstructive jaundice. Molecular biology reports 2010;37:2989-99.
[460] Liu ZH, Ma YL, Shen TY, Chen HQ, Zhou YK, Zhang P, et al. Identification of DC-SIGN as the receptor during the interaction of Lactobacillus plantarum CGMCC 1258 and dendritic cells. World J Microb Biot 2011;27:603-11.
[461] Frese SA, Benson AK, Tannock GW, Loach DM, Kim J, Zhang M, et al. The Evolution of Host Specialization in the Vertebrate Gut Symbiont Lactobacillus reuteri. PLoS Genet 2011;7:e1001314.
[462] Tuomola EM, Ouwehand AC, Salminen SJ. The effect of probiotic bacteria on the adhesion of pathogens to human intestinal mucus. FEMS Immunol Med Microbiol 1999;26:137-42.
[463] Izquierdo E, Medina M, Ennahar S, Marchioni E, Sanz Y. Resistance to simulated gastrointestinal conditions and adhesion to mucus as probiotic criteria for Bifidobacterium longum strains. Curr Microbiol 2008;56:613-8.

[464] Juge N. Microbial adhesins to gastrointestinal mucus. Trends in microbiology 2012;20:30-9.
[465] Boekhorst J, Helmer Q, Kleerebezem M, Siezen RJ. Comparative analysis of proteins with a mucus-binding domain found exclusively in lactic acid bacteria. Microbiology+ 2006;152:273-80.
[466] Pridmore RD, Berger B, Desiere F, Vilanova D, Barretto C, Pittet AC, et al. The genome sequence of the probiotic intestinal bacterium Lactobacillus johnsonii NCC 533. Proc Natl Acad Sci U S A 2004;101:2512-7.
[467] Kankainen M, Paulin L, Tynkkynen S, von Ossowski I, Reunanen J, Partanen P, et al. Comparative genomic analysis of Lactobacillus rhamnosus GG reveals pili containing a human- mucus binding protein. Proc Natl Acad Sci U S A 2009;106:17193-8.
[468] Connell I, Agace W, Klemm P, Schembri M, Marild S, Svanborg C. Type 1 fimbrial expression enhances Escherichia coli virulence for the urinary tract. Proc Natl Acad Sci U S A 1996;93:9827-32.
[469] Macias-Rodriguez ME, Zagorec M, Ascencio F, Vazquez-Juarez R, Rojas M. Lactobacillus fermentum BCS87 expresses mucus- and mucin-binding proteins on the cell surface. J Appl Microbiol 2009;107:1866-74.
[470] Buck BL, Altermann E, Svingerud T, Klaenhammer TR. Functional analysis of putative adhesion factors in Lactobacillus acidophilus NCFM. Appl Environ Microbiol 2005;71:8344-51.
[471] Rojas M, Ascencio F, Conway PL. Purification and characterization of a surface protein from Lactobacillus fermentum 104R that binds to porcine small intestinal mucus and gastric mucin. Appl Environ Microbiol 2002;68:2330-6.
[472] Miyoshi Y, Okada S, Uchimura T, Satoh E. A mucus adhesion promoting protein, MapA, mediates the adhesion of Lactobacillus reuteri to Caco-2 human intestinal epithelial cells. Biosci Biotechnol Biochem 2006;70:1622-8.
[473] Jacobson GR, Rosenbusch JP. Abundance and membrane association of elongation factor Tu in E. coli. Nature 1976;261:23-6.
[474] Dallo SF, Kannan TR, Blaylock MW, Baseman JB. Elongation factor Tu and E1 beta subunit of pyruvate dehydrogenase complex act as fibronectin binding proteins in Mycoplasma pneumoniae. Mol Microbiol 2002;46:1041-51.
[475] Granato D, Bergonzelli GE, Pridmore RD, Marvin L, Rouvet M, Corthesy-Theulaz IE. Cell surface-associated elongation factor Tu mediates the attachment of

Lactobacillus johnsonii NCC533 (La1) to human intestinal cells and mucins. Infect Immun 2004;72:2160-9.
[476] Nakamura J, Ito D, Nagai K, Umehara Y, Hamachi M, Kumagai C. Rapid and sensitive detection of Hiochi bacteria by amplification of Hiochi bacterial common antigen gene by PCR method and characterization of the antigen. J Ferment Bioeng 1997;83:161-7.
[477] Ramiah K, van Reenen CA, Dicks LM. Expression of the mucus adhesion genes Mub and MapA, adhesion-like factor EF-Tu and bacteriocin gene plaA of Lactobacillus plantarum 423, monitored with real-time PCR. Int J Food Microbiol 2007;116:405-9.
[478] Lesuffleur T, Barbat A, Dussaulx E, Zweibaum A. Growth adaptation to methotrexate of HT-29 human colon carcinoma cells is associated with their ability to differentiate into columnar absorptive and mucus-secreting cells. Cancer Res 1990;50:6334-43.
[479] Lesuffleur T, Porchet N, Aubert JP, Swallow D, Gum JR, Kim YS, et al. Differential expression of the human mucin genes MUC1 to MUC5 in relation to growth and differentiation of different mucus-secreting HT-29 cell subpopulations. J Cell Sci 1993;106 (Pt 3):771-83.
[480] Gouyer V, Wiede A, Buisine MP, Dekeyser S, Moreau O, Lesuffleur T, et al. Specific secretion of gel-forming mucins and TFF peptides in HT-29 cells of mucin-secreting phenotype. Bba-Mol Cell Res 2001;1539:71-84.
[481] Lievin-Le Moal V, Servin AL. The front line of enteric host defense against unwelcome intrusion of harmful microorganisms: mucins, antimicrobial peptides, and microbiota. Clin Microbiol Rev 2006;19:315-37.
[482] D'Agostino EM, Rossetti D, Atkins D, Ferdinando D, Yakubov GE. Interaction of Tea Polyphenols and Food Constituents with Model Gut Epithelia: The Protective Role of the Mucus Gel Layer. J Agr Food Chem 2012;60:3318-28.
[483] Roos S, Lindgren S, Jonsson H. Autoaggregation of Lactobacillus reuteri is mediated by a putative DEAD-box helicase. Molecular Microbiology 1999;32:427-36.
[484] Mack DR, Ahrne S, Hyde L, Wei S, Hollingsworth MA. Extracellular MUC3 mucin secretion follows adherence of Lactobacillus strains to intestinal epithelial cells in vitro. Gut 2003;52:827-33.
[485] Zweibaum A. Differentiation of Human Colon Cancer-Cells. Nato Adv Sci I a-Lif 1991;218:27-37.

[486] Mack DR, Michail S, Wei S, McDougall L, Hollingsworth MA. Probiotics inhibit enteropathogenic E. coli adherence in vitro by inducing intestinal mucin gene expression. Am J Physiol 1999;276:G941-50.
[487] Prescher JA, Bertozzi CR. Chemical technologies for probing glycans. Cell 2006;126:851-4.
[488] Huet G, Hennebicq-Reig S, de Bolos C, Ulloa F, Lesuffleur T, Barbat A, et al. GalNAc-alpha-O-benzyl inhibits NeuAc alpha 2-3 glycosylation and blocks the intracellular transport of apical glycoproteins and mucus in differentiated HT-29 cells. Journal of Cell Biology 1998;141:1311-22.
[489] Huet G, Kim I, Debolos C, Loguidice JM, Moreau O, Hemon B, et al. Characterization of Mucins and Proteoglycans Synthesized by a Mucin-Secreting Ht-29 Cell Subpopulation. Journal of Cell Science 1995;108:1275-85.
[490] Manzi AE, Dell A, Azadi P, Varki A. Studies of Naturally-Occurring Modifications of Sialic Acids by Fast-Atom Bombardment Mass-Spectrometry - Analysis of Positional Isomers by Periodate Cleavage. Journal of Biological Chemistry 1990;265:8094-107.
[491] Woodward MP, Young WW, Bloodgood RA. Detection of Monoclonal-Antibodies Specific for Carbohydrate Epitopes Using Periodate-Oxidation. Journal of immunological methods 1985;78:143-53.
[492] Freitas W, Cayuela C, Antoine JM, Piller F, Sapin C, Trugnan G. A heat labile soluble factor from Bacteroides thetaiotaomicron VPI-5482 specifically increases the galactosylation pattern of HT29-MTX cells. Cellular Microbiology 2001;3:289-300.
[493] Sanchez B, Urdaci MC, Margolles A. Extracellular proteins secreted by probiotic bacteria as mediators of effects that promote mucosa-bacteria interactions. Microbiology+ 2010;156:3232-42.
[494] van Baarlen P, Wells JM, Kleerebezem M. Regulation of intestinal homeostasis and immunity with probiotic lactobacilli. Trends in immunology 2013;34:208-15.
[495] Elo S, Saxelin M, Salminen S. Attachment of Lactobacillus-Casei Strain Gg to Human Colon-Carcinoma Cell-Line Caco-2 - Comparison with Other Dairy Strains. Letters in Applied Microbiology 1991;13:154-6.
[496] Bernet MF, Brassart D, Neeser JR, Servin AL. Adhesion of human bifidobacterial strains to cultured human intestinal epithelial cells and inhibition of enteropathogen-cell interactions. Appl Environ Microbiol 1993;59:4121-8.
[497] Adlerberth I, Ahrne S, Johansson ML, Molin G, Hanson LA, Wold AE. A mannose-specific adherence mechanism in Lactobacillus plantarum conferring binding to the human colonic cell line HT-29. Appl Environ Microbiol 1996;62:2244-51.

[498] Tuomola EM, Salminen SJ. Adhesion of some probiotic and dairy Lactobacillus strains to Caco-2 cell cultures. International Journal of Food Microbiology 1998;41:45-51.
[499] Servin AL, Coconnier MH. Adhesion of probiotic strains to the intestinal mucosa and interaction with pathogens. Best Pract Res Cl Ga 2003;17:741-54.
[500] Coconnier MH, Klaenhammer TR, Kerneis S, Bernet MF, Servin AL. Protein-Mediated Adhesion of Lactobacillus-Acidophilus Bg2fo4 on Human Enterocyte and Mucus-Secreting Cell-Lines in Culture. Appl Environ Microb 1992;58:2034-9.
[501] Gopal PK, Prasad J, Smart J, Gill HS. In vitro adherence properties of Lactobacillus rhamnosus DR20 and Bifidobacterium lactis DR10 strains and their antagonistic activity against an enterotoxigenic Escherichia coli. Int J Food Microbiol 2001;67:207-16.
[502] Li XJ, Yue LY, Guan XF, Qiao SY. The adhesion of putative probiotic lactobacilli to cultured epithelial cells and porcine intestinal mucus. J Appl Microbiol 2008;104:1082-91.
[503] Gonzalez-Rodriguez I, Sanchez B, Ruiz L, Turroni F, Ventura M, Ruas-Madiedo P, et al. Role of Extracellular Transaldolase from Bifidobacterium bifidum in Mucin Adhesion and Aggregation. Appl Environ Microb 2012;78:3992-8.
[504] Gionchetti P, Rizzello F, Venturi A, Brigidi P, Matteuzzi D, Bazzocchi G, et al. Oral bacteriotherapy as maintenance treatment in patients with chronic pouchitis: a double-blind, placebo-controlled trial. Gastroenterology 2000;119:305-9.
[505] Ho SB, Luu Y, Shekels LL, Batra SK, Kandarian B, Evans DB, et al. Activity of recombinant cysteine-rich domain proteins derived from the membrane-bound MUC17/Muc3 family mucins. Bba-Gen Subjects 2010;1800:629-38.
[506] Pretzer G, Snel J, Molenaar D, Wiersma A, Bron PA, Lambert J, et al. Biodiversity-based identification and functional characterization of the mannose-specific adhesin of Lactobacillus plantarum. J Bacteriol 2005;187:6128-36.
[507] Jakubovics NS, Kerrigan SW, Nobbs AH, Stromberg N, van Dolleweerd CJ, Cox DM, et al. Functions of cell surface-anchored antigen I/II family and Hsa polypeptides in interactions of Streptococcus gordonii with host receptors. Infect Immun 2005;73:6629-38.
[508] Prakobphol A, Xu F, Hoang VM, Larsson T, Bergstrom J, Johansson I, et al. Salivary agglutinin, which binds Streptococcus mutans and Helicobacter pylori, is the lung scavenger receptor cysteine-rich protein gp-340. J Biol Chem 2000;275:39860-6.

[509] Jumblatt MM, Imbert Y, Young WW, Jr., Foulks GN, Steele PS, Demuth DR. Glycoprotein 340 in normal human ocular surface tissues and tear film. Infect Immun 2006;74:4058-63.

[510] Holmskov U, Lawson P, Teisner B, Tornoe I, Willis AC, Morgan C, et al. Isolation and characterization of a new member of the scavenger receptor superfamily, glycoprotein-340 (gp-340), as a lung surfactant protein-D binding molecule. J Biol Chem 1997;272:13743-9.

[511] Kukita K, Kawada-Matsuo M, Oho T, Nagatomo M, Oogai Y, Hashimoto M, et al. Staphylococcus aureus SasA is responsible for binding to the salivary agglutinin gp340, derived from human saliva. Infect Immun 2013;81:1870-9.

[512] Lelwala-Guruge J, Ljungh A, Wadstrom T. Haemagglutination patterns of Helicobacter pylori. Frequency of sialic acid-specific and non-sialic acid-specific haemagglutinins. APMIS : acta pathologica, microbiologica, et immunologica Scandinavica 1992;100:908-13.

[513] Robinson J, Goodwin CS, Cooper M, Burke V, Mee BJ. Soluble and cell-associated haemagglutinins of Helicobacter (Campylobacter) pylori. J Med Microbiol 1990;33:277-84.

[514] Hirmo S, Kelm S, Iwersen M, Hotta K, Goso Y, Ishihara K, et al. Inhibition of Helicobacter pylori sialic acid-specific haemagglutination by human gastrointestinal mucins and milk glycoproteins. FEMS Immunol Med Microbiol 1998;20:275-81.

[515] Evans DJ, Jr., Evans DG, Takemura T, Nakano H, Lampert HC, Graham DY, et al. Characterization of a Helicobacter pylori neutrophil-activating protein. Infect Immun 1995;63:2213-20.

[516] Boren T, Falk P, Roth KA, Larson G, Normark S. Attachment of Helicobacter pylori to human gastric epithelium mediated by blood group antigens. Science 1993;262:1892-5.

[517] Wadstrom T, Hirmo S, Boren T. Biochemical aspects of Helicobacter pylori colonization of the human gastric mucosa. Aliment Pharmacol Ther 1996;10 Suppl 1:17-27.

[518] Vimr ER, Troy FA. Identification of an inducible catabolic system for sialic acids (nan) in Escherichia coli. J Bacteriol 1985;164:845-53.

[519] Almagro-Moreno S, Boyd EF. Sialic acid catabolism confers a competitive advantage to pathogenic vibrio cholerae in the mouse intestine. Infect Immun 2009;77:3807-16.

[520] Olson ME, King JM, Yahr TL, Horswill AR. Sialic acid catabolism in Staphylococcus aureus. J Bacteriol 2013;195:1779-88.
[521] Henriksson A, Conway PL. Adhesion of Lactobacillus fermentum 104-S to porcine stomach mucus. Curr Microbiol 1996;33:31-4.
[522] Matsumura A, Saito T, Arakuni M, Kitazawa H, Kawai Y, Itoh T. New binding assay and preparative trial of cell-surface lectin from Lactobacillus acidophilus group lactic acid bacteria. J Dairy Sci 1999;82:2525-9.
[523] Chan RC, Reid G, Irvin RT, Bruce AW, Costerton JW. Competitive exclusion of uropathogens from human uroepithelial cells by Lactobacillus whole cells and cell wall fragments. Infect Immun 1985;47:84-9.
[524] Chauviere G, Coconnier MH, Kerneis S, Darfeuille-Michaud A, Joly B, Servin AL. Competitive exclusion of diarrheagenic Escherichia coli (ETEC) from human enterocyte-like Caco-2 cells by heat-killed Lactobacillus. FEMS Microbiol Lett 1992;70:213-7.
[525] Bernet MF, Brassart D, Neeser JR, Servin AL. Lactobacillus-Acidophilus La-1 Binds to Cultured Human Intestinal-Cell Lines and Inhibits Cell Attachment and Cell Invasion by Enterovirulent Bacteria. Gut 1994;35:483-9.
[526] Blomberg L, Henriksson A, Conway PL. Inhibition of adhesion of Escherichia coli K88 to piglet ileal mucus by Lactobacillus spp. Appl Environ Microbiol 1993;59:34-9.
[527] Bernet-Camard MF, Lievin V, Brassart D, Neeser JR, Servin AL, Hudault S. The human Lactobacillus acidophilus strain LA1 secretes a nonbacteriocin antibacterial substance(s) active in vitro and in vivo. Appl Environ Microbiol 1997;63:2747-53.
[528] Hudault S, Lievin V, Bernet-Camard MF, Servin AL. Antagonistic activity exerted in vitro and in vivo by Lactobacillus casei (strain GG) against Salmonella typhimurium C5 infection. Appl Environ Microbiol 1997;63:513-8.
[529] Corr SC, Gahan CGM, Hill C. Impact of selected Lactobacillus and Bifidobacterium species on Listeria monocytogenes infection and the mucosal immune response. Fems Immunol Med Mic 2007;50:380-8.
[530] Sgouras D, Maragkoudakis P, Petraki K, Martinez-Gonzalez B, Eriotou E, Michopoulos S, et al. In vitro and in vivo inhibition of Helicobacter pylori by Lactobacillus casei strain Shirota. Appl Environ Microb 2004;70:518-26.
[531] Ingrassia I, Leplingard A, Darfeuille-Michaud A. Lactobacillus casei DN-114 001 inhibits the ability of adherent-invasive Escherichia coli isolated from Crohn's disease patients to adhere to and to invade intestinal epithelial cells. Appl Environ Microb 2005;71:2880-7.